A statistical model of North Indian Ocean tropical cyclone genesis, tracks and landfall

Md Wahiduzzaman

MSc in Environmental Science (Environmental Systems Analysis)
B.Sc Hon's in Geography and Environment

A thesis submitted in fulfillment
of the requirements for the degree of
Doctor of Philosophy (PhD)

Institute for Marine and Antarctic Studies
University of Tasmania
Hobart, Tasmania, Australia

August 2017

STATEMENTS AND DECLARATIONS

1.1 Declaration of Originality

I certify that the work in this thesis entitled "**A statistical model of North Indian Ocean tropical cyclone genesis, tracks and landfall**" has not previously been submitted for a degree nor has it been submitted as part of requirements for a degree to any other university or institution other than Institute for Marine and Antarctic Studies, University of Tasmania.

I also certify that the thesis is an original piece of research and it has been written by me. Any help and assistance that I have received in my research work or the preparation of the thesis itself have been appropriately acknowledged. This thesis differs from a traditional thesis by including, in their traditional form, a series of authored and co-authored journal articles in II Papers.

1.2 Authority of Access

This thesis may be reproduced, archived, and communicated in any material form in whole or in part by the University of Tasmania, or its agents, and be made available for loan and limited copying in accordance with the Copyright Act 1968.

Signed:

Md. Wahiduzzaman

Date: 17th August, 2017

1.3 Statement of Co-authorship

The following people and institutions contributed to the publication of work undertaken as part of this thesis:

Candidate = Md Wahiduzzaman, Institute for Marine and Antarctic Studies, University of Tasmania, Hobart, Australia.

Author 1 = Mohammad (Md) Wahiduzzaman (candidate), Institute for Marine and Antarctic Studies, University of Tasmania, Australia.

Author 2 = Dr Eric C J Oliver, Institute for Marine and Antarctic Studies, University of Tasmania and Australian Research Council Centre of Excellence for Climate System Science, Hobart, Tasmania, Australia.

Author 3 = Dr Philip J Klotzbach, Department of Atmospheric Science, Colorado State University, Fort Collins, Colorado, USA.

Author 4 = Dr Simon J Wotherspoon, Institute for Marine and Antarctic Studies, University of Tasmania and Australian Antarctic Division, 203 Channel Highway, Kingston, TAS 7050, Australia.

Author 5 = A/Prof Neil J Holbrook, Institute for Marine and Antarctic Studies, University of Tasmania and Australian Research Council Centre of Excellence for Climate System Science, Hobart, Tasmania, Australia.

Author details and their roles:

Paper 1, ***A climatological model of North Indian Ocean tropical cyclone genesis, tracks and landfall*** (Located in chapter 2)

Md Wahiduzzaman (candidate) was the primary author and wrote and implemented the code with assistance by Simon Wotherspoon. Eric Oliver, Simon Wotherspoon and Neil Holbrook contributed to the idea, its formalisation and development and in an editorial capacity.

Author contributions*:*

Md Wahiduzzaman 85%

Eric Oliver 5%

Simon Wotherspoon 5%

Neil Holbrook 5%

Paper 2, ***A statistical seasonal forecast model of North Indian Ocean tropical cyclones using the Quasi-Biennial Oscillation*** (Located in chapter 3)

Md Wahiduzzaman (candidate) was the primary author and wrote and implemented the code with assistance by Simon Wotherspoon. Eric Oliver, Phil Klotzbach, Simon Wotherspoon and Neil Holbrook contributed to the idea, its formalisation and development and in an editorial capacity.

Author contributions*:*

Md Wahiduzzaman 80%

Eric Oliver 5%

Phil Klotzbach 5%

Simon Wotherspoon 5%

Neil Holbrook 5%

Paper 3, ***Seasonal forecasting of tropical cyclones in the North Indian Ocean region: The role of El Niño-Southern Oscillation*** (Located in chapter 4)

Md Wahiduzzaman (candidate) was the primary author and wrote and implemented the code with assistance by Simon Wotherspoon. Eric Oliver, Simon Wotherspoon and Neil Holbrook contributed to the idea, its formalisation and development and in an editorial capacity.

Author contributions*:*

Md Wahiduzzaman 85%

Simon Wotherspoon 5%

Eric Oliver 5%

Neil Holbrook 5%

Paper 4, ***Stochastic modelling of tropical cyclone landfall across the North Indian Ocean rim*** (Located in chapter 5)

Md Wahiduzzaman (candidate) was the primary author and wrote and implemented the code. Eric Oliver, Simon Wotherspoon and Neil Holbrook contributed to the idea, its formalisation and development and in an editorial capacity.

Author contributions*:*

Md Wahiduzzaman 85%

Simon Wotherspoon 5%

Eric Oliver 5%

Neil Holbrook 5%

We the undersigned agree with the above stated, "proportion of work undertaken" for each of the above accepted/published and under revision or preparation in peer-reviewed manuscripts contributing to this thesis:

Signed:

A/Prof Neil J Holbrook
Primary Supervisor
IMAS
University of Tasmania

Prof Richard Coleman
Executive Director
IMAS
University of Tasmania

Date: 17th August, 2017

ACKNOWLEDGEMENTS

First and foremost, I would like to thank my supervisors, Assoc Prof Neil Holbrook and Dr Simon Wotherspoon for their constant support, guidance, patience and encouragement and for always making themselves available for discussions throughout my PhD candidature at Institute for Marine and Antarctic Studies, University of Tasmania. I would like to give special thanks to Dr Eric Oliver and Phil Klotzbach for their discussions, comments and attending in the meetings.

I also want to thank the Higher Degree Research Office at University of Tasmania, Institute for Marine and Antarctic Studies, Australian Marine Sciences Association for providing me the various sources of funding during my candidature. It enabled me to attend many national and international conferences, which elevated my work to a higher level and helped me to maintain a large international network, and also gain the skill of communicating my results with increasing confidence. Finally, I would like to thank my family for their continual support throughout my PhD.

ABSTRACT

Extensive damage and loss of life can be caused by landfalling tropical cyclones (TCs). Seasonal forecasting of TC landfall probabilities is potentially beneficial to insurance/re-insurance companies, decision makers, government policy and planning departments, and residents in coastal areas. In this study, climatological and statistical seasonal forecast models are developed for TC genesis, tracks and landfall for North Indian Ocean (NIO) rim countries based on kernel density estimation, a generalised additive model (GAM) including an Euler integration step, and landfall detection using a country mask approach. To forecast TC activity in the NIO region, the relative roles of climate modes (stratospheric Quasi-Biennial Oscillation (QBO), El Niño – Southern Oscillation (ENSO), Indian Ocean Dipole (IOD)) as predictor variables in the modelling schemes have been investigated. Using a 35-year record (1979-2013) of tropical cyclone track observations from the Joint Typhoon Warning Centre (part of the International Best Track Archive Climate Stewardship Version 6), the distribution of cyclone genesis points is approximated by kernel density estimation and the observed cyclone tracks are fitted using the GAM as smooth functions of location in each season. The model simulated TCs are randomly selected from the fitted kernel (TC genesis) and cyclonic paths, with random innovations, are simulated (TC tracks) to generate a suite of landfall statistics. Lead-lag analysis is undertaken to assess the utility of various climate mode predictor timescales for TC forecast potential.

Three hindcast validation methods are applied to evaluate the integrity of the models. First, leave-one-out cross-validation is applied whereby the country of landfall is determined by the majority vote (considering the location by only the highest percentage of landfall) from the simulated tracks. Second, the probability distribution of simulated landfall is evaluated against the observed landfall. Third, the distances between the point of observed landfall and simulated landfall are compared and quantified. Overall, the models show very good cross-validated hindcast skill of modelled landfalling cyclones against observations for most NIO rim countries, with only a relatively small difference in the percentage of predicted landfall locations compared with observations. Finally, the developed models demonstrate that including information on the phase of the QBO (using the stratospheric QBO index) and ENSO (using the Southern Oscillation index (SOI)) can improve the skill of seasonal forecasts of TCs in the NIO region.

It is shown that the most skilful model (the model skill is assessed based on predictor leads of from 1-6 months) for ENSO as predictor is found using a three-month-averaged SOI with two-month lead ahead of each of the four NIO region designated TC seasons. Analogously, the three-month averaged QBO is found to be potentially most skilful at the three-month lead. Both models demonstrate clear improvements over climatology. The hindcast probabilities and distribution of TC landfall occurrences using QBO and ENSO as climate predictor modes, match remarkably well against observations over most of the study domain.

Finally, in a separate analysis, a Poisson regression model using the Markov Chain Monte Carlo method was also developed to forecast TC landfall probabilities in the NIO region. A combined three-predictor (sea surface temperature, ocean heat content, and SOI) model was found to perform best in this model formulation against climatology.

Table of Contents

I INTRODUCTION

1 Introduction

The hazard of tropical cyclones (TCs) affecting the North Indian Ocean (NIO) region is a topic of considerable importance to the welfare of populations and economies of NIO rim countries (Fig.1). The NIO is a breeding ground for tropical cyclones (Mohapatra *et al.* 2014; Shaji *et al.* 2014) and accounts for only 7% (Mohapatra *et al.* 2014; Sahoo and Bhaskaran 2016) of the world's tropical cyclones- (about 5/year (Mohapatra *et al.* 2014)– four in the Bay of Bengal (Alam *et al.* 2003; Vissa *et al.* 2013; Balaguru *et al.* 2014; Mohapatra *et al.* 2014; Rajasekhar *et al.* 2014) and one in the Arabian Sea (Alam *et al.* 2003; Rajeevan *et al.* 2013; Vissa *et al.* 2013; Balaguru *et al.* 2014; Mohapatra *et al.* 2014; Rajasekhar *et al.* 2014) – but the number of deaths from TCs that make landfall in the region can be staggering (Webster 2008; Islam and Peterson 2009; Lin *et al.* 2009; McPhaden *et al.* 2009; Ng and Chan 2012; Pattanaik and Mohapatra 2016). It is important therefore to assess the risks thoroughly and carefully. Models can be valuable tools for evaluation and management of the tropical cyclone risks by providing seasonal forecast and early warnings. Both dynamical and statistical model have been developed to forecast tropical cyclone in the NIO basin but there is very little skill is found using dynamical models (Pattanaik and Mohapatra 2016). In view of this, there is need to develop a suitable probabilistic seasonal forecast model.

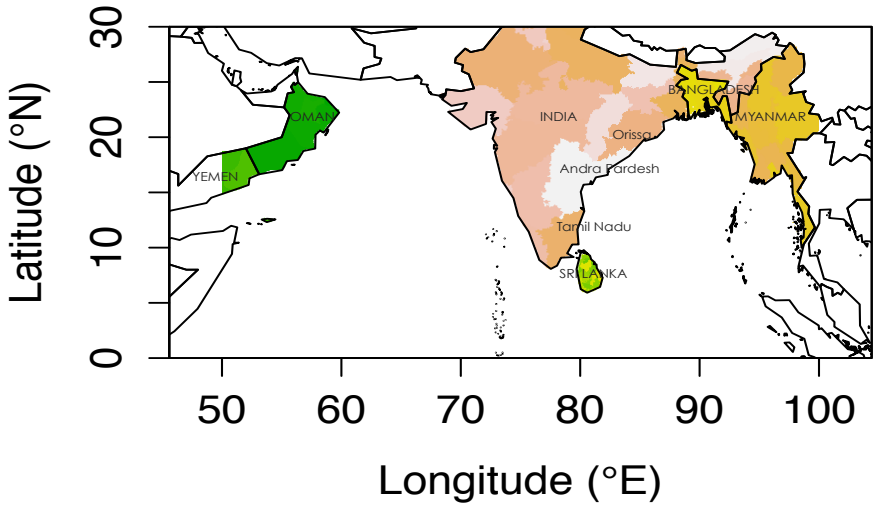

Fig.1 Geographic map showing the countries (and states) along the North Indian Ocean rim relevant to this thesis. The six countries affected by tropical cyclone landfall include India, Bangladesh, Myanmar, Sri Lanka, Oman and Yemen. Also indicated are the three Indian states (Orissa, Andhra Pradesh, Tamil Nadu) most strongly affected by tropical cyclone landfall.

Seasonal forecasting and early warnings of tropical cyclone can help decision-makers, and residents in vulnerable coastal areas, to consider and plan potential action months in advance (Taskin and Lodree Jr 2011). For example, tropical cyclone forecasts can be used to estimate demands for emergency supplies like non-perishable food items and gas-powered generators. This is used in households, and emergency evacuation shelter during and after a landfall cyclone. Also, tropical cyclone forecasts can be transformed into damage projections in monetary terms, which is of interest to insurance companies. At the government planning and policy levels, seasonal forecasting can be usefully adopted to inform and assist decision-making. For instance, decisions like whether a mandatory evacuation should be issued and if so then when, where emergency evacuation shelters should be located, and what are the appropriate quantities of emergency supplies that should be stocked at various locations in each hierarchy level of a state/country (Taskin and Lodree Jr 2011). A successful case can be mentioned about Cyclone *Sidr*, a Category IV storm, struck the southwestern coast of Bangladesh on November 15, 2007 killing 3,406 people. Compared with a similar Category IV storm Cyclone *Gorky* that struck Bangladesh in 1991 causing an estimated 140,000 fatalities, *Sidr* claimed far fewer lives. The low number of deaths is the result of cyclone forecasting and early warnings, and successful evacuation of coastal residents (Paul 2009). In order to model TC activity, it is necessary to understand the factors that influence TC genesis, propagation track, and landfall. Tropical cyclone activity over the North Indian Ocean is strongly influenced by El Niño - Southern Oscillation (Girishkumar and Ravichandran 2012; Girishkumar *et al.* 2015), Quasi-Biennial Oscillation (Fadnavis *et al.* 2011; Fadnavis *et al.* 2014), Pacific Decadal Oscillation (Girishkumar *et al.* 2014), Boreal Summer Intraseasonal Oscillation (Kikuchi and Wang 2010), Indian Ocean Dipole (Saji *et al.* 1999) Madden Julian Oscillation (Kikuchi and Wang 2010; Mohapatra and Adhikary 2011; Girishkumar *et al.* 2015).

This thesis discusses firstly the development of a statistical seasonal model of tropical cyclone genesis, tracks and landfall for the North Indian Ocean – that represents a climatological model of tropical cyclones for the region. The TC genesis model is based on kernel density estimation, the tracks are estimated using a generalised additive model, and landfall is detected by an Euler integration step with a country mask approach. This thesis also investigates the contributions of El Niño - Southern Oscillation (ENSO) and Quasi-Biennial Oscillation (QBO) as predictor variables of TC activity over the NIO.

Considering these predictors, statistical seasonal forecast models are developed for tropical cyclone genesis, tracks and landfall across the NIO rim countries using the aforementioned approaches. A Poisson regression model is also developed to forecast TC landfall probabilities in the NIO region.

Chapter 1 is structured with four subsections. Chapter 1.1 addresses the physical mechanisms of a tropical cyclone and the necessary conditions for development, classification and movement of TCs over the NIO. Chapter 1.2 describes known important atmospheric and oceanic modes in the NIO region and their large-scale effects on the climatology of the NIO region. Chapter 1.3 gives a history of statistical seasonal forecasting approach. Finally, Chapter 1.4 presents the objectives and structure of the thesis.

1.1 Tropical cyclones over the North Indian Ocean

1.1.1 Tropical cyclone structure

The structure of a tropical cyclone is divided into three parts like the eye, the eyewall and the widespread rain/feeder/spiral bands (Riehl 1954; Palmen 1956; Yanai 1964; Gray 1968, 1979; Frank 1987; Holland 1987; Gray 1990; Montgomery and Farrell 1993; McBride 1995; UNDP 2009; Werner 2011). The centre of eye can be identified by the area of lowest pressure and little or no wind and often a cloudless sky. The eye (Fig.2) is usually 40 km in diameter but can vary less than 10km to more than 100km. The eyewall (Fig.2) is the wall of dense convective cloud rising about 15-17km into the atmosphere surrounding the eye (Riehl 1954; Palmen 1956; Yanai 1964; Gray 1968, 1979; Frank 1987; Holland 1987; Gray 1990; Montgomery and Farrell 1993; McBride 1995; UNDP 2009). The strongest winds and heaviest rainfall can be found in the eyewall near the surface whereas the highest pressure gradients are towards the storm centre (UNDP 2009). The radius of maximum winds varies strongly between the different TC basins and the range is 10-100 km with increasing of the radius height (Riehl 1954; Palmen 1956; Yanai 1964; Gray 1968, 1979; Frank 1987; Holland 1987; Gray 1990; Montgomery and Farrell 1993; McBride 1995; Gray 1998; UNDP 2009). The feederbands (Fig.2) around the eyewall are approximately 10 km width and a height between 3 and 15 km (Emanuel 1991).

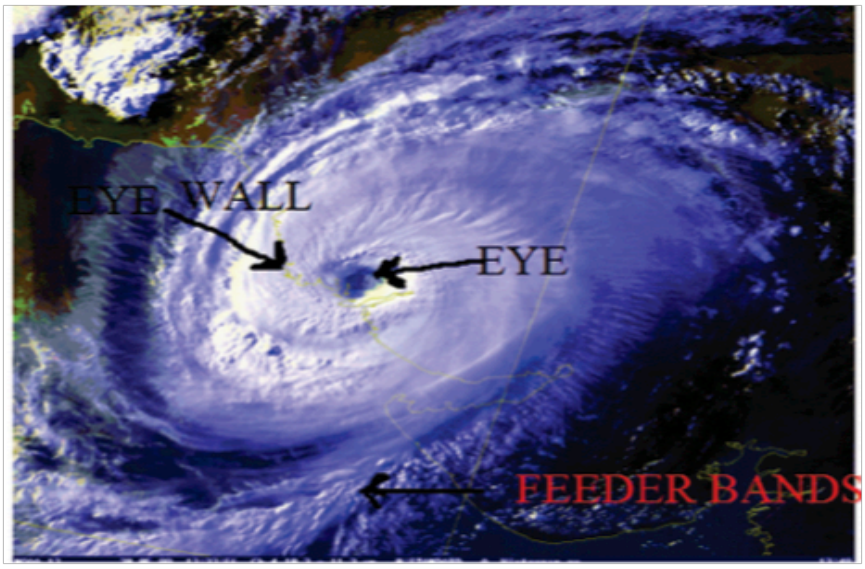

Fig.2 Structure of a tropical cyclone (UNDP 2009). It is divided as eye, eyewall and the feeder bands

The energy source of a mature TC is the thermodynamic disequilibrium between the lower atmosphere and the oceans and this disequilibrium is not reflected in an actual temperature difference between the lower troposphere and the ocean, but in the undersaturation of surface-near air (Kleinschmidt 1951; Holland 1997; Werner 2011). Emanuel (1986) described an idealized TC as a Carnot machine (Fig.3) where heat gets converted into mechanical energy. For acquiring a more thermodynamic equilibrium of the ocean and lower troposphere, surface air flows cyclonically towards the boundary layer of the storm center and then it rises close to the moist adiabatic state into the mid- and upper troposphere (Emanuel 1991). Therefore increased surface winds lead to increase heat transfer from the ocean and to subsequent intensification and so on (Holland 1997). These processes lead to the development of maximum potential intensity of a tropical cyclone (Emanuel 1988). Later this theory has been critised by Smith *et al.* (2008) and they pointed a major deficiency of the theory is the tacit assumption of gradient wind balance in the boundary layer. They noted if a more complete boundary-layer formulation is included using the gradient wind profiles obtained from Emanuel's theory, the tangential wind speed in the boundary layer becomes supergradient that invalidates the assumption of gradient wind balance and they show the degree to which the tangential wind is supergradient depends on the assumed boundary layer depth. The full boundary-layer solutions require a knowledge of the tangential wind profile above the boundary layer in the outer region where there is subsidence into the layer which is

depend on the breadth of this profile. This effect is not considered in Emanuel's theory. Holland (1997) also descried a theory for maximum potential intensity by the central pressure of a cyclone and used published empirical relationships to calculate the maximum winds for a given central pressure.

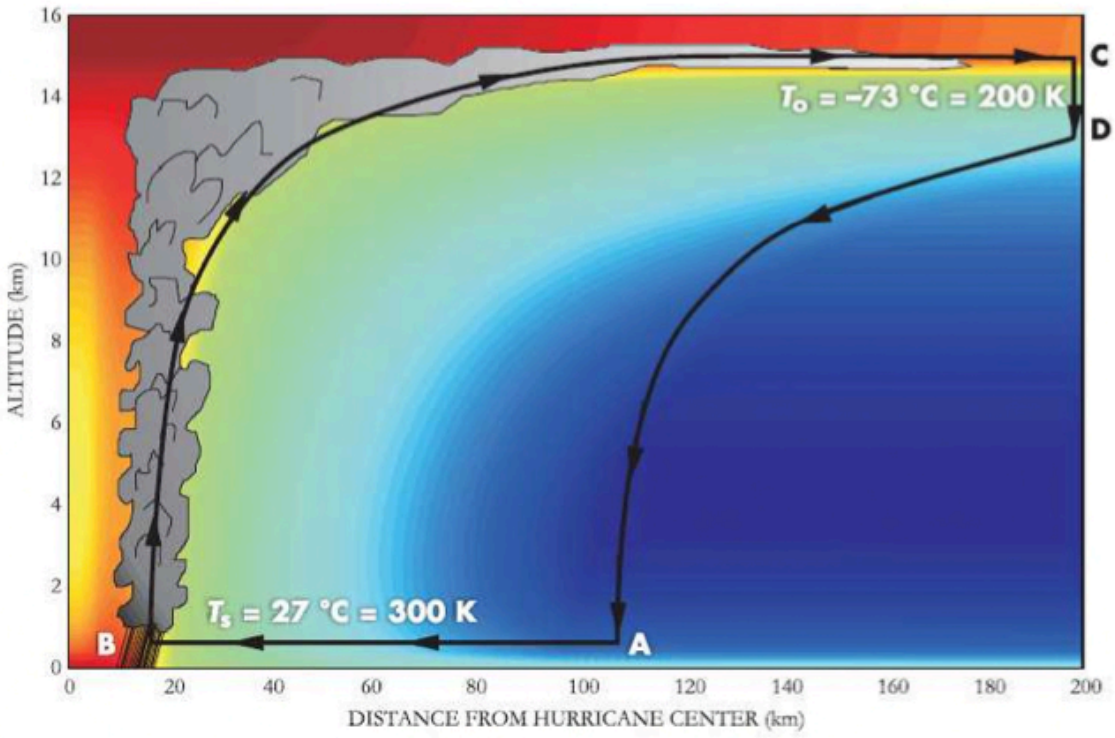

Fig.3 A tropical cyclone as a Carnot heat engine (Emanuel 1988; Emanuel 2006). **A** indicates a low-pressure system formation with inbound surrounding air by isothermally abd gain entropy through water vapor over the warm ocean. B shows the upward air flow and from C to D air travels along the outflow of tropical cyclone where it has neutral buoyancy and finally from D to A air flows back to surface.

1.1.2 Tropical cyclogenesis

TC formation (genesis) can occur when certain atmospheric and oceanic conditions are favorable. Gray (1968) outlined environmental factors that he deemed relevant to tropical cyclone formation and these are sea surface temperature (SST), conditional instability in the lower to mid-troposphere, absolute vorticity in the lower troposphere, mid-troposphere relative humidity, divergence in the upper troposphere, and low vertical shear of the horizontal winds between the lower and upper troposphere. Later in several studies

(e.g., (Gray 1975; McBride and Zehr 1981; Gray *et al.* 1992, 1993) showed the climatological aspects of the seasonal frequency of tropical cyclone formation at any location by six seasonally averaged parameters where three are dynmical potential and rest three are thermal potential. Gray (1998) explained the multiplication both of dynamic (the Coriolis parameter, low-level relative vorticity and inverse of the tropospheric vertical wind shear) and thermal potential (ocean thermal energy as ocean temperatures greater than 26 ~ to a depth of 60 meters, equivalent potential temperature gradient as the difference in equivalent potential tem- perature between the surface and 500mb and mid-tropospheric relative humidity) which specifies seasonal genesis parameter that provides very good estimates of the long term frequency of occurrence of tropical cyclone at all global basins for each season of the year.

Also, Gray (1998) explained the following background requirements to make a possible tropical cyclone formation-(1) climatology is right (for example region, season, SST etc), (2) synoptic flow pattern is right (For instance monsoon trough, high vorticity with small vertical wind shear etc) and (3) active mesoscale convention system is present within a cloud cluster system. He also added if these three equirements are met then there will have still uncertainties unless the presence or lack of concentrated wind convergence at the centre of a tropical convergence is considered. It is widely acknowledged that tropical cyclones form in moist unstable environments with low-level tropical disturbances like easterly waves, tropical cloud clusters and warm sea surface temperatures (Montgomery and Farrell 1993). Tropical cyclone formation needs a background understanding of tropical convection (Gray 1998).

Tropical cyclone can be form from an African easterly wave (Hopsch *et al.* 2010); broad scale vorticity convergence (Yanai 1964); upper tropospheric troughs (Ramage 1950), the Inter Tropical Convergence Zone (Tanabe 1963), ordinary cold fronts (Emanuel 2005b), monsoon troughs (Ritchie and Holland 1999), a baroclinic-barotropic instability of the African easterly jet (Landsea 1993), easterly (shift from north-easterly to south-easterly) waves (Montgomery and Farrell 1993), large-scale environmental conditions (Camargo *et al.* 2007a; McGauley and Nolan 2011), temperature - potential energy (Emanuel 2005a), vertical wind shear (Paterson *et al.* 2005; Tang and Emanuel 2010), a humid environment (Emanuel *et al.* 2008) and the convective available potential energy (Camargo *et al.* 2007c).

North Indian Ocean consists Bay of Bengal and Arabian Sea where Bay of Bengal is the active region for tropical cyclone development. During pre-monsoon (March-May) and post-monsoon (October-November), westward propagating minor tropical disturbances near and south of Bay of Bengal develop into cyclones. The Inter tropical convergence zone is the meeting zone of winds from Norther and Southern hemisphere, which play a vital role for cyclone development in Bay of Bengal (UNDP 2009; Akter and Tsuboki 2014; Akter 2015; Goyal *et al.* 2016).

1.1.3 Classification and movement of cyclonic disturbances in the NIO

Tropical cyclones are known by many terms across the basin like hurricanes, typhoons, cyclones etc. Though they have different names but they are classified according to wind speed. Based on the wind speed, the cyclonic disturbances formed in the Bay of Bengal and the Arabian Sea are classified (WMO 1997; UNDP 2009) as below:

Table 1. Classifications of cyclonic disturbances for the Bay of Bengal and the Arabian Sea region

Weather System	Maximum wind speed	
	knots	kp/h
1. Low Pressure area	< 17	< 31
2. Depression	17 - 33	31 - 61
3. Cyclonic storm	34-47	62-88
4. Severe cyclonic storm	48-63	89-118
5. Very Severe cyclonic storm	64-119	119-221
6. Super cyclonic storm	≥ 120	≥ 222

The season wise directions of movement of cyclonic storms that form in the Bay of Bengal and the Arabian Sea are given below (IMD 1979; SMRC 1998).

In winter (December-February), a few tropical storms occur in the Bay of Bengal. They usually form between 5° N and 8° N, move in a westward or northwestward direction and make landfall at north Tamil Nadu coast or the eastern coast of Sri Lanka. Tropical storms do not occur in the Arabian Sea during these months.

During pre-monsoon (March-May), Most of the Bay storms in this month originate between 8° N and 15° N and east of 85° E. They initially move towards northwest or north; later they recurve towards northeast and make landfall at at the eastern coast of India, the coastal areas of Bangladesh or the Arakan coast of Myanmar. The tropical storms over the Arabian Sea move initially towards northwest or north. After recurving they move towards the Gujrat-Sind Mekran coast.

In monsoon (June-September), almost all the Bay storms (mostly depressions / deep depressions) in this month originate between 16° N and 21° N and west of 85° E. Majority of them move towards the north-westward and weaken into depressions after crossing the coast. Then they recurve towards the north or north-northeast. Most of the storms in the Arabian sea in this season are practically confined to the area north of 15° N and east of 65° E. Movement is mainly westwards or northwestwards.

During post-monsoon (October-November), majority of the storms form between 8° N and 13° N and move in a west-northwestward direction making landfall at north Tamil Nadu coast and adjoining south Andhra coast, Bangladesh coast and emerge into the Arabian Sea and reintensify. The storms that form in more northern latitudes over the Bay of Bengal move northwest and then recurve towards the northeast. In the Arabian Sea, the initial movement of the storms is northwestward. The storms which proceed north of 15° N generally recurve towards the northeast making landfall at north Maharashtra-South Gujrat coast.

1.1.4 Bimodal characteristics of tropical cyclones in the NIO region

Bimodal characteristics of tropical cyclones are observed in the NIO region (Yanase *et al.* 2012; Li *et al.* 2013; Xing and Huang 2013; Akter and Tsuboki 2014) . A distictly bimodal cyclone season in the NIO is pre-monson and post-monsoon (Camargo *et al.* 2007c; Kikuchi and Wang 2010; Akter and Tsuboki 2014; Wahiduzzaman *et al.* 2016) with the primary (secondary) peak in cyclone frequency is in November (May). This seasons are also characterized by summer and winter prevailing wind directions. During summer (winter) southwesterly (northwesterly) monsoon winds blow form the western Arabian Sea (Bay of Bengal) to Bay of Bengal (Arabian Sea). The opposite directions of monsoon winds between two seasons show seasonal difference of TC genesis (Shankar *et al.* 2002).

Climatologically, the seasonal spatial variation in the cyclone distribution is linked with the seasonal variation in the monsoon trough location which is formed between the westerly or southwesterly monsoon winds and the easterly trade winds. During the pre-monsoon (post-monsoon), the trough crosses the northernmost (middle) BoB. Dynamic and thermodynamic parameters for cyclogenesis, namely the areal average of the seasonal relative vorticity at 850 hPa, SST, vertical wind shear between 850 and 200 hPa, relative humidity at 700 hPa, and the difference in equivalent potential temperature between the surface and 500 hPa, were compared between the pre- and post-monsoon by Akter and Tsuboki (2014) and they found in both seasons, the values of these dynamic and thermodynamic parameters for TC genesis were similar to values in the western North Pacific. They concluded that during the pre-monsoon large wind shear caused by a northern shift of the monsoon trough negatively affects cyclogenesis in the southern BoB, and large convective inhibition aloft caused by the advection of hot, dry air suppresses convective activity in the northern BoB. Therefore, both the seasonal monsoon trough location and the environmental convective inhibition account for the less frequent cyclogenesis during the pre-monsoon over the BoB.

Previous studies (Gray 1968; Camargo *et al*. 2007c; Evan and Camargo 2011; Yanase *et al*. 2012; Li *et al*. 2013) suggested that the bimodal feature of TC frequency in the BoB and AS is attributable to the annual cycle of the background vertical shear. Li *et al*. (2013) found very low genesis frequency in monsoon period and discussed that the first increase of cyclone frequency is seen in pre-monsoon compared with the level in winter. The key process responsible for such a rapid increase is the abrupt increase of the midlevel atmosphere relative humidity. It plays the dominant role and contributes 87% of the total genesis potential index (GPI) increase. The first decrease of cyclone frequency occurs in monsoon compared with the level in pre-monsoon. The combined effect of atmospheric vertical wind shear, vorticity, and potential intensity is responsible for this decrease. The second increase of cyclone frequency occurs in post-monsoon with reference to the level in monsoon. It is mainly attributed to the decrease of the vertical shear. The second decrease of cyclone frequency occurs in winter with reference to the level in post-monsoon. This is primarily caused by the decrease of the environmental relative humidity and relative vorticity. The period of winter is dominated by the boreal winter northeast monsoon, which is much weaker and drier than the boreal south-west monsoon (Li *et al*. 2013)

Another study by Xing and Huang (2013) is shown that the bimodal distribution of TC genesis events is due to potential intensity and vertical wind shear. The primary reason is the change of wind direction linked with the onset and withdrawal of the summer monsoon over the BoB. The decreases of relative humidity in winter and vorticity in summer play a minor role in the contributions to the seasonal variation (Xing and Huang 2013).

1.2 Ocean-atmosphere modes affecting the Indian Ocean region

The Indian Ocean is the smallest of the world oceans. The east-west dimension is about 7800 km (between Australia and southern Africa) and the north-south dimension is about 9600 km (from Antarctica to the Bay of Bengal); the average depth is 3800 m, but contains two ridge systems namely the Central Indian Ridge and Ninety East Ridge. Ocean currents are influenced by the existence of numerous ridges and plateaus (Tomczak and Godfrey 1994) and the propagation of long planetary waves (Wang *et al.* 2001; Killworth and Blundell 2003, 2003; Tailleux 2003).

The climate of the Indian Ocean region is strongly influenced by ocean variability on various spatial and temporal scales (Schott and McCreary Jr 2001). It is dominated by two large-scale interannual climate modes: El Niño - Southern Oscillation (ENSO) in the Pacific basin and Indian Ocean Dipole (IOD) in the Indian Ocean (Philander 1990; Saji *et al.* 1999; Webster *et al.* 1999). ENSO is attributed to 30% (using empirial orthogonal function analysis) of the total variation of anomalous Indian Ocean SST while the IOD explains around 12% of the total (Saji *et al.* 1999). Further studies (Cai *et al.* 2001; Ashok *et al.* 2003; Meyers *et al.* 2007; Ramsay *et al.* 2008; Lim *et al.* 2009; Ummenhofer *et al.* 2009) discuss these modes and their effects. In the following section, both of these large-scale ocean-atmosphere signals (ENSO and IOD), and their interannual modulation of the large-scale tropical and subtropical atmosphere and their effects on the NIO climate are discussed.

1.2.1 The El Niño -Southern Oscillation

ENSO is the dominant interannual mode of ocean-atmosphere variability in the Pacific and affects the large-scale climate all over the globe (Lau 1985; Philander 1985; Cane *et al.* 1986; Allan 1988; Philander 1990, 1992; Ropelewski and Halpert 1996). Its effects on tropical cyclones are long observed in North Atlantic (Gray 1984), Western North Pacific

(Chan 1985) and Northern Australia (Nicholls 1979).

'Normal' conditions in the tropical Pacific comprise of a deep thermocline (around 200m) in the western equatorial Pacific, associated with the Western Pacific warm pool, and a cold tongue extending zonally westward from the equatorial Eastern Pacific into the central Pacific. Low-pressure and convection is typical in the West Pacific warm pool region while high-pressure and subsidence tends to occur in the eastern tropical Pacific – the low level westward flow and upper level eastward flow that closes this loop forms the walker circulation. By piling up water in the tropical West Pacific, the surface trade winds further enhance the east-west gradient in temperature and further pushing down the thermocline in that region (Philander 1990). Bjerknes (1969) showed that this represented a positive feedback mechanism on an initial perturbation at the equatorial thermocline (Bjerknes 1969). The equatorial SST dipole in the Pacific introduces zonal easterly trade winds towards the tropical Western Pacific warm pool. This enables a further enhancement of the SST dipole due to increasing the tropical thermocline's slope and increasing upwelling of cold water in the East Pacific. The strength of the Bjerknes feedback between ocean and atmosphere in the normal climatological conditions or in the ENSO phases is dependent on the east-west slope of the tropical thermocline. The pressure gradient weakens because of the resulting reduction in SST gradient across the equatorial Pacific, and therefore a weakening of the easterly trade winds and a flattening of the thermocline slope. This mechanism finally ends with a breakdown of the Walker circulation and an interruption of the equatorial upwelling in the Eastern Pacific, leading to El Niño conditions. Conversely, a La Niña event corresponds to an enhancement of the cold tongue in the equatorial East Pacific (Philander 1992).

ENSO is a coupled phenomenon that is related with Southern Osillation Index which is defined as varying difference in atmospheric pressure between Darwin, Australia and Tahiti, Hawaii and tropical pacific sea surface temperature. A schematic of ENSO phenomenon is shown in Fig.4.

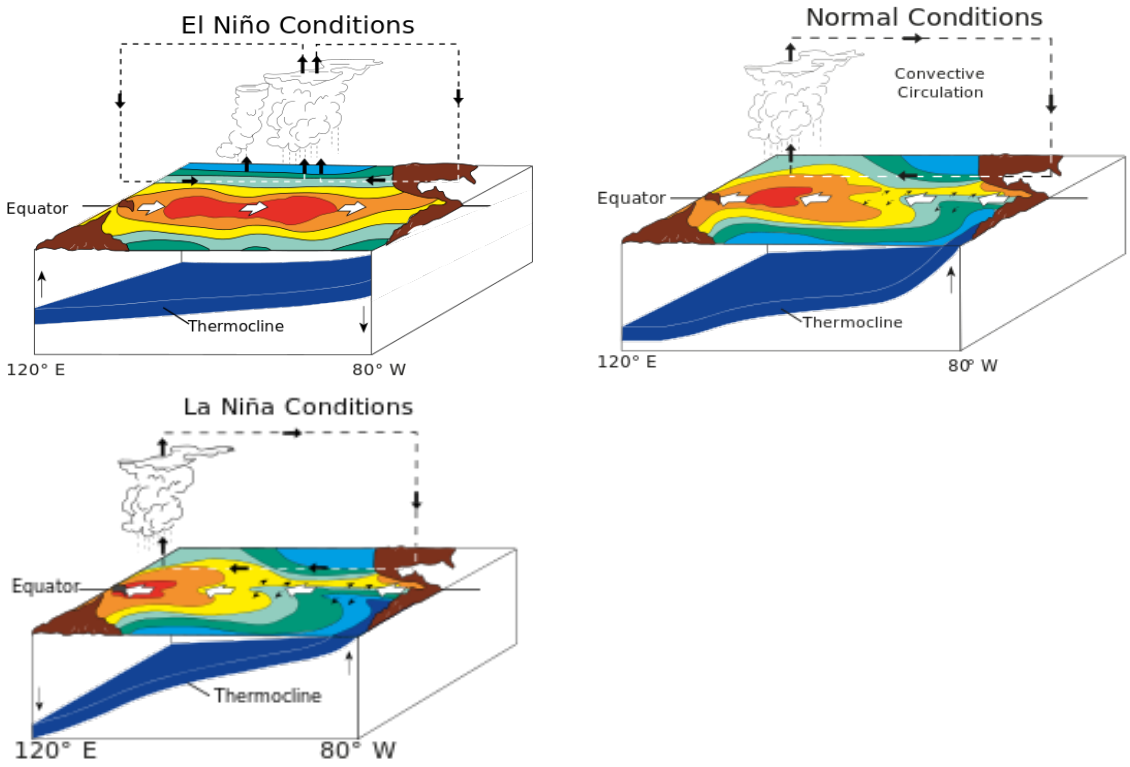

Fig.4 A schematic showing the atmospheric circulation and tilt of the thermocline during El Niño (upper left), Normal (upper right) and La Niña (bottom left) (NCDC June 2009)

Generally the duration of a single ENSO event is ~18 months, and the quasi-periodicity of ENSO is characterized between 2-8 years (Rasmusson 1984; Wright *et al.* 1984), and tends to oscillate with the seasonal cycle (Philander 1985). Due to ENSO, sea level pressure or SST anomalies are responsible for the large-scale changes in the climatology. Different studies are looking into the large-scale modulation of the atmosphere as a result of ENSO on different time-scales (e.g., (Van Loon and Shea 1987; Karoly 1989; Drosdowsky and Williams 1991; Zhang *et al.* 1997; Garreaud and Battisti 1999; Lu *et al.* 2008).

ENSO is the largest single predictable factor that influences the global tropical cyclone frequency, genesis, tracks and landfall on seasonal time-scales (Camargo *et al.* 2008; Camp *et al.* 2015) Many earlier studies have investigated the relationship between ENSO and seasonal TC activity in NIO basins (Ho *et al.* 2006; Kuleshov *et al.* 2008; Girishkumar *et al.* 2012; Srikanth *et al.* 2012; Girishkumar *et al.* 2014; Camp *et al.* 2015; Girishkumar *et al.* 2015). Girishkumar *et al.* (2012) studied the influences of ENSO on tropical cyclone activity in the Bay of Bengal (BoB) during October–December. The

study showed that more TCs formed under La Niña years than El Niño years in the post-monsoon season, which is the peak TC season. In the La Niña phase, it was shown that 70% of TCs that formed in the eastern part of the BoB tend to move north-westward and make land fall north of 15°N on the east coast of India. During El Niño years, most of the TCs that formed in the western BoB took a westward track towards the east coast of India, particularly south of 15°N. Girishkumar *et al.* (2012) also examined the physical mechanism that links ENSO to TC activity. They found that during La Niña (El Niño), the existence of low-level cyclonic (anticyclonic) vorticity, enhanced (suppressed) convection, and high (low) tropical cyclone heat potential in the Bay of Bengal provided favorable (unfavorable) conditions of TC activity (frequency, genesis location and intensity. This work was later extended by adding an MJO relationship (Girishkumar *et al.* 2015) on TC activity under El Niño and La Niña phases of ENSO.

Related studies have also been undertaken. Singh *et al.* (2001) examined the relationship between ENSO and tropical cyclonic activity in the BoB during the summer monsoon season (July–August). Their study revealed that more tropical depressions formed in the BoB during El Niño years where they only focused on the monsoon period only. Singh *et al.* (2000) showed that there was a reduction in cyclonic storms in two peak seasons (Pre and Post Monsoon) over the BoB during El Niño years. Camargo *et al.* (2007) demonstrated the effect of ENSO on the genesis potential index (useful metric for gauging the performance of global climate models to simulate TC genesis) in all ocean basins, and concluded that there tends to be a shift in genesis potential from the northern to southern part of the BoB due to wind shear in La Niña years as compared to El Niño years.

1.2.2 Indian Ocean Dipole Mode

The Indian Ocean Dipole (IOD) is a coupled ocean-atmosphere phenomenon in the Indian Ocean that is described by an anomalous cold and warm SST in the southeastern equatorial Indian Ocean and western equatorial Indian Ocean. “Dipole” mode was first introduced independently in two studies in 1999, by groups from the USA (Webster *et al.* 1999) and Japan (Saji *et al.* 1999). Both studies suggested that the IOD is a local mode of the Indian Ocean that exists independently from the Pacific. Saji *et al.* (1999) introduced the term IOD that reflects a zonal structure of the phenomenon with two maxima of different polarity. This anomaly is found not only in SST but also in other oceanic and

atmosphere fields like sea surface heights, wind, pressure, rainfall, and outgoing long wave radiation over the Indian Ocean. Later the this IOD pattern is proposed as the Indian Ocean Zonal Mode (Black *et al.* 2003; Clark *et al.* 2003) or Indian Ocean Dipole Zonal Mode (Annamalai *et al.* 2005; Song *et al.* 2007) because it matches the out-of-phase development of the SST extreme in the east and west Indian Ocean.

The IOD is a tropical phenomenon that is strongly locked to the annual cycle and reaches a peak during boreal autumn in September-October (Huang and Kinter Iii 2002). It has positive and negative phases. Not only the anomalously cold SST in the east and warm in the west but also the anomalous easterlies equatorial wind illustrates the positive IOD (Fig.5) that causes excessive rain at the eastern African coast and drought in Australia. The negative IOD (Fig.5) has an opposite pattern. During the negative phase of the IOD it is found that there are warmer than average SSTs near Indonesia and cooler than average SSTs in the western Indian Ocean that results in stronger westerly winds across the Indian Ocean, greater convection near Australia, and enhanced rainfall in the Australian region (Australian Bureau of Meteorology, http://www.bom.gov.au/watl/about-weather-and-climate/australian-climate-influences).

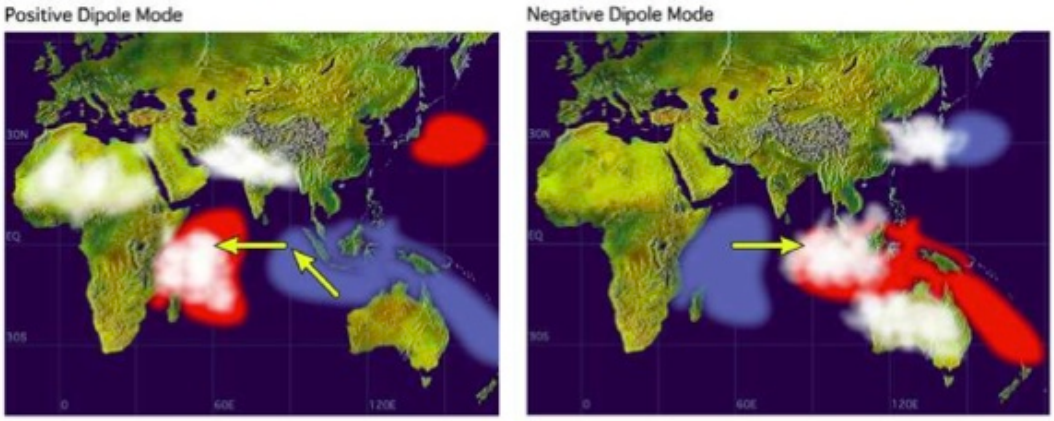

Fig.5 A schematic showing the IOD phenomenon during positive (left) and negative phase (right). Red and blue indicate warm and cold SST anomalies respectively. Also white patches show the increased convective activities, and yellow arrow directs the anomalous wind.

The mechanism for more landfalls over India during negative IOD is discussed by Yuan et al. (2013) who examined NIO TC activity under different phases of IOD and their study revealed that under negative IOD there are anomalous easterlies over BoB, which would steer TCs toward the east coast of India. Historically there were also many more

landfalls over east coast of India under negative IOD.

1.2.3 Quasi-Biennial Oscillation

The (stratospheric) Quasi-biennial Oscillation (QBO) is a quasi-periodic oscillation of the equatorial zonal wind that dictates the variability of the equatorial stratosphere (16–50 km height above the surface) and affects downward propagating easterly and westerly wind regimes, with a variable period averaging approximately 28 months (Baldwin *et al.* 2001). The structure of the QBO (Naujokat 1986; Baldwin *et al.* 2001) is as follows and a schematic diagram is shown in Fig.6.

- Alternating easterly and westerly wind regimes propagate downward with time;
- Westerlies move down faster and more regularly than easterlies;
- The transition to easterlies is often delayed between 30 and 50 hPa;
- Easterlies are generally stronger (30-35 m/s) than westerlies (15-20 m/s);
- Maximum amplitudes of both phases typically occur near 20-hPa;
- The average period is a little over 2 years;
- Both the period and amplitude considerably vary from cycle to cycle.

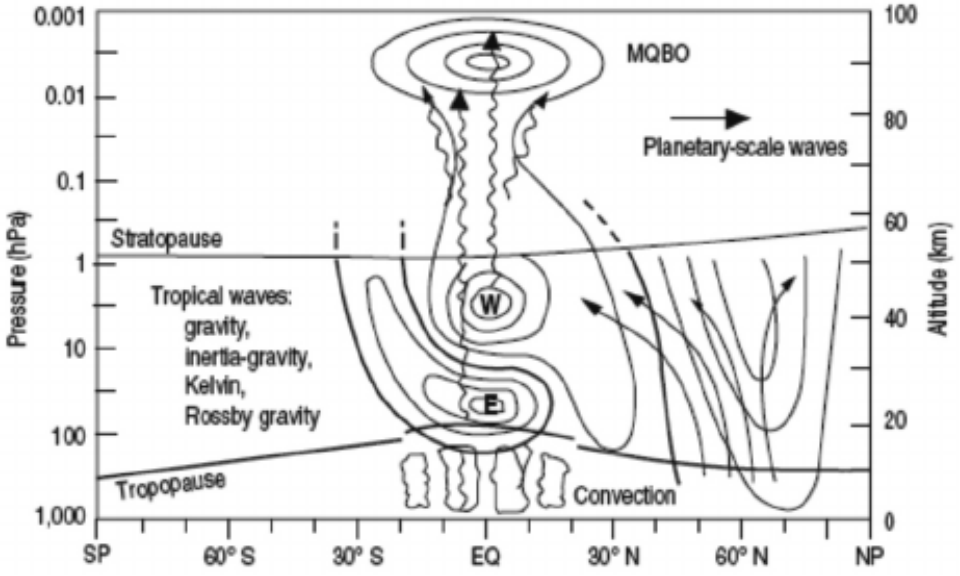

Fig.6 A schematic QBO showing the circulation where the string and black arrow show tropical and planetary waves respectively (Sağır *et al.* 2015).

The propagation of the QBO extends below the tropopause and modulates the water vapor mixing ratios in air entering the stratosphere through the cold tropical tropopause region (Zhou *et al.* 2004; Liang *et al.* 2011). The QBO has been shown to modulate tropical, deep convection (Collimore *et al.* 2003; Ho *et al.* 2009; Liess and Geller 2012), the incidence of Atlantic hurricanes (Gray 1984) and typhoon tracks in the western North Pacific (Ho *et al.* 2009). Gray (1984) pointed out an apparent influence of the QBO on Atlantic TC activity and found TC activity in the Atlantic was greater during the QBO westerly phase, or during the transition to the westerly phase, than during the easterly phase. It was found that more intense Atlantic hurricanes occurred during westerly QBO years (Gray 1984). Subsequently, the QBO influence on Atlantic hurricane activity has been discussed by other authors (Shapiro 1989; Hess and Elsner 1994; Landsea *et al.* 1998; Elsner and Kara 1999; Arpe and Leroy 2009) as a factor in a specific year's level of activity or in the general variability of the Atlantic basin. Camargo and Sobel (2010) have also explored the relationship between the QBO and TC activity in the North Atlantic. They found a statistically significant relationship from the 1950s to the 1980s but did not find a significant relationship in recent years. Camargo and Sobel (2010) also found that the QBO-TC frequency relationship was generally weak in most global TC basins.

Recently, a potentially useful climatic relationship has been demonstrated between the stratospheric Quasi-Biennial Oscillation (QBO) and TC tracks in the Bay of Bengal region of the NIO (Fadnavis *et al.* 2014). The QBO influence is observed to be significantly stronger during the easterly phase compared to the westerly phase. Also, numbers of cyclones are higher during the easterly phase than during the westerly phase, at least during the more active pre-monsoon and post-monsoon seasons. This follows earlier research work that has also proposed relationships between the stratospheric QBO and hurricane activity in the North Atlantic region (Gray *et al.* 1992, 1994), although the use of the QBO as a predictor for North Atlantic TC activity has been discontinued in recent years (Klotzbach 2007, Camargo and Sobel 2010). Other studies have also examined the influence of the QBO on TC activity in the western North Pacific (Chan 1995; Baik and Paek 1998; Lander and Guard 1998; Ho *et al.* 2009), the eastern North Pacific (Whitney and Hobgood 1997), the North Indian Ocean (Balachandran and Guhathakurta 1999) and the South Indian Ocean (Jury 1993; Jury *et al.* 1999).

1.3 Statistical modelling of tropical cyclones

Statistical modelling approaches have been developed and improved for predicting TC activity in various basins and sub-basins since 1980 (Klotzbach *et al.* 2010). Nicholls (1979) described the first statistical seasonal forecast model of TC activity for the Australian region and Gray (1984) for the North Atlantic, and later again in the North Atlantic showing climatic relationships with hurricane activity based on the Quasi-Biennial Oscillation and African rainfall (Gray *et al.* 1992, 1994). A co-relationship between intense hurricanes and the Sahel monsoon rainfall was also shown (Landsea and Gray 1992). The forecast skill of climatology and persistence was confirmed and improved based on Gray's operational Atlantic seasonal TC forecasts for the analyzed period from 1984–2001 (Owens and Landsea 2003; Saunders and Lea 2005; Klotzbach 2007). Other relevant statistical forecasts include model predictions of hurricane counts using Poisson regression models in the North Atlantic (Elsner and Schmertmann 1993; Lehmiller *et al.* 1997) and Australian region (McDonnell and Holbrook 2004a, 2004b). Later, the Poisson method was extended using a Bayesian approach to investigate seasonal TC counts and landfall over the USA (Elsner and Jagger 2004, 2006) and northern Australia (Werner and Holbrook 2011), and this approach was also used to improve multiseason forecasting of Atlantic hurricane activity (Elsner *et al.* 2008), and seasonal forecasting of TCs affecting the Fiji, Samoa and Tonga regions (Chand and Walsh 2010) and the central North Pacific (Chu and Zhao 2007). A Projection pursuit regression (PPR) has been used to forecast seasonal TC totals and associated TC predictands (Chan *et al.* 1998; Chan and Shi 1999; Chan *et al.* 2001; Liu and Chan 2012) in the northwest Pacific and Australian region and also a statistical scheme based on ENSO related indices has been developed for predicting the annual number of TCs making landfall along the south China coast (Liu and Chan 2003). The modes from an empirical orthogonal analysis of climate factors have been used as predictors of TC behavior in a statistical model also for the South China region (Goh and Chan 2010).

Solow and Nicholls (1990) described the first Poisson regression based statistical forecast model for the Australian region using the Southern Oscillation Index (SOI) as a predictor of Australian region total TC counts. A Poisson regression model using the September lead saturated equivalent potential temperature gradient between 1000hPa and 500hPa and SOI was developed to forecast upcoming season TC genesis (TCG) totals across the

Australian region (McDonnell and Holbrook 2004a, 2004b). This model has also been applied to forecast subregional TCG totals in the eastern Indian Ocean, Northern Australia and southwest Pacific regions (McDonnell *et al.* 2006). Another study (Liu and Chan 2012) presented a seasonal forecast model for the Australian region based on a PPR using generally known predictors such as the NINO4, trade wind index, and the outgoing long-wave radiation index from the U.S. Climate Prediction Center.

So far, little skill has been shown in seasonal forecasts for the NIO region using dynamical models (Camargo *et al.* 2007a; Camp *et al.* 2015). Camp *et al.* (2015) suggested that the seasonal TC cycle in the North Indian Ocean is poorly simulated by ERA-Intertim and GloSea4 and GloSea5 models. Also Camargo *et al.* (2005) and Shaevitz *et al.* (2014) noted that both low and high-resolution models are generally unable to properly simulate the seasonal cycle. Yahyai (2014) describes the dynamical High Resolution Model (HRM) and consortium for small scale modelling (COSMO) models in the NIO. They showed that their performance was insufficient for predicting landfall points compared to those observed, due to limited spatial resolution. In a separate study, Ray *et al.* (2012) used an artificial neural network system for the North Indian Ocean region to point out the error of prediction between the landfall point by simulated eastward track and observed tracks.

On the other hand, statistical models draw conclusions from the statistical record to relate current and previous TC positions as predictors of the next position and behaviour. A number of models have been developed for probabilistic cyclone forecasting. The HURRAN (Hurricane Analog) model searches for historical analogs to the track being simulated, and calculates probabilities for the simulated track's next position from these historical analogs (Neumann 1972). A multiple regression model, CLIPER (Climatology-Persistence), based on a set of polynomial regression, has been used to relate a selected number of TC predictors to predictands (Vickery *et al.* 2000). Emanuel *et al.* (2006) used Markov Chain Monte Carlo (MCMC) approach to simulate tropical cylone tracks.

We have developed both a climatological and a statistical seasonal forecast model of tropical cyclone genesis, tracks and landfall for the North Indian Ocean based on kernel density estimation, a generalised additive model, and an Euler integration with country mask approach, as well as separately using a Poisson regression model. Three hindcast

514 methods have also been used to cross-validate and measures the skill of the model.

515 ## 1.4 Thesis objectives and structure

516 The key aims of this thesis are:

517 1. To develop a climatological model of North Indian Ocean (NIO) region tropical
518 cyclone genesis, trajectories and landfall.
519 2. To develop statistical seasonal forecast models of TC genesis, tracks and landfall
520 probabilities, on a state-by-state basis across the NIO rim coutnries, utilising
521 information from important climate modes relevant to the region.
522 3. To evaluate the skill of the models against historical observations using cross-
523 validation techniques.

524 The seasonal forecast models are intended to better inform vulnerable populations for
525 tropical cyclone risks in the upcoming season(s).

526 The thesis is organised as follows. Chapter 2 is presented in the form of an accepted paper
527 to be publised in *Climate Dynamics* that addresses developing a climatological model of
528 TC genesis, track and landfall. Chapter 3 investigates the value of using a QBO index as a
529 climate predictor variable for statistical seasonal forecast modelling of TC genesis, tracks
530 and landfall, and represents a paper for revision to *Climate Dynamics*. Chapter 4 describes
531 an analogous statistical forecast model but instead considering ENSO as the important
532 climate mode, and using the SOI as predictor variable. Chapter 4 is also presented in the
533 form of a manuscript for submission to *Climate Dynamics*. Chapter 5 comprises a paper
534 for submission to *Climate Dynamics* that exploits stochastic modelling of seasonal TC
535 landfall frequency in relation with intesnity. Finally, in Chapter 6, the results of
536 climatological model, two seasonal forecast model using QBO and ENSO, Possion
537 regression and GAM approach with intensity and future research are outlined before we
538 summarise the key achievements of this study.

II PAPERS

2 DEVELOPMENT OF CLIMATOLOGICAL MODEL FOR TROPICAL CYCLONE GENESIS, TRACKS AND LANDFALL IN THE NORTH INDIAN OCEAN REGION

2.1 Chapter Overview

This chapter introduces a climatological model of North Indian Ocean region tropical cyclone genesis, tracks and landfall based on the observational data from 1979-2013. The development of climatological model of tropical cyclone genesis, tracks and landfall for North Indian Ocean rim countries are based on kernel density estimation, a generalised additive model including an Euler integration step, and landfall detection using a country mask approach. The model is fitted to the observed cyclone track velocities as a smooth function of location in each season and the distribution of cyclone genesis points is approximated by kernel density estimation. The model simulated TCs are randomly selected from the fitted kernel and the cyclonic tracks represented by the model together with the application of stochastic innovations at each step and simulated the first point of landfall. Leave one out cross validation with majority vote approach, probability distribution and distance calculation between observed and simulated landfall validation hindcast methods are used to analyse the skill of model.

The main text of this chapter is an accepted paper to be published in the journal of *Climate Dynamics (*Wahiduzzaman M, Oliver E, Wotherspoon S, Holbrook N (2016) A climatological model of North Inidan Ocean tropical cyclone genesis, tracks and landfall, Climate Dynamics, pp.1-19)

2.2 Wahiduzzaman *et al.* 2016; *Climate Dynamics*

A climatological model of North Indian Ocean tropical cyclone genesis, tracks and landfall

Mohammad Wahiduzzaman[1, 2], Eric C.J. Oliver[1, 3], Simon J. Wotherspoon[1,4], Neil J. Holbrook[1,3]

[1]Institute for Marine and Antarctic Studies (IMAS), University of Tasmania, Australia

[2] Department of Geography and Environment, Jahangirnagar University, Dhaka, Bangladesh

[3]Australian Research Council Centre of Excellence for Climate System Science, Hobart, Tasmania, Australia

[4] Australian Antarctic Division, 203 Channel Highway, Kingston, TAS 7050, Australia

Accepted December 2016 *Climate Dynamics*

Corresponding author address: Neil J. Holbrook, Institute for Marine and Antarctic Studies (IMAS), University of Tasmania, TAS 7001 Australia | E-mail: **neil.holbrook@utas.edu.au**

Keywords Cyclone Genesis, Cyclone Tracks, Tropical Cyclones, Tropical Cyclone Landfall, North Indian Ocean

Abstract

Extensive damage and loss of life can be caused by tropical cyclones (TCs) that make landfall. Modelling of TC landfall probability is beneficial to insurance/re-insurance companies, decision makers, government policy and planning, and residents in coastal areas. In this study, we develop a climatological model of tropical cyclone genesis, tracks and landfall for North Indian Ocean (NIO) rim countries based on kernel density estimation, a generalised additive model (GAM) including an Euler integration step, and landfall detection using a country mask approach. Using a 35-year record (1979-2013) of tropical cyclone track observations from the Joint Typhoon Warning Centre (part of the International Best Track Archive Climate Stewardship Version 6), the GAM is fitted to the observed cyclone track velocities as a smooth function of location in each season. The distribution of cyclone genesis points is approximated by kernel density estimation. The model simulated TCs are randomly selected from the fitted kernel (TC genesis), and the cyclone paths (TC tracks), represented by the GAM together with the application of stochastic innovations at each step, are simulated to generate a suite of NIO rim landfall statistics. Three hindcast validation methods are applied to evaluate the integrity of the model. First, leave-one-out cross validation is applied whereby the country of landfall is determined by the majority vote (considering the location by only highest percentage of landfall) from the simulated tracks. Second, the probability distribution of simulated landfall is evaluated against the observed landfall. Third, the distances between the point of observed landfall and simulated landfall are compared and quantified. Overall, the model shows very good cross-validated hindcast skill of modelled landfalling cyclones against observations in each of the NIO tropical cyclone seasons and for most NIO rim countries, with only a relatively small difference in the percentage of predicted landfall locations compared with observations.

1 Introduction

Tropical cyclones (TCs) are considered to be the most devastating weather phenomena that affect North Indian Ocean (NIO) rim countries, producing major impacts over significantly large areas (Tyagi *et al.* 2010; Girishkumar and Ravichandran 2012; Nath *et al.* 2015). TCs have affected NIO rim communities since the earliest days of settlement (O'Hare 2001) and can have substantial impacts on the coastal countries of the Bay of Bengal and the Arabian Sea (Belanger *et al.* 2012).

The NIO is a breeding ground for tropical cyclones (Mohapatra *et al.* 2014; Shaji *et al.* 2014) but accounts for only 7% (Mohapatra *et al.* 2014; Sahoo and Bhaskaran 2016) of the world's tropical cyclones (about 5/year (Mohapatra *et al.* 2014)) – four in the Bay of Bengal (Alam *et al.* 2003; Vissa *et al.* 2013; Balaguru *et al.* 2014; Mohapatra *et al.* 2014; Rajasekhar *et al.* 2014) and one in the Arabian Sea (Rajeevan *et al.* 2013; Mohapatra *et al.* 2014; Rajasekhar *et al.* 2014) – but the number of deaths from TCs that make landfall in the region can be staggering (Webster 2008; Islam and Peterson 2009; Lin *et al.* 2009; McPhaden *et al.* 2009; Ng and Chan 2012; Pattanaik and Mohapatra 2016). Examples of the devastating effects of TCs in this region include the impacts of the Category-5 TC (*TC 02B*) that hit the Chittagong district of Bangladesh in 1991, and *TC Nargis* that hit Myanmar in 2008, with each resulting in around 140,000 lives lost and US$2.4 billion and $10 billion in damages respectively (Mydans and Cowell 2008; Alam and Collins 2010; Nath *et al.* 2015). Further, between 2007 and 2010, there were significant losses associated with at least one event in each year (Haggag and Badry 2012). In short, the human and financial costs annually due to TCs making landfall across NIO rim coastlines can be enormous.

In the present study, we develop a climatological TC model that takes account of the characteristics of past tropical cyclones and that can be used as a fundamental baseline for understanding the seasonality of TC genesis, tracks and landfall. Modelling of seasonal TC landfall probabilities has the potential to assist decision-makers, and residents in vulnerable coastal areas, to consider and plan. At the government planning and policy levels, seasonal modelling can be usefully adopted to inform and assist decision-making. Ultimately skilful prediction and careful assessment of the possible risk and extent of losses in areas affected by tropical cyclones can be beneficial to insurance companies (Rumpf *et al.* 2007).

Seasonal forecast modelling of tropical cyclone activity represents a major challenge for dynamical models (Camargo 2013; Shaevitz *et al.* 2014; Camp *et al.* 2015). Dynamical seasonal forecast model skill depends on the model used, the model resolution and the intrinsic predictability of the large-scale circulation regimes (Camargo *et al.* 2005; Bengtsson *et al.* 2007; Camargo and Barnston 2009). Camargo *et al.* (2007a) assume the poor performance of dynamical model (European Centre for Medium-range Weather Forecasts (ECMWF) and the UK Met Office predict tropical storm frequency based on dynamical models) to predict the tropical storm frequency due to model error and lack of predictability. Camp *et al.* (2015) describe the seasonal forecast skill of the UK Met Office Hadley Centre GloSea5 model, which is a high-resolution dynamical seasonal forecast system with an atmospheric horizontal grid of 0.83° longitude x 0.55° latitude (~53 km at 55°N) and 0.25° in the global ocean. Model skill of tropical storm predictions was evaluated across various basins for the period 1992 – 2013. While GloSea5 and ERA-Interim have been shown to be remarkably skilful in most basins across the globe, these model systems show no seasonal forecast skill over the NIO region (Camp *et al.* 2015) – a region notably characterised by a double-peak in tropical cyclone occurrences throughout the annual cycle (maxima during the pre-monsoon (April-May) and post-monsoon (October-November) periods). Yahyai (2014) describes the ability of the dynamical High Resolution Model (HRM) and Consortium for Small-scale Modelling (COSMO) models in the NIO to predict the probabilities of tropical cyclone landfall, but their performance was insufficient for predicting landfall points compared to those observed, due to limited spatial resolution.

In a separate study, Ray *et al.* (2012) used an artificial neural network system for the North Indian Ocean region to point out the prediction error between the landfall points of the simulated eastward tracks and the observed tracks. Zhao *et al.* (2009) explored global atmospheric dynamical models (with a horizontal grid scale of 50 km) to show that tropical cyclone activity (the frequency and interannual variability of tropical cyclones with intensities above a threshold of 33 m/s) are simulated quite realistically in the Atlantic and Northwest Pacific basin. However, the simulation for the NIO is not as close to the observations, with too many storms simulated in the Arabian Sea and too few in the Bay of Bengal. Knutson *et al.* (2014) concluded that while reasonable results have been found for the North Atlantic and Northwest Pacific basins, a substantially larger intensity

680 bias was found for simulations in the NIO region using the Geophysical Fluid Dynamics
681 Laboratory (GFDL) hurricane model (with a horizontal grid scale of 9 km) in a seasonal
682 forecast mode.

683 Interestingly, statistical models have shown some promise for TC count prediction in the
684 NIO region (Nath *et al.* 2015). Skilful TC track studies have been previously also
685 demonstrated using statistical forecast models in western North Pacific (Rumpf *et al.*
686 2010), North Atlantic (Emanuel *et al.* 2006) and South Pacific (James and Mason 2005)
687 regions. There is no guarantee that statistical TC models, developed for the Atlantic and
688 Pacific, will be similarly beneficial in the NIO in a seasonal context, since the seasonal
689 cycle is characterised by the double peak that exists in the pre-monsoon and post-
690 monsoon periods. Compared to other ocean basins across the globe, the Indian Ocean has
691 also received much less attention for statistical seasonal prediction of cyclones (Nath *et*
692 *al.* 2015). Therefore, in the first instance, an attempt has been made here to develop a
693 climatological model of the four TC seasons in the NIO region, i.e. that best characterises
694 the winter (December-February), pre-monsoon (March-May), monsoon (June-September)
695 and post-monsoon (October-November) seasons.

696 This paper discusses the development of a statistical seasonal model of tropical cyclone
697 genesis, tracks and landfall for the North Indian Ocean – that represents a climatological
698 model of tropical cyclones for the region. The genesis model is based on kernel density
699 estimation, and the tracks are estimated using a generalised additive model. Three
700 hindcast methods are used to cross-validate the model. The structure of the paper is as
701 follows: The data on which the model is based and how the model works are described in
702 section 2. The kernel density estimation for tropical cyclone genesis distribution, the
703 generalised additive model used for cyclone tracks, and country and state-based hazard
704 zone mapping for landfall probabilities, are also described in Section 2. Section 3 presents
705 the simulation and cross-validation results from the model, and evaluates these against
706 observed data. Results are discussed in Section 4, and some concluding remarks are
707 provided in Section 5.

708 **2 Data and Methods**

709 2.1 Data from IBTrACS

710 Tropical cyclone track data for the North Indian Ocean region (Fig.1) were obtained from
711 the International Best Track Archive for Climate Stewardship (IBTrACS), National
712 Climatic Data Center (www.ncdc.noaa.gov/oa/ibtracs/).

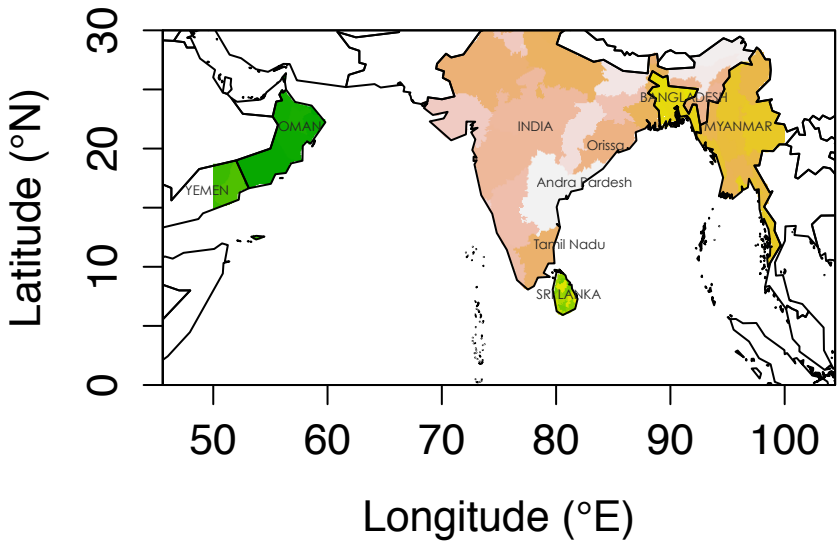

713

714 Fig.1 Geographic map showing the countries (and states) along the North Indian Ocean rim
715 relevant to this study. The six countries affected by tropical cyclone landfall include India,
716 Bangladesh, Myanmar, Sri Lanka, Oman and Yemen.

717 IBTrACS provides global tropical cyclone best track data, in a centralised location, to aid
718 understanding of the distribution, frequency, and intensity of TCs worldwide. In
719 combining track and intensity estimates from many sources, this consolidated collection
720 of TC data provides an extensive global climatology and insight into data uncertainty,
721 which is a critical consideration for climate trending (Knapp *et al.* 2010; Kossin *et al.*
722 2013). Specifically, we have used data from the Joint Typhoon Warning Centre (JTWC)
723 for the 35-year period from 1979-2013. The JTWC data are a contributed subset within
724 IBTrACS version 6, which are the data most commonly used by researchers worldwide
725 (Knapp *et al.* 2010). The parameters used in our analysis of 'storms' include date,
726 position (degrees of latitude and longitude) and wind speed. Note that we also take
727 account of tropical depressions that have not reached tropical cyclone intensity, as well as
728 tropical cyclone intensity storms (i.e. those storms that occurred where wind speeds have
729 reached at least 34 knots, or 17.5 m s^{-1}).

730

For the genesis model, we determined the time and position along each track that the tropical storm winds first exceeded the critical speed of 34 kt to determine that the storm had reached tropical cyclone intensity. For tropical cyclone pathways in the North Indian Ocean (NIO) region, we note that both tropical depressions and tropical cyclones follow tracks that are not really any different (Warrick *et al.* 2000; Mohapatra *et al.* 2012; Brian 2015). By including the tracks from both tropical cyclones and storms, we increase the overall sample size (since the historical database of tropical cyclones for the NIO region is not large (Paliwal *et al.* 2011)), and hence improve the overall statistical representation, based on this assumption that the tracks are not significantly different between tropical storms or tropical cyclones. Notably, we have ignored TCs prior to 1979 to improve reliability of the observational database (Evan and Camargo 2010; Weinkle *et al.* 2012).

2.2 Methods

Skilful basin-wide statistical models have been developed by several researchers (Gray 1984; Nicholls 1985; Wilks 1995; Nicholls *et al.* 1998; Elsner and Jagger 2004; Camargo *et al.* 2005; James and Mason 2005; Saunders and Lea 2005; Elsner and Jagger 2006; Emanuel *et al.* 2006; Hall and Jewson 2007; Holland and Webster 2007; Landsea 2007; Rumpf *et al.* 2007; Leroy and Wheeler 2008; Elsner and Jagger 2010; Jagger and Elsner 2010; Elsner and Jagger 2013; Hall and Yonekura 2013; Kang *et al.* 2016). A crucial component of basin-wide TC modelling is the TC track – i.e. the trajectory from genesis (Hall and Jewson 2007). First, TC genesis modelling can be performed in several ways, including sampling from historical genesis sites (Vickery *et al.* 2000), interpolating historical genesis locations (James and Mason 2005), binning historical genesis events through a probability density function (PDF) (Emanuel *et al.* 2006), or the application of a near-neighbour approach to develop and sample a genesis kernel PDF (Rumpf *et al.* 2007). Second, TC track modelling can also be approached in different ways. For example, Vickery *et al.* (2000) and James and Mason (2005) used autoregressive models to increment TC track direction. Casson and Coles (2000) draw from the historical tracks, translating TC tracks through small random displacements. Emanuel *et al.* (2006) propagate tracks by sampling a transition matrix for TC track direction, and Rumpf *et al.* (2007) described a stochastic model for the separation of tropical cyclone tracks based on the geographic characteristics and applied kernel probability density function and direction increment to simulate the tracks.

Our approach has been to develop a statistical climatological model of TC genesis, tracks and landfall for the NIO, and based on some similar methods employed by Hall and Jewson (2007) for the North Atlantic Ocean and Yonekura and Hall (2011) for the Western North Pacific region. The basic modelling approach comprises of kernel density estimation for TC genesis, application of a generalised additive model for the TC tracks (fitting and baseline for simulation) and Euler integration, and takes account of a country mask for determining points of landfall.

The genesis model developed here closely follows the previous work of Hall and Jewson (2007) for the North Atlantic and Yonekura and Hall (2011) for the Western North Pacific. In their research, genesis is sampled from a Poisson distribution and an empirical kernel-density function and genesis has no climate state sensitivity. Our approach fits and utilises a kernel density function for random sampling (using a standard plug in estimator), with the kernel density estimates masked over shallow water and land for the genesis distribution.

TC tracks are modelled as successive 4-step (i.e. 6-hr) track displacements each day. The choice of a 6-hr increment is consistent with that applied by Hall and Jewson (2007) and Yonekura and Hall (2011). However, in those previous studies, auto regression was applied for the tracks. In a separate study, Mestre and Hallegatte (2009) used a GAM approach to predict the number and intensity of TCs in the North Atlantic. Here, we used a GAM approach instead to model the storm track velocity field in the NIO.

The landfall detection closely follows the work of Weinkle *et al.* (2012) for the North Atlantic, Eastern and Western Pacific, North Indian Ocean, and the Southern Hemisphere. They used an operational sea surface temperature product as a land mask with $1/20^0$ global grid spacing to detect the first landfall. In the present study, we used a $1/12^0$ mask approach with Euler integration to detect landfall across country and state boundaries.

In the following subsections, we present the approaches that we have applied to model tropical cyclone genesis, tracks and landfall, and also to cross-validate the models.

2.2.1 Tropical cyclone genesis: Kernel density estimation

In the present study, we have applied a Kernel density approach to model the spatial distribution of observed tropical cyclone genesis locations. This approach has been

794 previously used successfully by, for example, Vickery *et al.* (2000); James and Mason
795 (2005); Emanuel *et al.* (2006) and Rumpf *et al.* (2007). Kernel density estimation is a
796 method to estimate the probability density function (PDF) of a random variable in a non-
797 parametric way. This distribution is defined by a smoothing function and a bandwidth
798 value (length scale) that controls the smoothness of the resulting density curve.
799 Bandwidth selection can be undertaken in various ways, including by "rule of thumb", by
800 cross-validation, by "plug-in" methods, or by other means (Turlach 1993; Bashtannyk and
801 Hyndman 2001).

802 More formally, Kernel estimators smooth out the contribution of each observed data point
803 over the local neighbourhood of that data point, with the neighbourhood defined by the
804 bandwidth. The contribution of data point $x(i)$ to the estimate at some point x depends on
805 how far apart $x(i)$ and x are situated. If we denote the kernel function as K and its
806 bandwidth by h, the estimated density at any point x is

807 $$\hat{f}(x) = \frac{1}{n}\sum_{i=1}^{n} K\left(\frac{x - x(i)}{h}\right)$$

808 In essence, the convolution smooth out the contribution of each observed data point over
809 a local neighbourhood of that data point. The extent of this contribution is dependent
810 upon the shape of the kernel function, K, and the chosen bandwidth, h. A larger
811 bandwidth increases the region influenced by each x_i, resulting in a smoother estimate.

812 The kernel K must satisfy the constraint $\int K(x)dx = 1$, but is otherwise arbitrary. The
813 Gaussian kernel,

814 $$K(x) = (2\,\pi)^{-1} \exp\left(-\frac{x^2}{2}\right)$$

815 is a common choice and the one we use here.

816 In our analysis, we calculate the kernel bandwidth for the kernel density function using a
817 standard plug in estimator. This approach has been shown to be a simple but effective
818 method for estimating relevant bandwidths (Rigollet and Vert 2009) and makes for
819 pragmatic calculations. Hence, kernel density estimation is also used in the present study
820 to model and quantify the probability distribution (function) of observed tropical cyclone

821 genesis locations and occurrences from which we can randomly sample.

822 The choice of bandwidth is a crucial issue in kernel density estimation. The plug in
823 method is based on a simple idea that gives an estimate ($\hat{f}$) of the bias of the unknown
824 function *f*. A pilot estimate of *f* is then "plugged in" to derive an estimate of the bias and
825 hence an estimate of the mean integrated squared error. The optimal bandwidth (*h*)
826 minimises the error/estimated measure of fit (Loader 1999). Essentially, the kernel
827 density estimator places a Gaussian kernel of specified bandwidth over each observation
828 and sums. Samples are drawn from the estimated density by treating the estimate as a
829 Gaussian mixture - first a component of the mixture is chosen and then a sample deviate
830 is drawn from that component of the mixture.

831 In the absence of any modification, simple application of the kernel estimator enables TC
832 genesis over land, which is most apparent for longer smoothing (bandwidth) scales.
833 While there are a few isolated cases when TCs have been observed to form over land,
834 such occurrences are largely atypical. To address this issue, we restrict genesis to ocean
835 regions by masking the kernel density function over land areas and also choose to reject
836 genesis in regions where water depths are shallower than some critical depth – we assume
837 this to be for water depths <200m, i.e. typically across the continental shelf. This process
838 is iterated to generate a sample of the correct size.

839 For genesis, we determined the time and position along each track that the tropical storm
840 winds exceeded the critical speed of 34 knots, defined as becoming tropical cyclone
841 strength (WMO 1997). It was found that <10% (9.4%) of the estimated genesis locations
842 were either very close to the coast or over land, which were removed by our mask. As a
843 simulation set, we extracted 50 genesis points from the kernel to set up the climatology.

844 2.2.2 Tropical cyclone tracks: Generalised Additive Model

845 Cyclone trajectories were modelled by fitting a generalised additive model (GAM) to the
846 incremental track velocities. The GAM is an extension of the generalised linear model
847 (GLM), which in turn is an extension of the standard linear model (LM) (Guisan *et al.*
848 2002). GAMs are a generalisation of linear regression in which the linear terms are
849 replaced by smooth transformations of the predictors.

One of the most popular and useful tools in data analysis is the linear regression model or simply the "linear model". Standard regression models assume the response, y, is normally distributed about its mean, μ, with variance σ^2

$$y \sim N(\mu, \sigma^2).$$

In the regression case, the mean, μ, can be modelled as a linear combination of predictor variables, $X_1, X_2, \ldots, X_m$

$$\mu = \beta_0 + \beta_1 X_1 + \beta_2 X_2 + \cdots + \beta_m X_m$$

where β_0 ,β_m are the regression coefficients to be estimated.

The generalised linear model extends the linear model in two key ways. First, the generalised linear model assumes the response may be distributed about its expected value according to any distribution F from any exponential family of distributions (including the Poisson, Binomial and Normal families)

$$y \sim F(\mu)$$

And secondly, that the predictors enter the model through the linear predictor η which is related to the expected response μ by a monotonic function ℓ, called the link function

$$\ell(\mu) = \eta = \beta_0 + \beta_1 x_1 + \beta_2 x_2 + \cdots + \beta_p x_p$$

These extensions relax the restrictions imposed by the linear model on both the distribution of the data and the functional relation between the response and predictors. Note that if F is the Normal family of distributions and the link function ℓ is the identity, then the generalised linear model reduces to the linear model.

The generalised additive model further relaxes the functional relation between the response and the predictors by assuming the linear predictor is related to the predictors through a number of smooth transformations $f_1, f_2, \ldots, f_p$

$$\ell(\mu) = \eta = \beta_0 + f_1(x_1) + f_2(x_2) + \cdots + f_p(x_p)$$

Where a LM or GLM seek to estimate the regression coefficients $\beta_0, \beta_1, \ldots, \beta_p$, a GAM seeks to estimate the smooth functions $f_1, f_2, \ldots, f_p$ of the predictors.

The advantage of the generalised additive model scheme is that it is a data driven approach and can automatically discover relationships in the data. The smooth functions $f_1, f_2, \ldots, f_p$ are not prescribed by any rigid parametric representation, but instead are typically estimated by smoothing.

The disadvantage of the generalised additive model is that it cannot easily represent interactions amongst terms. Rather, it assumes each term contributes additively. To a limited degree, interactions can be modelled by including multivariate smooth terms, that is terms of the form $f_{ij}(x_i, x_j)$. However, multivariate smooth terms require much greater volume of data to be reliably estimated (Hastie *et al.* 2009).

In this paper, generalised additive models are used to model the two components of the velocity field that define the trajectory of the cyclones. First, track velocities are generated by calculating the increment in identifiable tropical storm positions at each time step to estimate the storm track velocities along their tracks. Then, the GAM is fitted to these storm track velocities. A separate GAM is fitted to each velocity component in the x (east) and y (north) directions, to allow the vector velocity field to be predicted. In this simple model we fit each velocity as a smooth function of location in each season.

Cyclone trajectories are simulated using the fitted GAM to predict mean increment velocities at each step along the simulated track, together with random (stochastic) innovations also at each step – starting from randomly selected genesis locations drawn from the kernel for each NIO region TC season. Based on the mean vector field estimated by the GAM fit, an Euler step is used to project trajectories forward in time from this genesis point. A stochastic innovation is added at each time step to account for the variable nature of the vector field that is not captured by the GAM, with a variance determined by the residual error of the GAM fit. For each simulated genesis point, 50 trajectories (and each trajectory has an independent set of innovations applied) were simulated 7 days forward in time with a 6 hourly time step.

We have endeavoured to be both pragmatic with our lifetime choice and consistent with typical TC lifetime scales for the region in our modelling. This choice of a 7-day lifetime for TCs in the model is based both reported research and our own analysis of historical NIO region TC observations from genesis to landfall. Cyclone lifetimes over the NIO range from 1-12 days (1-9 days has been reported by Evan and Camargo (2010) for the

907 Arabian Sea in the period 1979-2008), with an average TC lifetime of 4.8 days, with most
908 TCs making landfall by the 7th day. Almost 80% (79.3%) of NIO region TC lifetimes are
909 within 7 days of genesis, and we therefore consider this to be a reasonable and
910 appropriate choice for our climatological model. Our analysis shows that the model-
911 simulated landfall is 80% for a choice of 7-day for the cyclone lifetime, which is
912 consistent with observations (75%). If we run the model with a lifetime of 12 days the
913 simulated landfall becomes too large (94%) and if we run the model with a lifetime of 2
914 days then the simulated landfall becomes too small (23%). Overall, by considering the
915 maximum TC lifetime over the NIO and our sensitivity analysis the 7-day choice of
916 lifetime is the most representative.

917 2.2.3 Landfall locations

918 To determine the points of landfall, each trajectory is interpolated in time to finer
919 increments, with successive points along the trajectory compared to the land mask and the
920 first land mask crossing is taken to be the point of landfall. The estimated precise point of
921 landfall accuracy depends on the resolution to which the trajectory is interpolated. One
922 limitation of this approach is that only the first point of landfall is identified. For a
923 cyclone that passes over the Andaman or Nicobar islands, this will be the recorded point
924 of landfall, even if the cyclone carries on to possibly strike elsewhere. To functionally
925 solve this problem, we removed the islands from the mask in our analysis (although they
926 appear on the geographical map), so the model simply allows the cyclone track to
927 continue.

928 From the literature and our own analysis, we note that multiple landfalls are rare in the
929 NIO region; it is almost never seen that a cyclone strikes a country in the NIO rim and
930 then comes back again to strike land a second time (Evan and Camargo 2010; Weinkle *et*
931 *al.* 2012; Alam and Dominey-Howes 2015). In the study period, 95.2% of NIO region
932 TCs made landfall (95.7% is reported by Alam and Dominey-Howes (2015) based on
933 their long-term catalogue (from 1000AD to 2009) of landfall occurrences in surrounding
934 countries of the Bay of Bengal) and none make secondary landfalls. Based on this
935 observation, we have only considered the first point of landfall for this region, while
936 being consistent with other previous research across other basins by Weinkle *et al.* (2012)
937 where they assume that even in TC multiple landfall cases, only the first point of landfall
938 is counted.

939 2.2.4 Model validation

940 To assess the integrity and potential utility of the model, we have applied three separate
941 model validation methods. These are introduced as follows.

942 2.2.4.1 Cross-validation

943 Cross-validation is a resampling procedure where the available data are repeatedly
944 divided into development and verification (prediction) subsets (Wilks 1995). It tries to
945 simulate actual forecasts and provide an accurate estimate of the predictive skill of the
946 model or algorithms (Hess and Elsner 1994; McDonnell and Holbrook 2004a). Cross
947 validation endeavours to assess how well the developed model will perform in forecasting
948 the unknown future (Elsner and Schmertmann 1993).

949 We develop instead a climatological model of tropical cyclones, where the model
950 represents our best fit to the observed seasonal cycle. The model is developed through
951 standard cross-validation procedures, whereby we leave out individual tracks and fit on
952 the remaining data, which is in itself a test of model capability against data not included
953 in the fit. Given that our climatological represents our best estimate of the seasonal cycle,
954 holding out the last 10 years of observations would not be particularly instructive since it
955 would compare climatological seasonal forecasts against interannually changing
956 conditions. We point out though that in ongoing separate work, we build forecast model
957 versions using indices of El Niño – Southern Oscillation and the stratospheric Quasi-
958 Biennial Oscillation as predictor variables for forecasting. In those model cases, we
959 indeed do assess forecast skill against independent data and our climatological model
960 forecasts.

961 Here, we apply leave-one-out cross-validation where we:

962 1. Remove each storm track in turn, and fit the model to the remaining data;
963 2. Simulate each of the removed storm trajectories based on the model fit to the
964 reduced data set; and
965 3. For each simulated track determine the country of landfall, and from all landfalls
966 determine the most likely country of landfall by majority vote (we only identified
967 one state/country where most of the tracks make landfall).
968

969 2.2.4.2 Probability distribution

970 Because India has the longest coastal boundary of any country along the NIO rim, India is
971 exposed to higher rates of landfall than other neighbouring countries, such as Bangladesh.
972 As such, a 'majority vote' approach means that India results in greater occurrences of
973 landfall. To address this, we considered an alternative approach whereby we examined
974 the probability distribution of simulated landfall with relation to the observed landfall.
975 Here, we ran the GAM simulation 40 times and averaged the results in turn for each TC
976 season. From the results, we also calculated the standard deviation and compared the
977 simulation with the observed data.

978 2.2.4.3 Distance between simulated and observed landfall

979 Finally, we evaluated the model by calculating the distance between the observed and
980 simulated landfall points, for tracks that correspondingly originate from the same
981 observed genesis points. Each landfall location, from a simulated track, was measured
982 against the corresponding observed landfall location, and a probability distribution was
983 developed based on the differences.

984 **3 Results**

985 3.1 Model fits of TC genesis and tracks

986 Fig. 2 shows the observed genesis locations (panel a) and tracks (panel b) for the 35-year
987 record of storms contained in the JTWC database for the period of 1979-2013. During this
988 period, a total of 105 storms reached tropical cyclone strength. Most of the TCs in the
989 NIO region originate between 5° N and 15° N and east of 85° E. A greater proportion of
990 TCs formed in the Bay of Bengal (72.4%) compared to the Arabian Sea (27.6%). In the
991 Bay of Bengal, most TCs initially move towards the northwest or north; later on in their
992 lifetime a few have been seen to recurve towards the northeast. In the Arabian Sea, these
993 storms generally move westward. Not all TCs made landfall: 25% decayed to below TC
994 strength while still located over the ocean. In the Bay of Bengal, cyclones typically made
995 landfall along the southeast coast of India, Bangladesh and Myanmar. For the Arabian
996 Sea, TC landfall mainly occurred along the Oman and Yemen coasts, and very few
997 crossed the western coast of India – with most cyclones dying out in the Arabian Sea.

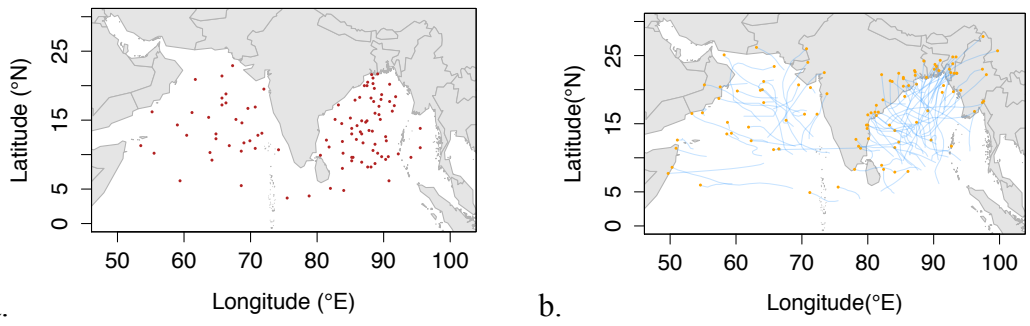

Fig. 2 Observed (a) tropical cyclone genesis locations, and (b) tracks of the corresponding storms that reach tropical cyclone intensity at the genesis points. Red dots in (a) identify the tropical cyclone genesis points in the North Indian Ocean region (0^0 to 30^0 N and 50^0 to 100^0E) for the JTWC storm record in the 35-year period from 1979-2013. The blue lines indicate the tropical cyclone tracks with the last recorded location of the tropical storm intensity tracks indicated as a yellow dot.

Annually, tropical cyclones form most frequently (44% of annual totals) during the post-monsoon (October-November) season (Fig. 3), whereas winter (December-February) represents the quietest season (15% of annual totals) for tropical cyclones, with only about one third of the post-monsoon season occurrences. The monsoon (June-September) season (18% of annual totals) displays similar numbers to winter while the pre-monsoon season (March-May) contributes slightly more than half of the total number of TCs formed during the post-monsoon season (23% of annual totals). There is a clear latitudinal shift of genesis locations with season. In winter, genesis tends to occur south of 10^0 N, but occurs north of 10^0 N in the other seasons. In winter and during the monsoon season, cyclones move in a westward or north-westward direction. In the Bay of Bengal, these storms tend to track westwards and north-westwards into the east coast of India during the post-monsoon season, and north-eastwards into Bangladesh and Myanmar during the pre-monsoon. The distribution of observed storm tracks corresponding to each TC season (Fig. 3) illustrates that most TCs during the post-monsoon season make landfall along the western and north-western coastal fringe of the Bay of Bengal – in particular, the Indian state of Andra Pradesh (see Fig.1) and the southwest Bangladesh state of Khulna. During the pre-monsoon season, TCs tend to make landfall in the north-eastern part of the Bay of Bengal, including the south-eastern part of Bangladesh and Myanmar. In winter, TCs tend to track towards the Tamil Nadu coast of India (i.e., the south-western fringe of the Bay of Bengal). During the monsoon season, storms tend to track towards the Orissa coast of India (i.e., north-western fringe of the Bay of Bengal).

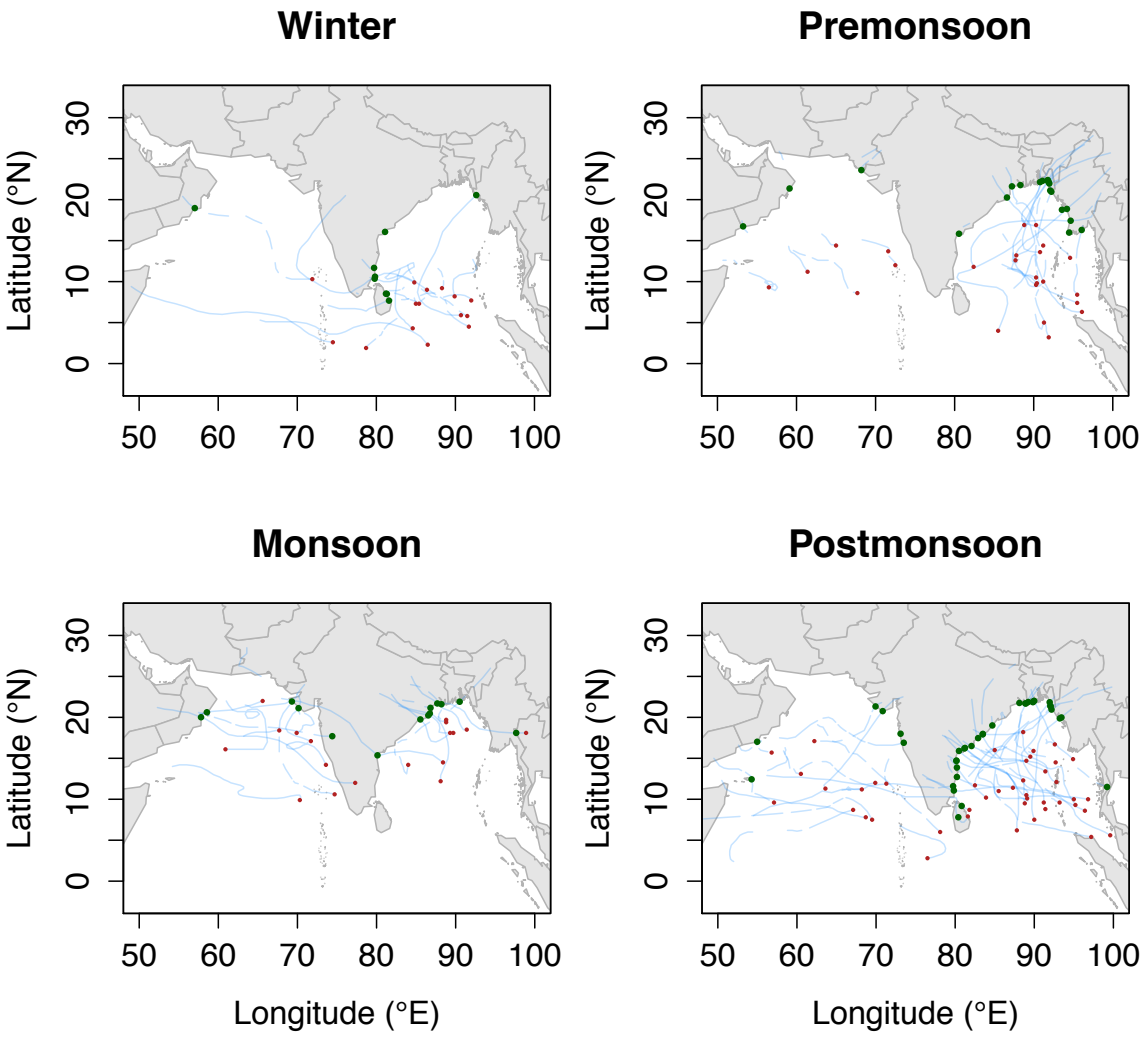

Fig.3 Seasonal distribution of North Indian Ocean region (0^0 to 30^0 N and 50^0 to 100^0E) observed tropical cyclone genesis locations (identified by red dots), tracks (identified by blue lines) and landfall locations (identified by green dots) over the 35-year period of 1979-2013.

The modelled distribution of genesis points, approximated by the kernel density estimation, is shown in Fig. 4. Highest density estimates are found in the Bay of Bengal (consistent with the observed genesis locations seen in Fig. 2). By season, highest densities are found in the post-monsoon season followed by the pre-monsoon. In the post-monsoon season the highest density is nearest to the Indian state of Andra Pradesh, while in the monsoon and winter seasons the highest genesis densities are closer to the Bangladesh and Sri Lanka coasts, respectively.

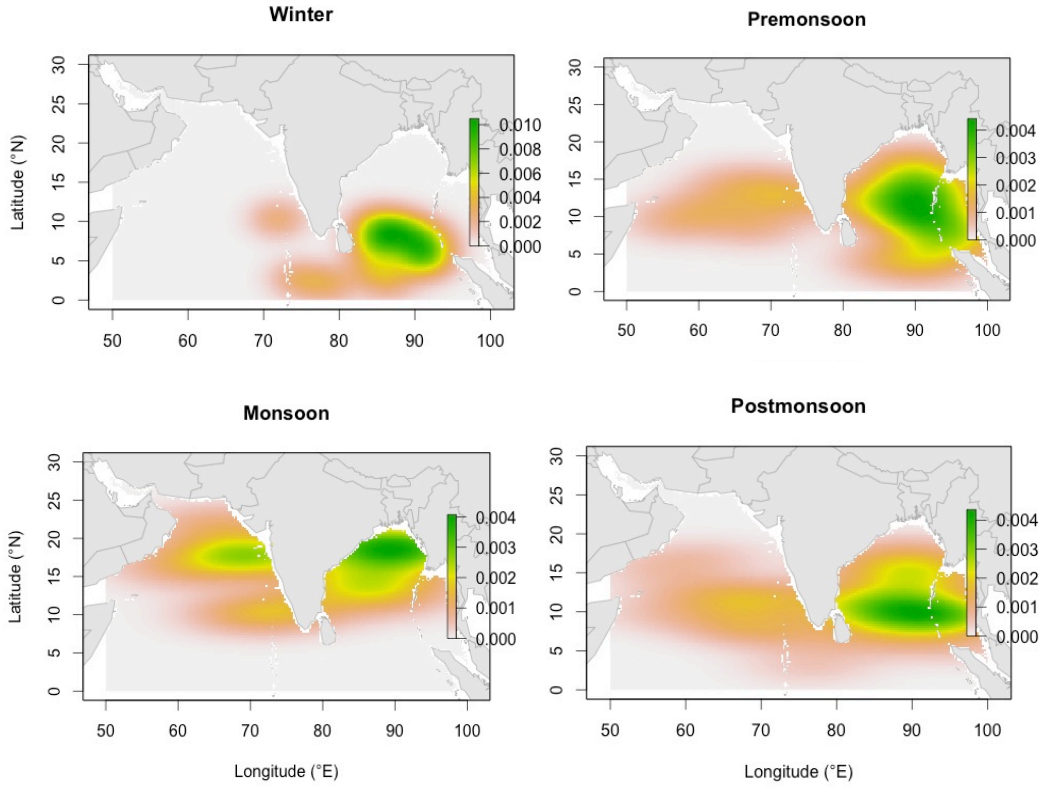

Fig.4 Modelled seasonal distributions of tropical cyclone genesis based on kernel density estimates across the observations in the North Indian Ocean region (0^0 to 30^0 N and 50^0 to 100^0E) based on the 35-year JTWC data record from 1979-2013. Green colour shows the highest density (concentration of TC numbers/km^2) area of genesis.

For each country around the NIO rim, the total numbers (and percentage within season) of TCs that make landfall as a function of season are provided in Table 1. Looking along rows (and thus across columns) we can see how landfall rates vary by season for each country (%*). Alternatively, looking down columns (and thus across rows) we can see how landfall rates vary by country within each season (%$^\#$). We see that 71% of NIO region TCs make landfall in two of the four TC seasons, annually – these are the post-monsoon (44% of the time) and pre-monsoon (23% of the time) seasons. Further, the pre-monsoon period represents the season with the highest annual number of TC landfall occurrences in Myanmar (50%) and Bangladesh (47%). The most landfall occurrences for India have been observed during the post-monsoon season, with 52% of India's annual tropical cyclone landfalls. For Yemen, there was only one recorded landfall during the entire record, and this occurred during the post-monsoon. For Oman, the seasons with the most landfalls were the monsoon and pre-monsoon seasons (each with 33%). For Sri

Lanka, the most landfall occurrences (60%) have been in winter (a total number of 15 (14% of annual total) TCs make landfall).

Among the NIO rim countries, the total numbers, and percentage, of observed tropical cyclones that make landfall as a function of season are also provided in Table 1. Among the 6 countries, the highest percentage of landfall occurrences are in the pre-monsoon season (20 out of 24 TCs, ~83%), followed by the post-monsoon season (36 out of 47 TCs, ~76%); whereas 60% (9 TCs make landfall out of 15) of cyclones make landfall in winter and ~74% (14 TCs make landfall out of total 19) make landfall in the monsoon season. Among the 6 NIO countries, almost 45% of cyclone landfalls occur in India during the post-monsoon season whereas Bangladesh (34%) is the favourable zone for TC landfalls in the pre-monsoon season.

Table 1. For each country around the NIO rim, we show here the observed total numbers (and percentage) of tropical cyclones that make landfall as a function of season. For each country, the season with highest landfalls in that country is indicated by bold percentages. For each season, the country with highest landfalls in that season is indicated by bold with underlined percentages.

	Winter			Premonsoon			Monsoon			Postmonsoon			Total	
Country ~	No	% *	%#	No	% *	%#	No	% *	%#	No	% *	%#	No	% *
IND	4	10	**<u>26.6</u>**	5	12.5	20.8	10	25	**<u>52.6</u>**	21	**52.5**	**<u>44.7</u>**	**40**	100
MYN	1	10	6.7	5	**50**	20.8	1	10	5.3	3	30	6.4	10	100
BAN	0	0	0	8	**47.1**	**<u>33.4</u>**	1	5.8	5.3	8	**47.1**	17	17	100
SLN	3	**60**	20	0	0	0	0	0	0	2	40	4.3	5	100
YEM	0	0	0	0	0	0	0	0	0	1	**100**	2.1	1	100
OMAN	1	16.7	6.7	2	**33.3**	8.3	2	**33.3**	10.5	1	16.7	2.1	6	100
Landfall	9		60	20		83.3	14		73.7	36		76.6	79	
NON	6	---	40	4	---	16.7	5	---	26.3	11	---	23.4	26	--
TOTAL	15	---	100	24	---	100	19	---	100	**<u>47</u>**	--	100	**<u>105</u>**	--

~ (IND=India; MYN=Myanmar, BAN=Bangladesh, SLN= Sri Lanka, YEM= Yemen, OMN=OMAN, NON=No landfall recorded

*(across season) and #(across countries)

We next look at how landfall is distributed with time since genesis, for each TC season (Fig. 5). Landfall tends to occur with greatest likelihood around 1-4 days after genesis in winter (100% of the time) and 2-4 days after genesis during the pre-monsoon (47%). During the monsoon, it tends to occur 0-1 day after genesis (70%) and during the post-monsoon 0-2 days after genesis (68%).

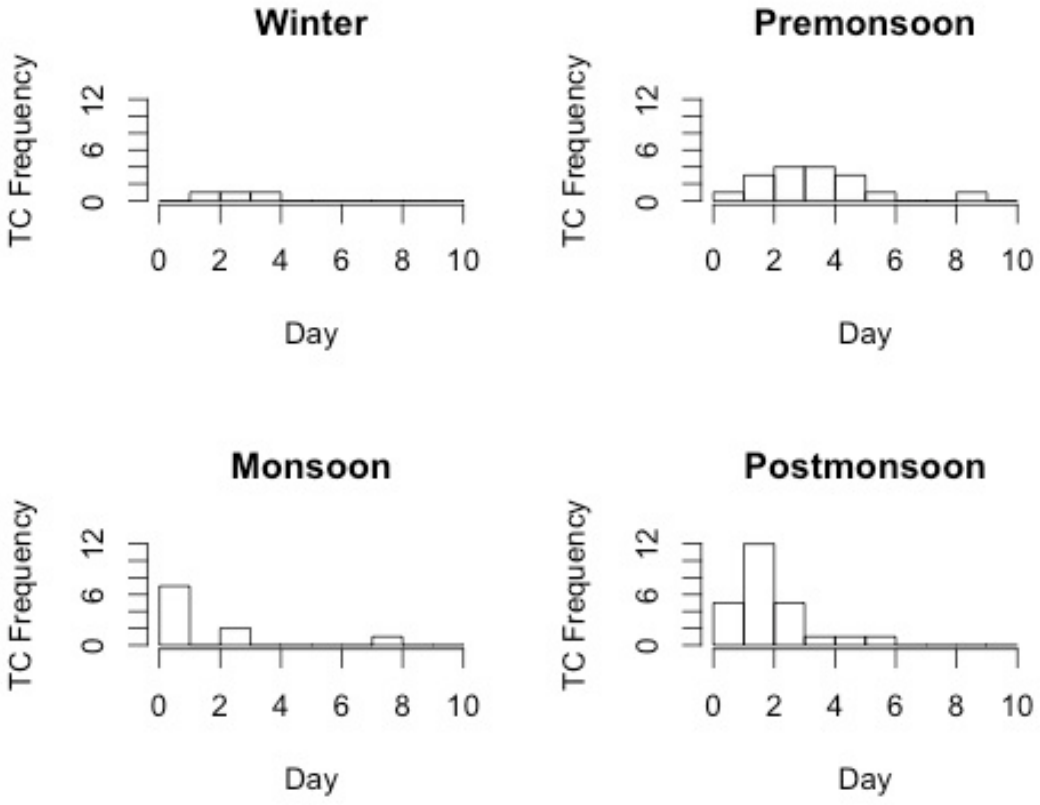

Fig.5 Observed TC landfall frequency for each season, measured as a function of the number of days from genesis to landfall, within the North Indian Ocean region (0^0 to 30^0 N and 50^0 to 100^0E) over the 35-year record (1979-2013).

The GAM fit to the observed TC tracks acts to smooth estimates of the TC velocities as a function of space, independently for each season (Fig. 6). In winter, the GAM velocity field indicates a westward or north-westward movement (10-20^0 N) of the fitted TC tracks. In the pre-monsoon season, the GAM fit shows a tendency for TCs to move towards the northwest or north (10-20^0 N), and then recurve towards the northeast (20^0 N above) in the Bay of Bengal or northwest/north (15-20^0 N) in the Arabian Sea. During the monsoon season, movement is towards the northwest (8-22^0 N) in the Bay of Bengal and west and north-westward (12-22^0 N) over the Arabian Sea. In the post-monsoon season,

the initial movement of storms is north-westward (10-18^0 N) followed by north-eastward curvature (18^0 N above).

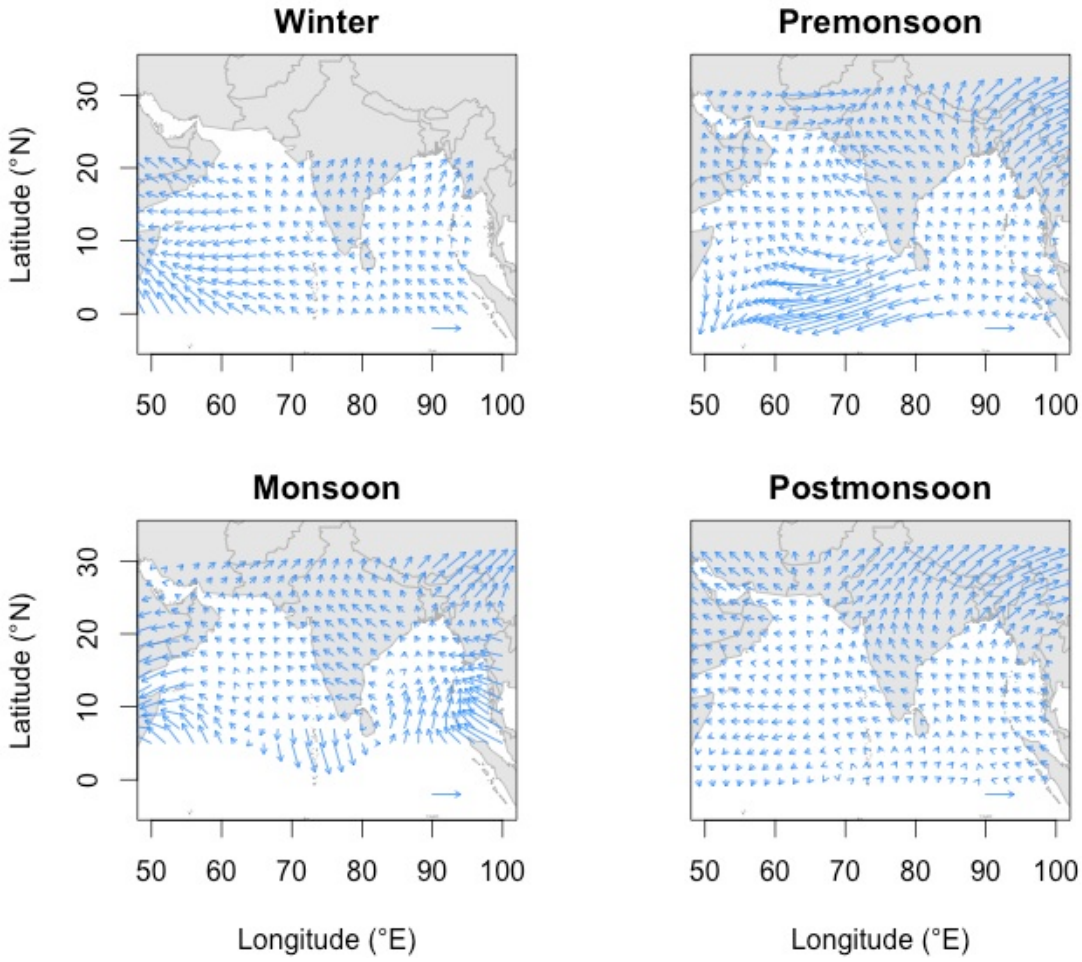

Fig.6 Seasonal distribution of fitted tropical cyclone track velocities (data from 1979-2013) across the North Indian Ocean estimated using a generalised additive model approach. The length of the reference arrow corresponds to velocity magnitudes of 10m/s.

3.2 Simulated cyclone tracks and landfall locations

Simulations of TC tracks (Fig. 7) indicate how the modelled storms tend to track and where they tend to make landfall. In winter, the modelled TCs tend to track in a westward or north-westward direction over the Bay of Bengal and most of them make landfall along the northern Tamil Nadu coast or the eastern coast of Sri Lanka. Over the Arabian Sea, the storms tend to move towards the west, although some of them move towards the north and northeast. This is generally consistent with observations. During the pre-monsoon season, storms initially move northwest or north over the Bay of Bengal and later recurve towards the northeast and make landfall along the Arakan coast of Myanmar. Over the

Arabian Sea, the simulated storms move initially towards the northwest or north, and then after recurving they move towards the Gujrat-Sind Mekran coast of India (consistent with observations). A greater propensity of storms is seen in the Arabian Sea during the monsoon where a majority of the simulated storms move towards the northwest (consistent with observations) and then recurve towards the north or north-northeast, resulting in increased landfall occurrences in the Middle East, which is also evident to a lesser degree in the post-monsoon season. Finally during the post-monsoon season, simulated storms move in a north-westward direction and then recurve towards the northeast (in contrast to the observations in which cyclones move both in north-westward and eastward directions).

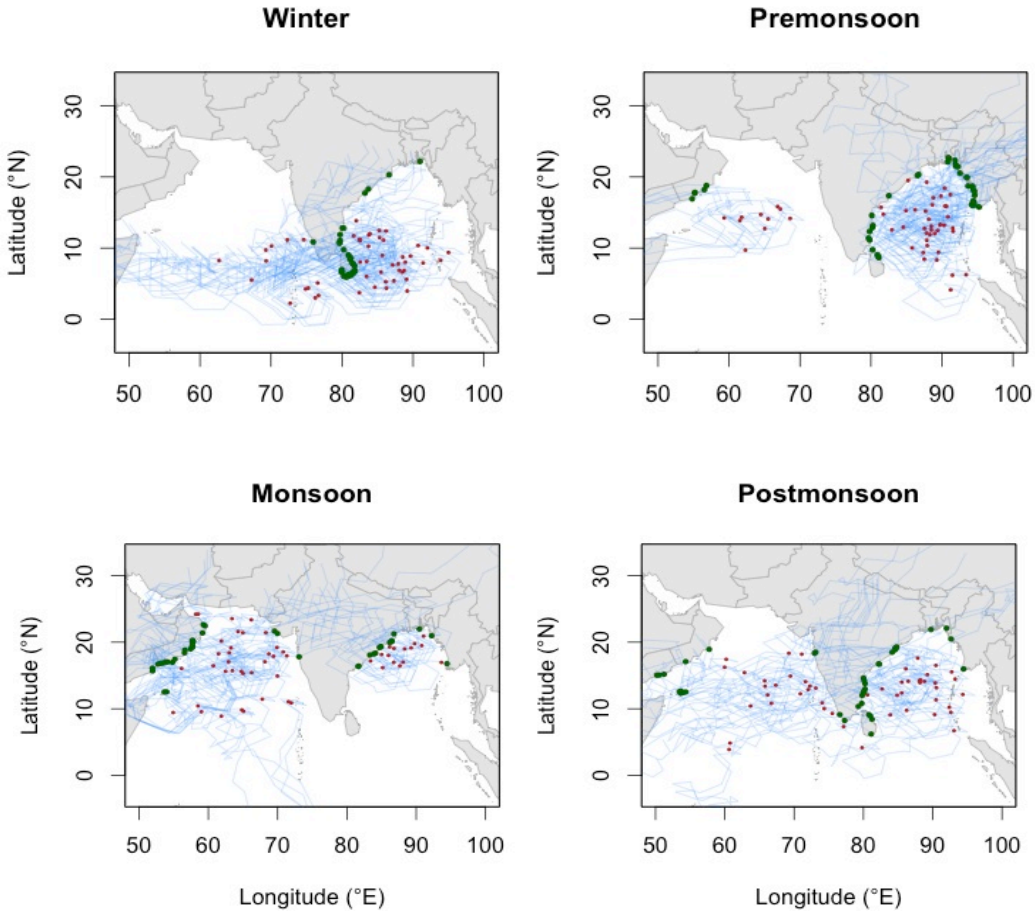

Fig.7 Simulation of tropical cyclones across the North Indian Ocean region as a function of season. A total of 50 tropical cyclone genesis points were randomly selected from the modelled kernel density and the tropical cyclone tracks were simulated using the fitted generalised additive model combined with the random innovations. Red dots show the TC genesis points, blue lines indicate the tropical cyclone tracks, and green dots indicate landfall locations.

The simulated total number (and percentage) of TCs that make landfall as a function of season are provided in Table 2 for each country around the NIO rim. Looking along rows (and thus across columns) we can see how the landfall rates vary by season for a single country (%*). It is seen that 80% of the simulated TCs make landfall across the NIO rim, similar to the observed value of 75%. Myanmar (56.5%) and Bangladesh (50%) were predicted to have the largest number of tropical cyclone landfalls during the pre-monsoon season, consistent with observations. The most active period for India is apparent during the post-monsoon season when 29.9% of the country's annual tropical cyclone landfalls occurred. For Yemen, a highest number of 4 TCs (~66.7%) make landfall during the post-monsoon. For Oman, the maximum of 57.1% of annual landfalls occur during the monsoon and the most landfall was in winter for Sri Lanka (63.6%).

By looking down columns (and thus across rows) we can see how landfall rates vary by country within a season (%#). The model simulations predict that India would have the highest proportion (52%) of tropical cyclones that make landfall during the post-monsoon season, consistent with the observations. 60% (30 TCs make landfall out of 50) of cyclones make landfall in winter and 76% (38 TCs make landfall out of 50) in the monsoon season. Among the 6 NIO countries, Myanmar (56.5%) and Bangladesh (50%) is the favourable zone for landfalls in the pre-monsoon season.

Table 2. For each country around the NIO rim, we show here ***the GAM fitted*** total numbers (and percentage) of tropical cyclones that make landfall as a function of season. Maxima are in bold and underlined. Format is the same as in Table 1.

	Winter			Pre-monsoon			Monsoon			Post-monsoon			Total	
Country ~	No	% *	% #	No	% *	%#	No	% *	%#	No	% *	%#	No	% *
IND	21	24.1	**42**	21	24.1	**42**	19	21.8	**38**	26	29.9	**52**	**87**	100
MYN	1	4.3	2	13	**56.5**	26	6	26.1	12	3	13.1	6	23	100
BAN	0	0	0	6	**50**	12	1	12.5	2	5	**37.5**	10	12	100
SLN	7	**63.6**	14	4	36.4	8	0	0	0	0	40	0	11	100
YEM	1	16.7	2	1	16.7	2	0	0	0	4	**66.6**	8	6	100
OMAN	0	0	0	3	14.3	6	12	**57.1**	24	6	28.6	12	21	100

Landfall	30		60	48		96	38		76	44		88	160	
NON	20	---	40	2	---	4	12	---	24	6	---	12	40	--
TOTAL	50	---	100	50	---	100	50	---	100	50	--	100	200	--

~ (IND=India; MYN=Myanmar, BAN=Bangladesh, SLN= Sri Lanka, YEM= Yemen, OMN=OMAN, NON=No landfall recorded; *(across season) and #(across countries)

Geographically, the simulated percentages of TC landfall as a function of season across the NIO rim countries are presented in Fig. 8. During winter, the model simulates the highest proportion of TC landfall occurrences for the states of Tamil Nadu and Andra Pardesh in India and across a few states in Bangladesh. In the pre-monsoon season, the states of Ayeyarwady, Rakhine and Tanintharyi in Myanmar, states of Oman, and the western Indian state of Orissa, are all predicted to have the largest proportion of TC landfalls relative to other NIO rim countries. During the post-monsoon, the Indian states of Andra Pradesh, Orissa and Tamil Nadu, and the coastal states of Myanmar, are predicted to have the largest proportion of TC landfalls during that season. In the monsoon season, Orissa in India, Chittagong in Bangladesh, and Myanmar states are predicted to have the highest proportion of TC simulated landfall occurrences, with elevated numbers also predicted for Al Wusta, Ash Sharqiyah and Dhofar in Oman.

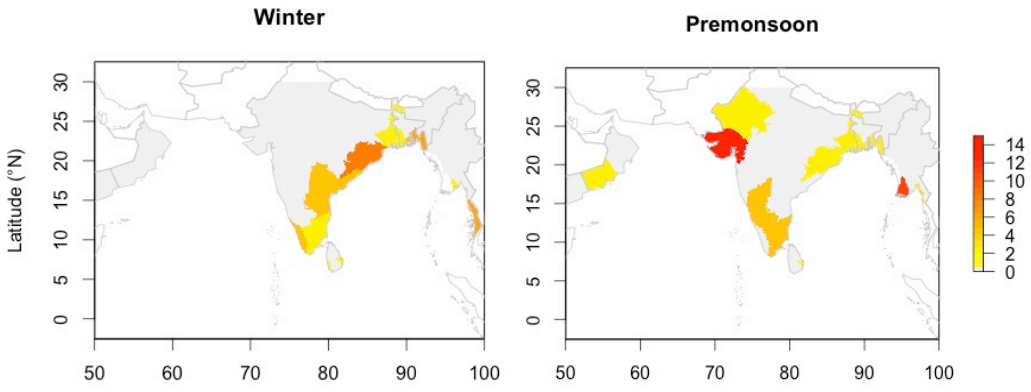

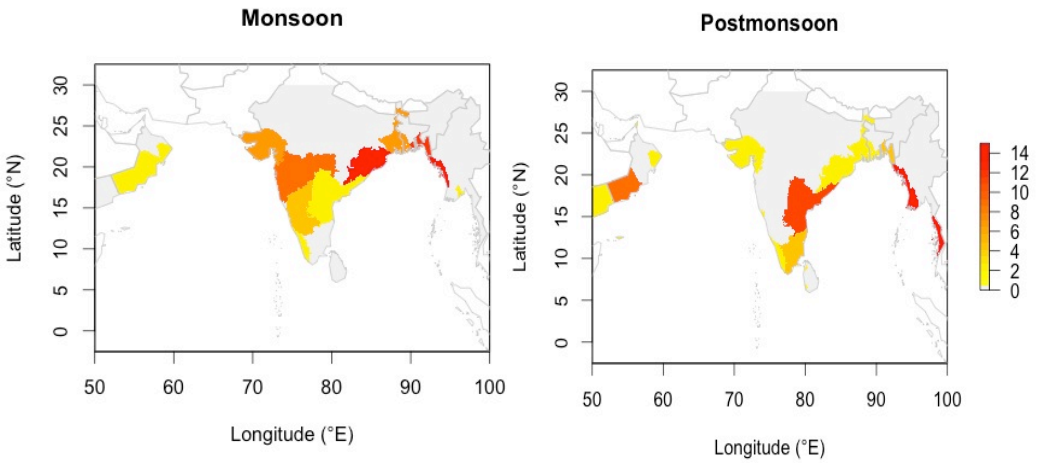

Fig.8 Geographic distribution of model simulated percentage probabilities of tropical cyclone landfall by state across the NIO rim country boundaries. Colours range from yellow to red (according to percentage) corresponding from the lowest to highest model simulated percentage probabilities by TC landfall. Grey indicates a percentage of zero landfalls.

The highest percentage of modelled landfall occurrences are seen in 0-2 days after genesis in the winter (80%) and pre-monsoon (69.5%) seasons, whereas for the monsoon season (62.5%) it occurs in 0-1 day and within 0-2 days during the post monsoon season (74.4%) (Fig.9). These simulated landfall times match well with the observations, except in the pre-monsoon season where the highest landfall rates occur in 2-4 days after genesis.

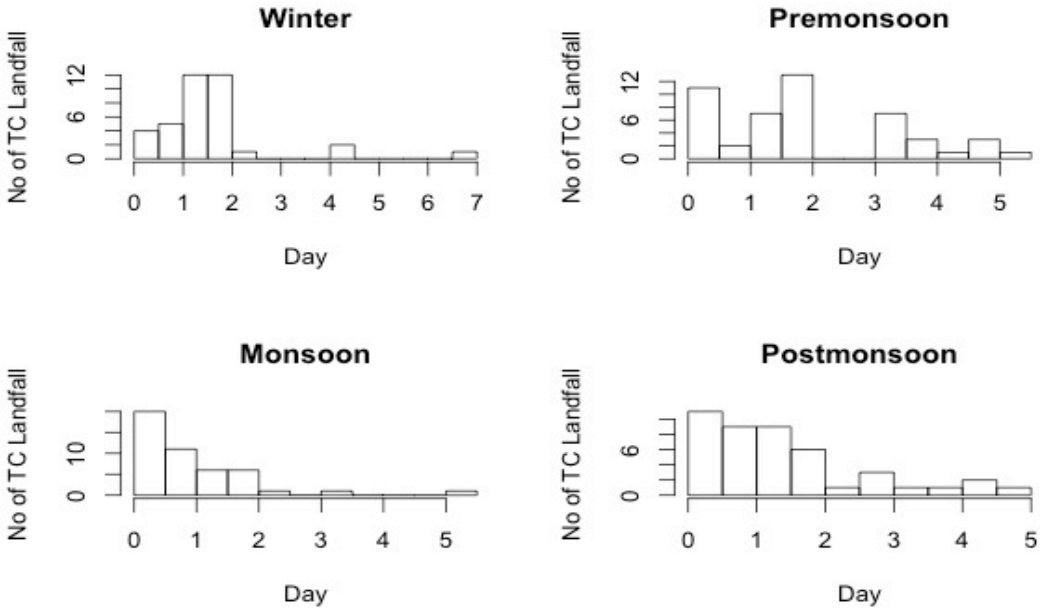

Fig.9 Model simulated TC landfall frequency for each season, measured as time estimated in the number of days from genesis to landfall, for the North Indian Ocean region (0^0 - 30^0 N and 50^0 - 100^0E).

3.3 Prediction skill of model measured against observations

Leave-one-out cross validation (LOOCV) is performed by removing each track in turn and then simulating the trajectories corresponding to the deleted tracks based on the reduced data set, but from the observed genesis point corresponding to the removed track. For each simulated track, we predict the most likely country and point of landfall, by the majority vote from the simulated tracks. Based on comparison of the percentages of country-based statistics of cyclone landfalls between the observations and the model simulations, it was found that the model performs very well overall (except Bangladesh) according to the majority vote approach (Table 3).

The highest percentages of both observed and simulated landfall totals are in India – 38% and 57%, respectively. The observed percentage (9.5%) for Myanmar is remarkably well simulated by the model (10%). The percentage difference in total landfall occurrences (Table 3) between the observations and simulated values is smallest for Myanmar (0%) and largest for Bangladesh (100%). The only exception to overall good model performance was for Bangladesh where the model failed to simulate landfall (Table 3 and 4). With Bangladesh's coastline being a relatively small target for tropical cyclones to strike (239 km long coastline, as compared with 7517 km for India), using a majority vote approach, where we decide on a single state/country that represents where most of the tracks make landfall, appears to be an inadequate approach.

Table 3. Number and percentages of observed and simulated annual probabilities of North Indian Ocean region tropical cyclones that landfall across each country coastline.

	Observation		Simulation	
Country	No	%	No	%
India	40	38.1	57	57
Myanmar	10	9.5	10	10
Bangladesh	17	16.2	0	0

Sri Lanka	5	4.8	4	4
Oman	6	5.7	7	7
Yemen	1	0.9	4	4
Total landfall	79	75.2	82	82
No landfall	26	24.8	18	18
Total	105	100	100	100

Assuming the vector fields depend only on season, the Table 3 contents analysis (vector fields depend on smooth function of longitude and latitude and the function varies with season) is extended to produce Table 4 where we see the highest observation (40%) and simulation percentages (61%) are shown in India and the lowest in Yemen (0.9%) across the NIO rim countries – except for Bangladesh which again fails due to the majority vote approach. The percentage difference in total landfall occurrences (Table 4) between the observations and simulated values is smallest for Yemen (0%) and largest for Bangladesh (100%).

Table 4 Number and percentages of annual total North Indian Ocean region observed and simulated tropical cyclones that landfall across each country coastline. In this analysis, vector fields depend only on season.

	Observation		Simulation	
Country	No	%	No	%
India	40	38.1	61	61
Myanmar	10	9.5	7	7
Bangladesh	17	16.2	0	0
Sri Lanka	5	4.8	3	3
Oman	6	5.7	8	7

Yemen	1	0.9	1	1
Total landfall	79	75.2	80	80
No landfall	26	24.8	20	20
Total	105	100	100	100

Following the second model validation approach (introduced in Section 2.2.4.2), we examined the probability distribution of simulated landfall occurrences against the observed landfall occurrences. The model was run 40 times and the statistical mean plus error was compared against the observations (Table 5a and 5b). This means that we have an ensemble of tracks, and therefore landfall locations, from which to build a distribution and compare its mean and spread against the observations. It is seen (Table 5a) that the percentage of simulated landfall occurrences (37.4%) matches well with the observed percentage (38.1%) of landfall occurrences for India. The observed values for all the other countries lie within the spread of the simulated ensemble. The only exception is Bangladesh, where the simulated probability is 0--9.6% but the observed percentage is 16.2%. When examining the results based on seasonal model fits (Table 5b) it is found that the predicted landfall probability with mean error for Bangladesh in the monsoon season (3.6%) is nearly similar to the observed. However, as a whole, the model performance for Bangladesh is poor across the other TC seasons. For example, the simulated landfall probability in the pre-monsoon season is only 6.6% compared to 33.4% for the observations. The model also over predicts landfall rates for Yemen in all seasons and for Myanmar in the post-monsoon. Overall the percentage of simulated landfall occurrences against the observed landfall occurrences matches well for all seasons, especially the pre-monsoon and post-monsoon periods (Table 5b).

Table 5 Results of the second model validation technique. Percentage frequency of total observed and predicted tropical cyclone landfall occurrences across country coastlines a) for all months, and b) for each season. Errors represent the standard deviation about the mean.

a)

	Observation	Prediction mean with error

Country	No	%	%
India	40	**38.1**	**37.4** ± 17.1
Myanmar	10	9.5	13.4 ± 13.5
Bangladesh	17	16.2	4.7 ± 4.9
Sri Lanka	5	4.8	7.2 ± 6.4
Oman	6	5.7	12.8 ± 9.6
Yemen	1	0.9	3.5 ± 3.5
Total landfall	79	**75.2**	**79**
No landfall	26	24.8	21
Total	105	100	100

1236

1237 b)

Country	Observation				Prediction mean with error			
	Win	Pre	Mon	Post	Win	Pre	Mon	Post
	No (%)	No (%)	No (%)	No (%)	%	%	%	%
IND	4(26.6)	5(20.8)	10(52.6)	21(44.7)	32.7±20.9	33.2±14.4	39.6±17.8	43.9±15.4
MYN	1(6.7)	5(20.8)	1(5.3)	3(6.4)	8.9±14.8	25.9±18.4	4.9±6.1	13.8±14.7
BAN	0(0)	8(33.4)	1(5.3)	8(17)	2.2±4.8	6.6±5.3	3.6±3.7	6.4±5.6
SLN	3(20)	0(0)	0(0)	2(4.3)	20.9±16.3	3.3±3.8	0.9±1.6	3.8±4
OMN	1(6.7)	2(8.3)	2(10.5)	1(2.1)	0.9±1.7	10.8±7.1	30.7±20.4	8.9±9.2
YEM	0(0)	0(0)	0(0)	1(2.1)	1.9±2.5	4.4±3.6	3±4.4	4.5±3.4
Landfall	9(60)	20**(83.3)**	14(73.7)	36(**76.6**)	67.5	**84.2**	82.7	**81.3**
NON	6(40)	4(16.7)	5(26.3)	11(23.4)	32.5	15.8	17.3	18.7
Total	15(100)	24(100)	19(100)	47(100)	100	100	100	100

1238

In the third model validation approach (introduced in Section 2.2.4.3), we calculated the distance between observed landfall and simulated landfall occurrences to evaluate model performance. The distribution of distances between the observed and simulated landfall points across all simulated tracks is presented in Fig. 10. It is found that the majority of simulated TC landfall occurrences (54.6%) occur within 0-500 km of the observed landfall locations, with the best model performances found in the winter, monsoon and post-monsoon seasons. For the pre-monsoon season, there is a greater spread of differences between modelled landfall locations and those observed, with the majority difference being at just over 1500 km from the observed. Given the spatial scale of tropical cyclones is typically O(1000 km), modelled landfall occurrences within ~500 km of the observations would suggest very good model performance, while those falling within ~1000km should still be deemed as skilful.

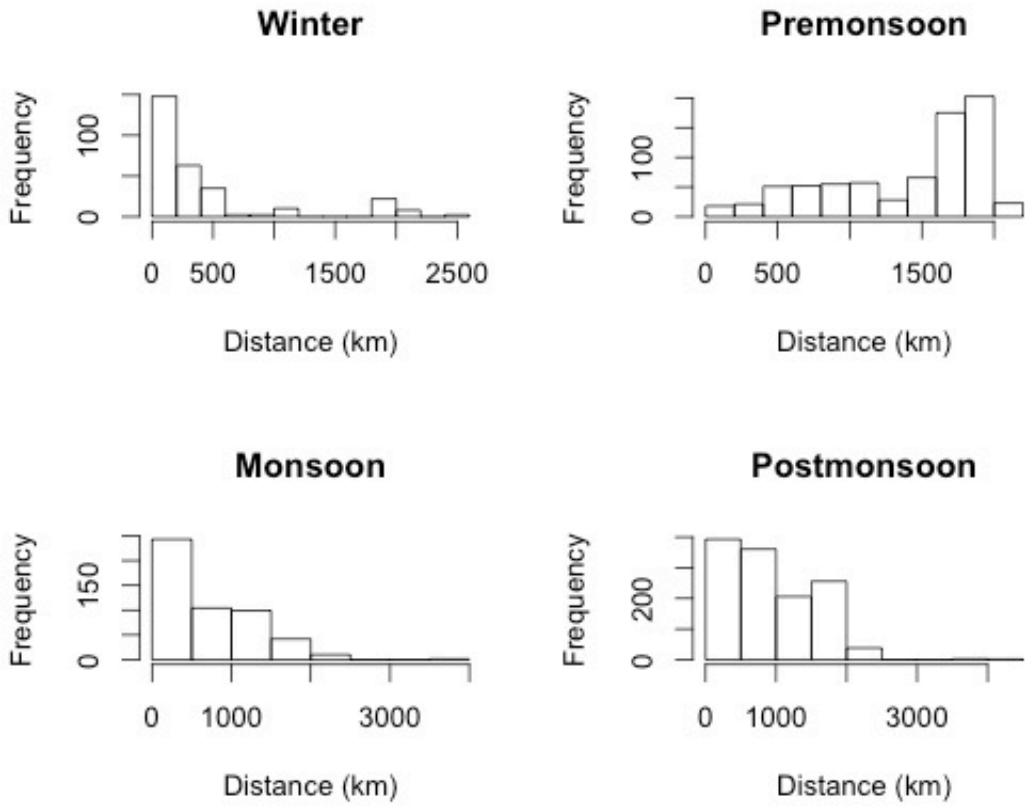

Fig. 10 Distribution of distances between observed and simulated landfall location over the NIO as per season.

4. Discussion

This study has described a new climatological statistical model of tropical cyclone genesis, tracks and landfall for the North Indian Ocean region. This climatological model is intended to represent a model baseline against which future TC forecast models might be developed and assessed for their seasonal forecast skill on year-to-year or longer time scales. The model presented here simulates tropical cyclone genesis, tracks and landfall as a function of season only, and takes no account of the influence of possible climatic prediction, or predictor, influences on year-to-year or longer time scales, such as the possible effects of El Niño – Southern Oscillation or the Indian Ocean Dipole. Hence, the model might be seen as a kind of climatological persistence model for TCs in the North Indian Ocean region.

So far, little skill has been shown in dynamical (climate) model seasonal forecasts of tropical cyclones for the NIO region (Camargo *et al.* 2007a; Camp *et al.* 2015). Specifically, Camargo *et al.* (2005) and Shaevitz *et al.* (2014) noted that both low and high-resolution models are generally unable to properly simulate the seasonal cycle. We have instead applied a statistical modelling approach here, where the tropical observed cyclone genesis is modelled by kernel density estimation, producing a probability density function (PDF) from which individual storms can be randomly sampled. Tracks are fitted using a generalised additive model, and model track simulations use random innovations at spatial increments to produce an ensemble of simulated tracks. The model is cross-validated in three separate ways to assess and ensure reliability of the results.

The simulation of a large number of tracks with an implementation of this model enables the calculation of landfall probabilities at any location of interest in the North Indian Ocean region affected by tropical cyclones. In our 35-year study period (1979-2013), a total number of 105 tropical cyclones (TCs) have been reported and are recorded in the JTWC database (within IBTrACS). Of these, 79 (75%) made landfall across six North Indian Ocean (NIO) rim countries, namely Bangladesh, India, Myanmar, Sri Lanka, Oman and Yemen. Almost half of the TCs that made landfall, have done so during the post-monsoon season, while 25.3% (20) made landfall during the pre-monsoon season – a total of 71% making landfall during only these two of the four seasons annually. Specifically, 50% of annual TC landfall events into Myanmar have occurred during the pre-monsoon season, while 47% of total annual TC landfall events also occurred during

this same season in Bangladesh. Conversely, 52% of landfall events into India have occurred during the post-monsoon season. In terms of time from genesis to landfall, it was found that it takes around 2-4 days since genesis for 47% of events to make landfall during the pre-monsoon season and from 0- 2 days (68% of events) during the post-monsoon season. Correspondingly, the model also predicts that the highest percentage of TC landfall events should occur in the pre-monsoon season for Myanmar and in the post-monsoon season for India. However, the model failed to predict the highest number of landfall occurrences in the pre-monsoon season for Bangladesh.

We have chosen three methods to cross-validate this statistical model. First, leave-one-out cross-validation was applied. We have shown that the percentages of annual total NIO region observed and simulated TCs that made landfall across each country coastline compare well. It was found that the model performs best in this sense for Myanmar, with the smallest prediction error of 0.5% difference. On the other hand, the worst performance is identified for Bangladesh where the model fails to predict. The cross validation analysis was repeated by assuming that the vector field depends on only season and then the model predicts well for Yemen and Myanmar, but again failed for Bangladesh due to the majority vote approach.

The second cross-validation approach considers the probability distribution of the simulated tracks, where the model is run several times and the statistical mean and error (standard deviation) are generated to assess whether the model results capture the percentage of observed landfalls within an error bound (standard deviation). The standard deviation represents the model error (±) around the model-predicted mean value, which encompasses the observed percentages of landfall occurrences for most of the six countries in the NIO rim. Exceptions are for Myanmar during the post-monsoon season (the model predicts 13.8% whereas the observations correspond to 6.4%) and Bangladesh in the pre-monsoon season (the model predicts 6.6% whereas the observations correspond to 33.4%).

The third and final cross-validation approach calculates the distance between observed and simulated landfall points, and reveals that the majority of modelled TC landfall occurrences are within a relatively short distance (0-500km) of the observed landfall locations. This confirms the model skill, given that the typical spatial scale of tropical cyclones (O(1000km)) is much larger than the typical error in landfall location.

Statistically an average of 500 km error is good relative to the average size of a tropical storm (approx. 1000 km). Second, a forecast with an error of 500km is still useful information as compared with no information, which would be the case in the absence of a forecast model. Third, we need to accept that this basin is hard to model due to double peak in seasonal cycle (Camargo *et al.* 2005; Shaevitz *et al.* 2014; Camp *et al.* 2015). An error in predicted landfall location of 500 km is similar to the errors of dynamical models for the region, which have errors on the order of 100's of km (e.g.,(Mallik *et al.* 2015; Rayhun *et al.* 2015)).

One limitation of the statistical modelling approach is the lower sharpness (the tendency of the forecast to predict extreme values) that comes with such models (Vitart *et al.* 2010). Statistical models rarely predict very low or very high probabilities largely because of the constraints provided by climatology (Slade and Maloney 2013). In other words, we are examining the expected seasonal state rather than the extreme events. There is also room for the TC genesis kernel density estimation to be better tuned to the observations. Specifically, the kernel does not capture the genesis locations particularly well near Sri Lanka. Future improvements to the genesis model may translate to a bias reduction in the track simulations and thus landfall estimates.

Our model presented here provides the climatological basis against which future developments of statistical forecasting applications, given climate predictors on interannual to decadal time scales, can be tested for their skill. In particular, the Quasi-Biennial Oscillation and El Niño – Southern Oscillation are potentially relevant climate modes of variability to the North Indian region tropical cyclone activity (Girishkumar and Ravichandran 2012; Fadnavis *et al.* 2014). These climate modes and skill in seasonally forecasting tropical cyclone activity afforded by the model developed on other relevant predictor variables will be investigated and discussed in separate studies.

5. Conclusions

The key aim of this paper has been to develop a climatological statistical model of tropical cyclone genesis, tracks and landfall for the North Indian Ocean region and its neighbouring rim countries that will be beneficial for forecast models to be compared against. The main findings are as follows:

1. An effective method has been developed to estimate the distribution of tropical cyclone

genesis points by kernel density estimation. This paper demonstrates that the masked kernel density estimates well the observed genesis points within each season.

2. A novel generalised additive model (GAM) has been introduced and fitted to track increments and used as a baseline for predicting the tropical cyclone velocity field in each season. In the winter and monsoon seasons, the GAM-fitted velocity field highlights the westward or north-westward cyclone movement during this time. Conversely, during the pre-monsoon season, the model fit highlights the north-westward/northward movement, and north-eastward recurvature. In the post-monsoon season, the GAM shows the cyclone movement is typically in a north-westward direction which later recurves towards the northeast.

3. The observations indicate the highest percentage of landfall occurrences in the pre-monsoon seasons are found in Myanmar (50%) and Bangladesh (47%), while for the post-monsoon season the largest percentage of landfall occurs in India (52%). Our model shows characteristically similar results with simulated highest percentage landfall occurrences for Myanmar (56.5%) and Bangladesh (50%) in the pre-monsoon season, and for India (30%) in the post-monsoon.

4. The characteristic number of days from tropical cyclone genesis to landfall can provide useful time scale information for coastal planning and emergency response. We determined the time since genesis that landfall occurs, and found the percentage in the observations and simulations are characteristically 2-4 days for the pre-monsoon season and 0-2 days for the post-monsoon season.

5. From analysis of the results by season, we find the highest number of model simulated cyclones move eastward during the pre-monsoon season and make landfall around the eastern part of Bay of Bengal, whereas they move westward making landfall in the western part of Bay of Bengal/eastern coast of India during the post-monsoon.

6. To validate the quality of the model hindcasts against the observed landfall occurrences across the NIO countries, three validation methods were introduced ((1) leave-one-out cross-validation, (2) probability distribution of country of landfall, and (3) distance between observed and simulated landfall locations), collectively

demonstrating that the model performs well as a climatological baseline.

In summary, we have developed a new and skilful seasonal climatological model of tropical cyclone genesis, tracks, and landfall for the North Indian Ocean region. It is found that our model produces skilful hindcasts of these tropical cyclone characteristics. An important outcome of this paper is the development of seasonal TC genesis distributions using kernel density estimation, and trajectory simulation and landfall detection using a generalised additive model with stochastic innovations that impinge on a country mask. Efforts are currently underway to adapt the presented model approach to develop a statistical seasonal forecasting model that incorporates interannual climate predictors, including simple metrics for the stratospheric Quasi-Biennial Oscillation or El Niño – Southern Oscillation.

Acknowledgments. We would like to sincerely thank the two anonymous reviewers for their inshightful comments that helped us to significantly improve the quality of this manuscript. Mohammad Wahiduzzaman was supported by University of Tasmania Graduate Research Scholarship (TGRS) for this PhD research undertaken at the University of Tasmania, Hobart, Tasmania, Australia.

References

Alam E, Collins AE (2010) Cyclone disaster vulnerability and response experiences in coastal Bangladesh. Disasters 34(4):931-954

Alam E, Dominey-Howes D (2015) A new catalogue of tropical cyclones of the northern Bay of Bengal and the distribution and effects of selected landfalling events in Bangladesh. International Journal of Climatology 35(6):801-835

Alam MM, Hossain MA, Shafee S (2003) Frequency of Bay of Bengal cyclonic storms and depressions crossing different coastal zones. International Journal of Climatology 23(9):1119-1125

Balaguru K, Taraphdar S, Leung LR, Foltz GR (2014) Increase in the intensity of postmonsoon Bay of Bengal tropical cyclones. Geophysical Research Letters 41(10):3594-3601

Bashtannyk DM, Hyndman RJ (2001) Bandwidth selection for kernel conditional density estimation. Computational Statistics & Data Analysis 36:279-298

1409 Belanger JI, Webster PJ, Curry JA, Jelinek MT (2012) Extended prediction of North Indian Ocean
1410 tropical cyclones. Weather and Forecasting 27(3):757-769

1411 Bengtsson L, Hodges KI, Esch M (2007) Tropical cyclones in a T159 resolution global climate
1412 model: Comparison with observations and re-analyses. Tellus, Series A: Dynamic
1413 Meteorology and Oceanography 59 A(4):396-416

1414 Brian B (2015) Tropical Cyclone ACE Climatology. Climate Blog Published on 8th Nov, 2015

1415 Camargo SJ (2013) Global and regional aspects of tropical cyclone activity in the CMIP5 models.
1416 Journal of Climate 26(24):9880-9902

1417 Camargo SJ, Barnston AG (2009) Experimental dynamical seasonal forecasts of tropical cyclone
1418 activity at IRI. Weather and Forecasting 24(2):472-491

1419 Camargo SJ, Barnston AG, Klotzbatch PJ, Landsea CW (2007a) Seasonal Tropical cyclone
1420 forecasts. Bulletin of the World Meterological Organization 56:297-307

1421 Camargo SJ, Barnston AG, Zebiak SE (2005) A statistical assessment of tropical cyclone activity
1422 in atmospheric general circulation models. Tellus, Series A: Dynamic Meteorology and
1423 Oceanography 57(4):589-604

1424 Camp J, Roberts M, Maclachlan C, Wallace E, Hermanson L, Brookshaw A, Arribas A, Scaife
1425 AA (2015) Seasonal forecasting of tropical storms using the Met Office GloSea5 seasonal
1426 forecast system. Quarterly Journal of the Royal Meteorological Society 141(691):2206-
1427 2219

1428 Casson E, Coles S (2000) Simulation and extremal analysis of hurricane events. Journal of the
1429 Royal Statistical Society. Series C: Applied Statistics 49(2):227-245

1430 Elsner JB, Jagger TH (2004) A hierarchical Bayesian approach to seasonal hurricane modeling.
1431 Journal of Climate 17(14):2813-2827

1432 Elsner JB, Jagger TH (2006) Prediction models for annual U.S. hurricane counts. Journal of
1433 Climate 19(12):2935-2952

1434 Elsner JB, Jagger TH (2010) Hurricanes and climate change. Springer, pp 1-419

1435 Elsner JB, Schmertmann CP (1993) Improving extendedrange seasonal predictions of intense
1436 Atlantic hurricane activity. Wea. Forecasting 8:345-351

1437 Emanuel K, Ravela S, Vivant E, Risi C (2006) A Statistical Deterministic Approach to Hurricane
1438 Risk Assessment. Bulletin of the American Meteorological Society 87(3):299-314

1439 Evan AT, Camargo SJ (2010) A Climatology of Arabian Sea Cyclonic Storms. Journal of Climate
1440 24(1):140-158

1441 Fadnavis S, Ernest Raj P, Buchunde P, Goswami BN (2014) In search of influence of
1442 stratospheric Quasi-Biennial Oscillation on tropical cyclones tracks over the Bay of Bengal
1443 region. International Journal of Climatology 34(3):567-580

1444 Girishkumar MS, Ravichandran M (2012) The influences of ENSO on tropical cyclone activity in
1445 the Bay of Bengal during October-December. Journal of Geophysical Research: Oceans
1446 117(2)

1447 Gray WM (1984) Atlantic seasonal hurricane frequency, Part I: El Nino and 30 mb Quasi-
1448 Biennial Oscillation influences. Monthly Weather Review 112(9):1649-68

1449 Guisan A, Edwards Jr TC, Hastie T (2002) Generalized linear and generalized additive models in
1450 studies of species distributions: Setting the scene. Ecological Modelling 157(2-3):89-100

1451 Haggag M, Badry H (2012) Hydrometeorological Modeling Study of Tropical Cyclone Phet in
1452 the Arabian Sea in 2010 Atmospheric and Climate Sciences 2:174-190

1453 Hall T, Yonekura E (2013) North American tropical cyclone landfall and SST: A statistical model
1454 study. Journal of Climate 26(21):8422-8439

1455 Hall TM, Jewson S (2007) Statistical modelling of North Atlantic tropical cyclone tracks. Tellus,
1456 Series A: Dynamic Meteorology and Oceanography 59 A(4):486-498

1457 Hastie T, Tibshirani R, Friedman J (2009) The Elements of Statistical learning: Data Mining,
1458 Inference, and Prediction. Springer Series in Statistics Second Edition:295-333

1459 Hess JC, Elsner JB (1994) Extended-range hindcasts of tropical-origin Atlantic hurricane activity.
1460 Geophysical Research Letters 21(5):365-368

1461 Holland GJ, Webster PJ (2007) Heightened tropical cyclone activity in the North Atlantic: Natural
1462 variability or climate trend? Philosophical Transactions of the Royal Society A:
1463 Mathematical, Physical and Engineering Sciences 365(1860):2695-2716

1464 Islam T, Peterson RE (2009) Climatology of landfalling tropical cyclones in Bangladesh 1877-
1465 2003. Natural Hazards 48(1):115-135

1466 Jagger TH, Elsner JB (2010) A consensus model for seasonal hurricane prediction. Journal of
1467 Climate 23(22):6090-6099

James MK, Mason LB (2005) Synthetic tropical cyclone database. Journal of Waterway, Port, Coastal and Ocean Engineering 131(4):181-192

Kang NY, Lim MS, Elsner JB, Shin DH (2016) Bayesian updating of track-forecast uncertainty for tropical cyclones. Weather and Forecasting 31(2):621-626

Knapp KR, Kruk MC, Levinson DH, Diamond HJ, Neumann CJ (2010) The international best track archive for climate stewardship (IBTrACS). Bulletin of the American Meteorological Society 91(3):363-376

Knutson TR, Zeng F, Wittenberg A, Kim SH, Sirutis J, Bender M, Zhao M, Tuleya R (2014) Recent Research at GFDL on Surface Temperature Trends and Simulations of Tropical Cyclone Activity in the Indian Ocean Region. U.C. Mohanty MM, O.P. Singh, B.K. Bandyopadhyay, L.S. Rathore (ed) Monitoring and Prediction of Tropical Cyclones in the Indian Ocean and Climate Change. Springer, pp 50-62

Kossin JP, Olander TL, Knapp KR (2013) Trend analysis with a new global record of tropical cyclone intensity. Journal of Climate 26(24):9960-9976

Landsea CW (2007) Counting Atlantic tropical cyclones back to 1900. Eos 88(18):197-208

Leroy A, Wheeler MC (2008) Statistical prediction of weekly tropical cyclone activity in the southern hemisphere. Monthly Weather Review 136(10):3637-3654

Lin II, Chen CH, Pun IF, Liu WT, Wu CC (2009) Warm ocean anomaly, air sea fluxes, and the rapid intensification of tropical cyclone Nargis (2008). Geophysical Research Letters 36(3):L03817

Loader CR (1999) Bandwidth Selection: Classical or Plug-In? The Annals of Statistics 27(2):415-438

Mallik MAK, Ahsan MN, Chowdhury MAM (2015) Simulation of Track and Landfall of Tropical Cyclone Viyaru and Its Associated Strom Surges Using NWP Models. American Journal of Marine Science 3(1):11-21

McDonnell KA, Holbrook NJ (2004a) A Poisson regression model of tropical cyclogenesis for the Australian-southwest Pacific Ocean region. Weather and Forecasting 19(2):440-455

McPhaden MJ, Foltz GR, Lee T, Murty VSN, Ravichandran M, Vecchi GA, Vialard J, Wiggert JD, Yu L (2009) Ocean-atmosphere interactions during cyclone nargis. Eos 90(7):53-54

Mestre O, Hallegatte S (2009) Predictors of tropical cyclone numbers and extreme hurricane intensities over the North Atlantic using generalized additive and linear models. Journal of Climate 22(3):633-648

Mohapatra M, Bandyopadhyay BK, Tyagi A (2012) Best track parameters of tropical cyclones over the North Indian Ocean: A review. Natural Hazards 63(3):1285-1317

Mohapatra M, Bandyopadhyay BK, Tyagi A (2014) Status and Plans for Operational Tropical Cyclone Forecasting and Warning Systems in the North Inidan Ocean Region. U.C. Mohanty MM, O.P. Singh, B.K. Bandyopadhyay, L.S. Rathore (ed) Monitoring and Prediction of Tropical Cyclones in the Indian Ocean and Climate Change. Springer, pp 149-162

Mydans S, Cowell A (2008) "Myanmar Mourns Victims of Cyclone".New York Times

Nath S, Kotal SD, Kundu PK (2015) Seasonal prediction of tropical cyclone activity over the North Indian Ocean using the neural network model. Atmosfera 28(4):271-281

Ng EKW, Chan JCL (2012) Interannual variations of tropical cyclone activity over the north Indian Ocean. International Journal of Climatology 32(6):819-830

Nicholls N (1985) Predictability of interannual variations of Australian seasonal tropical cyclone activity. Monthly Weather Review 113(7):1144-1149

Nicholls N, Landsea C, Gill J (1998) Recent trends in Australian region tropical cyclone activity. Meteorology and Atmospheric Physics 65(3-4):197-205

O'Hare G (2001) Hurricane 07B in the Godivari Delta, Andhra Pradesh, India: Vulnerability, mitigation and the spatial impact. Geographical Journal 167(1):23-38

Paliwal M, Patwardhan A, Sarda NL (2011) Analyzing tropical cyclone tracks of North Indian Ocean.COM.Geo 11 Proceedings of the 2nd International Conference on Comupting for Geospatial Research & Applications, Article No.18, ACM New York, USA.

Pattanaik DR, Mohapatra M (2016) Seasonal forecasting of tropical cyclogenesis over the North Indian Ocean. Journal of Earth System Science 125(2):231-250

Rajasekhar M, Kishtawal CM, Prasad MYS, Seshagiri Rao V, Rajeevan M (2014) Extended range tropical cyclone predictions for East Coast of India. U.C. Mohanty MM, O.P. Singh, B.K. Bandyopadhyay, L.S. Rathore (ed) Monitoring and Prediction of Tropical Cyclones in the Indian Ocean and Climate Change. pp 137-148

1527 Rajeevan M, Srinivasan J, Niranjan Kumar K, Gnanaseelan C, Ali MM (2013) On the epochal
1528 variation of intensity of tropical cyclones in the Arabian Sea. Atmospheric Science Letters
1529 14(4):249-255

1530 Ray A, Jaiswal N, Kishtawal CM (2012) Cyclone tracking over North Indian Ocean using
1531 Artificial Neural Network Models and implementation of regional and seasonal
1532 stratification, Second WMO International Conference on Indian Ocean Tropical and
1533 Cyclone Change (IOTCCC-2012). New Delhi

1534 Rayhun KMZ, Quadir DA, Chowdhury MAM, Ahsan MN, Haque MS (2015) Simulation of
1535 structure, track and landfall of tropical cyclone Bijli using WRF-ARW model. J.
1536 Bangladesh Acad. Sci 39(2):157-167

1537 Rigollet P, Vert R (2009) Optimal rates for plug-in estimators of density level sets. Bernoulli
1538 15(4):1154-1178

1539 Rumpf J, Weindl H, Faust E, Schmidt V (2010) Structural variation in genesis and landfall
1540 locations of North Atlantic tropical cyclones related to SST. Tellus, Series A: Dynamic
1541 Meteorology and Oceanography 62(3):243-255

1542 Rumpf J, Weindl H, Höppe P, Rauch E, Schmidt V (2007) Stochastic modelling of tropical
1543 cyclone tracks. Mathematical Methods of Operations Research 66(3):475-490

1544 Sahoo B, Bhaskaran PK (2016) Assessment on historical cyclone tracks in the Bay of Bengal, east
1545 coast of India. International Journal of Climatology 36(1):95-109

1546 Saunders MA, Lea AS (2005) Seasonal prediction of hurricane activity reaching the coast of the
1547 United States. Nature 434(7036):1005-1008

1548 Shaevitz DA, Camargo SJ, Sobel AH, Jonas JA, Kim D, Kumar A, Larow TE, Lim YK,
1549 Murakami H, Reed KA, Roberts MJ, Scoccimarro E, Vidale PL, Wang H, Wehner MF,
1550 Zhao M, Henderson N (2014) Characteristics of tropical cyclones in high-resolution models
1551 in the present climate. Journal of Advances in Modeling Earth Systems 6(4):1154-1172

1552 Shaji C, Kar SK, Vishal T (2014) Storm surge studies in the North Indian Ocean: A review.
1553 Indian Journal of Marine Sciences 43(2):125-147

1554 Slade SA, Maloney ED (2013) An intraseasonal prediction model of atlantic and east Pacific
1555 tropical cyclone genesis. Monthly Weather Review 141(6):1925-1942

1556 Turlach BA (1993) Bandwidth Selection in Kernel Density Estimation: A Review. CORE and
1557 Institut de Statistique 19:1-33

1558 Tyagi A, Bandyopadhyay BK, Mohapatra M (2010) Monitoring and prediction of cyclonic
1559 disturbances over North Indian ocean by regional specialised meteorological centre, New
1560 Delhi (India): Problems and prospective. In: Indian Ocean Tropical Cyclones and Climate
1561 Change. pp 93-103

1562 Vickery PJ, Skerjl P, Steckley AC, Twinsdale L (2000) Simulation of hurricane risk in the united
1563 states using an empirical storm track modeling technique. Journal of structural engineering
1564 126:1222-1237

1565 Vissa NK, Satyanarayana ANV, Prasad Kumar B (2013) Intensity of tropical cyclones during pre-
1566 and post-monsoon seasons in relation to accumulated tropical cyclone heat potential over
1567 Bay of Bengal. Natural Hazards 68(2):351-371

1568 Vitart F, Leroy A, Wheeler MC (2010) A comparison of dynamical and statistical predictions of
1569 weekly tropical cyclone activity in the Southern Hemisphere. Monthly Weather Review
1570 138(9):3671-3682

1571 Warrick RA, MAccines KL, Pittock AB, Kench PS (2000) Climate change, severe storms and sea
1572 level. Floods edited by Dennis J. Parker Taylor and Francis group, London, p-139

1573 Webster PJ (2008) Myanmar's deadly daffodil. Nature Geoscience 1(8):488-490

1574 Weinkle J, Maue R, Pielke R (2012) Historical global tropical cyclone landfalls. Journal of
1575 Climate 25(13):4729-4735

1576 Wilks DS (1995) Statistical Methods in the Atmospheric Sciences. Academic Press, pp.467

1577 WMO (1997) Tropical Cyclone Operational Plan for the Bay of Bengal and the Arabian Sea,
1578 WMO Report 1997.

1579 Yahyai SSA (2014) NWP forecast Guidance during Phet at Oman Meteorological Service. U.C.
1580 Mohanty MM, O.P. Singh, B.K. Bandyopadhyay, L.S. Rathore (ed) Monitoring and
1581 Prediction of Tropical Cyclones in the Indian Ocean and Climate Change, Springer, pp
1582 240-262

1583 Yonekura E, Hall TM (2011) A Statistical model of tropical cyclone tracks in the western North
1584 Pacific with ENSO-dependent cyclogenesis. Journal of Applied Meteorology and
1585 Climatology 50(8):1725-1739

1586 Zhao M, Held IM, Lin SJ, Vecchi GA (2009) Simulations of global hurricane climatology,
1587 interannual variability, and response to global warming using a 50-km resolution GCM.
1588 Journal of Climate 22(24):6653-6678

2.3 Chapter Summary

This chapter addresses the thesis aims of development of a climatological model to model the tropical cyclone genesis, tracks and landfall in the North Indian Ocean region. The model consists three components which are genesis distribution by kernel density estimation, tracks by generalised additive model, landfall by eular intergration with country mask approach. Also the model hindcast skills are quantified.

In detail, we have presented a new statistical climatological model to develop climatological baseline for tropical cyclone genesis, tracks and landfall in the North Indian Ocean region. Overall, the model has good cross-validated hindcast skill (the very good skill is found in Myanmar but worse skill is seen in Bangladesh due to majority vote approach).

3 DEVELOPMENT OF STATISTICAL SEASONAL FORECAST MODEL FOR TROPICAL CYCLONE GENESIS, TRACKS AND LANDFALL IN THE NORTH INDIAN OCEAN REGION AND ROLE OF QBO

3.1 Chapter Overview

This chapter builds a seasonal forecast model of North Indian Ocean region tropical cyclone genesis, tracks and landfall by considering Quasi-Biennial Oscillation as predictor where the observational data is used from 1980-2009 and rest 2010-13 period is used for forecast. The development of forecast model of tropical cyclone genesis, tracks and landfall for North Indian Ocean rim countries are based on kernel density estimation, a generalised additive model including an Euler integration step, and landfall detection using a country mask approach. Lead-lag analysis is used to assess the best predictor timescales for TC forecast potential.The model is fitted to the observed cyclone track velocities as a smooth function of location in each phase jointly with season and the distribution of cyclone genesis points is approximated by kernel density estimation. Trajectories are then simulated by drawing new random genesis points from the fitted density estimates, and then tracing the cyclonic paths from the fitted velocity fields to determine the point of landfall. Two validation hindcast methods (Leave one out cross validation with majority vote approach, and distance calculation between observed and simulated landfall) are used to analyse the skill of model.

The main text of this chapter is a paper under revision for *Climate Dynamics (*Wahiduzzaman M, Oliver E, Klotzbach, P, Wotherspoon S, Holbrook N (2017) A statistical seasonal forecast model of North Indian Ocean tropical cyclones using Quasi-Biennial Oscillation, Climate Dynamics, under revision)

3.2 Wahiduzzaman *et al.* 2017; *Climate Dynamics*

A statistical seasonal forecast model of North Indian Ocean Tropical Cyclones using the Quasi-Biennial Oscillation

Mohammad Wahiduzzaman[1], Eric C.J. Oliver[1, 2], Philip J. Klotzbach[3], Simon J. Wotherspoon[1,4], Neil J. Holbrook[1,2]

[1]Institute for Marine and Antarctic Studies, University of Tasmania, Hobart, Tasmania, Australia

[2]Australian Research Council Centre of Excellence for Climate System Science, Hobart, Tasmania, Australia

[3] Department of Atmospheric Science, Colorado State University, Fort Collins, Colorado, USA

[4] Australian Antarctic Division, 203 Channel Highway, Kingston, TAS 7050, Australia

Under revision for *Climate Dynamics*

Corresponding author address: Mohammad Wahiduzzaman, Institute for Marine and Antarctic Studies, University of Tasmania, TAS 7001 Australia | E-mail: **md.wahiduzzaman@utas.edu.au**

Keywords Cyclone Genesis, Quasi-Biennial Oscillation, Storm tracks, TCs, Landfall, Statistical modelling, North Indian Ocean

Abstract

Previous studies have shown that the skill of seasonal forecasts of tropical cyclone (TC) activity over the North Indian Ocean (NIO) tends to be poor. This paper investigates the forecast potential of TC genesis, trajectories and landfall in the NIO region using an index of the stratospheric Quasi-Biennial Oscillation (QBO) as the predictor variable in a new statistical seasonal forecast model. Genesis was modelled by kernel density estimation, tracks were fitted using a generalised additive model (GAM) approach with an Euler integration step, and landfall detection was estimated using a country mask. The model was trained on a 35-year record of TC track observations (1979-2013) from the Joint Typhoon Warning Center and the QBO index at lags from 0-6 months. Over this time period, within each season and QBO phase, the distribution of genesis points was modelled by the kernel density estimator, and the cyclone tracks were velocity fits using the GAM along the observed cyclone tracks as smooth functions of location. Trajectories were simulated by first randomly selecting genesis points from the fitted kernel density estimates, and then ensembles of cyclone paths were traced, with random innovations, informed by the GAM-fitted velocity fields, to determine the points of landfall. Lead-lag analysis was used to assess the best predictor timescales for TC forecast potential. We found that the best model utilises the QBO index with a 3-month lead. Two hindcast validation methods were applied. First, leave-one-out cross validation was applied whereby the country of landfall was determined by the majority vote of the simulated tracks (the country with the highest percentage of landfalls). Second, the distances between the landfall locations in the observations and simulations were compared and quantified. Overall, the model shows good cross-validated hindcast skill across the region and for landfall into most NIO rim countries. Application of an independent forecast analysis further indicated that including information on the state of the QBO has the potential to improve the skill of TC seasonal forecasts in the NIO region.

1 Introduction

Tropical cyclones (TCs) are one of the most threatening weather hazards in the tropics and represent a major hazard to North Indian Ocean (NIO) rim countries (Alam *et al.* 2003; Ali *et al.* 2007; Alam and Collins 2010; Girishkumar *et al.* 2012; Mohapatra *et al.* 2012; Paliwal and Patwardhan 2013; Fadnavis *et al.* 2014; Girishkumar *et al.* 2014; Mohapatra *et al.* 2014; Rajasekhar *et al.* 2014; Girishkumar *et al.* 2015; Nath *et al.* 2015). Globally, the impacts of TCs can be devastating, with numerous previous events causing enormous loss of life and property damage, representing significant financial risk to insurance and reinsurance companies (Rumpf *et al.* 2007). As one of the most destructive weather systems on the planet, TCs can involve multiple hazards (e.g., storm surge, heavy rain, strong winds) over the course of several days (Ebert *et al.* 2010). One remarkable example was TC Nargis in 2008, which killed over 135,000 people (Webster 2008; Lin *et al.* 2009) in Myanmar and ranked as the second deadliest disaster in the decade from 2000-2009 according to the Centre for Research on Epidemiology of Disasters (Rodriguez *et al.* 2009). Due to the significant loss of life as well as economic damage caused by TCs making landfall in NIO rim countries (Webster 2008; Islam and Peterson 2009; Ng and Chan 2012; Mohapatra *et al.* 2014; Pattanaik and Mohapatra 2016) it is important to assess and/or anticipate risks as much as possible. Due to the threats that TCs pose to life and property, accurate TC landfall probability forecasts can be potentially beneficial to local populations regarding risks (Tolwinski-Ward 2015).

Skilful forecasts of TC tracks have particular importance (Fraedrich and Leslie 1989; Carter and Elsner 1997; Carson 1998; Elsner *et al.* 2006; Chu and Zhao 2007; Camargo *et al.* 2007a; Basu and Bhagyalakshmi 2010; Chu *et al.* 2010; Chand and Walsh 2011; Balachandran and Geetha 2012; Camp *et al.* 2015). In the present study, we have developed a statistical model to better understand and predict NIO region TC activity in the upcoming TC season. The NIO region accounts for 7% of the total number of TCs generated globally (Mohapatra *et al.* 2014; Sahoo and Bhaskaran 2016), averaging about 5 TCs per year (Mohapatra *et al.* 2014). Despite the relatively small percentage of the total global number, the socio-economic impact of TCs in this region is much greater than those in other TC basins (Singh 2010) due to the high population density along coastlines in low-lying areas as well as physical and socioeconomic factors, particularly in

Bangladesh (Hossain and Paul 2015). Furthermore, NIO region TCs are characterized by shorter life cycles, and their development relatively close to the coast compared with other basins allows less time for preparedness. So, any improvement in the analysis and forecasting for these regions can provide significant benefits (Singh *et al.* 2012).

Recently, a potentially useful climatic relationship has been demonstrated between the stratospheric Quasi-Biennial Oscillation (QBO) and TC tracks in the Bay of Bengal region of the NIO (Fadnavis *et al.* 2014). The QBO influence is observed to be significantly stronger during the easterly phase compared to the westerly phase. Also, numbers of cyclones are higher during the easterly phase than during the westerly phase, at least during the more active pre-monsoon and post-monsoon seasons. This follows earlier research work that has also proposed relationships between the stratospheric QBO and hurricane activity in the North Atlantic region (Gray *et al.* 1992, 1994), although the use of the QBO as a predictor for North Atlantic TC activity has been discontinued in recent years (Klotzbach 2007, Camargo and Sobel 2010). Other studies have also examined the influence of the QBO on TC activity in the western North Pacific (Chan 1995; Baik and Paek 1998; Lander and Guard 1998; Ho *et al.* 2009), the eastern North Pacific (Whitney and Hobgood 1997), the North Indian Ocean (Balachandran and Guhathakurta 1999) and the South Indian Ocean (Jury 1993; Jury *et al.* 1999).

The QBO is the leading mode of variability of the tropical stratosphere. It represents a quasi-periodic (with a mean period of 28-29 months) oscillation of the equatorial easterly (E) and westerly (W) zonal winds in the stratosphere that controls the variability of the equatorial stratosphere (Baldwin *et al.* 2001). The major features of the QBO (Naujokat 1986; Baldwin *et al.* 2001) are as follows:

- Downward propagating easterly and westerly wind regimes;
- Downward propagation of westerlies is usually faster and more regular than that of easterlies;
- Transition to easterlies is often delayed between 30 and 50 hPa;
- Easterly anomalies are generally stronger (30-35 m/s) than westerly anomalies (15-20 m/s);
- Maximum amplitudes of both E and W phases typically occur near 20 hPa;
- Average periodicity is slightly greater than 2 years;
- Oscillation period and amplitude vary considerably from cycle to cycle.

The propagation of the QBO extends below the tropopause and modulates the water vapor mixing ratios in air entering the stratosphere through the cold tropical tropopause region (Zhou *et al.* 2004; Liang *et al.* 2011). The QBO has been shown to modulate tropical, deep convection (Collimore *et al.* 2003; Ho *et al.* 2009; Liess and Geller 2012), the incidence of Atlantic hurricanes (Gray 1984) and typhoon tracks in the western North Pacific (Ho *et al.* 2009). Gray (1984) pointed out an apparent influence of the QBO on Atlantic TC activity and found TC activity in the Atlantic was greater during the QBO westerly phase, or during the transition to the westerly phase, than during the easterly phase. It was found that more intense Atlantic hurricanes occurred during westerly QBO years (Gray 1984). Subsequently, the QBO influence on Atlantic hurricane activity has been discussed by other authors (Shapiro 1989; Hess and Elsner 1994; Landsea *et al.* 1998; Elsner and Kara 1999; Arpe and Leroy 2009) as a factor in a specific year's level of activity or in the general variability of the Atlantic basin. Camargo and Sobel (2010) have also explored the relationship between the QBO and TC activity in the North Atlantic. They found a statistically significant relationship from the 1950s to the 1980s but did not find a significant relationship in recent years. Camargo and Sobel (2010) also found that the QBO-TC frequency relationship was generally weak in most global TC basins. This manuscript follows in the line of Fadnavis *et al.* (2014) with a primary emphasis on TC track modulation (as opposed to TC frequency modulation) by the QBO.

This paper discusses the development of a statistical seasonal forecast model of TC genesis, track and landfall for the North Indian Ocean – incorporating the QBO index as the key predictor variable. The genesis model is based on kernel density estimation, and the tracks are estimated using a generalised additive model. The structure of this paper is as follows: The data on which the model is based and the model details are described in Section 2. The kernel density estimation for modelling the TC genesis distribution, the generalised additive model for track simulation, and country- and state-based hazard zone mapping for landfall probabilities are also described in Section 2. In Section 3 the simulation and cross-validation results from the model are presented and compared against observations. A discussion along with a summary and conclusions are provided in Section 4.

2 Data and Methods

TC genesis models using kernel densities and subsequent simulation of TC cyclone

trajectories have been developed by several researchers (Casson and Coles 2000; James and Mason 2005; Emanuel 2006; Rumpf *et al.* 2007). We adopt a similar approach for modelling TC activity in the North Indian Ocean region, following the approach of Hall and Jewson (2007) for the North Atlantic Ocean and Yonekura and Hall (2011) for the Western North Pacific region. Here we specifically consider the QBO as a predictor (excluding the influence of strong (>1.5° C SST (running 3-month mean) anomalies for the Niño 3.4 region) El Niño-Southern Oscillation (ENSO)) events. The procedure for the simulation of TC tracks can be outlined as follows. We first sample a genesis point from the kernel density model. Then the initial segment of a TC track is generated by calculating the latitudinal and longitudinal difference of TCs starting in the vicinity of this genesis point as a function of QBO phase and season. With this segment and the underlying velocity field, fitted using a generalised additive model (GAM), a new position for the simulated TC track can be found. The trajectories are based on a 7-day life span with a 6-hour time step interval. From this model, a number of synthetic but realistic storm tracks are simulated that are much larger than the number of storms provided by the historical data, and these resulting storm tracks are used to perform landfall hazard zone mapping.

2.1 TC Data

We have used data from the Joint Typhoon Warning Center (JTWC) as archived in the International Best Track Archive for Climate Stewardship (IBTrACS) version 6 for the 35-year period from 1979-2013 (Knapp *et al.* 2010). We have utilized JTWC data as opposed to the official World Meteorological Organization TC data provided by the Indian Meteorological Department, as wind estimates are not provided by the IMD until 1990. The parameters used in our analysis of TCs include date, position and wind speed. We also take into account tropical depressions that have not reached tropical storm intensity, as well as TC intensity storms (cyclone intensity storms where the one-minute sustained wind speeds are >34 knots (>17.5 m s^{-1})). We examined all available depression and tropical storm tracks, as both depressions and TC intensity storms follow similar tracks (Warrick *et al.* 2000; Mohapatra *et al.* 2012; Brian 2015). This helps to increase the overall sample size due to the relative paucity of TCs in the NIO region (Paliwal *et al.* 2011). TCs prior to 1979 are excluded from this dataset, as there is significant uncertainty in North Indian Ocean TC intensity prior to this time (Evan and Camargo

2010; Weinkle *et al.* 2012). We define the North Indian Ocean region to be bounded meridionally from 0°-30°N and zonally from 50°E-100°E (Fig.1).

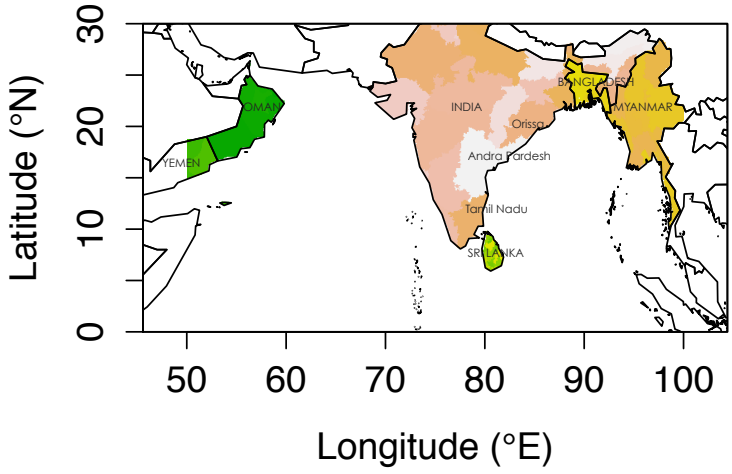

Fig.1 Map showing the countries (and states) along the North Indian Ocean rim relevant to this study. The six countries potentially affected by TC landfall are India, Bangladesh, Myanmar, Sri Lanka, Oman and Yemen. Also indicated are the three Indian states (Orissa, Andhra Pradesh, and Tamil Nadu) most strongly affected by TC landfall (Wahiduzzaman *et al.* 2016).

2.2 Quasi-Biennial Oscillation index

The Quasi-Biennial Oscillation (QBO) index is based on a time series of National Centers for Environmental Prediction (NCEP) Reanalysis zonal mean wind shear at the equator. We have calculated the QBO index as the east-west wind velocity difference between the 30hPa and 50hPa levels (30hpa-50hpa). Huesmann and Hitchman (2001) have previously compared this form of the QBO index anomalies with the Singapore index of stratospheric winds, and the NCEP index represents the QBO better than indices obtained from radiosonde observations at Singapore (Huesmann and Hitchman 2001; Ho *et al.* 2009; Fadnavis *et al.* 2011; Fadnavis *et al.* 2014). As the zonal wind shear in the lowest stratospheric layer influences near-tropopause variations, we utilize the NCEP reanalysis zonal mean wind shear anomaly time series at the equator as the preferred QBO index. The QBO index is computed for every month, and the QBO index is then defined to be either in a westerly (W-QBO) or easterly (E-QBO) phase. The easterly phase (i.e. wind shear (difference between 30hPa and 50hPa levels) is defined by a negative QBO index while a positive index denotes the westerly phase. Within a season (e.g. winter) if the index is negative for two months, we consider the QBO phase of that entire season as

being in the easterly phase. This approach is likewise adopted for the westerly (positive) phase. We have separated cyclone tracks by easterly (E-QBO) and westerly (W-QBO) phase during each cyclone season.

2.3 Methodology

A number of studies (Balachandran and Guhathakurta 1999; Camargo and Sobel 2010; Fadnavis *et al.* 2011; Yadav 2012; Fadnavis *et al.* 2014) suggest that the QBO has a notable and potentially important influence on TC frequency and track. However, Chan (1995) finds that the relationship between TCs and the QBO does not hold well during strong ENSO events. Our analysis in the present study therefore takes this into account and excludes data for previously classified strong ENSO events (either strong El Niño or strong La Niña). Years of strong El Niño and La Niña events are listed in Table 1. Only those years in which the El Niño and La Niña events are strong are considered as ENSO years, while the remaining years are assumed to be relatively ENSO-neutral for the purposes of our analysis. The years of strong El Niño and La Niña events follow the classification provided by the NOAA Climate Prediction Centre (http://www.cpc.ncep.noaa.gov/products/analysis_monitoring/ensostuff/ensoyears.shtml).

Table.1 Years of strong El Niño and La Niña during the study period (1979–2013), classified by the NOAA CPC based on the Oceanic Niño Index (http://www.cpc.ncep.noaa.gov/products/analysis_monitoring/ensostuff/ensoyears.shtml) - the running 3-month mean SST anomaly for the Niño 3.4 region (i.e., 5°N-5°S, 120°-170°W). Events are defined as 5 consecutive overlapping 3-month periods at or above the +0.5°C anomaly for warm (El Niño) events and at or below the -0.5°C anomaly for cold (La Niña) events. The threshold is further broken down into Weak (with a 0.5° to 0.9° SST anomaly), Moderate (1.0 ° to 1.4 °), Strong (1.5° to 1.9 °) and Very Strong (≥ 2.0°) events.

Year	ENSO Event	Year	ENSO Event	Year	ENSO Event
1979		1991	Strong El Niño	2002	
1980		1992	Strong El Niño	2003	
1981		1993		2004	
1982	Strong El Niño	1994		2005	
1983	Strong El Niño	1995		2006	
1984		1996		2007	
1985		1997-98	Strong El Niño	2008	

1987		1999	2010	Strong El Niño
1988	Strong La Niña	2000	2011	
1989	Strong La Niña	2001	2012	
1990		2002	2013	

A few studies have investigated the frequency and tracks of TCs in the Bay of Bengal and their relationship with the QBO (Balachandran and Guhathakurta 1999; Fadnavis *et al.* 2011; Fadnavis *et al.* 2014), but no previous study that we are aware of has developed a statistical forecast model to simulate and forecast TC tracks as well as provide probabilistic forecasts of landfall months in advance. Here, we have developed a statistical seasonal forecast model of TC genesis, tracks and landfall in the North Indian Ocean region for four seasons, utilising the QBO as a predictor. The four seasons are defined as follows: winter (December-February), pre-monsoon (March-May), monsoon (June-September), and post-monsoon (October-November). The QBO index used in this study is smoothed using a 3-month running average, and then a 1 to 6 month lead-lag analysis is performed to assess the best predictor timescale based on TC forecast skill. Using a 30-year record of TC track observations (1980-2009) and QBO data extending also one-year prior (1979-2009), the distribution of cyclone genesis points is approximated by kernel density estimation (Section 2.3.1), and the paths of the subsequent cyclone tracks are simulated by modelling the velocity along the observed cyclone tracks as smooth functions of location in each phase and season using a generalised additive model (GAM) (Section 2.3.2). Trajectories are then simulated by first randomly selecting genesis points from the fitted kernel density estimates, and then tracing the cyclonic paths from the fitted velocity fields, with randomised innovations at every step to determine the point of landfall. The model results have been cross-validated (Section 2.4) and assessed to estimate hindcast skill (Section 2.5). Several years of independent forecasts (2010-13) have also been assessed for skill.

2.3.1 TC genesis: Kernel Density Estimation

We have applied a kernel density approach to model the spatial distribution of observed TC genesis locations in each QBO phase and TC season. This approach has been successfully used previously in a variety of studies including those by Vickery *et al.* (2000), James and Mason (2005), Emanuel *et al.* (2006), and Rumpf *et al.* (2007). Kernel density estimation is a method to estimate the probability density function (PDF) of a

random variable in a non-parametric way. This distribution is defined by a smoothing function and a bandwidth value that controls the smoothness of the resulting density curve. The details of the kernel density estimation are explained in the appendix. In our analysis, we calculate the kernel bandwidth for the kernel density function using a standard plug-in estimator. This approach has been shown to be a simple but effective method (Rigollet and Vert 2009) for estimating relevant bandwidths and makes for pragmatic calculations. Hence, our modelled distribution of genesis points is represented by the kernel density estimation, in effect as a probability distribution (function) across the TC genesis observations.

To define the genesis locations, we determined the time and position along each track that the TC exceeded 34 knots, which we take as the definition of the transition to TC strength (WMO 1997). It was found that 9% of all genesis locations were in close proximity to the coast and were therefore restricted by the masked kernel density. Kernel density estimation places a Gaussian kernel of specified bandwidth over each observation and sums all of the kernels together. The distribution of genesis points as a function of QBO phase and/or season is approximated by kernel density estimation. Samples are drawn from the kernel by treating the estimate as a Gaussian mixture - first a component of the mixture is chosen and then a sample deviate is drawn from that component of the mixture. In the absence of any modification, simple application of the kernel estimator enables TC genesis over land which is most apparent for longer smoothing (bandwidth) scales. To address this issue, we restricted genesis to ocean regions by masking the kernel density function over land areas and choosing to reject any points generated above a threshold water depth of 200m.

2.3.2 TC tracks: Generalised Additive Model

Cyclone trajectories were modelled by fitting a GAM to the incremental track velocities. GAMs are a generalisation of linear regression in which the linear terms are replaced by smooth transformations of the predictors (Hastie *et al.* 2009). In linear regression models, the expected value μ of the response or dependent variable Y is modelled as a linear combination of the predictor variables $X_1, X_2, \ldots, X_p$,

$$\mu = E(Y|X_1, X_2, \ldots, X_p) = \beta_0 + \beta_1 X_1 + \beta_2 X_2 + \cdots \beta_p X_p.$$

where $\beta_0, \beta_1, \ldots, \beta_p$ are regression coefficients to be estimated. In a generalised additive model, the linear terms are replaced by smooth transformations of the predictors

$$\mu = E(Y|X_1, X_2, \ldots, X_p) = \beta_0 + f_1(X_1) + f_2(X_2) + \cdots f_p(X_p).$$

Hence, where linear regression estimates the regression coefficients $\beta_0, \beta_1, \ldots, \beta_p$, the GAM estimates the smooth transformations $f_1, f_2, \ldots, f_p$. Typically, these functions are estimated by smoothing and do not have an easily represented parametric form. The GAM is explained in more detail in the appendix.

Individual storms are incremented uniformly in time to estimate the storm track velocities along their tracks, and the GAM is fitted to each velocity component in the *x* (east) and *y* (north) directions, to allow the vector velocity field to be modelled as a function of QBO phase and season. Simulated cyclone trajectories are generated by using the fitted GAM to predict mean increment velocities at each step along the track. For each combination of season and QBO phase, simulated cyclone genesis points represent random selections from the estimated kernel (Section 2.3.1). Based on the mean vector field estimated by the GAM, an Euler step was used to project trajectories forward in time from this initial location. A stochastic innovation was added at each time step to account for the variable nature of the vector field that was not captured by the GAM with a variance determined by the residual error variance of the GAM fit. For each simulated genesis point, 50 trajectories were simulated 7 days forward in time with a 6-hourly time increment. We consider a 7-day lifetime as a reasonable choice for the model based on the fact that approximately 80% of NIO region TC lifetimes are less than 7 days (Wahiduzzaman *et al.* (2016).

2.3.3 Landfall locations

Multiple landfalls are rare in the NIO region (Evan and Camargo 2010; Weinkle *et al.* 2012; Alam and Dominey-Howes 2015), and consequently we have only considered the first point of landfall for this region. To determine the positions of landfall, a fine scale raster mask (1/12°) of the North Indian Ocean rim countries was first constructed. Then, for each TC, we traced along the trajectory to detect the first point where the TC struck land. We also recorded the country and state in which landfall occurred. The first time

and location crossing of the land mask was taken to be the point of landfall.

One limitation of this approach is that it only records the first point of landfall. For the case that a cyclone first crossed the land mask boundary for the small Andaman or Nicobar Islands, these islands would be recorded as the point of landfall, even though the cyclone may carry on to strike elsewhere. This is a limitation of the model in its basic form. We have removed the islands from the mask which allows the cyclone tracks to continue. However, the islands remain on the geographical map for reference.

2.2.3.1 2.3.4 Model validation

To assess the integrity and potential utility of the model, we have applied two separate validation methods. These are introduced as follows:

2.3.4.1 Validation method 1

Leave-one-out cross validation (LOOCV) was performed by removing each track in turn and then simulating the trajectories corresponding to the deleted tracks based on a model fit to the reduced data set. For each track we predicted the state/country by majority vote from the simulated tracks (where the highest percentage of tracks made landfall).

2.3.4.2 Validation method 2

We also evaluated the model by calculating the distance between the observed and simulated landfall points in tracks generated from the observed genesis points. Each landfall from a simulated track was measured against the observed track to find the location of simulated landfall and calculated as the distance from the observed location of landfall. The frequency of simulated TC landfall is presented as a function of distance between the simulated and observed locations.

2.4 Best predictor timescale for TC forecast potential

We assessed the best predictor timescale based on a lead-lag analysis between the QBO index and the TCs by considering two approaches to assess the overall model skill. The first approach was based on LOOCV. The second approach was based on the distance between the observed and simulated landfall points. For each lead-lag period, the percentages of TC landfall that fell within this range are provided in Table 2. The highest percentage (68%) is seen for a 3-month lead of the QBO predictor. We therefore use this QBO 3-month lead for the remainder of our analysis.

1993 **Table 2.** For each lead month around the NIO rim, the percentage of simulated TCs that
1994 made landfall within 500 km of the observed location. The bold number highlights the
1995 best lag based on percentage of TC landfall.

Lead (Months)	TC landfall (percentage)
1	8
2	35
3	**68**
4	64
5	46
6	31

1996

1997 We also calculated these results independently for each country (Table 3). Simulations of
1998 TC landfall using a 3-month lead QBO predictor compares well against observations and
1999 is consistent with the country-independent results presented in Table 3. For Myanmar, the
2000 simulated number of TCs is not well matched against observations, except at the 3-month
2001 lead. Considering the results overall, we chose a 3-month lead QBO as the predictor for
2002 our forecast model.

2003 **Table 3.** For each QBO predictor lead in months (ahead of the TC season), we show here
2004 the observed and simulated number of TCs that made landfall in each country. The bold
2005 number highlights the best lag for each country.

Country*	Observed landfall	Lead month-1	Lead month-2	Lead month-3	Lead month-4	Lead month-5	Lead month-6
IND	40	34	63	51	63	49	**37**
BAN	7	**3**	1	**3**	1	0	13
SRI	4	0	1	**2**	1	8	0
YEM	0	0	0	3	1	0	0
OMN	3	1	**2**	8	15	10	1
NON	40	18	16	25	20	**34**	16

2006

*IND=India; MYN=Myanmar; BAN=Bangladesh; SRI=Sri Lanka; YEM=Yemen; OMN=Oman; NON=No landfall and/or landfall in other countries that are not considered in this model.

3. Results

3.1 Genesis and track model fits as a function of QBO phase

The observed distribution of TC genesis points appears to have a clear dependence on the QBO phase (Fig.2), with a higher frequency of total genesis occurrences observed during the easterly QBO phase (60% of the total) than in the westerly QBO phase (40%), in keeping with the findings of Fadnavis *et al.* (2014). A comparison of the observed TC tracks between the two QBO phases (Fig.2) also shows further differences. Specifically, it is seen that during the easterly QBO phase, more TCs make landfall in the southwestern part of the Bay of Bengal (Tamil Nadu and Andhra Pradesh in India), the southwestern part of Bangladesh (Khulna), and along the northwestern part of India (near the Pakistan border). Landfall occurrence in Oman from TCs tracking across the Arabian Sea also occurs in the easterly QBO. Conversely, during the westerly QBO phase, more TCs make landfall in the north and northeastern portions of the Bay of Bengal, specifically the southeastern part of Bangladesh (Chittagong) and Myanmar.

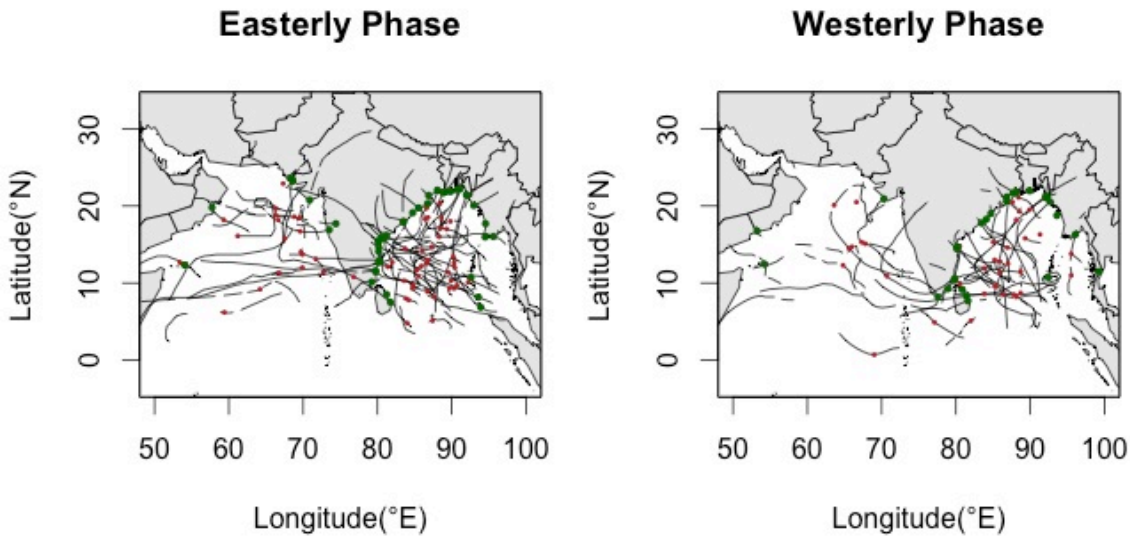

Fig.2 Observed TC genesis, tracks, and landfall over the North Indian Ocean (0° to 30°N and 50° to 100°E) for the easterly (left panel) and westerly (right panel) phases of the QBO from 1980-2009. Red dots identify the TC genesis points and black lines indicate the TC tracks, with the recorded locations of landfall indicated as a green dot.

The modelled distribution of TC genesis points, approximated by kernel density estimation, is shown for each QBO phase in Fig. 3. Highest densities are found in the Bay of Bengal for each phase of the QBO (consistent with the observed genesis locations seen in Fig. 2). Marginally higher genesis densities are found in the easterly QBO phase than in the westerly QBO phase. For both the easterly and westerly QBO phases, the highest density of genesis is seen in the latitudinal range from 8-15°N for the Bay of Bengal, whereas there are two lower density spatial peaks identifiable in the Arabian Sea for the easterly QBO phase and one in the westerly QBO phase.

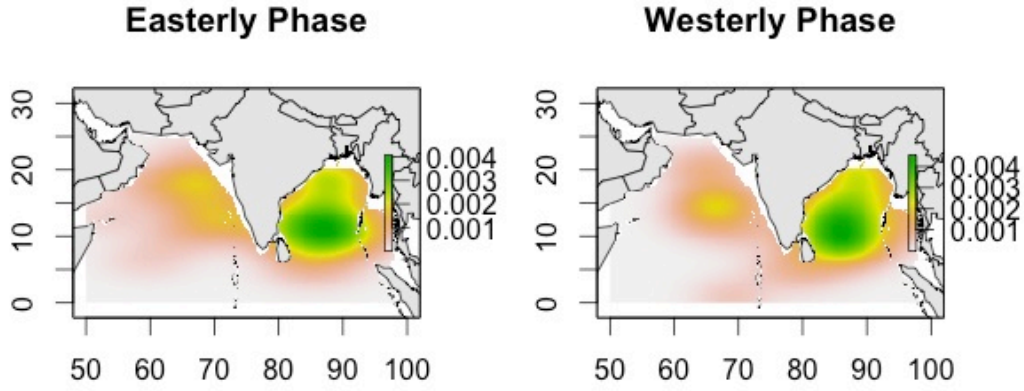

Fig.3. Modelled distributions of TC genesis locations based on kernel density estimates across the observations in the North Indian Ocean region (0° to 30°N and 50° to 100°E) for the easterly (left panel) and westerly (right panel) QBO phases, based on data from 1980-2009. The green colour shows the highest density (concentration of TC numbers/km^2) area of genesis.

For each country around the NIO rim, the total number of TCs that made landfall as a function of QBO phase are provided in Table 4. A total of 35 cyclones made landfall in the easterly QBO phase compared with 26 in the westerly QBO phase. India had the highest frequency of TC landfalls for any NIO rim country in both easterly and westerly QBO phases, but with a higher overall number of landfalling TCs in easterly QBO phases (25) compared with westerly QBO phases (15). All other countries have relatively few TC landfalls overall, so it is hard to make too many broad statements about differences in TC landfall based on QBO phases.

Table 4. Observed total numbers (and percentage) of TCs that made landfall as a function of QBO phase for each NIO rim country. Looking along a row, and thus across the columns, we can see how the landfall rates vary by QBO phase for a single country (%$^{\#}$). Alternatively, looking down a column and thus across the rows we can see how landfall

rates vary by country for a particular QBO phase (%*). For each country, the phase with the highest landfalls in that country is indicated by bold percentages. For each phase, the country with the highest landfalls in that phase is indicated by bold with underlined percentages.

Country	Easterly QBO Phase			Westerly QBO Phase		
	No	* (%)	# (%)	No	* (%)	# (%)
India	25	**63**	**<u>41</u>**	15	38	**<u>38</u>**
Myanmar	3	43	5	4	**57**	10
Bangladesh	4	**57**	7	3	43	8
Sri Lanka	1	25	2	3	**75**	8
Yemen	0	0	0	0	0	0
Oman	2	**67**	3	1	33	3
Total landfall	35	57	57	26	43	65
NON*	26		43	14		35
Total	61		100	40		100

* No landfall and/or landfall in other countries that are not considered in this model

There is a difference in the time from genesis to landfall observed between the QBO phases (Fig. 4). Corresponding to the easterly QBO phase, we found that landfall tends to

occur with the greatest likelihood around 3-4 days after genesis (22% of the time). In contrast, we found that the highest percentage of time periods from genesis to landfall was around 2-3 days, followed by a second peak at 4-5 days in the westerly QBO phase.

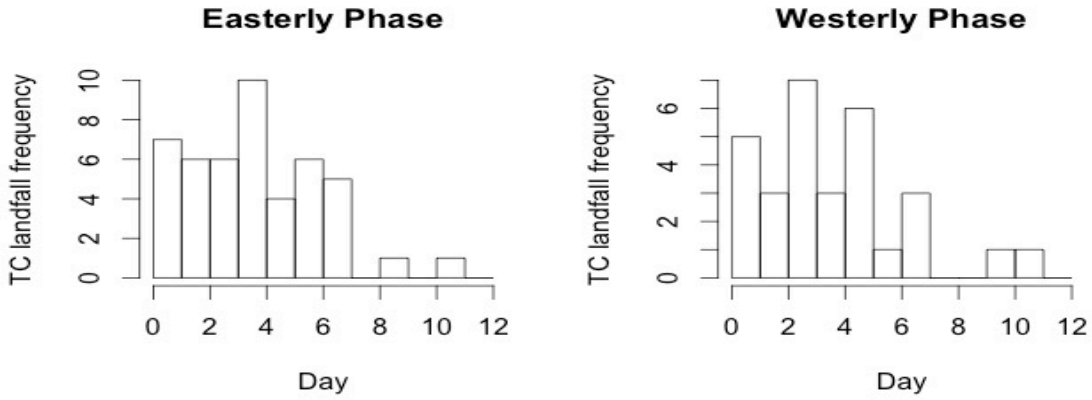

Fig.4. Observed TC landfall frequency in the North Indian Ocean region (0° to 30°N and 50° to 100°E) as a function of the number of days from genesis to landfall (1980-2009) for each QBO phase.

The GAM fit to the observed TC tracks acts to smooth estimates of the TC velocities as a function of phase of the QBO. The direction of cyclone movement in each QBO phase is displayed in Fig. 5. During the easterly QBO phase, the velocity field indicates westward to northward movement in the Bay of Bengal. In the Arabian Sea, velocities are mostly westward with a northward tendency in the northern portion of the basin. In the westerly QBO phase, the GAM-fitted TC velocity vectors indicate northward and north-eastward movement over the Bay of Bengal and mostly north-westward movement over much of the Arabian Sea.

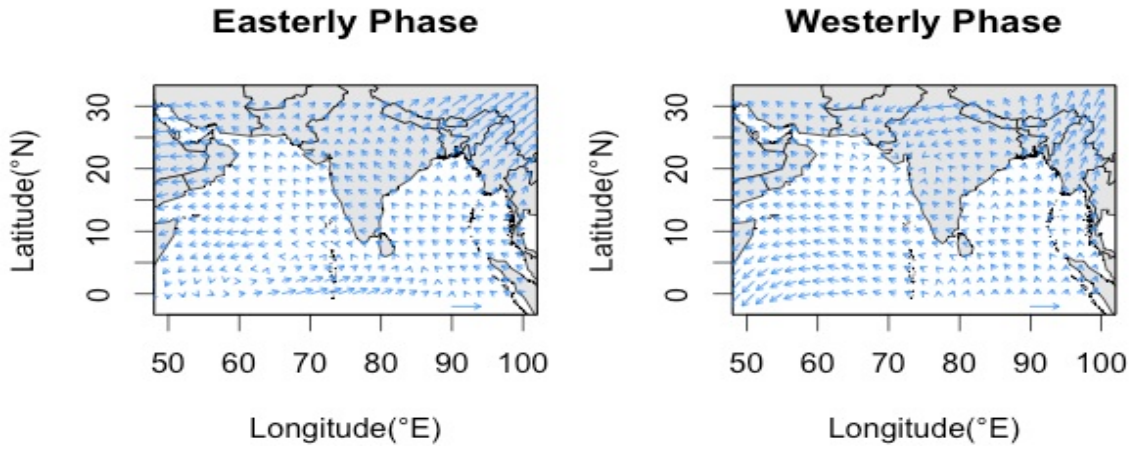

Fig.5. Distribution of fitted TC track velocities (data from 1980-2009) for each QBO phase across the North Indian Ocean estimated using a generalised additive model. The length of the reference arrow corresponds to velocity magnitudes of 10 ms^{-1}.

3.2 Simulated cyclone tracks and landfall locations

Model simulated cyclone tracks and landfalls are shown in Fig. 6. In the easterly QBO phase, TCs tend to track northwestward with most of them make landfall along the coast of the western Bay of Bengal and a greater number making landfall in India than in the westerly QBO phase. In the Arabian Sea, Oman and northwest India are modelled to receive the greatest number of landfalls. During the westerly QBO phase, it is seen that TCs tend to track towards the north and northeast over the Bay of Bengal with a preferred tendency to make landfall along the Orissa coast in India and Chittagong in Bangladesh and Myanmar. Over the Arabian Sea, TCs tend to move west with a preferred tendency to make landfall in Oman.

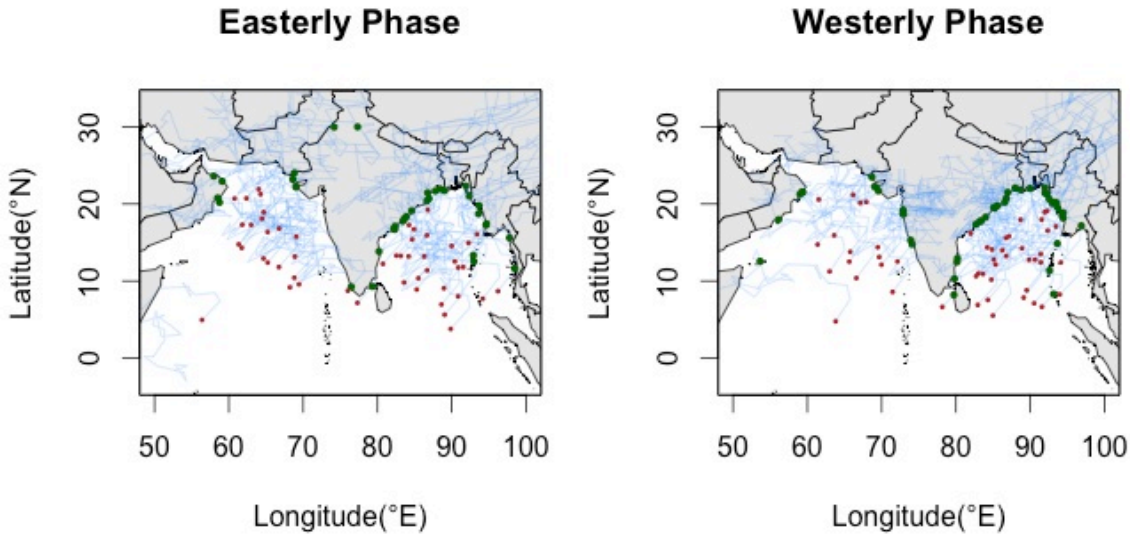

Fig.6. Simulation of TC tracks and landfall across the North Indian Ocean region as a function of QBO phase. A total of 50 TC genesis points were randomly selected from the modelled kernel, and the TC tracks were simulated using the pre-fitted generalised additive model combined with the random innovations. Red dots show the TC genesis points, blue lines indicate the TC tracks, and green dots show landfall locations.

The simulated percentage of TCs that make landfall as a function of QBO phase are provided in Table 5 for each country in turn. In the easterly QBO phase, the highest percentage of simulated TC landfall occurrences are in India and Oman. Conversely, during the westerly QBO phase, Bangladesh, Myanmar and Sri Lanka are modelled to

have higher frequency of landfall occurrences. Yemen has no TC landfall in each QBO phase. Variations in simulated landfall rates by country for a particular QBO phase are also shown in Table 5 (#%). In both QBO phases, 60% of simulated TCs made landfall (20 TCs made no landfall or landfall in other countries/island that is not considered into model), almost similar with the observed value of 61%. In the easterly QBO phase, it is seen that 38% of all simulated TCs made landfall in India with the second highest percentage landfall strike rate of 8% each into Oman and Myanmar. There is a simulated landfall rate of 6% in Bangladesh, and no recorded landfall in Sri Lanka and Yemen. In the westerly QBO phase, India was struck by almost half (46%) of the total simulated landfalling TCs. Myanmar received the second highest percentage of simulated landfall occurrences (12%). A total of 10% of the model simulated TCs made landfall in Bangladesh, 2% in Sri Lanka and 4% for Oman.

Table 5. ***GAM-fitted*** total numbers (and percentage) of TCs that make landfall as a function of QBO phase are displayed for each country along the NIO Rim. By looking along a row, and thus across the columns, fluctuations in landfall rates based on QBO phase for a single country (%*) are displayed. Alternatively, by looking down a column and thus across the rows, we can see how landfall rates vary by country for a particular QBO phase (%#). Maxima are in bold and underlined. Format is the same as in Table 4.

Country	Easterly Phase			Westerly Phase		
	No	* (%)	# (%)	No	* (%)	# (%)
India	19	**54**	**38**	16	46	**32**
Myanmar	4	40	8	6	**60**	12
Bangladesh	3	38	6	5	**62**	10
Sri Lanka	0	0	0	1	**100**	2
Yemen	0	0	0	0	0	0

Oman	4	**67**	8	2	33	4
Total landfall	30		60	30		60
NON*	20		40	13		40
Total	50		100	50		100

*No landfall and/or landfall in other countries that is not considered into model

Fig. 7 shows the frequency distribution of simulated times in days from TC genesis to landfall for each QBO phase. A slightly higher percentage of TCs make landfall 0-1 day after genesis in the westerly phase than in the easterly phase. In general, TCs generated in the westerly phase of the QBO make landfall more rapidly after genesis than in the easterly phase.

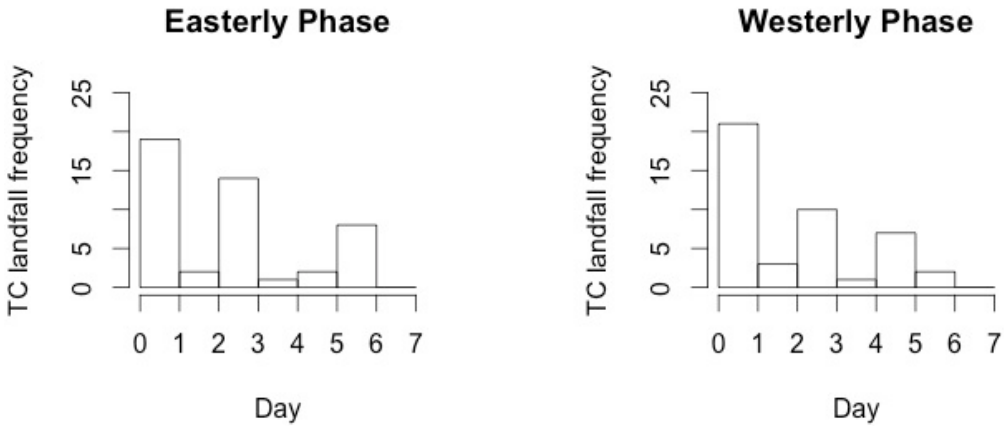

Fig.7. Model simulated frequency of TC landfall rates for each QBO phase, measured as days from genesis to landfall, within the North Indian Ocean region (0°- 30°N and 50° - 100°E).

Fig. 8 shows the geographic distribution of model simulated percentage probabilities of TC landfall by state across the NIO rim for both QBO phases. For the easterly QBO phase, Andhra Pradesh in India is modelled to have the highest percent simulated landfall probability, followed by the state of Orissa in India and then Myanmar. The state of Gujarat in India (bordering the northeast Arabian Sea) exhibits a larger percentage probability of simulated TC landfall during the westerly QBO phase. The model simulates the highest percentages of TC landfall during the westerly QBO phase in Myanmar, followed by Orissa, Andhra Pradesh, and Gujarat.

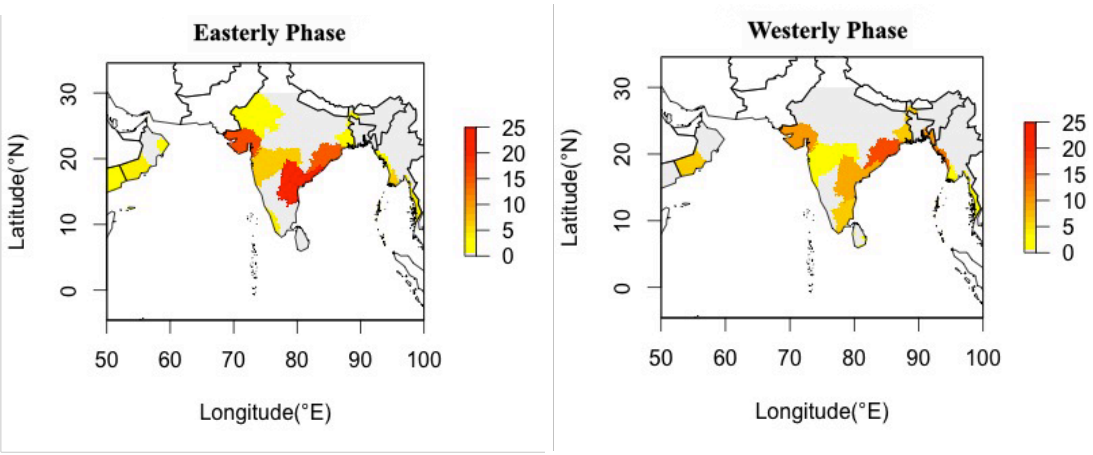

Fig.8. Geographic distribution of model simulated percentage probabilities of TC landfall by state across the NIO rim for both QBO phases. Colours range from yellow to red (as a percentage) indicating the lowest to highest model simulated percentage probabilities of TC landfall. Grey indicates no landfalls.

3.3 Genesis and track model fits as a function of both QBO phase and season

The QBO influence is observed to be significantly stronger across most NIO region TC seasons during the QBO easterly phase as compared to the westerly phase. The total number of observed cyclones is higher during the easterly QBO phase (61) than during the westerly QBO phase (40). The highest genesis occurrences are seen in the post-monsoon season for both phases of the QBO. In easterly QBO phases, 39% of genesis events occur in the post-monsoon season, whereas in westerly QBO phases, 50% of genesis events occur in the post-monsoon season. During easterly QBO phases, 21% of genesis events occur in the monsoon season, with both the winter and pre-monsoon seasons generating 20% of all genesis events. In westerly QBO phases, 25% of genesis events occur in the winter, followed by the pre-monsoon season (18%). Only 8% of genesis events occur during the monsoon season in the westerly QBO phase (Table 6).

Table 6. Observed total numbers (and percentage) of NIO region TC genesis occurrences as a function of QBO phase for each season. By looking along a row, and thus across the columns, we can see how the TC genesis occurrences vary by QBO phase for a single TC season (%*). Alternatively, by looking down a column, and thus across the rows, we can see how TC genesis occurrences vary by season for a particular QBO phase (%$^{\#}$). For each season, the phase with the highest genesis for the NIO Rim is indicated by bold percentages. For each phase, the season with highest genesis in that season is indicated by

2181 bold with underlined percentages.

Season	Easterly Phase			Westerly Phase		
	No	%*	%#	No	%*	%#
Winter	12	**55**	20	10	45	25
Pre-monsoon	12	**63**	20	7	37	18
Monsoon	13	**81**	21	3	19	8
Post-monsoon	24	**55**	**39**	20	46	**50**
Total	61		100	40		100

2182

2183 Fig. 9 displays how TCs have tracked and where they have made landfall for each season
2184 and QBO phase. In the winter season and in the easterly QBO phase, cyclones in the NIO
2185 region tended to track westward, with most of them made landfall along the Tamil Nadu
2186 coast in India. In contrast, during the westerly QBO phase, TCs tended to track in a north-
2187 eastward direction over the NIO, with most of them making landfall in Myanmar. In the
2188 pre-monsoon season, cyclones tended to track northward and north-eastward where they
2189 make landfall in Andhra Pradesh in India, Chittagong in Bangladesh during the easterly
2190 QBO phase during the westerly QBO phase, whereas they tended to track north-eastward
2191 and make landfall into south-east Bangladesh and Myanmar (eastern boundary of the Bay
2192 of Bengal). In the monsoon season, cyclones tended to track westward and made landfall
2193 along the Orissa and Gujarat coasts in India as well as Oman during the easterly QBO
2194 phase whereas the small number of observed cyclones typically tracked west to north-
2195 westward and made landfall in the state of west Bengal in India during the westerly QBO
2196 phase. Finally, in the post-monsoon season, cyclones have been observed to preferentially
2197 track north-westward to make landfall along the Tamil Nadu, Andhra Pradesh and West
2198 Bengal coasts in India during the easterly QBO phase, whereas cyclones tend to more
2199 preferentially track northward during the westerly QBO phase and made landfall in
2200 Orissa, India and Bangladesh.

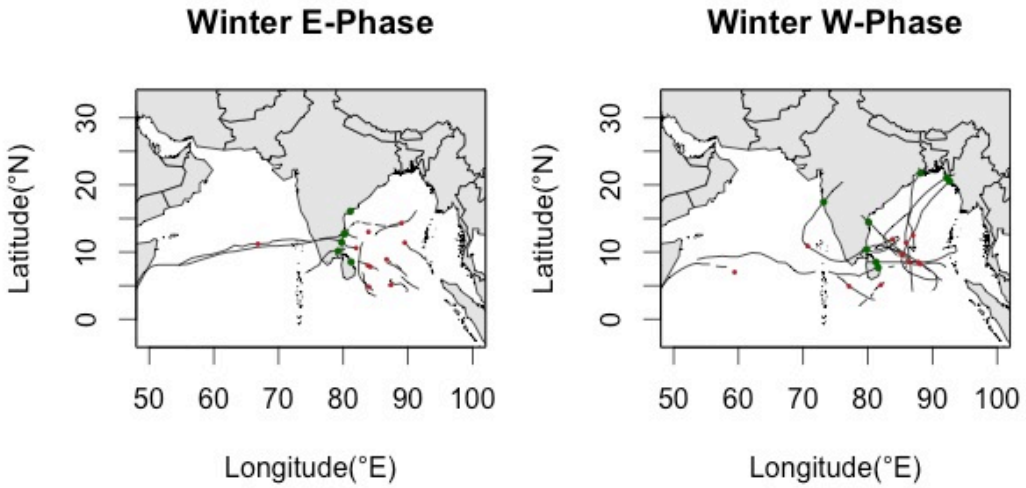

2201

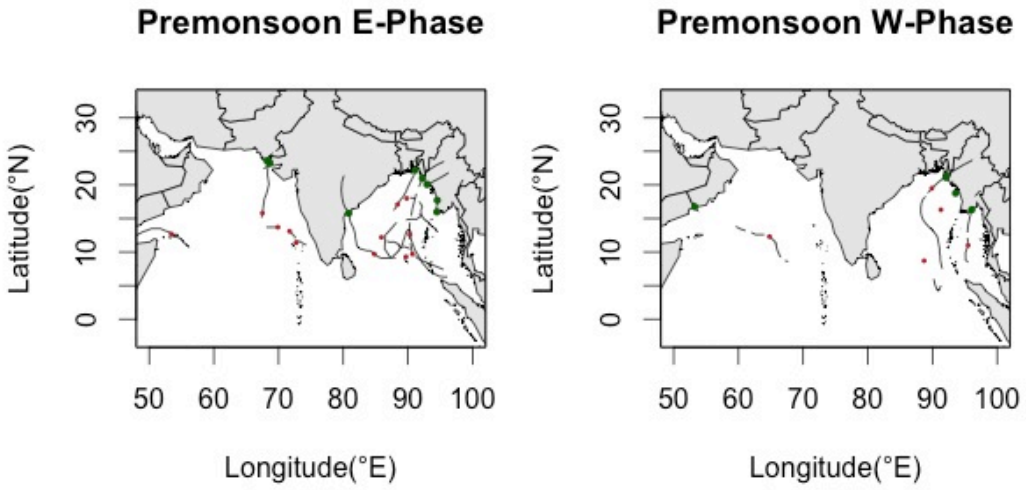

2202

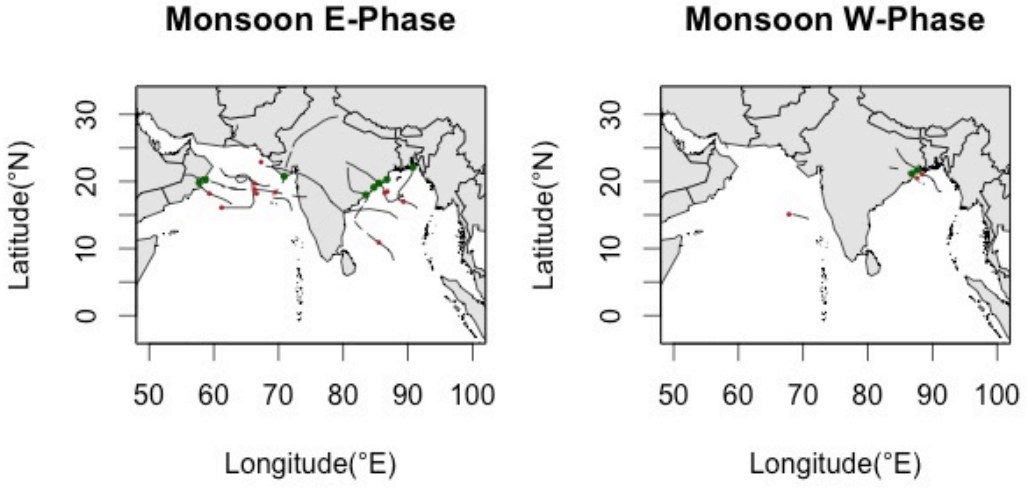

2203

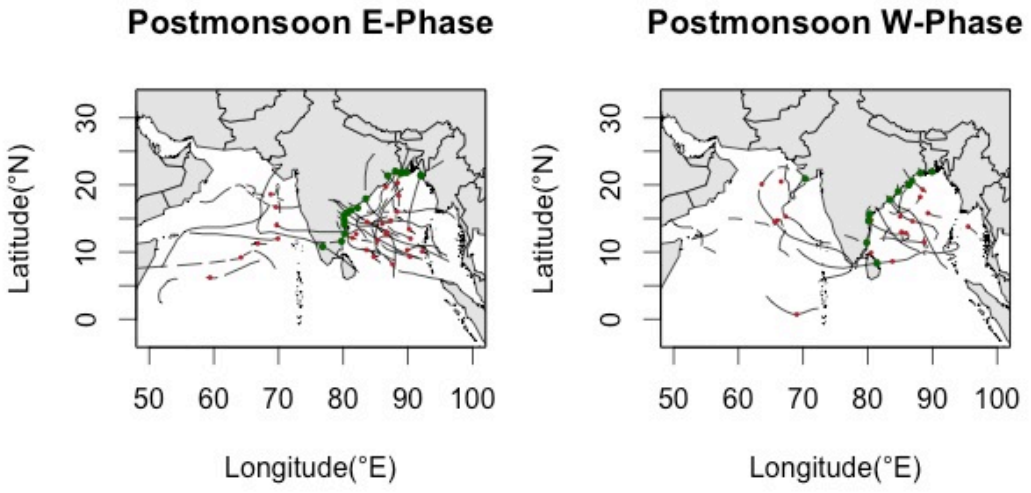

Fig.9 Observed TC genesis, tracks and landfall over the North Indian Ocean for the easterly QBO phase (E-Phase) in each of four seasons (left panels), and westerly QBO phase (W-Phase) in each of four seasons (right panels). Red dots identify the TC genesis points in the North Indian Ocean region (0° to 30°N and 50° to 100°E) from 1980-2009. The blue lines indicate the observed TC tracks, with the recorded locations of landfall indicated as green dots.

The modelled joint distributions (TC season and QBO phase) of TC genesis locations, based on kernel density estimates of the observed TC genesis occurrences recorded in the North Indian Ocean region, are shown in Fig. 10. Highest genesis densities are typically found in the Bay of Bengal, except for during the westerly QBO phase in the monsoon season (consistent with the observed genesis locations seen in Fig. 9). In the winter season, the highest genesis densities are estimated to be closer to 5-14°N in the Bay of Bengal during the easterly QBO phase, while the highest genesis densities are estimated from 8-11^{0}N in the Bay of Bengal and from 10-12^{0}N in the Arabian Sea during the westerly QBO phase. Genesis tends to take place slightly farther southwest in easterly QBO phases than in westerly QBO phases. In the pre-monsoon season, the highest genesis densities are found from 10-15° N in the Bay of Bengal and Arabian Sea during the easterly QBO phase and from 10-20°N during the westerly QBO phase. TCs tend to form closer to the coast in the pre-monsoon season in the westerly QBO phase. In the monsoon season, the highest genesis densities are seen from 18-20°N for the Bay of Bengal and 17-19°N for the Arabian Sea in the easterly QBO phase, while the highest densities are estimated from 14-16°N in the Arabian Sea during the westerly QBO phase. This northward shift during the monsoon season is due to the large-scale monsoon circulation and associated position of the monsoon trough. In the post-monsoon season, the highest genesis densities are estimated from 10-15°N in the Bay of Bengal for both

QBO phases and from 13-15°N in the Arabian Sea during the westerly QBO phase. A more distinct preference for TC formation in the Arabian Sea is noted in the westerly QBO phase than in the easterly QBO phase.

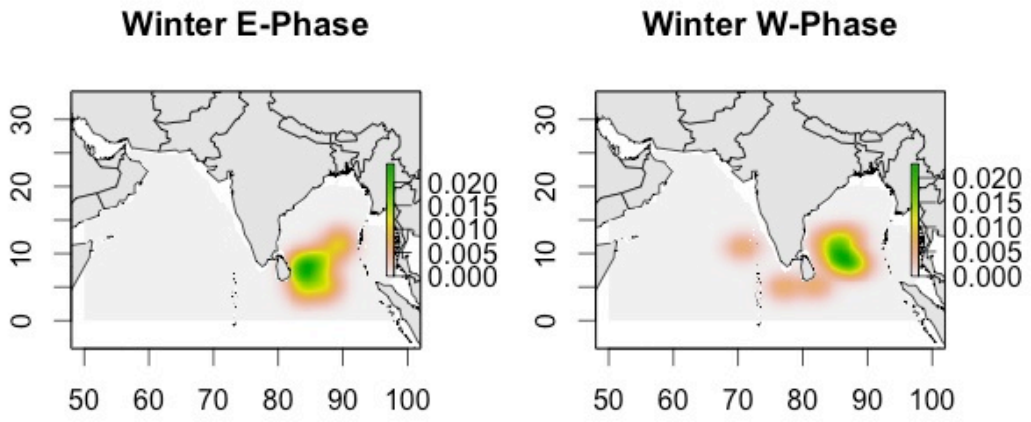

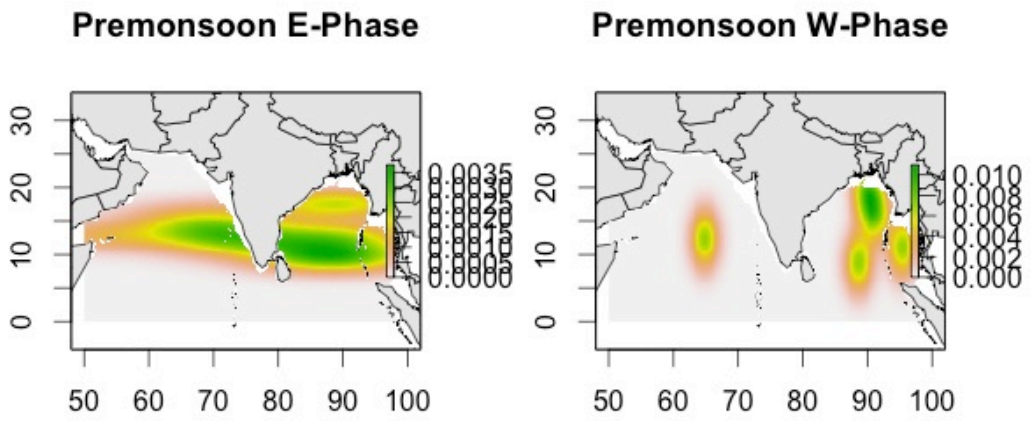

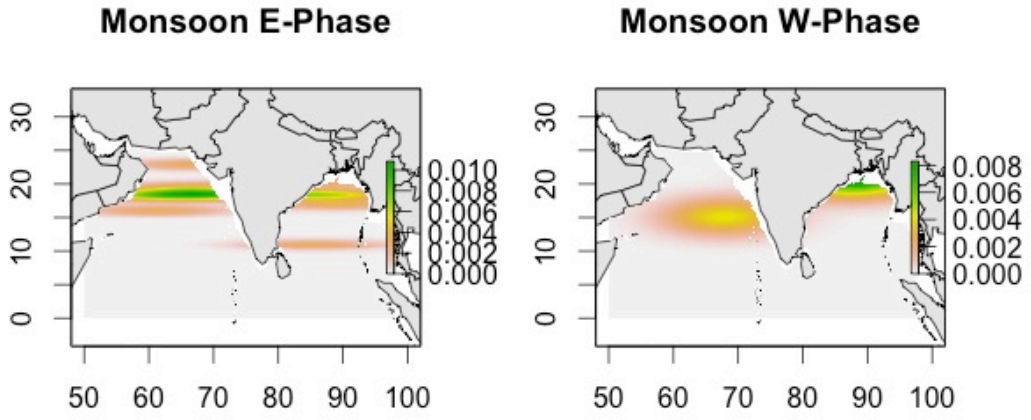

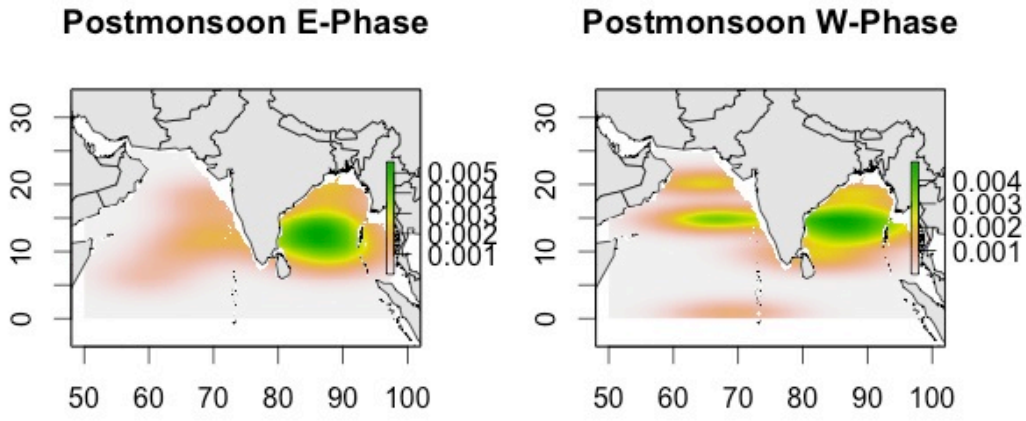

Fig.10 Modelled joint distributions (season and QBO phase) of TC genesis locations based on kernel density estimates of the observed TC genesis occurrences recorded in the North Indian Ocean region (0° to 30°N and 50° to 100°E), for both the easterly QBO phase (E-Phase) (left panels) and westerly QBO phase (W-Phase) (right panels) (strong ENSO years removed), based on data from 1980-2009. The green colour shows the highest density (concentration of TC numbers/km^2) area of genesis.

As reported earlier, a generalised additive model was fit to each velocity component of the observed TC tracks to generate a smoother and more complete velocity field over the entire domain. This was undertaken independently for each season and jointly with each phase of the QBO (Fig. 11). In the winter season, the fitted velocity field shows the westward flow field south of 15°N in the Bay of Bengal and Arabian Sea but their direction changes (north of 15°N) towards the northeast in the Bay of Bengal and towards the west-northwest in the Arabian Sea for the winter season corresponding to the easterly QBO phase. In contrast, the fitted velocity field shows the northwestward flow field (movement) in the Bay of Bengal south of 15°N before recurving towards the northeast during the westerly QBO phase, while mostly westward flows are modelled for the Arabian Sea, For the pre-monsoon season, during the westerly QBO phase the flow is mostly northward in the Bay of Bengal and westward and less variable in the Arabian Sea whereas the GAM-fitted velocity field shows a mostly northward flow in the Bay of Bengal and a westward flow, albeit highly variable, in the Arabian Sea during the easterly QBO phase. In the monsoon season, the velocity field predominantly shows a north-westward flow across the NIO region during both QBO phases. Finally, in the post-monsoon season, during the easterly QBO phase, predominately westward flows are seen, except north of 17°N where northward flow is visible for the Bay of Bengal, and eastward flow is seen for the northern portion of the Arabian Sea. In contrast, the GAM-fitted

velocity field shows westward, northward and north-westward flow over the Bay of Bengal and Arabian Sea during westerly QBO phase.

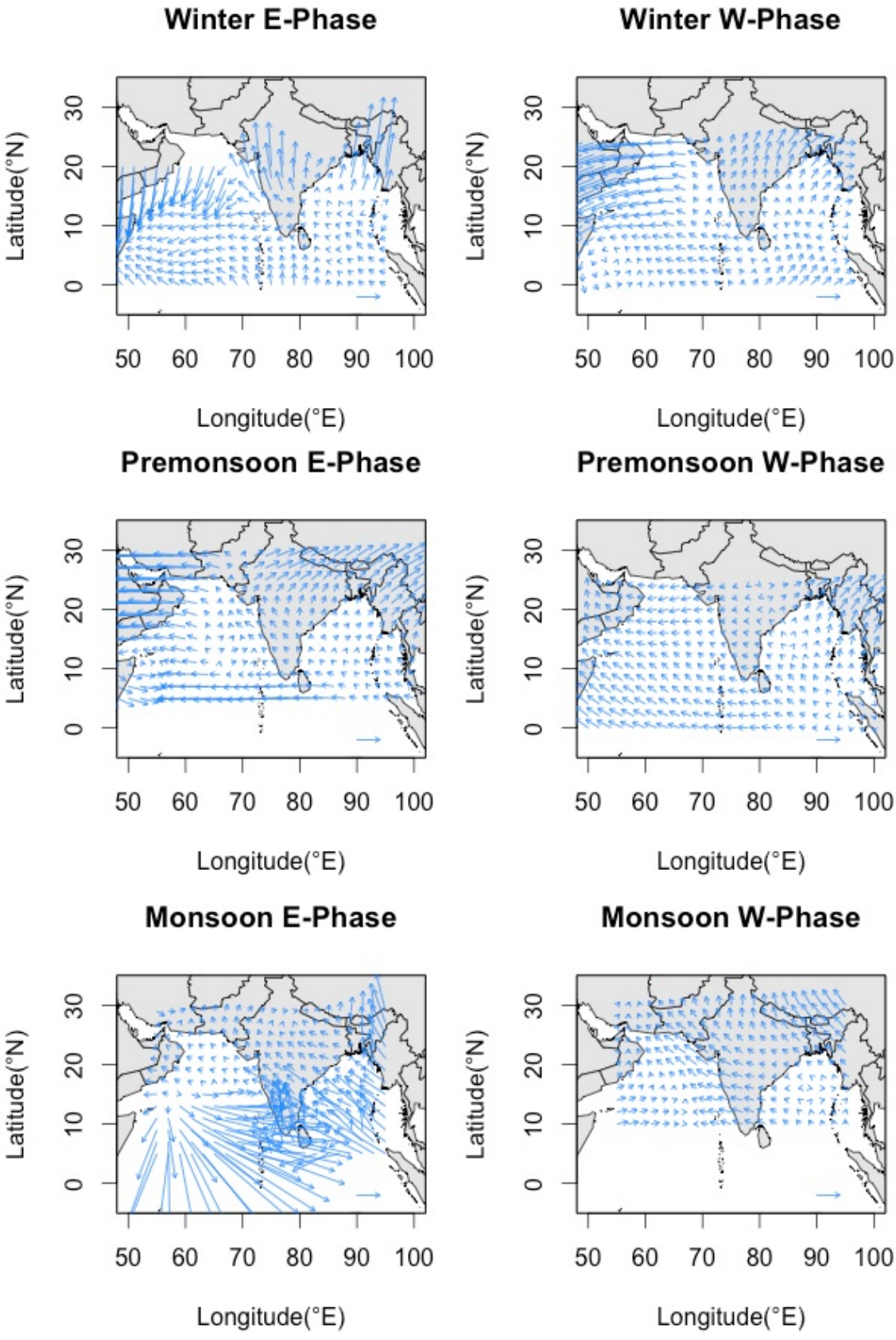

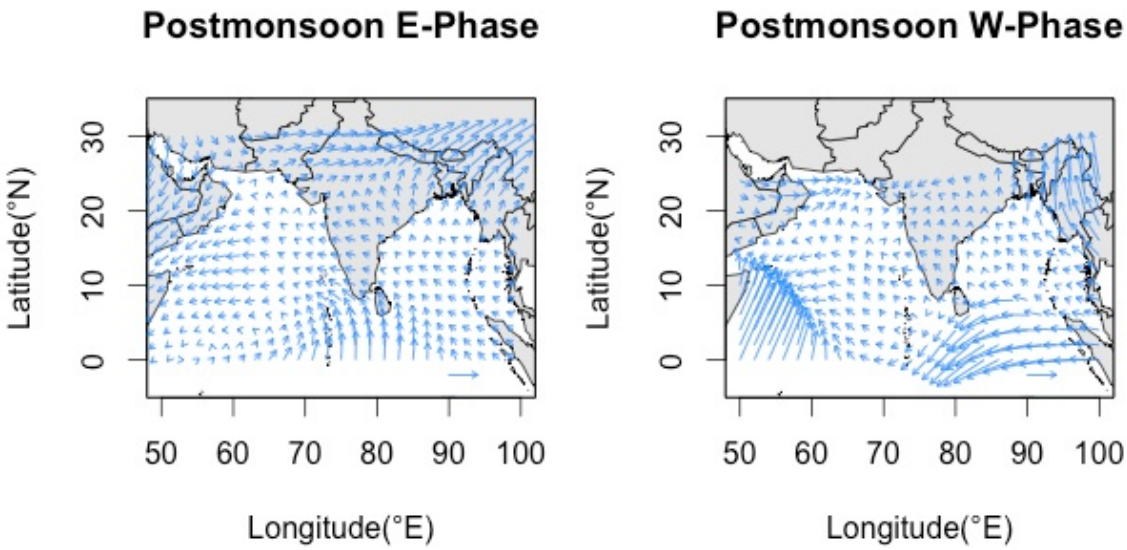

Fig.11 Distribution of GAM-fitted TC track velocities (data from 1980-2009) for each QBO phase jointly with season across the North Indian Ocean. The length of the reference arrow corresponds to velocity magnitudes of 10 ms^{-1}.

Geographically, the simulated percentages of TC landfall occurrences as a function of season and QBO phase across the NIO rim countries are presented in Fig. 12. During the winter season for both QBO phases, the model simulates the highest number of TC landfalls in Tamil Nadu, India. The model simulations identify Myanmar as the country most likely to result in the largest number of TC landfalls in the pre-monsoon season and during the westerly QBO phase, whereas Gujarat, Andhra Pradesh, Orissa in India, Oman and portions of Bangladesh, are simulated to be the most likely landfall locations in the easterly QBO phase. During the monsoon easterly QBO phase, the states of Andhra Pradesh, Orissa and West Bengal in India and Oman all correspond to the highest number of simulated TC landfalls whereas Andhra Pradesh and Orissa in India, Khulna in Bangladesh and Oman experience a large number of simulated TC landfalls in the westerly QBO phase. In the post-monsoon season, the highest simulated numbers of TC landfall occurrences are seen in the Andhra Pradesh, Tamil Nadu, Orissa and Gujarat states of India during the easterly QBO phase, whereas Andhra Pradesh, Orissa and Tamil Nadu in India are simulated to result in the largest number of TC landfalls during the westerly QBO phase.

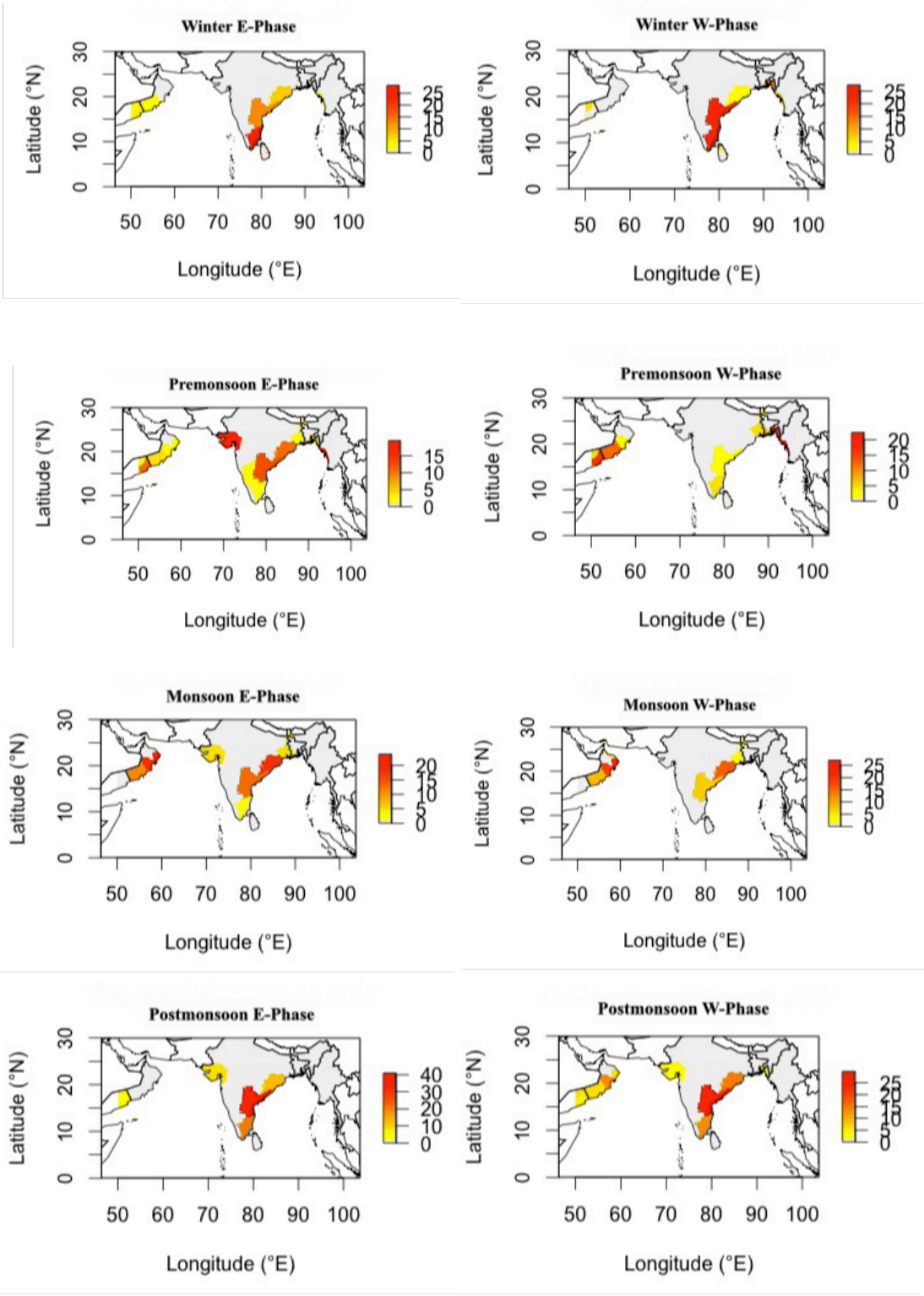

Fig.12 Geographic distribution of model simulated percentage probabilities of TC landfall by TC season and QBO phase across NIO rim states and countries. Colours range from yellow to red (as a percentage) indicating the lowest to highest model simulated percentage probabilities by TC landfall.

3.4 Dynamical mechanism to determine TC movement

The steering flow is the driving force that determines the movement of a TC. The beta effect and air sea interaction also impact the track taken by a TC (Williams and Chan 1994; Fadnavis *et al.* 2014). George and Gray (1976) showed that cyclone motion direction is best explained by 500mb winds. Here, we examined 500mb vector wind anomalies for the pre-monsoon (March-May) and post-monsoon (October-November) seasons in the NIO for easterly and westerly QBO phases. These two seasons are the most active seasons for TC formation in the NIO.

The distribution of steering winds during easterly QBO, westerly QBO and the difference between westerly and easterly QBO phases are shown in Fig. 13. In the pre-monsoon season, during the QBO easterly phase, anomalous northeasterly steering winds prevail in the northern portion of the Arabian Sea with generally weaker anomalies farther south in the basin. In the Bay of Bengal, anomalous southerly flow is evident in the northern portion of the basin, with anomalous easterly flow farther south (Fig. 13a). Anomalous easterly flow dominates both the northern portion of the Bay of Bengal and the Arabian Sea in QBO westerly phase during the pre-monsoon season, with generally weaker flow farther south in both basins (Fig. 13b). The difference between the westerly and easterly QBO phases in the pre-monsoon season highlights anomalous westerly flow in the southern portions of both the Bay of Bengal and Arabian Sea in westerly QBO phases (Fig. 13c). In the post-monsoon season, during easterly phase QBO (Fig.13d), anomalous northeasterly flow is evident in the Bay of Bengal, with predominately easterly anomalies farther south in the basin. Weaker anomalies are generally evident across the southern portion of the Arabian Sea, with southerly anomalies in the northern portion of the basin (Fig. 13d). A pronounced anomalous anti-cyclone is evident in the 500-mb steering flow in westerly phase QBO in the post-monsoon season, with anomalous westerly flow in the northern portion of the Bay of Bengal and anomalous easterly flow in the southern part of the Bay of Bengal. Anomalous southerly steering flow dominates most of the Arabian Sea (Fig. 13e). The difference between westerly and easterly QBO phase displays southwest winds across the western part of the Bay of Bengal, highlight a tendency for TCs to track farther to the northeast in westerly QBO phase episodes during the post-monsoon season (Fig. 13f).

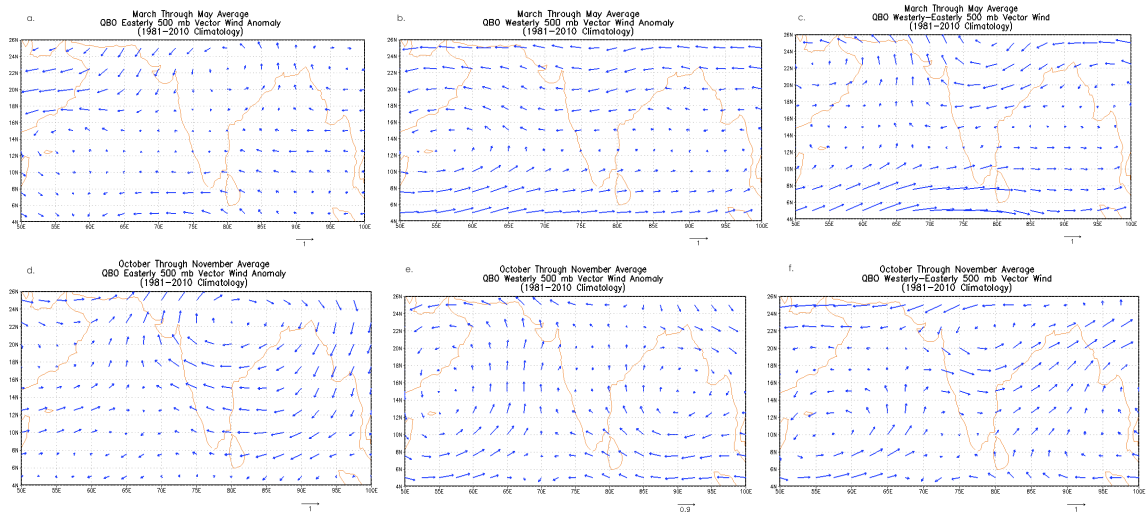

Fig.13 Distribution of steering winds (ms^{-1}) composite of study period excluding strong ENSO years in the pre-monsoon (March through May) during a) easterly QBO, b) westerly QBO, and c) westerly minus easterly QBO, and post-monsoon (October through November) season during d) easterly QBO, e) westerly QBO, and f) westerly minus easterly QBO.

3.5 Validation of model against observations

We validated the model using two different methods: (1) LOOCV by a majority vote approach, and (2) distance calculation between observed and simulated landfall. A comparison of the percentages of country-based statistics of cyclone landfalls from the observations against the model simulations was performed where the model was found to replicate climatology reasonably well (Wahiduzzaman *et al.* (2016). In a seasonal climatological context, they showed that the percentages of NIO region simulated TCs that made landfall across each country's coastline compared well with observations. They found that the model performed best for Myanmar and worst for Bangladesh.

For this QBO forecast model version, the highest numbers (we have 101 storms) of both observed and simulated landfall totals are in India – 40 and 51, respectively. The observed number (7) for Myanmar is well simulated by the model (9) (Table 7). Overall, the model shows good performance. With Bangladesh's coastline being a relatively small target for TCs to strike (239 km long coastline, as compared with 7517 km for India), using a majority vote approach where we decide on a single state/country that represents where most of the tracks make landfall is a factor that provides a clear opportunity for future improvements (Wahiduzzaman *et al.* 2016).

Table 7. Number of the annual total observed and simulated TC landfall occurrences across each country around the North Indian Ocean rim.

Country	Observed Number	Simulated Number
India	40	51
Myanmar	7	9
Bangladesh	7	3
Sri Lanka	4	2
Oman	3	8
Yemen	0	3
Total landfall	61	76
NON*	40	25
Total	101	101

*No landfall and/or landfall in other countries that is not considered into model

Applying the second model validation approach (Section 2.3.4.2), we calculated the distance between observed landfall and simulated landfall occurrences to evaluate model performance. The distribution of distances between the observed and simulated landfall points across all simulated tracks is presented in Fig. 14. It was found that the majority of simulated TC landfalls occurred within 500 km of the observed landfall locations. Given the spatial scale of TCs is typically on the order of 1000 km (Harold *et al.* 1999), modelled landfall occurrences within ~500 km of the observations can be considered indicative of good model performance for both QBO phases, noting however that there is also a secondary peak (source of error) at ~1500km during the easterly QBO phase. As the NIO basin is difficult to model due to a double peak in the pre-monsoon and the post-monsoon season (Camargo *et al.* 2005; Shaevitz *et al.* 2014; Camp *et al.* 2015). In

addition, average 5-day forecast track errors of individual TCs from dynamical models are several hundred kilometers (Mallik *et al.* 2015; Rayhun *et al.* 2015). Consequently, we believe that this model showed relatively good performance.

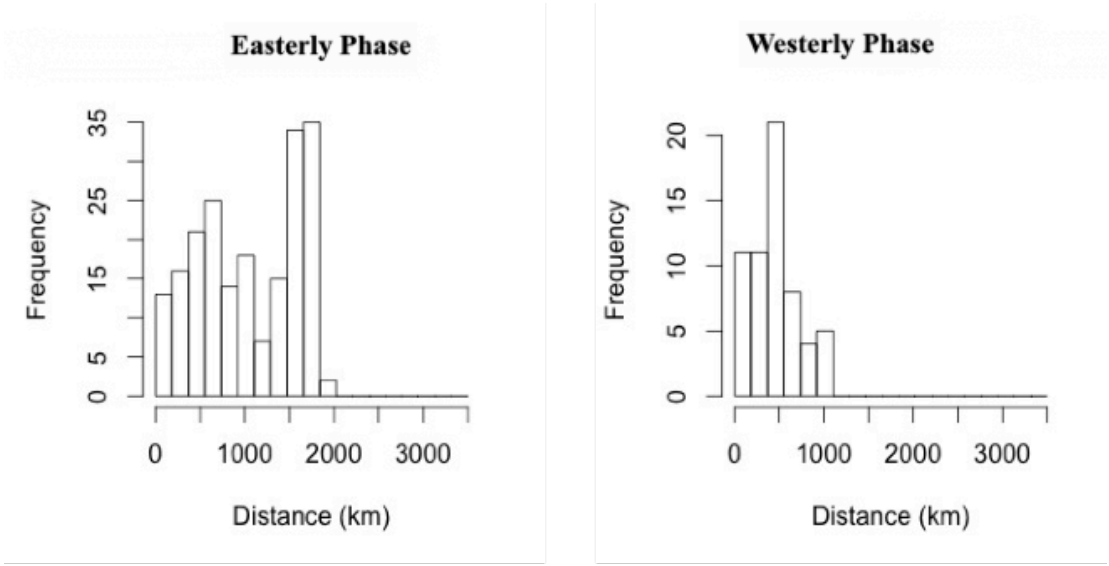

Fig. 14 Distribution of distances between observed and simulated landfall locations across NIO rim countries.

3.6 Prediction skill of model measured against observations

A comparison of the percentages of country-based statistics of cyclone landfalls from observations against the model simulations was also performed to assess the model skill when the predictor is used in model forecasts. It was found that the model performs better overall compared to the climatological model of Wahiduzzaman *et al.* (2016). The QBO-predictor model version presented here (cross-validated from 1980 to 2009) predicted landfall for Myanmar (9%), with similar frequency to observations (7%). The QBO-predictor model predicts half of all TCs making landfall (51%) for India, which is fairly close to observations (40%). Oman shows an 8% probability of TC landfall, Yemen and Bangladesh each show a 3% probability of TC landfall followed by Sri Lanka at 2% for the QBO-predictor model. Overall, the QBO-predictor model shows a total of 75% probability of TC landfall whereas the observations and climatological model predicted 60% and 79% respectively (Table 8).

Table 8. Numbers and percentages of annual total observed and simulated (by

2384 climatology and QBO predictor) TC landfall occurrences across each country of the
2385 North Indian Ocean rim.

Country	Observation		Simulation (Climatology)		Simulation (QBO Predictor)	
	No	%	No	%	No	%
India	40	40	44	43	51	51
Myanmar	7	7	22	22	9	9
Bangladesh	7	7	0	0	3	3
Sri Lanka	4	4	8	8	2	2
Oman	3	3	6	6	8	8
Yemen	0	0	0	0	3	3
Total landfall	61	60	80	79	76	75
NON*	40	40	21	22	25	25
Total	101	100	101	100	101	100

2386 *No landfall and/or landfall in other countries that is not considered into model

2387 In the distance calculation approach, it was found that the majority of simulated TC
2388 landfall occurrences (73%) were within 0-500 km of the observed landfall locations. For
2389 the climatological model, only 63% satisfied the 0-500km criteria, and so the forecast
2390 model presented here provides approximately 25% improvement over climatology for this
2391 error metric (Fig.15).

2392

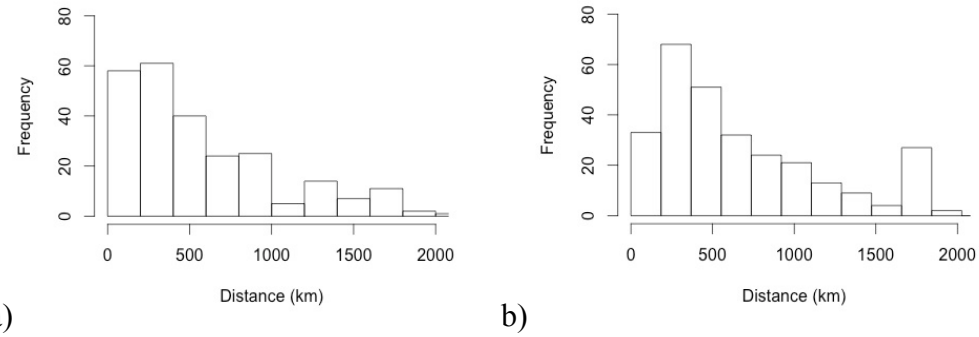

a) b)

Fig. 15 Distribution of distances between observed and simulated landfall location over the NIO for a) climatology and b) climatology plus QBO.

Separately, we have also explored the skill of independent model forecasts (hindcasts) for each season of the year for data from 2010-2013, taking into account the QBO phase. TCs occurred during the pre- and post-monsoon season in 2010, during the winter and post-monsoon season in 2011, during the post-monsoon season in 2012, and during the pre-monsoon season in 2013. The model hindcasts of TC activity in each season performed well against the observations (Fig. 16). Fig. 16 shows the observations of TC landfall as well as the QBO-prediction and model anomalies (QBO minus climatology). In the 2010 pre-monsoon season, observed TCs made landfall in Andhra Pradesh of India as well as in Oman (Fig.16a), and the QBO-prediction model presented the highest probability in Andhra Pradesh & Orissa of India and Myanmar (Fig.16b). The QBO minus climatology anomalies highlighted an increased likelihood in Andhra Pradesh and along the West Bengal coast in India with a decreased likelihood in Karnataka, Orissa in India, Oman and Rakhine in Myanmar (Fig 16c). During the post-monsoon season in 2010, a TC made landfall along the Myanmar coast (Fig.16d), although the QBO-prediction model showed the highest percentage chance of landfall in Andhra Pradesh, Orissa, and Gujarat in India (Fig.16e). The QBO model, however, did present a higher probability for Orissa and Myanmar than did the climatological model (Fig 16f).

During the 2011 winter season, a TC made landfall along the Tamil Nadu coast (Fig. 16g). The QBO-prediction model presented the highest percentage of probabilities in Orissa, Andhra Pradesh followed by Tamil Nadu of India (Fig.16h). Probabilities along most of the east coast of India were elevated from the climatological model (Fig 16i). During the post-monsoon season of 2011, a TC made landfall in Chittagong of Bangladesh (Fig.16j), and the QBO-prediction model presented the highest probability in Andhra Pradesh, Orissa and Tamil Nadu of India (Fig.16k). These probabilities were less

than in the climatological model (Fig 16l).

In the 2012 post-monsoon season, a TC made landfall along the Tamil Nadu coast (Fig.16m). The QBO-prediction model focused its highest probabilities in the western part of Bay of Bengal (Fig.16n), and the QBO model showed positive anomalies relative to climatology for Orissa and Tamil Nadu (Fig 16o).

In 2013, a TC made landfall in Bangladesh during the pre-monsoon season (Fig.16p). Both the QBO-prediction model (Fig.16q) and the QBO model relative to climatology (Fig.16r) showed an increased probability of landfall along the Bangladesh and Myanmar coasts.

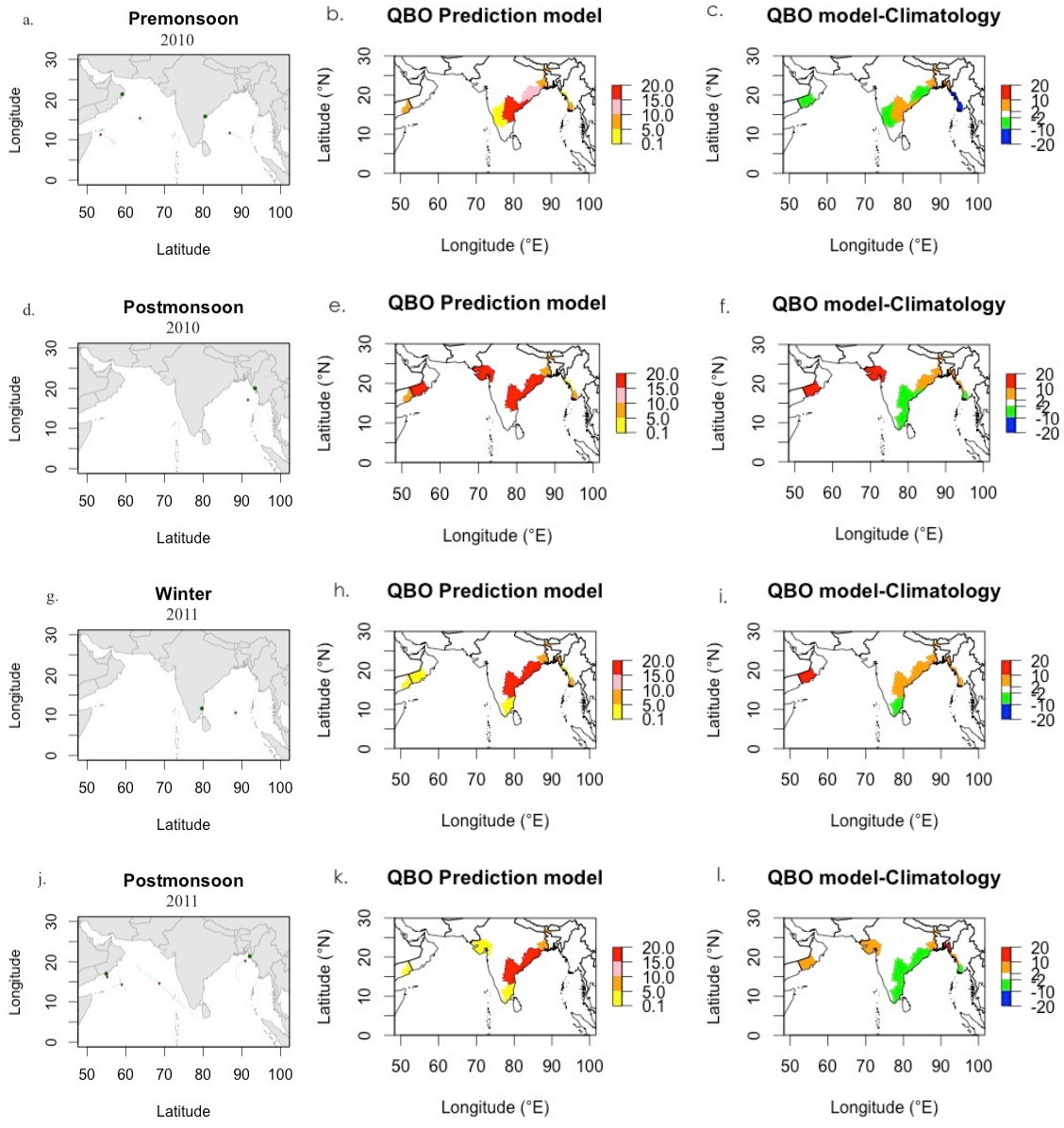

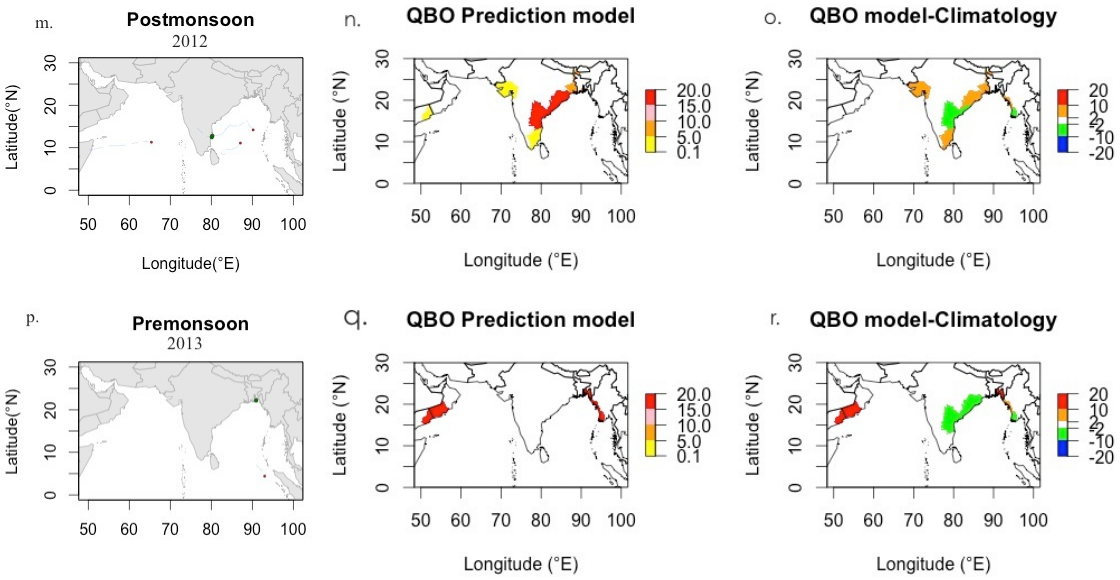

Fig.16 Observed (left) and hindcast QBO-prediction model (middle) and the difference between the QBO forecast and the climatological model (right) probabilities of landfall across the North Indian Ocean rim countries (0° to 30°N and 50° to 100°E) for a,b,c) 2010 pre-monsoon; d,e,f) 2010 post-monsoon; g,h,i) 2011 winter; j,k,l) 2011 post-monsoon; m,n,o) 2012 a post-monsoon and p,q,r) 2013 pre-monsoon, based on QBO phase information.

To assess the forecast skill more broadly, we have performed a hold-one-out validation by running the model 30 times, each time holding out one year and validating based on that held-out year. For example, we hold out 1980, then fit over 1981-2009, and predict for 1980. Then we aggregate the validation statistics by averaging across all these results to get single maps, by season and QBO phase, showing the landfall probabilities across all years for the QBO forecast model and the change relative to the climatological model. We have only considered the pre-monsoon and post-monsoon seasons, since they are the peak seasons for TCs. The model forecast of TC activity in these seasons performed well against the observations. Fig. 17 shows, by season and QBO phase, the observations of TC landfall as well as the climatology and forecast model anomalies. During the pre-monsoon easterly phase (Fig. 17a), TCs made landfall in Andhra Pradesh and Gujarat in India and Rakhine and Ayeywardy in Myanmar. The QBO model also forecasted well in these regions (Fig. 17b) compared to the climatological model which is seen through the comparison with anomalies (Fig 17c). In the pre-monsoon westerly phase (Fig. 17d), TCs have made landfall in the eastern part of the Bay of Bengal (Chittagong in Bangladesh and Rakhine in Myanmar) and Dofar in Oman (Arabian Sea), and we found that the QBO

model predicts a maximum in these regions (Fig. 17e) with positive anomalies along these coasts (Fig. 17f), meaning the QBO forecast model predicts a higher landfall probability in the regions that were actually hit. During the post-monsoon westerly phase, TCs made landfall in Andhra Pradesh and Tamil Nadu in India and in the southeastern part of Bangladesh (Fig. 17g). The QBO model highlighted these areas with increased chances of landfall (Fig. 17h-i). In the post-monsoon easterly phase, TCs made landfall in the western part of the Bay of Bengal (Fig. 17j) which is forecast well by the QBO model (Fig. 17k-l). Overall, the skill of the QBO model forecasts of TC landfall is an improvement over the climatological model.

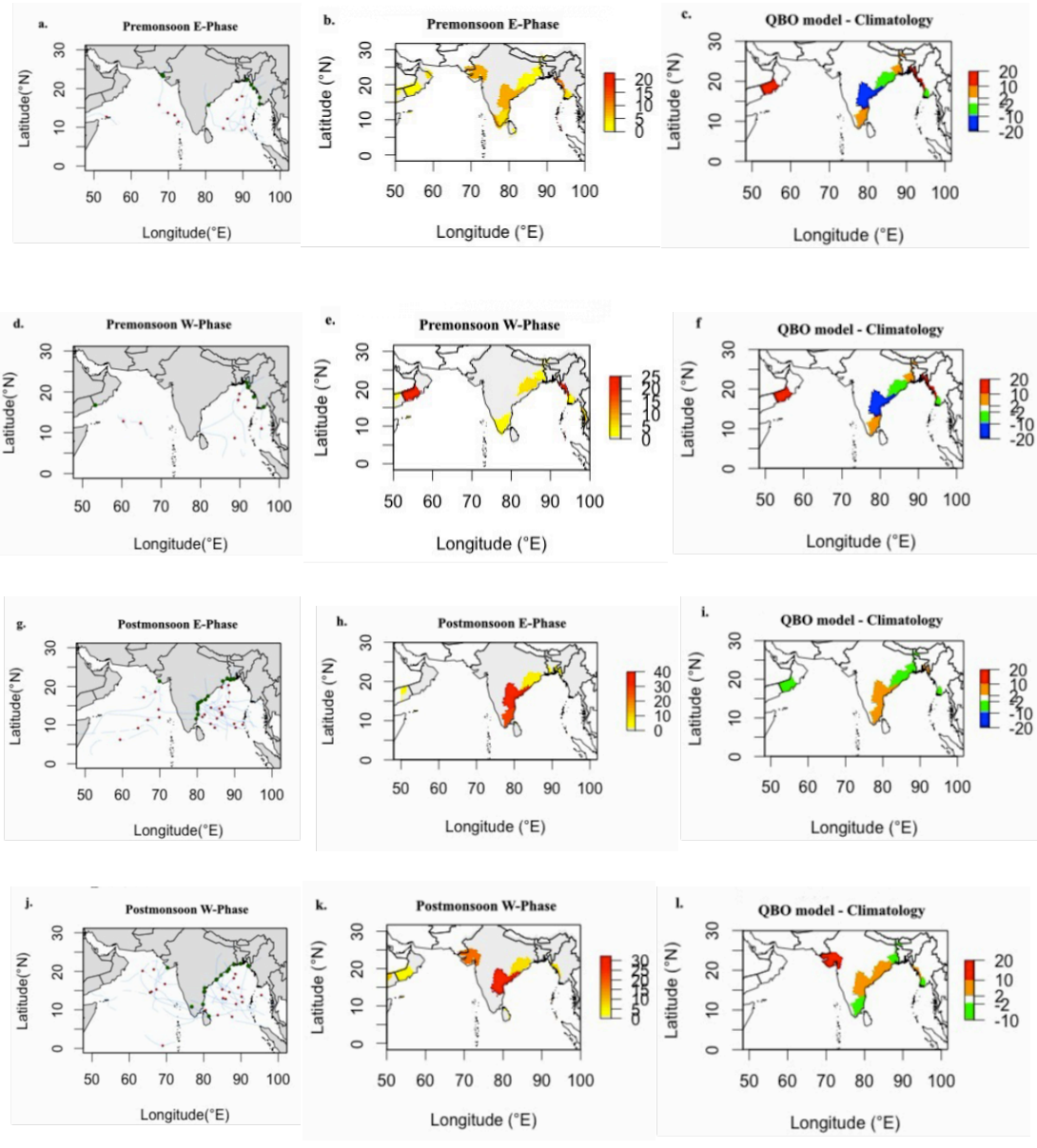

Fig.17 Observed (left), QBO forecast model (middle) and anomalies for the difference between the QBO forecast and climatological model (right) probabilities of landfall across the North

Indian Ocean rim countries (0° to 30°N and 50° to 100°E) for a,b,c) pre-monsoon and QBO easterly phase; d,e,f) pre-monsoon and QBO westerly phase; g,h,i) post-monsoon and QBO easterly phase; and j,k,l) post-monsoon and QBO westerly phase. Results have been aggregated across 30-years of leave-one-out cross validation.

3 Summary and Discussion

The significance of skillful seasonal forecasts is important for many societal sectors and the framework of developing climate services. In addition, it is valuable among the larger community by increasing the acceptance of climate forecasts (Doblas-Reyes *et al.* 2013). This study involved the development of a statistical seasonal forecast model of TC genesis, trajectories, and landfall for the North Indian Ocean (NIO) region, whereby a form of the stratospheric Quasi-Biennial Oscillation (QBO) shear index (30-50 hPa) has been incorporated as the key predictor variable. Fadnavis *et al.* (2014) have recently shown that there is a potentially useful climatic relationship between the QBO (excluding strong ENSO years) and TC tracks. Building on these recent research findings, we have used a generalised additive model (GAM) approach to fit the observed TC tracks as a smooth background trajectory (flow) field, and as a joint function of QBO-phase and TC season. The distribution of TC genesis points is approximated by kernel density estimation. The kernel bandwidth has been calculated with a standard plug in estimator. Model trajectories were simulated from randomly selected genesis points from the kernel, based on the GAM and an array of stochastic innovations applied at each time step. Two cross validation methods were applied. First, leave-one-out cross validation was applied whereby the country of landfall was determined using a majority vote approach. The second method involved calculating the distance (as an error metric) between the observed and simulated landfall locations.

The simulation of a large number of tracks with this model enabled the calculation of landfall probabilities at any location of interest around the NIO rim affected by TCs. In our 30-year study period (1980-2009), a total of 101 TCs were observed. Of these, 61 (60%) made landfall across five NIO rim countries, namely Bangladesh, India, Myanmar, Sri Lanka and Oman – while Yemen was also considered in this study, there were no observed landfall events in Yemen. We found that a greater percentage of TC genesis occurrences have been observed during the easterly QBO phase (60%) compared with the westerly QBO phase (40%). We further found that the highest percentage of TC genesis

occurrences have been observed in the post-monsoon season for both phases of the QBO. Our model simulations also show that there are significant differences in the directions of the cyclonic trajectories as a function of season and QBO phase that are consistent with the observations.

Based on leave-one-out cross-validation, we have shown that the percentages of annual total NIO region observed and simulated TCs that made landfall across each country coastline compared well. It was found that the model performs best for Myanmar, with relatively good simulation ability for several other countries. Based on our second cross-validation approach, which calculated the distance between observed and simulated landfall points, it was found that the majority of modelled TC landfall occurrences were within a relatively short distance (0-500km) of the observed landfall locations. Given the typical spatial scale of TCs (~1000km) is much larger than the typical error in landfall location, this demonstrates that the model is relatively skilful – at least within error estimates characterised by the physical scales of TCs, and typical error scales of dynamical models.

There is no currently available statistical model work that utilizes the QBO as a predictor in the NIO so we have instead applied a statistical seasonal forecast modelling approach here and found that the model is successful at forecasting TCs. Based on a sensitivity analysis, we chose a predictor time scale of 3 months for the QBO to lead TC activity within each TC season. Overall, our model shows skill exceeding that of climatology for the NIO rim. Also, it shows skill for individual year forecasts and from a suite of hindcast simulations, we found that the seasonal forecast model performed with approximately 25% improvement over results from the corresponding climatological model. However, there is also room for the genesis kernel density estimation in the model to be better tuned to the observations. Future improvements to the genesis model may translate to a bias reduction in the track simulations and thus landfall estimates. We are currently extending this research to consider the role of El Niño – Southern Oscillation as a separately important climate predictor with the aim to further improve TC prediction potential in the NIO region.

2534 Acknowledgments. Mohammad Wahiduzzaman was supported by a University of
2535 Tasmania Graduate Research Scholarship from the University of Tasmania.

2536 **References**

2537 Alam E, Collins AE (2010) Cyclone disaster vulnerability and response experiences in coastal
2538 Bangladesh. Disasters 34(4):931-954

2539 Alam E, Dominey-Howes D (2015) A new catalogue of tropical cyclones of the northern Bay of
2540 Bengal and the distribution and effects of selected landfalling events in Bangladesh.
2541 International Journal of Climatology 35(6):801-835

2542 Alam MM, Hossain MA, Shafee S (2003) Frequency of Bay of Bengal cyclonic storms and
2543 depressions crossing different coastal zones. International Journal of Climatology
2544 23(9):1119-1125

2545 Ali MM, Kishtawal CM, Jain S (2007) Predicting cyclone tracks in the north Indian Ocean: An
2546 artificial neural network approach. Geophysical Research Letters 34(4):L04603

2547 Arpe K, Leroy SAG (2009) Atlantic hurricanes-Testing impacts of local SSTs, ENSO,
2548 stratospheric QBO-Implications for global warming. Quaternary International 195(1-2):4-14

2549 Baik JJ, Paek JS (1998) A climatology of sea surface temperature and the maximum intensity of
2550 western North Pacific tropical cyclones. Journal of the Meteorological Society of Japan
2551 76(1):129-137

2552 Balachandran S, Geetha B (2012) Statistical prediction of seasonal cyclonic activity over North
2553 Indian Ocean. Mausam 63(1):17-28

2554 Balachandran S, Guhathakurta P (1999) On the influence of QBO over North Indian Ocean storm
2555 and depression tracks. Meteorology and Atmospheric Physics 70(1-2):111-118

2556 Baldwin MP, Gray LJ, Dunkerton TJ, Hamilton K, Haynes PH, Randel WJ, Holton JR, Alexander
2557 MJ, Hirota I, Horinouchi T, Jones DBA, Kinnersley JS, Marquardt C, Sato K, Takahashi M
2558 (2001) The quasi-biennial oscillation. Reviews of Geophysics 39(2):179-229

2559 Bashtannyk DM, Hyndman RJ (2001) Bandwidth selection for kernel conditional density
2560 estimation. Computational Statistics & Data Analysis 36:279-298

2561 Basu BK, Bhagyalakshmi K (2010) Forecast of the track and intensity of the tropical cyclone
2562 AILA over the bay of bengal by the global spectral atmospheric model VARSHA. Current
2563 Science 99(6):765-774

2564 Brian B (2015) Tropical Cyclone ACE Climatology. Climate Blog Published on 8th Nov, 2015

2565 Camargo SJ, Barnston AG, Klotzbatch PJ, Landsea CW (2007a) Seasonal Tropical cyclone
2566 forecasts. Bulletin of the World Meterological Organization 56:297-307

2567 Camargo SJ, Barnston AG, Zebiak SE (2005) A statistical assessment of tropical cyclone activity
2568 in atmospheric general circulation models. Tellus, Series A: Dynamic Meteorology and
2569 Oceanography 57(4):589-604

2570 Camargo SJ, Sobel AH (2010) Revisiting the influence of the quasi-biennial oscillation on
2571 tropical cyclone activity. Journal of Climate 23(21):5810-5825

2572 Camp J, Roberts M, Maclachlan C, Wallace E, Hermanson L, Brookshaw A, Arribas A, Scaife
2573 AA (2015) Seasonal forecasting of tropical storms using the Met Office GloSea5 seasonal
2574 forecast system. Quarterly Journal of the Royal Meteorological Society 141(691):2206-2219

2575 Carson DJ (1998) Seasonal forecasting. Quarterly Journal of the Royal Meteorological Society
2576 124:1-26

2577 Carter MM, Elsner JB (1997) A Statistical Method for Forecasting Rainfall over Puerto Rico.
2578 Weather and Forecasting 12(3):515-525

2579 Casson E, Coles S (2000) Simulation and extremal analysis of hurricane events. Journal of the
2580 Royal Statistical Society. Series C: Applied Statistics 49(2):227-245

2581 Chan JCL (1995) Tropical cyclone activity in the western North Pacific in relation to the
2582 stratospheric quasi-biennial oscillation. Mon. Wea. Rev. 123:2567-2571

2583 Chand SS, Walsh KJE (2011) Forecasting tropical cyclone formation in the Fiji region: A probit
2584 regression approach using bayesian fitting. Weather and Forecasting 26(2):150-165

2585 Chu P-S, Zhao X (2007) A Bayesian Regression Approach for Predicting Seasonal Tropical
2586 Cyclone Activity over the Central North Pacific. Journal of Climate 20(15):4002-4013

2587 Chu PS, Zhao X, Ho CH, Kim HS, Lu MM, Kim JH (2010) Bayesian forecasting of seasonal
2588 typhoon activity: A track-pattern-oriented categorization approach. Journal of Climate
2589 23(24):6654-6668

2590 Collimore CC, Martin DW, Hitchman MH, Huesmann A, Waliser DE (2003) On the relationship
2591 between the QBO and tropical deep convection. Journal of Climate 16(15):2552-2568

2592 Doblas-Reyes FJ, García-Serrano J, Lienert F, Biescas AP, Rodrigues LRL (2013) Seasonal
2593 climate predictability and forecasting: Status and prospects. Wiley Interdisciplinary
2594 Reviews: Climate Change 4(4):245-268

2595 Ebert EE, Turk M, Kusselson SJ, Yang J, Seybold M, Keehn PR, Kuligowski RJ (2010) Ensemble
2596 Tropical Rainfall Potential (eTRaP) Forecasts. Weather and Forecasting 26(2):213-224

2597 Elsner JB, Kara AB (1999) Hurricanes of the North Atlantic: Climate and Society, Oxford
2598 University press, pp.466

2599 Elsner JB, Murnane RJ, Jagger TH (2006) Forecasting U.S. hurricanes 6 months in advance.
2600 Geophysical Research Letters 33(10)

2601 Emanuel K (2006) Hurricanes: Tempests in a greenhouse. Physics Today 59(8):74-75

2602 Emanuel K, Ravela S, Vivant E, Risi C (2006) A Statistical Deterministic Approach to Hurricane
2603 Risk Assessment. Bulletin of the American Meteorological Society 87(3):299-314

2604 Evan AT, Camargo SJ (2010) A Climatology of Arabian Sea Cyclonic Storms. Journal of Climate
2605 24(1):140-158

2606 Fadnavis S, Chakraborty T, Ghude SD, Beig G, Ernest Raj P (2011) Modulation of Cyclone
2607 tracks in the Bay of Bengal by QBO. Journal of Atmospheric and Solar-Terrestrial Physics
2608 73(13):1868-1875

2609 Fadnavis S, Ernest Raj P, Buchunde P, Goswami BN (2014) In search of influence of
2610 stratospheric Quasi-Biennial Oscillation on tropical cyclones tracks over the Bay of Bengal
2611 region. International Journal of Climatology 34(3):567-580

2612 Fraedrich K, Leslie LM (1989) Estimates of cyclone track predictability. I: Tropical cyclones in
2613 the Australian region. Quarterly Journal of the Royal Meteorological Society 115(485):79-92

2614 George JE, Gray WM (1976) Tropical cyclone motion and surrounding parameter relationships.
2615 Journal of Applied Meteorology 15(12):1252-1264

2616 Girishkumar MS, Ravichandran M, Pant V (2012) Observed chlorophyll-a bloom in the southern
2617 Bay of Bengal during winter 2006-2007. International Journal of Remote Sensing
2618 33(4):1264-1275

2619 Girishkumar MS, Suprit K, Vishnu S, Prakash VPT, Ravichandran M (2015) The role of ENSO
2620 and MJO on rapid intensification of tropical cyclones in the Bay of Bengal during October–
2621 December. Theoretical and Applied Climatology 120(3-4):797-810

2622 Girishkumar MS, Thanga Prakash VP, Ravichandran M (2014) Influence of Pacific Decadal
2623 Oscillation on the relationship between ENSO and tropical cyclone activity in the Bay of
2624 Bengal during October–December. Climate Dynamics 44(11-12):3469-3479

2625 Gray WM (1984) Atlantic seasonal hurricane frequency, Part I: El Nino and 30 mb Quasi-
2626 Biennial Oscillation influences. Monthly Weather Review 112(9)

2627 Gray WM (1984) Atlantic seasonal hurricane frequency. Part II: forecasting its variability.
2628 Monthly Weather Review 112(9):1669-1683

2629 Gray WM, Landsea CW, Mielke Jr PW, Berry KJ (1992) Predicting Atlantic seasonal hurricane
2630 activity 6-11 months in advance. Weather & Forecasting 7(3):440-455

2631 Gray WM, Landsea CW, Mielke Jr PW, Berry KJ (1994) Predicting Atlantic Basin seasonal
2632 tropical cyclone activity by 1 June. Weather & Forecasting 9(1):103-115

2633 Hall TM, Jewson S (2007) Statistical modelling of North Atlantic tropical cyclone tracks. Tellus,
2634 Series A: Dynamic Meteorology and Oceanography 59 A(4):486-498

2635 Harold JM, Bigg GR, Turner J (1999) Mesocyclone activity over the North-East Atlantic. Part 1:
2636 Vortex distribution and variability. International Journal of Climatology 19(11):1187-1204

2637 Hastie T, Tibshirani R, Friedman J (2009) The Elements of Statistical learning: Data Mining,
2638 Inference, and Prediction. Springer Series in Statistics Second edition, pp.295-333

2639 Hess JC, Elsner JB (1994) Historical developments leading to current forecast models of annual
2640 Atlantic hurricane activity. Bulletin - American Meteorological Society 75(9):1611-1620

2641 Ho CI, Kim HS, Jeong JH, Son SW (2009) Influence of stratospheric quasi-biennial oscillation on
2642 tropical cyclone tracks in the western North Pacific. Geophysical Research Letters 36(6)

2643 Hossain MN, Paul SK (2015) Simulation of physical and socioeconomic factors of vulnerability
2644 to cyclones and storm surges using GIS: a case study. GeoJournal

2645 Huesmann AS, Hitchman MH (2001) The stratospheric quasi-biennial oscillation in the NCEP
2646 reanalyses: Climatological structures. Journal of Geophysical Research: Atmospheres
2647 106(D11):11859-11874

2648 Islam T, Peterson RE (2009) Climatology of landfalling tropical cyclones in Bangladesh 1877-
2649 2003. Natural Hazards 48(1):115-135

2650 James MK, Mason LB (2005) Synthetic tropical cyclone database. Journal of Waterway, Port,
2651 Coastal and Ocean Engineering 131(4):181-192

Jury MR (1993) A preliminary study of climatological associations and characteristics of tropical cyclones in the SW Indian Ocean. Meteorology and Atmospheric Physics 51(1-2):101-115

Jury MR, Pathack B, Parker B (1999) Climatic determinants and statistical prediction of tropical cyclone days in the southwest Indian Ocean. Journal of Climate 12(6):1738-1746

Klotzbach PJ (2007) Recent developments in statistical prediction of seasonal Atlantic basin tropical cyclone activity. Tellus 59A, 511-518.

Knapp KR, Kruk MC, Levinson DH, Diamond HJ, Neumann CJ (2010) The international best track archive for climate stewardship (IBTrACS). Bulletin of the American Meteorological Society 91(3):363-376

Lander MA, Guard CP (1998) A look at global tropical cyclone activity during 1995: Contrasting high Atlantic activity with low activity in other basins. Monthly Weather Review 126(5):1163-1173

Landsea CW, Bell GD, Gray WM, Goldenberg SB (1998) The extremely active 1995 Atlantic hurricane season: Environmental conditions and verification of seasonal forecasts. Monthly Weather Review 126(5):1174-1193

Liang CK, Eldering A, Gettelman A, Tian B, Wong S, Fetzer EJ, Liou KN (2011) Record of tropical interannual variability of temperature and water vapor from a combined AIRS-MLS data set. Journal of Geophysical Research: Atmospheres 116(6):D06103

Liess S, Geller MA (2012) On the relationship between QBO and distribution of tropical deep convection. Journal of Geophysical Research: Atmospheres 117(3):D03108

Lin II, Chen CH, Pun IF, Liu WT, Wu CC (2009) Warm ocean anomaly, air sea fluxes, and the rapid intensification of tropical cyclone Nargis (2008). Geophysical Research Letters 36(3):L03817

Loader CR (1999) Bandwidth Selection: Classical or Plug-In? The Annals of Statistics 27(2):415-438

Mallik MAK, Ahsan MN, Chowdhury MAM (2015) Simulation of Track and Landfall of Tropical Cyclone Viyaru and Its Associated Strom Surges Using NWP Models. American Journal of Marine Science 3(1):11-21

Mohapatra M, Bandyopadhyay BK, Tyagi A (2012) Best track parameters of tropical cyclones over the North Indian Ocean: A review. Natural Hazards 63(3):1285-1317

Mohapatra M, Bandyopadhyay BK, Tyagi A (2014) Status and Plans for Operational Tropical Cyclone Forecasting and Warning Systems in the North Inidan Ocean Region. U.C. Mohanty MM, O.P. Singh, B.K. Bandyopadhyay, L.S. Rathore (ed) Monitoring and Prediction of Tropical Cyclones in the Indian Ocean and Climate Change. Springer, pp 149-162

Nath S, Kotal SD, Kundu PK (2015) Seasonal prediction of tropical cyclone activity over the North Indian Ocean using the neural network model. Atmosfera 28(4):271-281

Naujokat B (1986) An update of the observed quasi-biennial oscillation of the stratospheric winds over the Tropics. Journal of the Atmospheric Sciences 43(17):1873-1877

Ng EKW, Chan JCL (2012) Interannual variations of tropical cyclone activity over the north Indian Ocean. International Journal of Climatology 32(6):819-830

Paliwal M, Patwardhan A (2013) Identification of clusters in tropical cyclone tracks of North Indian Ocean. Natural Hazards:1-12

Paliwal M, Patwardhan A, Sarda NL (2011) Analyzing tropical cyclone tracks of North Indian Ocean. COM.Geo 11 Proceedings of the 2nd International Conference on Comupting for Geospatial Research & Applications, Article No.18, ACM New York, USA.

Pattanaik DR, Mohapatra M (2016) Seasonal forecasting of tropical cyclogenesis over the North Indian Ocean. Journal of Earth System Science 125(2):231-250

Rajasekhar M, Kishtawal CM, Prasad MYS, Seshagiri Rao V, Rajeevan M (2014) Extended range tropical cyclone predictions for East Coast of India. U.C. Mohanty MM, O.P. Singh, B.K. Bandyopadhyay, L.S. Rathore (ed) Monitoring and Prediction of Tropical Cyclones in the Indian Ocean and Climate Change. pp 137-148

Rayhun KMZ, Quadir DA, Chowdhury MAM, Ahsan MN, Haque MS (2015) Simulation of structure, track and landfall of tropical cyclone Bijli using WRF-ARW model. J. Bangladesh Acad. Sci 39(2):157-167

Rigollet P, Vert R (2009) Optimal rates for plug-in estimators of density level sets. Bernoulli 15(4):1154-1178

Rodriguez J, F. Vos., R. Below., Guha-Sapir D (2009) Annual disaster statistical review 2008. In: Centre for Research on the Epidemiology of Disasters (CRED), Brussels, Belgium, p 33

Rumpf J, Weindl H, Höppe P, Rauch E, Schmidt V (2007) Stochastic modelling of tropical cyclone tracks. Mathematical Methods of Operations Research 66(3):475-490

Sahoo B, Bhaskaran PK (2016) Assessment on historical cyclone tracks in the Bay of Bengal, east coast of India. International Journal of Climatology 36(1):95-109

Shaevitz DA, Camargo SJ, Sobel AH, Jonas JA, Kim D, Kumar A, Larow TE, Lim YK, Murakami H, Reed KA, Roberts MJ, Scoccimarro E, Vidale PL, Wang H, Wehner MF, Zhao M, Henderson N (2014) Characteristics of tropical cyclones in high-resolution models in the present climate. Journal of Advances in Modeling Earth Systems, 6(4):1154-72

Shapiro LJ (1989) The relationship of the quasi-biennial oscillation to Atlantic tropical storm activity. Monthly Weather Review 117(7):1545-1552

Singh OP (2010) Tropical cyclones: Trends, Forecasting and Mitigation. Natural and Anthropogenic Disasters: 256-274

Singh R, Kishtawal CM, Pal PK, Joshi PC (2012) Improved tropical cyclone forecasts over north Indian Ocean with direct assimilation of AMSU-A radiances. Meteorology and Atmospheric Physics 115(1-2):15-34

Tolwinski-Ward SE (2015) Uncertainty quantification for a climatology of the frequency and spatial distribution of North Atlantic tropical cyclone landfalls. Journal of Advances in Modeling Earth Systems, 7:305-19

Turlach BA (1993) Bandwidth Selection in Kernel Density Estimation: A Review. CORE and Institut de Statistique 19:1-33

Vickery PJ, Skerjl P, Steckley AC, Twinsdale L (2000) Simulation of hurricane risk in the united states using an empirical storm track modeling technique. Journal of structural engineering 126:1222-1237

Wahiduzzaman M, Oliver E, Wotherspoon S, Holbrook N (2016) A climatological model of North Inidan Ocean tropical cyclone genesis, tracks and landfall. Climate Dynamics DOI: 10.1007/s00382-016-3461-4

Warrick RA, MAccines KL, Pittock AB, Kench PS (2000) Climate change, severe storms and sea level. Floods edited by Dennis J. Parker Taylor and Francis group, London, p.139

Webster PJ (2008) Myanmar's deadly daffodil. Nature Geoscience 1(8):488-490

Weinkle J, Maue R, Pielke R (2012) Historical global tropical cyclone landfalls. Journal of Climate 25(13):4729-4735

Whitney LD, Hobgood JS (1997) The relationship between sea surface temperatures and maximum intensities of tropical cyclones in the eastern North Pacific Ocean. Journal of Climate 10(11):2921-2930

Williams RT, Chan JCL (1994) Numerical studies of the beta effect in tropical cyclone motion. Part II: zonal mean flow effects. Journal of the Atmospheric Sciences 51(8):1065-1076

WMO (1997) Tropical Cyclone Operational Plan for the Bay of Bengal and the Arabian Sea, WMO Report 1997.

Yadav RK (2012) Emerging role of Indian ocean on Indian northeast monsoon. Climate Dynamics:1-12

Yonekura E, Hall TM (2011) A Statistical model of tropical cyclone tracks in the western North Pacific with ENSO-dependent cyclogenesis. Journal of Applied Meteorology and Climatology 50(8):1725-1739

Zhou XL, Geller MA, Zhang M (2004) Temperature fields in the tropical tropopause transition layer. Journal of Climate 17(15):2901-2906

3.3 Chapter Summary

This chapter addresses the thesis aims of development of a seasoal statistical forecast model to forecast the tropical cyclone genesis, tracks and landfall in the North Indian Ocean region by considering QBO as a predictor. The model consists three components which are genesis distribution by kernel density estimation, tracks by generalised additive model, landfall by eular intergration with country mask approach. Also the model hindcast skills are quantified.

We have presented a new statistical forecast model where the model shows very good cross-validated hindcast performance of modelled landfalling cyclones against observations for most NIO rim countries. The components of model are found to be successful in forecasting TC activity of NIO region for the upcoming season. The model skill is assessed based on 1 to 6 months lead-lag analysis that confirms QBO is a good predictor for 3 months advance to forecast. The distribution of TC genesis, tracks and landfall probabilities over the study period, as well as the hindcasted probabilities of TC landfall during QBO events match remarkably well against observations over most of the study domain.

4 DEVELOPMENT OF STATISTICAL SEASONAL FORECAST MODEL FOR TROPICAL CYCLONE GENESIS, TRACKS AND LANDFALL IN THE NORTH INDIAN OCEAN REGION AND EFFECTS OF ENSO

4.1 Chapter Overview

This chapter produces a forecast model of North Indian Ocean region tropical cyclone genesis, tracks and landfall based on the observational data from 1979-2013. The development of forecast model of tropical cyclone genesis, tracks and landfall for North Indian Ocean rim countries are based on kernel density estimation, a generalised additive model including an Euler integration step, and landfall detection using a country mask approach with considering ENSO. Lead-lag analysis is used to assess the best predictor timescales for TC forecast potential. The model is fitted to the observed cyclone track velocities as a smooth function of location in each phase and jointly with season and the distribution of cyclone genesis points are approximated by kernel density estimation. The model simulated TCs are randomly selected from the fitted kernel and the cyclonic tracks represented by the model together with the application of stochastic innovations at each step. Two hindcasts validation methods (Leave one out cross validation with majority vote approach, and distance calculation between observed and simulated landfall) are used to analyse the skill of model.

The main text of this chapter is a paper for submission to *Climate Dynamics (*Wahiduzzaman M, Wotherspoon S, Oliver E, Holbrook N (2017) Seasonal forecasting of tropical cyclones in the North Indian Ocean region: the role of El Niño-Southern Oscillation, Climate Dynamics, in prep)

4.2 Wahiduzzaman *et al.* 2017; *Climate Dynamics*

Seasonal forecasting of tropical cyclones in the North Indian Ocean region: The role of El Niño-Southern Oscillation

Md Wahiduzzaman[1], Simon J. Wotherspoon[1,2], Eric C.J. Oliver[1, 3], Neil J. Holbrook[1,3]

[1]Institute for Marine and Antarctic Studies, University of Tasmania, Australia

[2] Australian Antarctic Division, 203 Channel Highway, Kingston, Tasmania 7050, Australia

[3]Australian Research Council Centre of Excellence for Climate System Science, Hobart, Tasmania, Australia

For submission to *Climate Dynamics*

Corresponding author address: Neil J. Holbrook, Institute for Marine and Antarctic Studies, University of Tasmania, TAS 7001 Australia | E-mail: **neil.holbrook@utas.edu.au**

Abstract

In this study, we have investigated the contributions and prediction skills of El Niño-Southern Oscillation (ENSO) to the tropical cyclone (TC) activity over the North Indian Ocean (NIO). A statistical seasonal forecast model is developed through kernel density estimation (KDE), a Generalized additive model (GAM), Euler integration step and a country mask approach for tropical cyclone formation, trajectories and landfall across the NIO rim countries using ENSO as a predictor. TC from the Joint Typhoon Warning Centre and Southern Oscillation index data have been used for a period of 35-year (1979-2013). KDE is used to model the distribution of cyclone genesis points and the paths of the subsequent cyclone tracks are simulated by modelling the velocity along the observed cyclone tracks as smooth functions of location in each phase and season for the forecast model. Trajectories are then simulated by drawing new random genesis points from the fitted density estimates and then tracing the cyclonic paths from the fitted velocity fields to decide the positions of landfall. The best predictor times for TC forecast potential is assessed based on 1 to 6 months' lead-lag analysis that confirms ENSO is a good predictor for 2-month advance to forecast. Two hindcast validation methods are applied to assess the reliability of the model. The components of the model are found to be successful in forecasting TC activity of the NIO region for the season. The distribution of TC genesis, tracks and landfall probabilities over the study period, as well as the hindcasted probabilities of TC landfall during ENSO events, match remarkably well against observations over most of the study domain.

Keywords Tropical Cyclones, El Niño-Southern Oscillation, Seasonal forecasting, Statistical modelling, North Indian Ocean

1 Introduction

Tropical cyclones (TCs) are one of the utmost threatening physical catastrophes to humans, particularly along densely populated coastlines. TCs can cause a substantial loss of life and very often cause significant damage to properties (Alam *et al.* 2003; Tyagi *et al.* 2010; Girishkumar and Ravichandran 2012; Vissa *et al.* 2013; Balaguru *et al.* 2014; Girishkumar *et al.* 2014; Mohapatra *et al.* 2014; Rajasekhar *et al.* 2014; Shaji *et al.* 2014; Girishkumar *et al.* 2015; Nath *et al.* 2015; Sahoo and Bhaskaran 2016). In the North Indian Ocean (NIO) region, there have been numerous devastating losses due to TCs that make landfall, even in recent years (Islam and Peterson 2009; Ng and Chan 2012; Mohapatra *et al.* 2014; Pattanaik and Mohapatra 2016). These include a number of 1,38000 people and $10 billion loss by 2008 *Nargis* cyclone (Webster 2008; Lin *et al.* 2009; Alam and Collins 2010; Nath *et al.* 2015). Aside from the clear costs to human life, this is also a massive financial risk to insurance and reinsurance companies (Rumpf *et al.* 2007).

Seasonal forecasting of tropical cyclone activity can help decision-makers and inhabitants in shoreline zones to think and make a blueprint potential action month in advance. At the government preparation and strategy points, seasonal forecasting can be practically agreed to advise and aid decision-making. In order to model TC activity, it is essential to know the factors that effect TC genesis, propagation track, and landfall. Because of a deficiency of observation and resources, the development, strengthening and trajectories of TCs have been understudied in the NIO region. A couple of research have examined the effect of the atmospheric and oceanic states on the variation of TC activity in the Bay of Bengal (BoB) (Liebmann *et al.* 1994; Goswami *et al.* 2003; Ali *et al.* 2007; Sengupta *et al.* 2007; Kikuchi *et al.* 2009; Lin *et al.* 2009; Girishkumar and Ravichandran 2012; Felton *et al.* 2013). Nevertheless, they didn't implement El Niño – Southern Oscillation (ENSO) predictors in a statistical model for seasonal forecasting of tropical cyclones.

ENSO is the supreme significant ocean-atmosphere phenomenon in the Pacific and affects the large-scale climate globally (Lau 1985; Philander 1985; Cane *et al.* 1986; Allan 1988; Philander 1990, 1992; Ropelewski and Halpert 1996; Wang and Chan 2002; Behera *et al.* 2006; Eichler and Higgins 2006; An *et al.* 2007; Ashok and Saji 2007; Belmadani *et al.* 2010; Zhao *et al.* 2010; Chand and Walsh 2011; Werner *et al.* 2012; Hsu

et al. 2013; Camp *et al.* 2015; Girishkumar *et al.* 2015; Mahala *et al.* 2015). Its effects on tropical cyclones are felt in various ocean basins (Chu 2004; Girishkumar and Ravichandran 2012; Larson *et al.* 2012; Tao *et al.* 2012; Werner *et al.* 2012; Zhang *et al.* 2012; Du *et al.* 2013; Hsu *et al.* 2013; Camp *et al.* 2015; Girishkumar *et al.* 2015; Mahala *et al.* 2015). Generally, the duration of a single ENSO event (either El Niño or La Niña) is 1.5-2 years with the seasonal cycle (Philander 1985) and events tend to reoccur on interannual time scales (2-8 years). It is the coupling between sea level pressure, expressed as the winds and wind stress, and the sea surface temperature anomalies associated with ENSO as well as its timing and spatial teleconnections that are responsible for the large-scale changes in the climate across the globe.

ENSO is the leading predictable factor that influences the global tropical cyclone frequency, genesis, tracks and landfall on seasonal time-scales (Camargo *et al.* 2008; Camp *et al.* 2015). In the NIO basin, the connection between tropical cyclone and ENSO have been examined by several researchers (Ho *et al.* 2006; Kuleshov *et al.* 2008; Girishkumar *et al.* 2012; Srikanth *et al.* 2012; Felton *et al.* 2013; Girishkumar *et al.* 2014; Camp *et al.* 2015; Girishkumar *et al.* 2015; Mahala *et al.* 2015). For example, Girishkumar *et al.* (2012) studied the effects of ENSO on TC activity in the BoB during post-monsoon season. The study showed that during La Niña (El Niño) phase 70% TCs formed in the eastern (western) part of the BoB, moved north-westward (westward) and made landfall north (south) of 15°N. This work was later extended by adding an MJO relationship (Girishkumar *et al.* 2015) on TC activity.

Related studies have also been undertaken. Singh *et al.* (2001) examined the relationship between ENSO and depression activity in the BoB during the summer monsoon season (July–August) and found more tropical depressions during El Niño years. In another study, Singh *et al.* (2000) showed that there was a reduction in cyclonic storms in two peak seasons (Pre and Post monsoon) over the BoB during El Niño years. Camargo *et al.* (2007) demonstrated the influence of ENSO on the genesis potential index (useful metric for gauging the performance of global climate models to simulate TC genesis) in all ocean basins and found genesis potential movement from the northern to the southern part of the BoB due to wind shear in La Niña years than El Niño years.

Now-a-days seasonal forecasting of tropical cyclone landfall by dynamical models is challenging (Camargo 2013; Shaevitz *et al.* 2014; Camp *et al.* 2015) and its skill varies

(Camargo *et al.* 2005; Bengtsson *et al.* 2007; Camargo and Barnston 2009). Little accuracy was found in the simulation of seasonal cycle over the NIO region by Camp *et al.* (2015). Other dynamical models, including the Dynamical High Resolution Model (HRM), Consortium for small Scale Modeling (COSMO) and Artificial Neural Network System models, have been shown not to be able to forecast cyclone landfall well because of limited spatial resolution (Yahyai 2014) and number of simulations (Ray *et al.* 2012).

This manuscript considers the development of a statistical seasonal forecast model of NIO tropical cyclone activity (formation, trajectories and landfall) using a metric of ENSO as the predictor variable. Kernel density estimation (KDE) and a Generalized Additive Model is used to model genesis and the trajectories. The arrangement of this manuscript is as bellows. The data and model descriptions is provided in section 2. Lead-lag analysis is also presented in this section. Section 3 discusses the results of the TC genesis by KDE and TC trajectory simulations carried out with this model and assess them alongside observation. The overall results are presented in section 3, and conclusions are delivered in section 4.

2 Data and Methods

Statistical models of TC tracks and TC genesis have been examined in numerous previous studies, including those by by Casson and Coles (2000), Vickery *et al.* (2000), James and Mason (2005), Emanuel *et al.* (2006), Rumpf *et al.* (2007), Hall and Jewson (2007) and Yonekura and Hall (2011). They have pointed out that the statistical model generates sets of synthetic set TCs much larger than the historical set and compute the direction of tracks from the synthetic sets by using KDE and autoregressive modelling. We developed a statistical seasonal forecast model for NIO TC formation, trajectories and landfall closely followed by Hall and Jewson (2007) and Yonekura and Hall (2011). The procedure for the simulation of TC trajectories is two-fold. First, TC genesis points are sampled from a spatial probability density function that has been calculated by kernel density estimation. Second, the TC track "velocity field" was generated by calculating latitudinal and longitudinal differences between observed TC positions in time along the observed cyclone tracks, and a GAM model was fitted to model the observed "velocity field" within a season and the ENSO phase. The predicted velocity was then used to advect TCs from the genesis point to generate the modelled TC tracks. This was performed for each ENSO phase and jointly with the season. The trajectories are based on

7 days of lifespan and a 6-hour step interval, i.e. 4 steps in a day. From this model, a number of synthetic but realistic storm tracks than observed in the historical data were simulated and these synthetic track statistics are used to generate probabilistic landfall hazard zone maps.

2.1 Tropical Cyclone Data

The International Best Track Archive for Climate Stewardship (IBTrACS) dataset was established by the NOAA National Climatic Data Center to integrate the best TC track data from all official Tropical Cyclone Warning Centres (TCWCs) and the WMO Regional Specialized Meteorological Centres (RSMCs). These data were available and have been downloaded from <www.ncdc.noaa.gov/oa/ibtracs/>.

The data have been used from the Joint Typhoon Warning Centre (JTWC) for the 35-year period from 1979-2013 (the data from 1979 is more reliable (Wahiduzzaman *et al*, 2016). The JTWC data have been used by most of the researchers (Knapp *et al.* 2010). We here define the NIO (Fig.1) as the region bounded meridionally from 0°--30°N and zonally from 50°E--100°E.

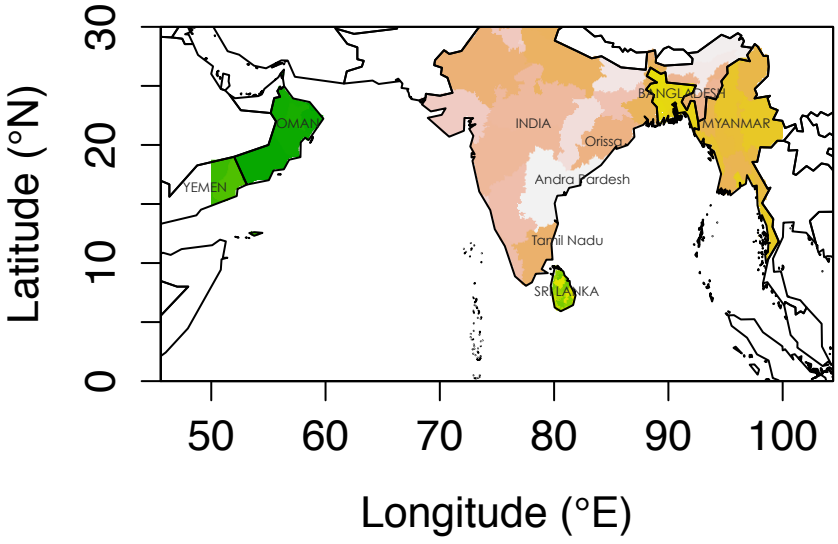

Fig.1 Countries (India, Bangladesh, Myanmar, Sri Lanka, Oman and Yemen) and three Indian states (Andhra Pradesh, Orissa and Tamil Nadu) along the NIO rim which is largely affected by tropical cyclone landfall.

2.2. Southern Oscillation Index (SOI)

The Southern Oscillation Index (SOI) is defined as the pressure difference between Tahiti

and Darwin (Ropelewski and Jones 1987) and presents a signal of the formation and strength of ENSO occurrences in the Pacific Ocean. A sustained value of the SOI index below −7 generally indicates El Niño while sustained values above +7 tend to indicate La Niña conditions.

The form of the SOI used by the Australian Bureau of Meteorology follows Troup (1965), that is, it is the standardised anomaly of the mean sea level pressure (MSLP) difference between Tahiti and Darwin:

$$SOI = 10\frac{P_{diff} - P_{avgdiff}}{SD(P_{diff})}$$

where P_{diff} = (average Tahiti MSLP for the month) - (average Darwin MSLP for the month), $P_{avgdiff}$ = long term average of P_{diff} for the month in question, and $SD(P_{diff})$ = long term standard deviation of P_{diff} for the month in question. The SOI was obtained from http://www.bom.gov.au/climate/current/soihtm1.shtml.

2.3 Methodology

A group of studies (Camargo *et al.* 2007c; Klotzbach 2011; Girishkumar and Ravichandran 2012; Felton *et al.* 2013; Li and Zhou 2013)have observed that TC modulating parameters vary substantially with ENSO. Few studies have investigated the TC frequency, trajectories in the BoB and its relationship with ENSO (Girishkumar and Ravichandran 2012; Ng and Chan 2012; Felton *et al.* 2013) but no single study that we aware of has developed the statistical forecast model to simulate TCs tracks and forecast landfall for months in advance. We developed a forecast model by considering ENSO as a predictor.

The SOI dataset was used in this study and it has a significant broad range from interannual to multidecadal timescales. The data is smoothed by averaging a 3-month period and then a 1 to 6-month lead-lag analysis is used to assess the best predictor timescales for TC forecast potential. Using a 30-year record of TC observations (1980-2009) and SOI data (1979-2009), the distribution of cyclone genesis points is estimated by kernel density. Then the paths of the subsequent cyclone tracks are simulated by modelling the velocity along the observed cyclone tracks as smooth functions of location in each phase and season with a Generalized Additive Model. Trajectories are then

simulated by drawing new random genesis points from the fitted density estimates and tracing the cyclonic paths from the fitted velocity fields to determine the point of landfall. Later the model is validated and assessed to measure the forecast skill.

2.3.1 Genesis modelling

The spatial distribution of tropical cyclone genesis points was modelled by KDE. The detailed concept of KDE is explained by Wahiduzzaman *et al* (2016). The estimator convolves the data with the kernel function to produce a smooth estimate of the density—here, specifically representing the spatial distribution of tropical cyclone genesis occurrences. The degree of smoothing is controlled by the dispersion or "bandwidth" of the kernel.

To define the genesis locations, we determined tropical cyclone by the >=34 knots wind speed (WMO 1997). The spatial distribution of genesis points was then estimated for each season and ENSO phase with a kernel density estimator using a two-dimensional Gaussian kernel and a simple plug-in estimator for the optimal bandwidth (Rigollet and Vert 2009). To generate simulated samples of TC genesis locations we draw the Probability Density Function.

2.3.2 Trajectories modelling

Cyclone tracks were estimated by fitting a Generalized Additive Model (GAM) to the observed trajectories velocity. The GAM is a simplification of linear regression in which the linear relationships are changed by smooth changes of the predictors (*Hastie et al.*, 2009).

Linear regression acts to model the expected value, μ, of the response or dependent variable Y as a linear amalgamation of the forecaster variables $X_1, X_2, \ldots, X_p$,

$$\mu = E(Y|X_1, X_2, \ldots, X_p) = \beta_0 + \beta_1 X_1 + \beta_2 X_2 + \cdots \beta_p X_p$$

where $\beta_0, \beta_1, \ldots, \beta_p$ are the regression coefficients to be estimated. In a Generalized Additive Model, the linear terms are replaced by smooth transformations of the predictors

$$\mu = E(Y|X_1, X_2, \ldots, X_p) = \beta_0 + f_1(X_1) + f_2(X_2) + \cdots f_p(X_p).$$

Where linear regression estimates the regression coefficients $\beta_0, \beta_1, \ldots, \beta_p$, the GAM estimates the smooth transformations $f_1, f_2, \ldots, f_p$. Typically, these functions do not have an easily represented parametric form.

The detailed concept of GAM is explained by Wahiduzzaman *et al.*, (2016). For the present application, the GAM is fitted to the observed tropical storm track velocities. Storm track velocities are calculated from storm tracks by differencing the latitudinal and longitudinal positions to generate velocities along the track increments. For each combination of season and ENSO phase, cyclone genesis points were drawn randomly from the kernel estimate of genesis points (a number of 50) and trajectories were simulated up to 7 days with a 4 times/day time step. As almost 80% of NIO region TC lifetimes are seen within 7 days from TC formation so 7-day will be a sensible and suitable choice for the model (Wahiduzzaman *et al.*, 2016).

2.3.3 Landfall modelling

For each simulated track it was also determined whether it made landfall by country mask approach. To make the identification of the landfall possible, a fine scale raster mask of the North Indian Ocean rim countries was first constructed. To determine the place and time of the landfall, each trajectory was interpolated to a finer time scale and successive points along this fine-scale trajectory were compared to the raster land mask, with the first point to fall on land considered to be the point of the landfall which we have considered for the model as multiple landfalls are rarely seen in the NIO region (Wahiduzzaman *et al.*, 2016).

2.4 Model Validation

Two validation methods were applied in this study.

2.4.1 Validation method 1

Leave-one-out cross-validation (LOOCV) was implemented by deleting each trajectory in turn and then predicting the trajectories related to the removed trajectories built on a model fit to the compact data set. For each trajectory we predicted the country of landfall by majority vote (Wahiduzzaman et al, 2016) from the simulated tracks.

2.4.2 Validation method 2

The second validation approach examines the distance between the observed and predicted landfalls for trajectories. For every observed landfall, a number of tracks originating from the same genesis point as the observed track were simulated, and histograms of the distance between the observed and simulated landfalls were

constructed.

2.5 The best predictor timescales for TC forecast potential

We evaluated the best predictor timescale for the ENSO lead-lag analysis by two approaches, the first based on the distance calculation, and the second based on comparing the simulated country of landfall (as determined by majority vote) to the observed country of landfall. Table 1 shows the percentage of simulated tracks that make landfall within 500 km of the observed landfall by lead month, and this percentage is converted to a skill score by decile. The highest (66.5%) percentage (skill score 7) is seen in a 2-month advance to forecast landfall, but the model also makes strong predictions for 5 and 6-month leads (skill 6), with the weakest performance at 3 and 4-month leads.

Table 1. For each lead month, the difference between observed and simulated tropical cyclones landfall is shown as ENSO predictor. The highest skill is denoted by bold percentages. The skill score 1 is defined as 1-10% and such that 10 is 91-100%.

Lead Month	TC landfall (in percentage)	Skill
1	47.9	5
2	**66.5**	**7**
3	22	3
4	24.1	3
5	53.5	6
6	53.5	6

Table 2 compares the observed number of TC landfall with the model predicted landfall from the simulated tracks for each ENSO lead month. In general, the model under-predicts landfall in Bangladesh and consistently over-predicts landfall in India and Sri Lanka. As the NIO rim countries have very different sizes and geometries, we chose to focus on point of landfall rather than country of landfall and chose the 2-month lead to forecast.

Table 2. For each lead month, the observed and simulated tropical cyclones landfall frequency as ENSO predictor is shown. For each country, the bold number highlights the best lag and the failure simulation in that lead month is denoted by bold with underlined percentages.

Country	Observed landfall (in number)	Lead month-1 (simulated number)	Lead month-2 (simulated number)	Lead month-3 (simulated number)	Lead month-4 (simulated number)	Lead month-5 (simulated number)	Lead month-6 (simulated number)
India	34	52	53	20	**37**	45	59
Myanmar	7	1	5	**8**	12	11	3
Bangladesh	14	**0**	**2**	**0**	1	**0**	**0**
Sri Lanka	3	7	**2**	17	7	9	5
Yemen	0	7	4	**0**	2	4	3
Oman	5	8	11	1	**6**	4	16
NON*	25	13	11	41	**23**	15	2

*NON=No landfall and/or landfall in other countries that is not considered into model.

3. Results

3.1 The genesis and track model fits per ENSO phase

Three phases of ENSO corresponding to El Niño, Neutral conditions and La Niña are considered here based on SOI values at the time. The highest average frequency of genesis (Fig.2) is observed in the La Niña years (3.67/yr), whereas El Niño and the Neutral years correspond to the 2.9 and 2.76 respectively over the NIO. This results are matching with previous studies done by Girishkumar and Ravichandran (2012); Felton *et al.* (2013) and Mahala *et al.* (2015) over the BoB. Observation of TC tracks (Fig. 2) indicates the movement of trajectories and point of landfall. In El Niño phase, tropical cyclones move in a westward direction (few of them to a northward direction) over the BoB and make landfall in the Tamil Nadu of India, Chittagong of Bangladesh, and Irrawaddy of Myanmar. During the Neutral phase over the BoB, most TC move towards the west (make landfall along the Andhra Pradesh and Orissa of India) and the north (make landfall along the eastern part of Bangladesh) and few of them are in the Irrawaddy coast of Myanmar. During La Niña phase, storms move towards the northwest in the BoB and make landfall along the east coast of India and the southern part of Bangladesh. Over the Arabia Sea (AS), cyclone moves towards Oman for El Niño and the Neutral phase of

ENSO. In short, during El Niño phase a large number of cyclones make landfall below 17°N whereas landfall above 15°N is seen in La Niña and the Neutral phase. Our results match with previous studies done by Girishkumar and Ravichandran (2012); Felton *et al.* (2013) and Mahala *et al.* (2015) over the BoB.

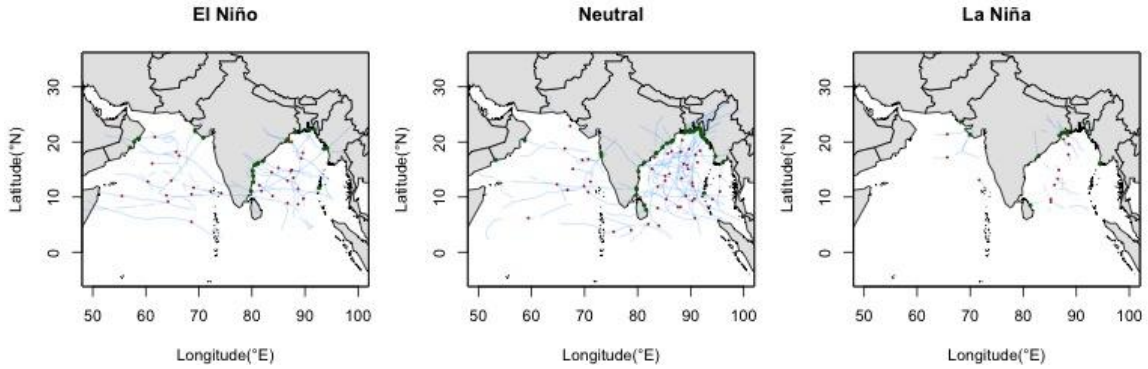

Fig.2 Observed TC genesis, trajectories and landfall for the El Niño (left), Neutral (middle) and La Niña (right) phases of the ENSO in the 30-year period from 1980-2009. Red (green) dots show the genesis (landfall) point in the NIO region (0° to 30°N and 50° to 100°E) and the blue lines specify the trajectories.

The modelled distribution of genesis points, approximated by KDE, is shown for each ENSO phase in Fig.3. The highest densities are found in the BoB for each phase of ENSO. In the Neutral phase the highest density is 7-21° in the BoB and 10-15° in the AS. In the El Niño phase the uppermost densities are nearer to 10-17° in the BoB and 10-13° in the AS, and in La Niña it is in 10-20° for the BoB and 15-18° in the AS.

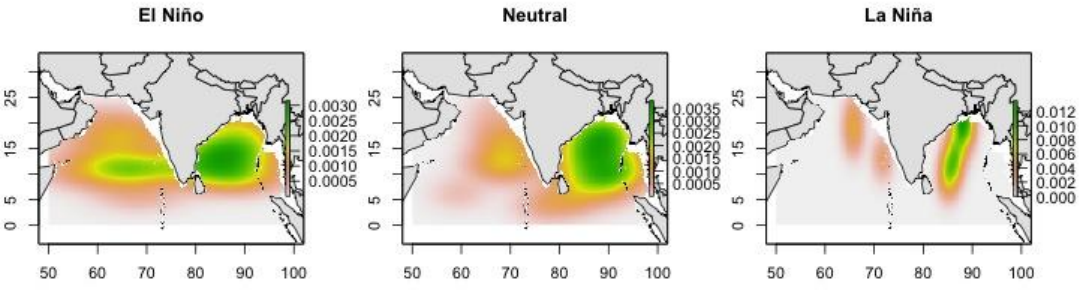

Fig.3 Modelled distributions of TC genesis locations from 1980-2009 based on KDE for the El Niño (left), Neutral (middle) and La Niña (right) phases of the ENSO. Green color shows the highest density (concentration of TC numbers/km^2) area of genesis.

Figure 4 shows the distribution with time since genesis by the ENSO phase. Highest

landfall rate is observed around 0 to 2 days after genesis in La Niña phase (86% of the time). During the Neutral phase it tends to occur 1 to 2 days after genesis (75.6%) and during the El Niño phase 0 to 1 day after genesis (51.1%).

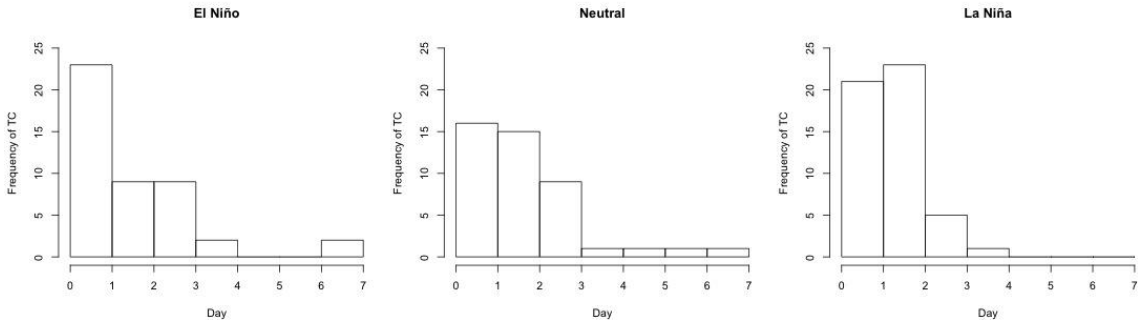

Fig.4 Frequency of observed TC landfall for each ENSO phase as a function of the days from genesis to landfall over the 30-year period (1980-2009).

The distribution of TC velocities by fitting GAM to the observed TC tracks for each ENSO phase is explained in Fig. 5. In the Arabian Sea in an El Niño or Neutral phase, the motion is predominantly westward in the south and more northwestward in the north. During a La Niña there is a more easterward component to the motion. In the BoB during the La Niña and Neutral phases, the motion is predominantly northeastern in the south, with cyclones more strongly directed to Sri Lanka and the tip of India in La Niña. In the North of the BoB, the motion is predominantly northwest in the west and northeast in the east, becoming increasingly so in the Neutral and La Niña phases.

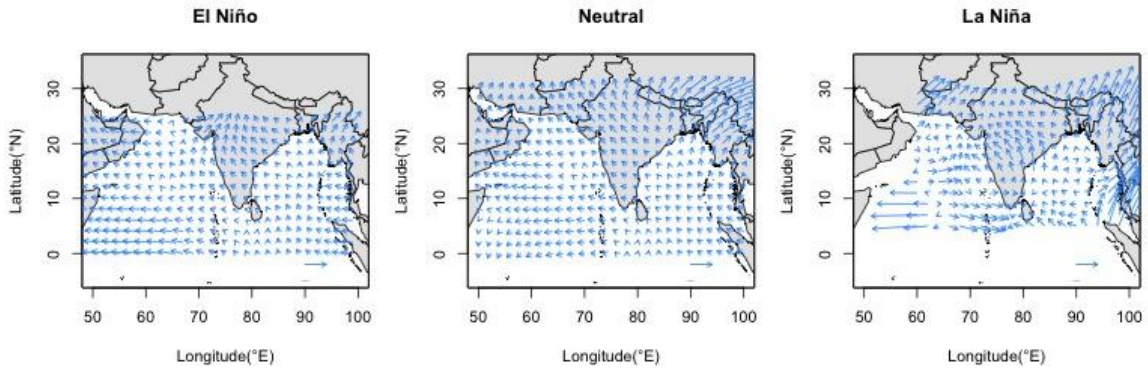

Fig.5 TC track velocities (data from 1980-2009) for each ENSO phase by fitting GAM across the NIO. The velocity magnitude of reference arrow is 10m/s.

3.2 Simulated cyclone tracks and landfall locations

Model simulations of TC trajectories (Fig. 6) shows their movement and point of landfall.

In El Niño phase, tropical cyclones move in a westward or northwestward (few of them towards north-east) direction over the BoB and majority make landfall near the northern Tamil Nadu and Orissa coast of India, the southwestern part of Bangladesh, Arakan and the Irrawaddy coast of Myanmar. This is generally consistent with the observations. Over the AS, storms move towards the north-west and they make landfall in the state of Salalah and the Sor coast of Oman and Yemen. During the Neutral phase over the BoB, many TCs move towards the northwest and make landfall along the Andhra Pradesh coast of India and the Irrawaddy coast of Myanmar. Over the AS, storms move towards the northwest and make landfall in Oman (consistent with observations except in the south-eastern part of Bangladesh). During the La Niña phase, storms move towards the northwest in the BoB and make landfall along the east coast of India, southeastern part of Bangladesh and eastern part of Sri Lanka. Over the Arabian Sea, cyclones move towards the northwest and very few of them to the east (consistent with observations).

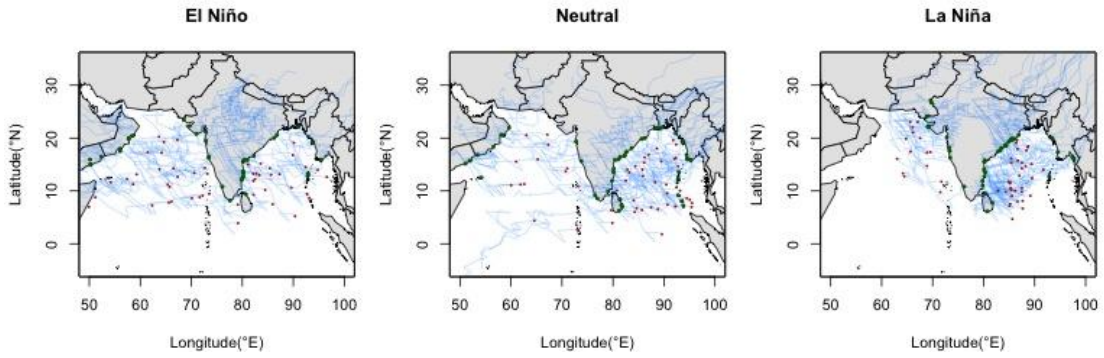

Fig.6 Simulated TC formation, trajectories and landfall over the NIO for the El Niño (left), Neutral (middle) and La Niña (right) phases of the ENSO. Red (green) dots show the TC genesis (landfall) point in the NIO region (0° to 30°N and 50° to 100°E) for a 30-year period from 1980-2009. The blue lines direct the TC trajectories.

In Fig. 7 the frequency of simulated landfall is discussed based on time after genesis across the phases . The maximum frequency is seen around 0-1 day after genesis in La Niña phase (61.2% of the time), El Niño phase (51.1% of the time) and the Neutral phase (44.7% of the time).

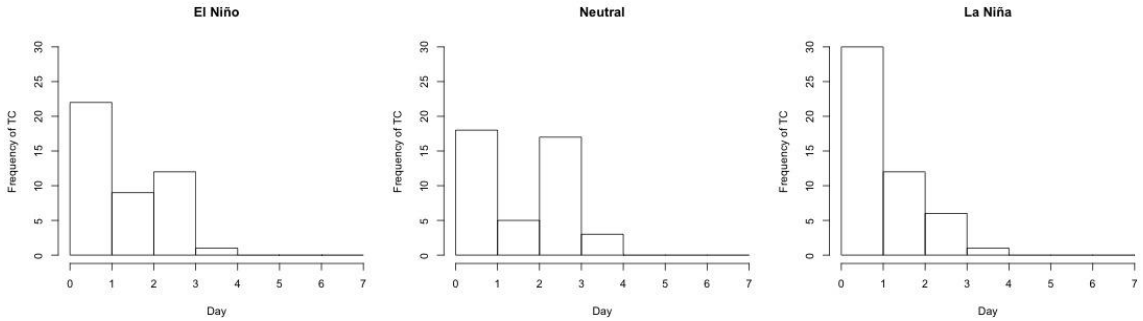

Fig.7 Simulated TC landfall frequency for each ENSO phase based on time from genesis to landfall.

3.3 Seasonwise tropical cyclone activities

Tropical cyclones form most frequently during the post-monsoon (Oct-Nov) season (Fig.8) and the pre-monsoon (Mar-May) contributes approximately half of the post-monsoon. Winter (Dec-Feb) is the the quietest season and the monsoon season also displays the same characteristics as winter though. The movement of tracks by seasons (Fig.8) illustrates most of the TC during post-monsoon moves westward and northwestward, and they make landfalls along the western and north-western coastal fringe of the BoB. However, in pre-monsoon season it tends to track northeastward and make landfall in the north-eastern part of the BoB. In winter, tropical cyclones tend to track towards the west and make landfalls in the south-western fringe of the BoB. During the monsoon season, storms tend to track towards the west or northwestward and make landfalls in the the north-western fringe of the BoB. Among season, pre- and post-monsoon season is the two-peak season for Bangladesh and both contribute a total of 88% landfall whereas individually the pre-monsoon season is the most concerning for Myanmar (about 66% of annual total tropical cyclones are seen to make landfall each year). The most active period (highest percentage of landfall) for India is seen during the post-monsoon season where 71% of annual tropical cyclone landfall is observed. For Sri Lanka, the highest percentage of annual landfall occurred during winter, and on the other hand, for Oman, the maximum annual landfall is seen during the monsoon season.

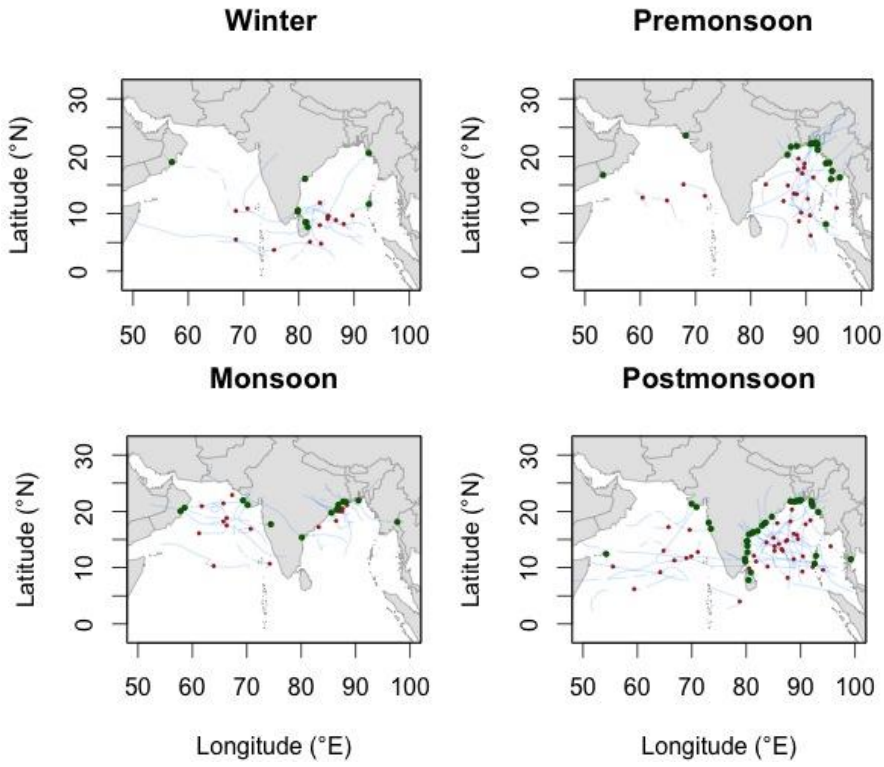

Fig.8 Seasonwise observed TC formation (red dots), trajectories (blue lines), and landfall positions (green dots) for 30-year period (1980-2009) in the NIO.

3.4 Tropical cyclone activities for both season and ENSO phase

Both season and phase wise observed TC tracks (Fig. 9) indicate the movement of TC and their landfall. In El Niño phase, during winter and pre-monsoon, tropical cyclones tend to track in a northward and northeastward direction over the BoB and majority make a landfall in the eastern part of the BoB, especially Chittagong in Bangladesh and the Irrawaddy coast of Myanmar. However, cyclones move towards the north or westward during the monsoon and post-monsoon season and majority make landfall along the Tamil Nadu and Andhra Pradesh coast in India and a few are on the western fringe of Bangladesh. Over the BoB and the AS, during the winter, monsoon and post-monsoon season in the neutral phase, storms move westward and make a landfall in Sri Lanka (during winter) and along the Orissa (in monsoon) and Andhra Pradesh (in post-monsoon) coast of India. However, north-eastward movement with landfall in the eastern part of Bangladesh and Myanmar is seen in the post-monsoon season. During the La Niña phase in all seasons, storms move westward or northwestward in the BoB and the AS and make a landfall along the east coast of India and the southern part of Bangladesh.

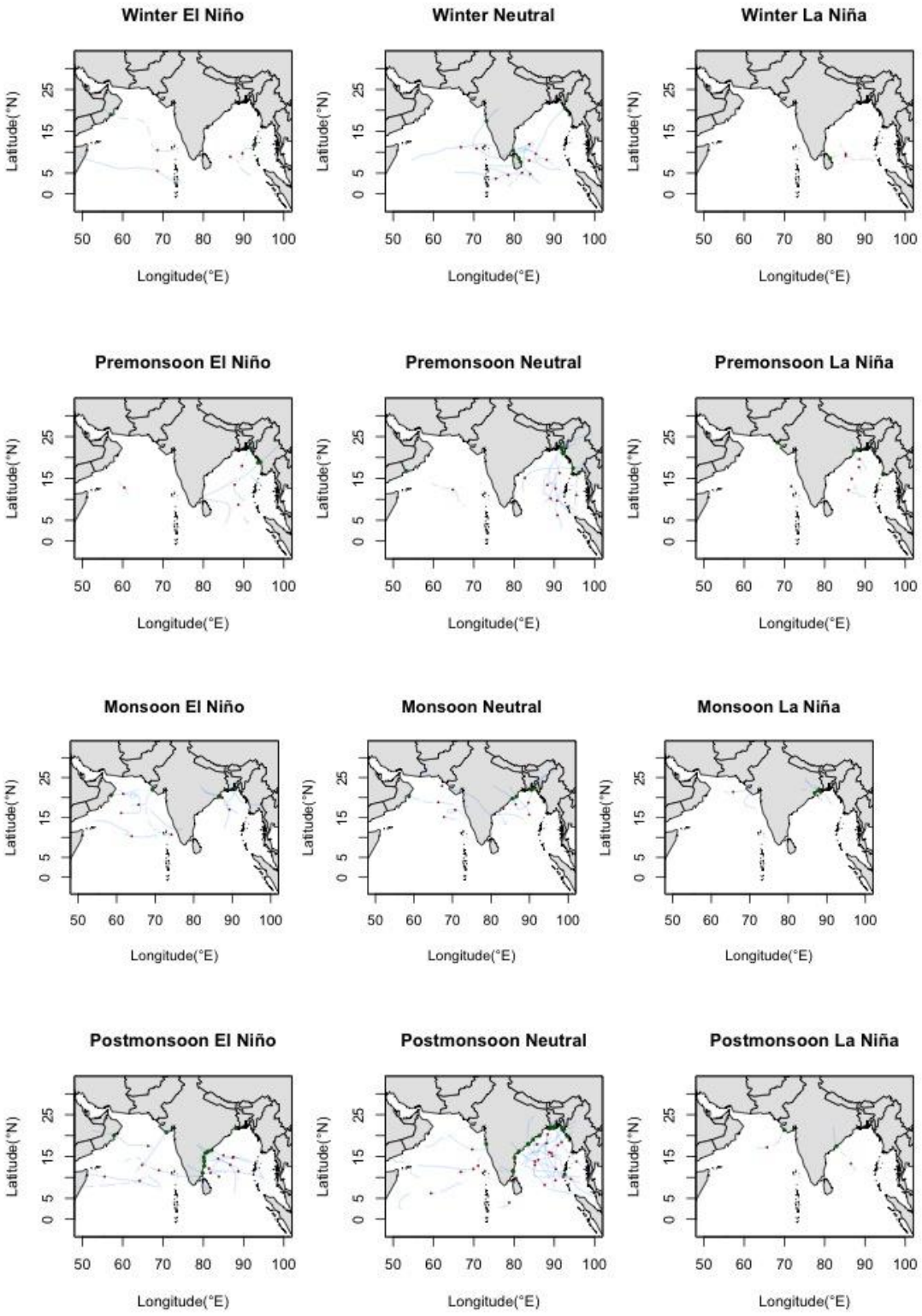

Fig.9 Observed TC formation, trajectories and landfall over the NIO for El Niño jointly with the season (left), Neutral jointly with the season (middle) and La Niña jointly with the season (right). Red dots show the TC genesis points. The blue lines direct the tropical cyclone trajectories with the first landfall point indicated as a green dot.

The modelled distribution of genesis points for each season and each ENSO phase is

shown in Fig.10. In winter, for all 3 phases of ENSO, the highest densities are seen 5-10° in the BoB and in the AS, while the highest genesis densities are closer to 10-20° in the BoB and 10-15° in the AS in the pre-monsoon. On the other hand, the highest densities are found 15-20° in the BoB and 10-20° in the AS in the monsoon season whereas post-monsoon shows highest densities in 10-20° for the BoB and the AS for all three phases of ENSO.

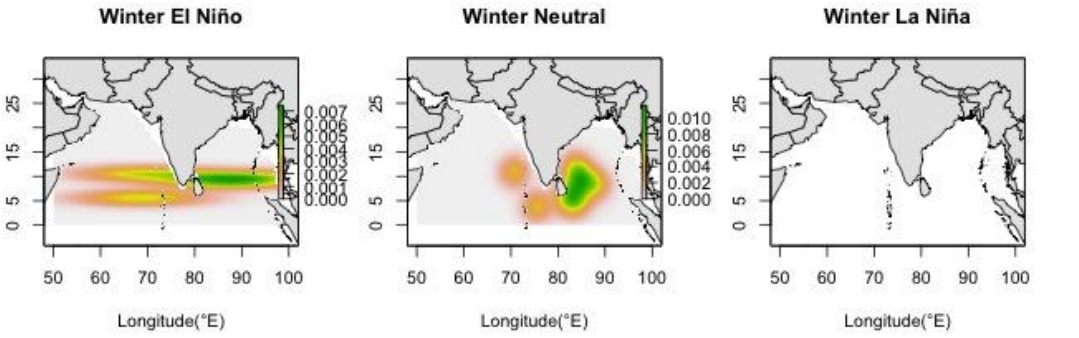

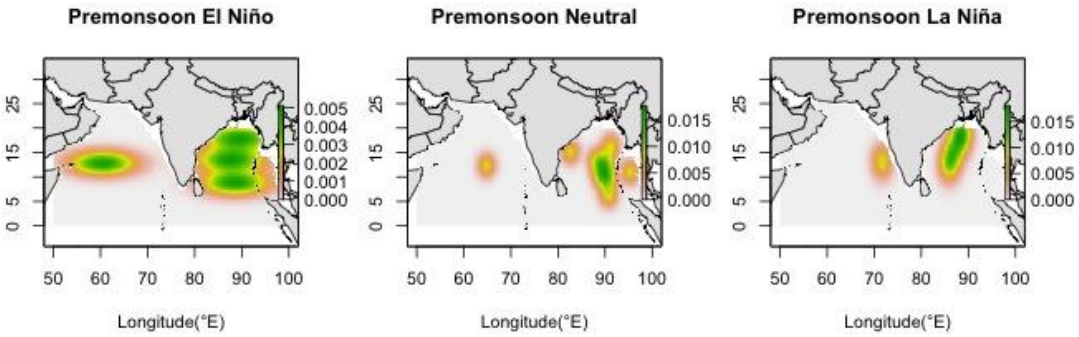

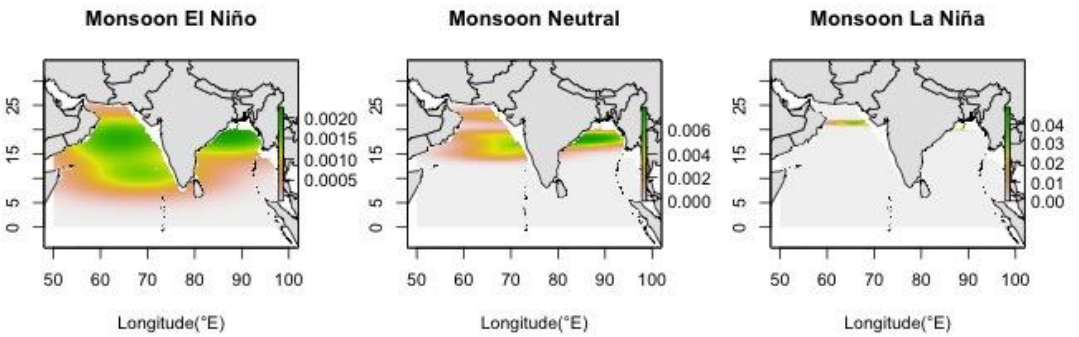

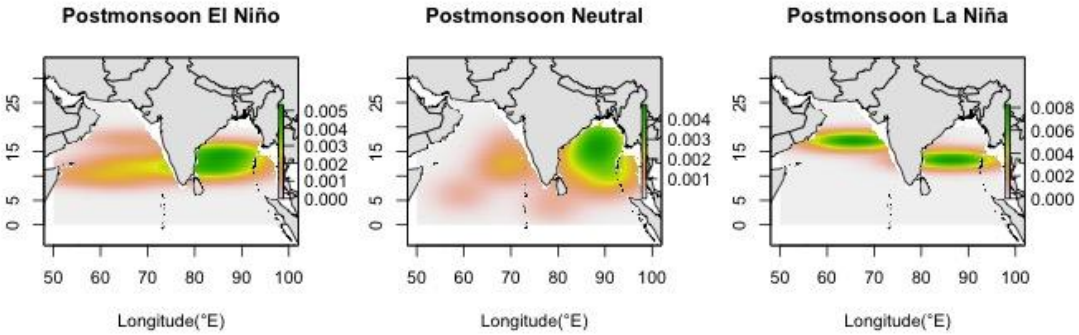

Fig.10 Modelled distributions of TC genesis locations in the NIO for the El Niño (left), Neutral (middle) and La Niña (right) phases of the ENSO with season based on the 30-year period 1980-2009. Green color shows the highest density (concentration of TC numbers/km^2) area of TC formation.

The distribution of TC velocities by fitting GAM to the observed TC tracks for each ENSO phase with season is explained in Fig. 11. In winter El Niño phase, the velocity field indicates a northeastward movement in NIO, whereas in both Neutral and La Niña phase the field is towards the west and later recurving towards the east. During pre-monsoon season each phase shows different characteristics of movement where the velocity field is towards the north in El Niño phase, east in Neutral phase as well as west and later eastward during La Niña phase in the BoB, whereas for the AS, the velocity field is towards the north-west (west) in El Niño and Neutral (La Niña) phase. During monsoon and post-monsoon, the velocity field indicates a westward movement for all three phases of ENSO except post-monsoon La Niña phase in which their movement turns west to east.

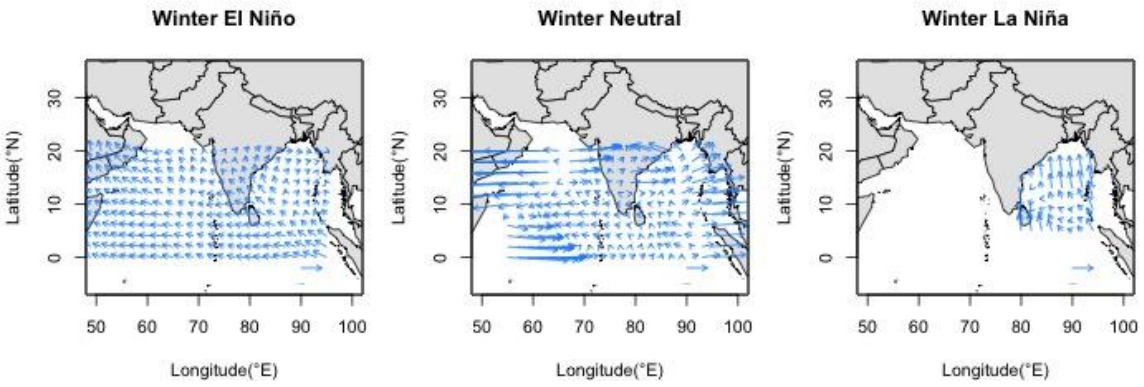

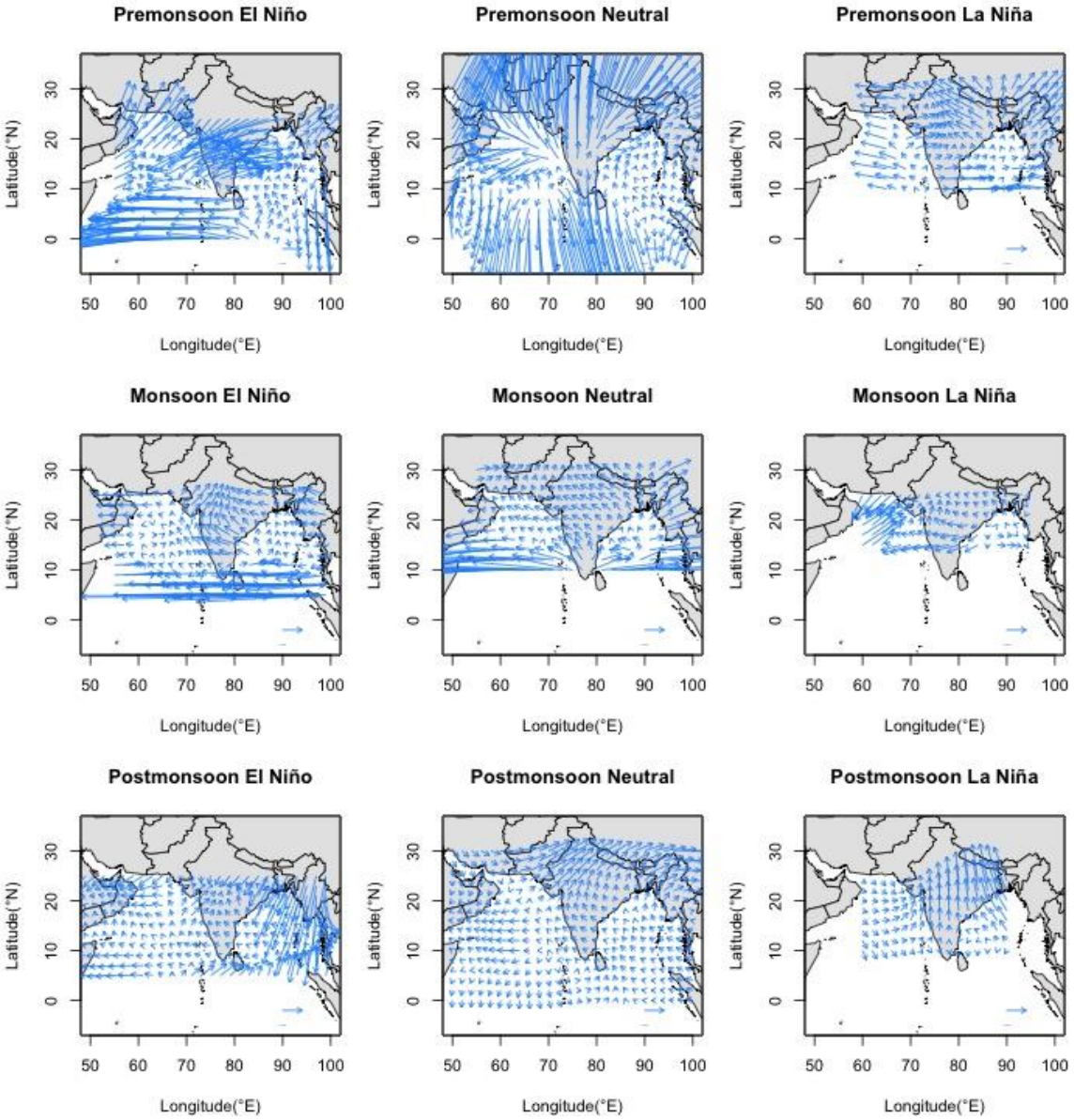

Fig.11 TC track velocities (data from 1980-2009) for each ENSO phase with season by fitting GAM across the NIO. The velocity magnitude of reference arrow is 10m/s.

Model simulations of TC tracks (Fig. 12) per season ENSO phase indicate the movement of trajectories and their point of landfall. During the winter and pre-monsoon El Niño phase, tropical cyclones tend to track towards northeastward over the BoB and majority make landfall in the eastern part of the BoB, especially Chittagong-Cox's bazar coast in Bangladesh and the coastal zone of Myanmar. However, cyclones move towards the north during the monsoon and most of them make landfall along the coastal fringe of Bangladesh, and also during the post-monsoon season cyclones move westward where they make landfall along the Tamil Nadu and Andra Pradesh coast in India. Over the AS,

during the El Niño phase for all four seasons, storms move westward and make landfalls in the coastal fringe of Oman, except in the winter as there is no simulated landfall. This is generally consistent with the observations. During the Neutral phase over the BoB, a majority of storms move northwards in winter, eastwards in the pre-monsoon, both eastwards and westwards in monsoon and west in the post-monsoon season. For all four seasons in La Niña phase, storms move towards the west (consistent with observations) in the BoB and make landfalls along the east coast of India and also the southeastern part of Bangladesh for monsoon and Myanmar for post-monsoon, whereas over the AS, cyclone movement varies with the season (consistent with observations).

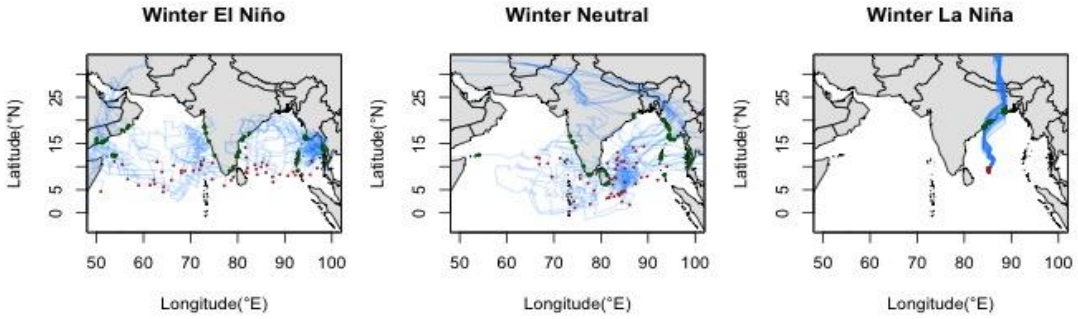

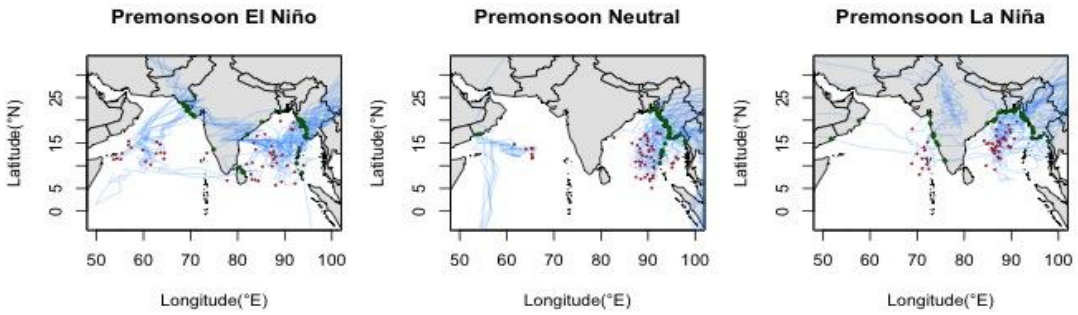

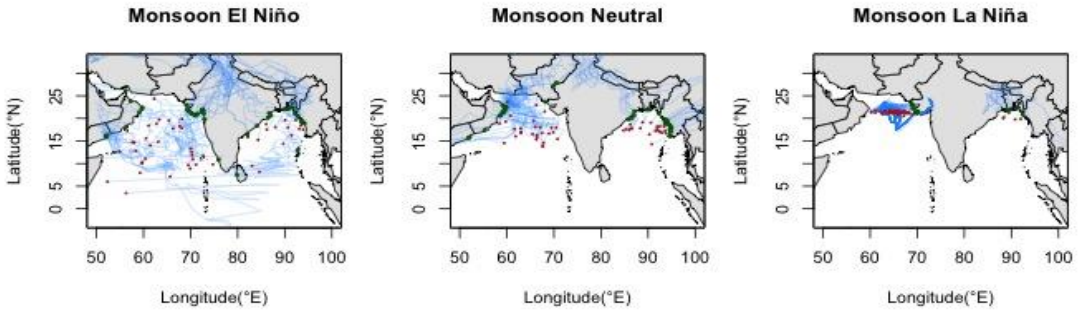

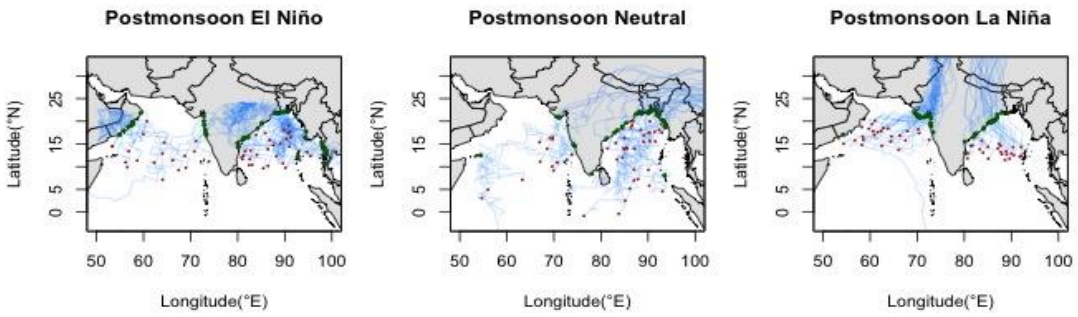

Fig.12 Simulated TC formation, trajectories and landfall during four seasons over the NIO for the El Niño (left), Neutral (middle) and La Niña (right) phases of the ENSO. Red (green) dots show the TC genesis (landfall) point in the NIO region (0° to 30°N and 50° to 100°E) for a 30-year period from 1980-2009. The blue lines direct the TC trajectories.

3.5 Dynamical mechanism determining TC movement

The movement of TC is determined by the driving force of steering flow (Fadnavis *et al.* 2014). Earlier studies by Girishkumar and Ravichandran (2012) found that 200 hPa wind patterns during ENSO regimes do not confirm any substantial difference however George (1976) explained 500 hpa wind patterns as best for TC motion. We have shown 500hpa wind patters for pre-monsoon and post-monsoon during ENSO phases.

The wind patterns during El Niño, Neutral and La Niña are shown in Fig.13. In the pre-monsoon during El Niño phase, the winds move towards westward below 12^0 N and eastward 16^0 N above for NIO (Fig. 13a). Neutral (Fig.13b) and La Niña followed the same characteristics with exception in between 12-16^0 N where winds move south-westward in AS (Fig.13c). In the post-monsoon during El Niño (Fig.13d) and Neutral (Fig.13e) phase, the winds move towards north-westward in BoB and westward in AS till 18^0 N. On the otherhand, during La Niña phase, the winds move towards westward in the NIO with exception around 6^0 N in BoB where wind moves eastward (Fig. 13f).

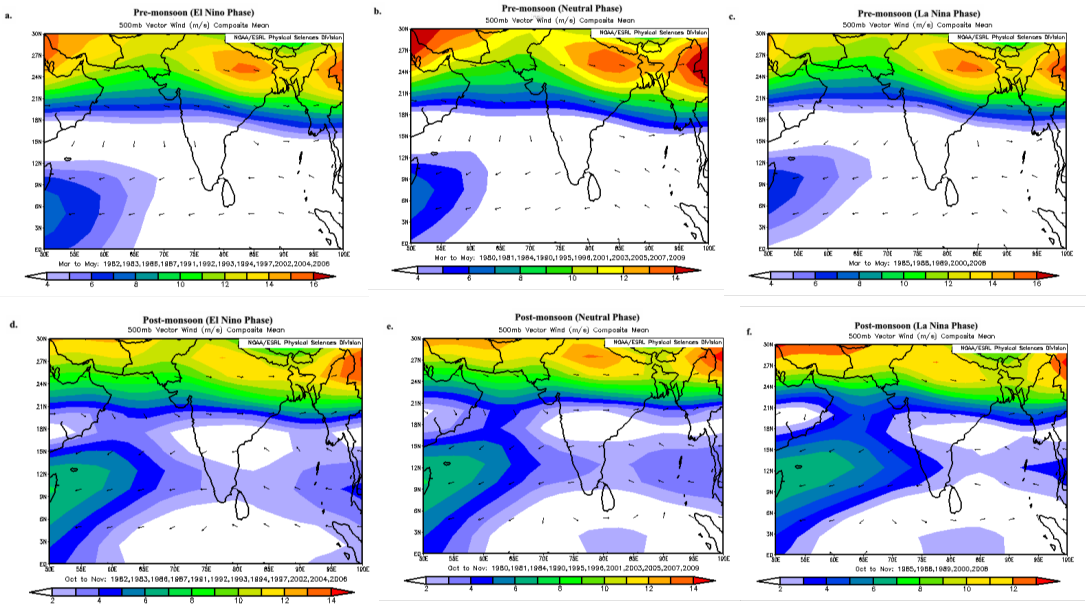

Fig.13 Distribution of 500 hPa winds (m/s) in the pre-monsoon season during a) El Niño, b) Neutral, and c) La Niña, and post-monsoon season during a) El Niño, b) Neutral, and c) La Niña.

3.6 Validation skill of model against observations

The model was validated by Leave-one-out cross-validation (LOOCV) with majority vote approach and distance calculation. Using the LOOCV with majority vote approach for a climatological model, Wahiduzzaman *et al.* (2016) found that the model prediction compared well with observation.

For this validation, the highest percentages of both observed and simulated landfall totals are 38% and 60%, respectively, in India. The observed percentage (7.9%) for Myanmar is simulated remarkably well by the model (5.7%). The percentage difference in total landfall occurrences (Table 3) between the observations and simulated values is smallest for Sri Lanka (1.1%) and Myanmar (2.2%).

Table 3. of Total annual observed and simulated Number and percentages of tropical cyclones landfall probability across the NIO rim

Country	Observation		Simulation	
	No	%	No	%
India	34	38.6	53	60.2

Myanmar	7	7.9	5	5.7
Bangladesh	14	15.9	2	2.3
Sri Lanka	3	3.4	2	2.3
Oman	5	5.7	11	12.5
Yemen	0	0	4	4.5
Total landfall	63	71.6	77	87.5
NON	25	28.4	11	12.5
Total	88	100	88	100

Following the second model validation approach, we calculated the distance between observed and simulated landfall and presented in Fig. 14b. The maximum simulated TC landfall (68.8%) happened within 500 km. By considering the spatial scale of TC (~1000 km), the landfall within ~500 km by model suggest a good model performance.

3.7 Forecast skill of model against observations

To assess the model skill, a comparison between observation and the model simulation is presented in Table 4. The model simulation considered both climatology and ENSO predictor. The seasonal forecast model is found to perform well in comparison with the purely climatological model. The forecast model predicted very well for Myanmar (5.7%) and Sri Lanka (2.3%) (consistent with observation). The climatology is showing a very good skill for India and Oman (consistent with observation).

Table 4. Number and percentages of annual total North Indian Ocean region's observed and simulated tropical cyclones by climatology and ENSO predictor with landfall probability across each country

Country	Observation		Simulation (Climatology)		Simulation (Forecast Model	
	No	%	No	%	No	%
India	34	38.6	38	43.2	53	60.2
Myanmar	7	7.9	1	1.1	5	5.7

Bangladesh	14	15.9	0	0	2	2.3
Sri Lanka	3	3.4	16	18.2	2	2.3
Oman	5	5.7	3	3.4	11	12.5
Yemen	0	0	2	2.3	4	4.5
Total landfall	63	71.6	60	68.2	77	87.5
NON	25	28.4	28	31.8	11	12.5
Total	88	100	88	100	88	100

In addition, following the distance calculation approach 68.8% of total TC landfalls were within 500 km whereas 63.3% of total TC landfalls were within 500 km by climatological model so the forecast model claims approximately 15% improvement over climatology (Fig.14).

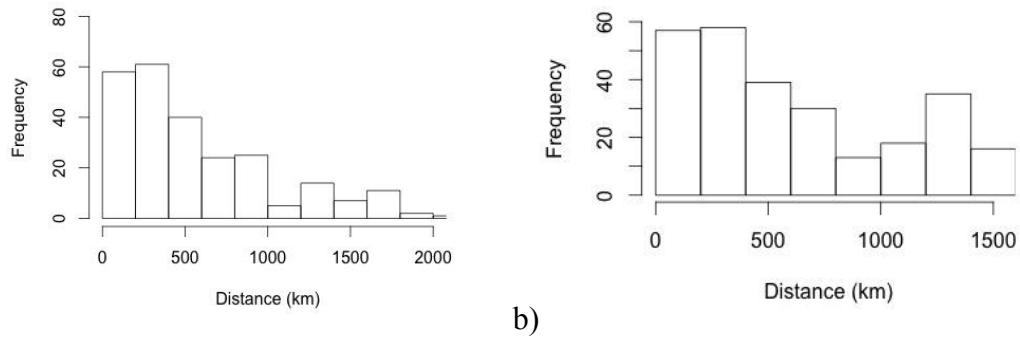

a) b)

Fig. 14 Distribution of distances between observed and simulated landfall location over the NIO a) during climatology b) when ENSO is considered as a predictor

The skill of model forecasts for each season of the year from 2010-2013 has been examined by considering ENSO phase. During this period of time TCs occurrence have been found in winter (2011), pre-monsoon (2010 and 2013) and post-monsoon (2010-12). The observation, model forecast and model anomalies (forecast model – climatological model) are shown in Fig 15. In the 2010 pre-monsoon period, observed landfall is seen in Andhra Pradesh of India, Oman (Fig 15.a) and the model forecasted highest probabilities in Andhra Pradesh, Orissa in India, Rakhine in Myanmar (Fig.15b). The forecast model minus climatology showed a maximum increased likelihood in Andhra Pradesh, Orissa of India with a decreased likelihood in Ayeyarwady, Myanmar (Fig.15c). For post-monsoon period, observed landfall is seen in Rakhine of Myanmar (Fig.15d) and the model

forecasted maximum probabilities along the Myanmar coast (Fig.15e). The forecast model minus climatology showed a maximum increased likelihood along the Myanmar coast with a decreased likelihood along the eastern part of India coast (Fig.15f).

In winter season 2011, TC made landfall in Tamil Nadu of India (Fig.15g) and the model predicted landfall towards head of Sri Lanka as well as Tamil Nadu of India (Fig.15h). Probability was more in Sri Lanka and less in Tamil Nadu of India than climatological model (Fig.15i). For post-monsoon, observed landfall is seen in Chittagong of Bangladesh as well as Dofar in Oman (Fig. 15j) and the model predicted maximum probabilities along the east coast of Bangladesh as well as Myanmar (Fig. 15k). The forecast model minus climatology showed a maximum increased likelihood along the Bangladesh (east coast)-Myanmar coast with a decreased likelihood along the eastern part of India coast as well as Dofar in Oman (Fig.15l).

During 2012 post-monsoon period, TC made landfall in Andhra Pradesh of India (Fig. 15m) and the model forecasted highest probabilities along the Myanmar coast followed by Andhra Pradesh, India (Fig. 15n) where positive anomalies are seen in Myanmar coast with negative anomalies along east coast of India (Fig. 15o).

In 2013 pre-monsoon season, observed landfall is seen in Chittagong coast of Bangladesh (Fig. 15p) and the model predicted maximum probabilities in Chittagong of Bangladesh, Rakhine in Myanmar, Andhra Pradesh and Orissa in India (Fig. 15q) where these regions showed positive anomalies and maximum negative anomalies are found in Barisal coast of Bangladesh and Ayeyarwady in Myanmar (Fig. 15r). Overall, the skill of model for each season shows well performance compared to climatological model.

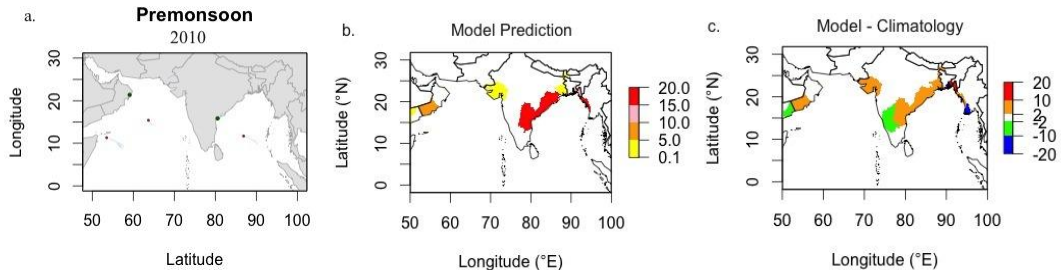

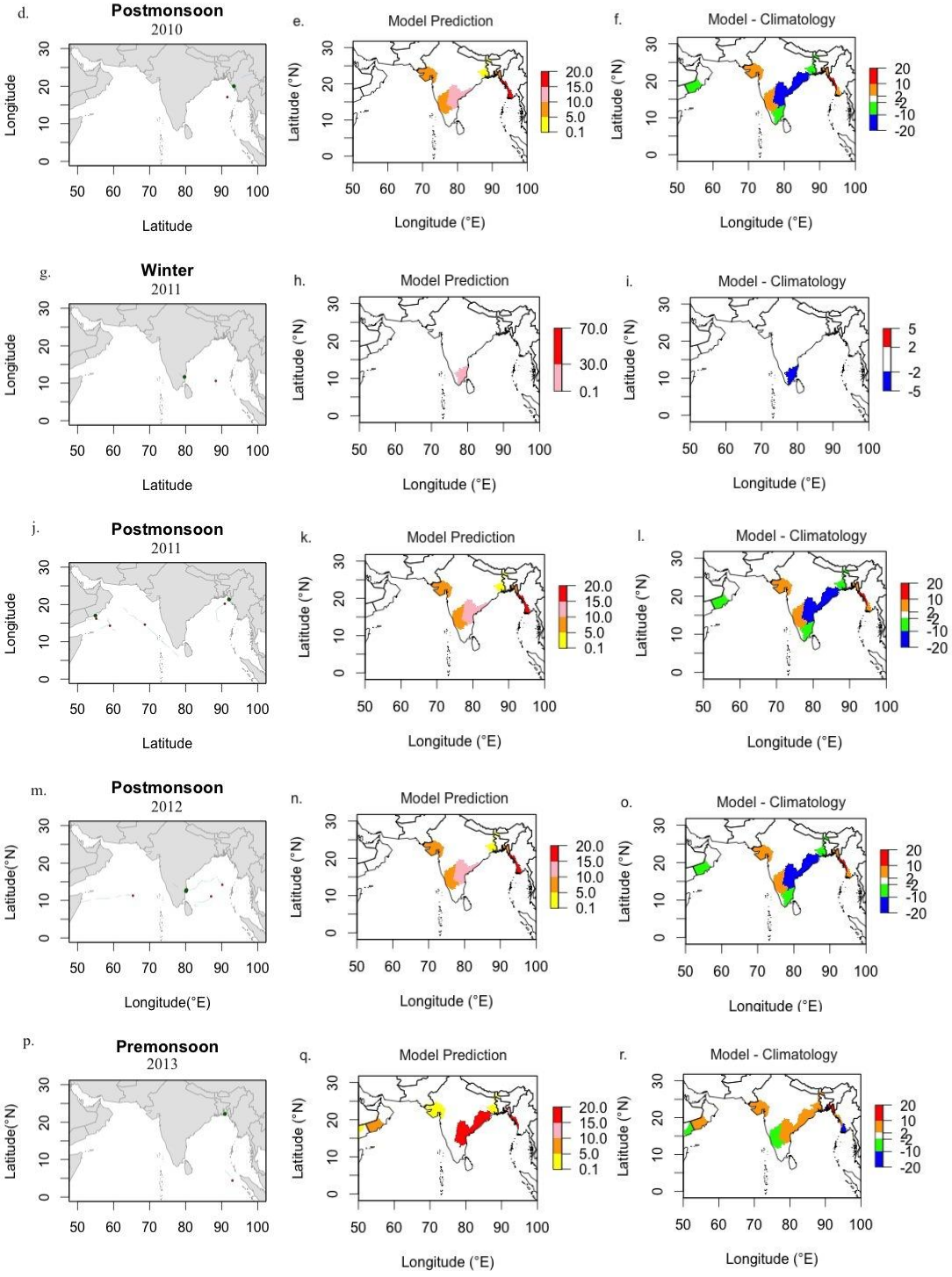

Fig.15 Observed (left) and hindcast model prediction (middle) and the difference between the two- model forecast (right) probabilities of landfall across the NIO rim countries for a,b,c) 2010 pre-monsoon; d,e,f) 2010 post-monsoon; g,h,i) 2011 winter; j,k,l) 2011 post-monsoon; m,n,o) 2012 a post-monsoon and p,q,r) 2013 pre-monsoon.

To examine the forecast skill more generally, we have presented a hold-one-out validation by running the model 30 times where each time holding out one year and validating based

on that held-out year. For instance, we hold out 1980 then fit over the rest of period (1981-2009) and predict for 1980. By averaging all the validation results we draw maps to focus the probabilities by forecast model as well as the difference with climatological model. The pre and post-monsoon (two major peak seasons) observation, model forecast and model anomalies (forecast model – climatological model) are shown in Fig. 16. In pre-monsoon El Niño phase, TC made landfall in Rakhine of Myanmar (Fig.16a) and the model forecasted maximum landfall probabilities along the Myanmar coast (Fig.16b) with positive anomalies in Ayeyarwady of Myanmar and negative anomalies in Rakhine of Myanmar and Andhra Pradesh & Orissa of India (Fig.16c). During the Neutral phase, TC made landfall in Chittagong of Bangladesh, Rakhine of Myanmar (Fig.16d) and the model forecasted well in these regions (Fig.16e) and positive anomalies are seen in Chittagong of Bangladesh (Fig. 16f). In La Niña phase, TC landfall is seen in West Bengal of India (Fig.16g) which is predicted well by forecast model (fig.16h) compared to climatology through anomalies (Fig.16i).

During post-monsoon El Niño phase, TC made landfall in Andhra Pradesh of India and Oman (Fig. 16j) and we found model predicts maximum in these regions (Fig.16k) with positive anomalies and negative anomalies are found in West Bengal of India (Fig. 16l). In Neutral phase, maximum landfall is seen in east coast of India (Fig.16m) and the model predicted maximum probabilities along the coast of Myanmar as well as south east of India (Fig. 16n). The forecast model minus climatology showed a maximum increased likelihood along the east coast of India except West Bengal (Fig.16o). During La Niña phase, TC made landfall in Andhra Pradesh and Gujarat of India (Fig. 16p) and the model forecasted well in these regions (Fig 16q) with positive anomalies (Fig.16r).

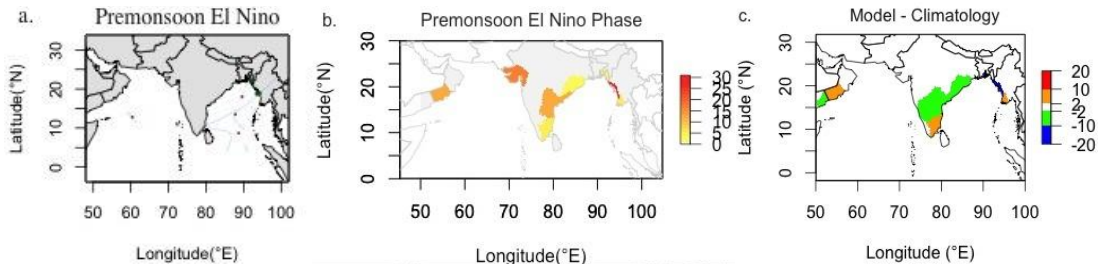

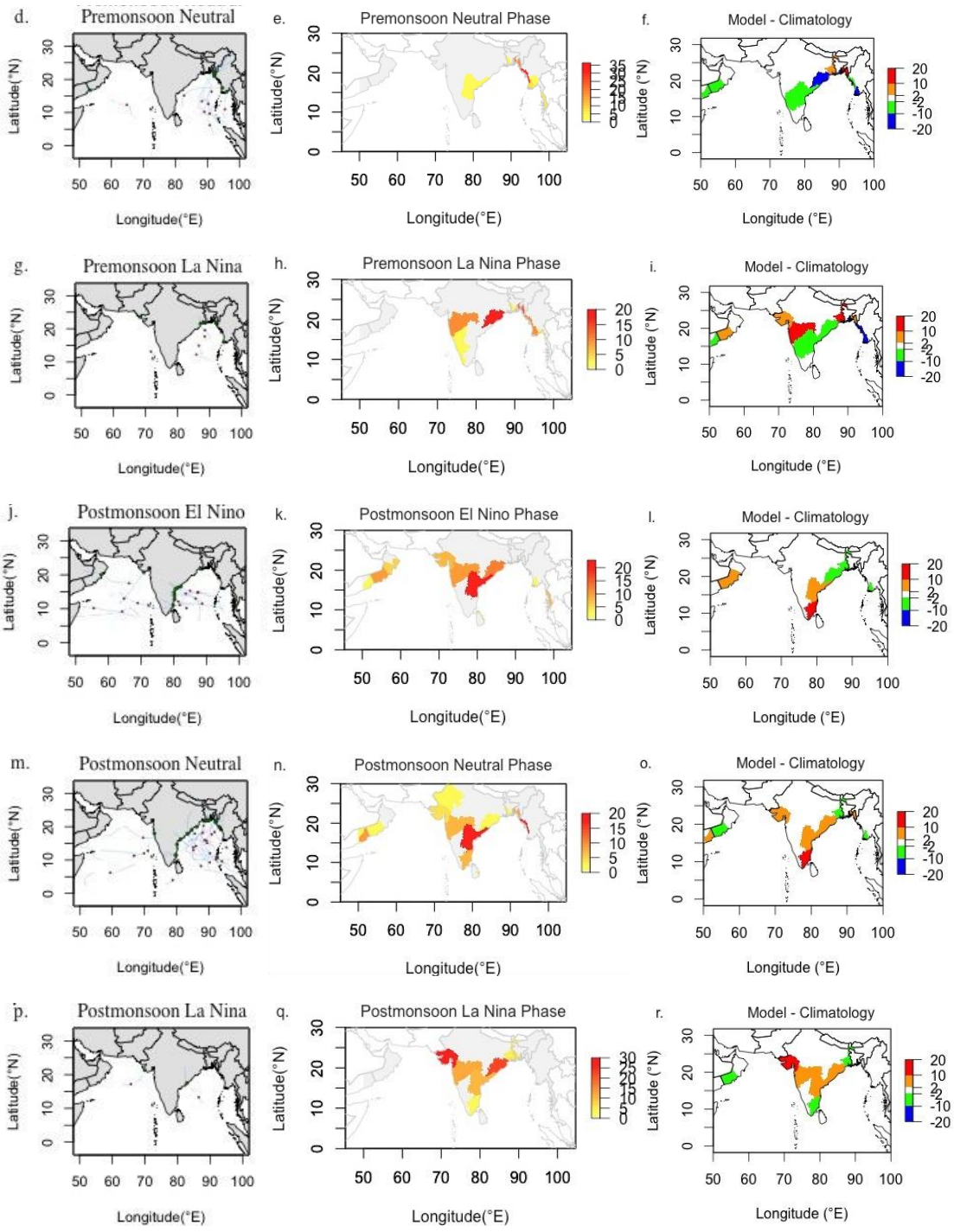

Fig.16 Observed (left), forecast model (middle) and the forecast - climatological model (right) probabilities of TC landfall over the NIO rim for a,b,c) pre-monsoon and El Niño phase; d,e,f) pre-monsoon and Neutral phase; g,h,i) pre-monsoon and La Niña phase; and j,k,l) post-monsoon and El Niño phase; m,n,o) post-monsoon and Neutral phase; and p,q,r) post-monsoon and La Niña phase. Results have been accumulated across 30-years of leave-one-out cross validation.

4. Summary and Discussion

This paper developed a statistical seasonal forecast model of TC activities while considering ENSO influence over the NIO. The paper addresses questions and carries out analyses using a variety of statistical methods and climate analysis tools for the seasonal forecast models.

Felton *et al.* (2013) have recently shown that there is a potential relationship between ENSO and TC. Building on these recent research findings we have used Kernel density estimation (KDE) to model the TC genesis points, then Generalized Additive Model (GAM) to model the TC tracks. By random genesis points based on the KDE, simulated TC tracks have been generated by the GAM from which landfall positions down to country scale have been modelled. By stratifying these practices of TC model based on the different phases of climate factors, including El Niño Southern Oscillation (ENSO), their impacts have been studied and seasonal forecast of future TC activity considering ENSO has been done.

During 30-year time (1980-2009), a total number of 88 tropical cyclones (TCs) have been observed and a number of 63 (71.6%) made landfall across six NIO rim countries. For the ENSO phase, the highest average frequency of genesis is seen in the La Niña years (3.67), whereas El Niño and the Neutral years correspond to the 2.9 and 2.76 respectively over the NIO. There is a significant change for the cyclonic movement during the season and the ENSO phase and this is consistent with the model simulation. The landfall probabilities for each phase and the season vary across phases and country of NIO rim.

During El Niño phase of ENSO, the GAM-fitted velocity field highlights westward/northwestward direction while during La Niña phase they move westward and northeastward. TC tracks, when stratified as per the phases of ENSO, show the evidence of an influence of ENSO on track direction and landfall. During El Niño phase of ENSO, cyclones move below 17°N while during La Niña phase they move above of 15°N to make landfalls. During La Niña period, cyclones head to the northwest direction; these cyclones are formed in the eastern part of the Bay of Bengal and make landfalls above 15°N on the east coast of India, particularly the Orissa coast and the southwestern fringe of Bangladesh. On the other hand, during the El Niño years most of the genesis is found in the western Bay of Bengal where TCs are moving in the westward direction (15°N) towards the east coast of India, particularly Tamil Nadu and Andhra Pradesh.

The KDE/GAM formalism as applied in this study is a unique method to model TC genesis and tracks. By generating random genesis points from the KDE distribution and then following the GAM velocity field, "future" TC tracks have been resulted. This formalism is different from regression-based forecast models. In regression-based forecast models, it is intended that the physical mechanisms behind how the predictors affect TC activity be represented, as least indirectly, in the models. Comparatively, the KDE/GAM is purely phenomenological model that replicates the climatological distribution.

Two methods have been applied to cross-validate this statistical forecast model. Based on first leave-one-out cross-validation the percentages of annual simulated TCs landfall across the NIO rim countries compare well with observation. The performance of the model was very good for Sri Lanka and Myanmar. Another cross-validation approach calculates the distance between observed and simulated landfall and it was found that the maximum predicted TC landfall are within a relatively short distance (0-500km). Given the typical spatial scale of TCs (~1000km) and compared to the typical error in landfall, this demonstrates that the model is relatively skilful.

The model skill is assessed based on 1 to 6 months lead-lag analysis that confirms ENSO is a good predictor for 2 months advance forecast so based on the sensitivity analysis, we chose the 2 months lead for ENSO predictor The validation approach is compared with the climatological model to assess the skill of the forecast model and it is claimed that the developed model demonstrates that including information on the state of ENSO can improve the skill of seasonal forecasts of TCs in the NIO region. By comparing with the climatology the forecast model shows skill exceeding that of climatology for the NIO rim. The model shows skill for individual year forecasts and from a suite of hindcast simulations, the model claims an approximately 15% improvement over climatology.

Acknowledgment. We would like to sincerely thank anonomous thesis examiner for his insightful comments that helped us to significantly improve the quality of this manuscript. University of Tasmania Graduate Research Scholarship from the University of Tasmania, Australia, supported Mohammad Wahiduzzaman.

3467 ## References

3468 Alam E, Collins AE (2010) Cyclone disaster vulnerability and response experiences in coastal
3469 Bangladesh. Disasters 34(4):931-954

3470 Alam MM, Hossain MA, Shafee S (2003) Frequency of Bay of Bengal cyclonic storms and
3471 depressions crossing different coastal zones. International Journal of Climatology
3472 23(9):1119-1125

3473 Ali MM, Jagadeesh PSV, Jain S (2007) Effects of Eddies on bay of Bengal cyclone intensity. Eos
3474 88(8):93-93

3475 Allan RJ (1988) El Nino Southern Oscillation influences in the Australasian region. Progress in
3476 Physical Geography 12(3):313-348

3477 An S-I, Kug J-S, Timmermann A, Kang I-S, Timm O (2007) The Influence of ENSO on the
3478 Generation of Decadal Variability in the North Pacific. Journal of Climate 20(4):667-680

3479 Ashok K, Saji N (2007) On the impacts of ENSO and Indian Ocean dipole events on sub-regional
3480 Indian summer monsoon rainfall. Natural Hazards 42(2):273-285

3481 Balaguru K, Taraphdar S, Leung LR, Foltz GR (2014) Increase in the intensity of postmonsoon
3482 Bay of Bengal tropical cyclones. Geophysical Research Letters 41(10):3594-3601

3483 Bashtannyk DM, Hyndman RJ (2001) Bandwidth selection for kernel conditional density
3484 estimation. Computational Statistics & Data Analysis 36:279-298

3485 Behera SK, Luo JJ, Masson S, Rao SA, Sakuma H, Yamagata T (2006) A CGCM Study on the
3486 Interaction between IOD and ENSO. Journal of Climate 19(9):1688-1705

3487 Belmadani A, Dewitte B, An S-I (2010) ENSO Feedbacks and Associated Time Scales of
3488 Variability in a Multimodel Ensemble. Journal of Climate 23(12):3181-3204

3489 Bengtsson L, Hodges KI, Esch M (2007) Tropical cyclones in a T159 resolution global climate
3490 model: Comparison with observations and re-analyses. Tellus, Series A: Dynamic
3491 Meteorology and Oceanography 59 A(4):396-416

3492 Camargo SJ (2013) Global and regional aspects of tropical cyclone activity in the CMIP5 models.
3493 Journal of Climate 26(24):9880-9902

3494 Camargo SJ, Barnston AG (2009) Experimental dynamical seasonal forecasts of tropical cyclone
3495 activity at IRI. Weather and Forecasting 24(2):472-491

Camargo SJ, Barnston AG, Klotzbatch PJ, Landsea CW (2007a) Seasonal Tropical cyclone forecasts. Bulletin of the World Meterological Organization 56:297-307

Camargo SJ, Barnston AG, Zebiak SE (2005) A statistical assessment of tropical cyclone activity in atmospheric general circulation models. Tellus, Series A: Dynamic Meteorology and Oceanography 57(4):589-604

Camargo SJ, Emanuel KA, Sobel AH (2007) Use of a genesis potential index to diagnose ENSO effects on tropical cyclone genesis. Journal of Climate 20(19):4819-4834

Camargo SJ, Emanuel KA, Sobel AH (2007c) Use of a Genesis Potential Index to Diagnose ENSO Effects on Tropical Cyclone Genesis. Journal of Climate 20(19):4819-4834

Camargo SJ, Robertson AW, Barnston AG, Ghil M (2008) Clustering of eastern North Pacific tropical cyclone tracks: ENSO and MJO effects. Geochemistry, Geophysics, Geosystems 9(6):1-23

Camp J, Roberts M, Maclachlan C, Wallace E, Hermanson L, Brookshaw A, Arribas A, Scaife AA (2015) Seasonal forecasting of tropical storms using the Met Office GloSea5 seasonal forecast system. Quarterly Journal of the Royal Meteorological Society 141(691):2206-2219

Cane MA, Zebiak SE, Dolan SC (1986) Experimental forecasts of El Nino. Nature 321(6073):827-832

Casson E, Coles S (2000) Simulation and extremal analysis of hurricane events. Journal of the Royal Statistical Society. Series C: Applied Statistics 49(2):227-245

Chand SS, Walsh KJE (2011) Influence of ENSO on Tropical Cyclone Intensity in the Fiji Region. Journal of Climate 24(15):4096-4108

Chu P-S (2004) ENSO and tropical cyclone activity. Hurricanes and Typhoons: Past, Present, and Potential. Columbia University Press.pp.297-328

Du YG, Song JJ, Tang JP (2013) Impacts of different kinds of ENSO on landfalling tropical cyclones in China. Journal of Tropical Meteorology 19(1):39-48

Eichler T, Higgins W (2006) Climatology and ENSO-Related Variability of North American Extratropical Cyclone Activity. Journal of Climate 19(10):2076-2093

Emanuel K, Ravela S, Vivant E, Risi C (2006) A Statistical Deterministic Approach to Hurricane Risk Assessment. Bulletin of the American Meteorological Society 87(3):299-314

Felton CS, Subrahmanyam B, Murty VSN (2013) ENSO-modulated cyclogenesis over the Bay of Bengal. Journal of Climate 26(24):9806-9818

Girishkumar MS, Ravichandran M (2012) The influences of ENSO on tropical cyclone activity in the Bay of Bengal during October-December. Journal of Geophysical Research: Oceans 117(2)

Girishkumar MS, Ravichandran M, Pant V (2012) Observed chlorophyll-a bloom in the southern Bay of Bengal during winter 2006-2007. International Journal of Remote Sensing 33(4):1264-1275

Girishkumar MS, Suprit K, Vishnu S, Prakash VPT, Ravichandran M (2015) The role of ENSO and MJO on rapid intensification of tropical cyclones in the Bay of Bengal during October–December. Theoretical and Applied Climatology 120(3-4):797-810

Girishkumar MS, Thanga Prakash VP, Ravichandran M (2014) Influence of Pacific Decadal Oscillation on the relationship between ENSO and tropical cyclone activity in the Bay of Bengal during October–December. Climate Dynamics 44(11-12):3469-3479

Goswami BN, Ajayamohan RS, Xavier PK, Sengupta D (2003) Clustering of synoptic activity by Indian summer monsoon intraseasonal oscillations. Geophysical Research Letters 30(8):14-21

Hall TM, Jewson S (2007) Statistical modelling of North Atlantic tropical cyclone tracks. Tellus, Series A: Dynamic Meteorology and Oceanography 59 A(4):486-498

Hastie T, Tibshirani R, Friedman J (2009) The Elements of Statistical learning: Data Mining, Inference, and Prediction. Springer Series in Statistics Second Edition, pp.295-333

Ho CH, Kim JH, Jeong JH, Kim HS, Chen D (2006) Variation of tropical cyclone activity in the South Indian Ocean: El Niño-Southern Oscillation and Madden-Julian Oscillation effects. Journal of Geophysical Research: Atmospheres 111(22):65

Hsu PC, Ho CR, Liang SJ, Kuo NJ (2013) Impacts of two types of El Niño and la Niña events on typhoon activity. Advances in Meteorology 2013

Islam T, Peterson RE (2009) Climatology of landfalling tropical cyclones in Bangladesh 1877-2003. Natural Hazards 48(1):115-135

James MK, Mason LB (2005) Synthetic tropical cyclone database. Journal of Waterway, Port, Coastal and Ocean Engineering 131(4):181-192

Kikuchi K, Wang B, Fudeyasu H (2009) Genesis of tropical cyclone Nargis revealed by multiple satellite observations. Geophysical Research Letters 36(6):L06811

Klotzbach PJ (2011) El Niño-Southern Oscillation's impact on Atlantic basin hurricanes and U.S. Landfalls. Journal of Climate 24(4):1252-1263

Knapp KR, Kruk MC, Levinson DH, Diamond HJ, Neumann CJ (2010) The international best track archive for climate stewardship (IBTrACS). Bulletin of the American Meteorological Society 91(3):363-376

Kuleshov Y, Qi L, Fawcett R, Jones D (2008) On tropical cyclone activity in the Southern Hemisphere: Trends and the ENSO connection. Geophysical Research Letters 35(14):L14S08

Larson S, Lee SK, Wang C, Chung ES, Enfield D (2012) Impacts of non-canonical El Niño patterns on Atlantic hurricane activity. Geophysical Research Letters 39(14)

Lau (1985) Elements of a stochastic-dynamical theory of the long-term variability of the El Niño/Southern Oscillation. J. Atmos. Sci. 42:1552-1558

Li RCY, Zhou W (2013) Modulation of western north pacific tropical cyclone activity by the ISO. Part II: Tracks and landfalls. Journal of Climate 26(9):2919-2930

Liebmann B, Hendon HH, Glick JD (1994) The relationship between tropical cyclones of the western Pacific and Indian Oceans and the Madden-Julian oscillation. J. Meteor. Soc. Japan 72:401-411

Lin II, Chen CH, Pun IF, Liu WT, Wu CC (2009) Warm ocean anomaly, air sea fluxes, and the rapid intensification of tropical cyclone Nargis (2008). Geophysical Research Letters 36(3)

Loader CR (1999) Bandwidth Selection: Classical or Plug-In? The Annals of Statistics 27(2):415-438

Mahala BK, Nayak BK, Mohanty PK (2015) Impacts of ENSO and IOD on tropical cyclone activity in the Bay of Bengal. Natural Hazards 75(2):1105-1125

Mohapatra M, Bandyopadhyay BK, Tyagi A (2014) Status and Plans for Operational Tropical Cyclone Forecasting and Warning Systems in the North Inidan Ocean Region. U.C. Mohanty MM, O.P. Singh, B.K. Bandyopadhyay, L.S. Rathore (ed) Monitoring and Prediction of Tropical Cyclones in the Indian Ocean and Climate Change. Springer, pp 149-162

Nath S, Kotal SD, Kundu PK (2015) Seasonal prediction of tropical cyclone activity over the North Indian Ocean using the neural network model. Atmosfera 28(4):271-281

Ng EKW, Chan JCL (2012) Interannual variations of tropical cyclone activity over the north Indian Ocean. International Journal of Climatology 32(6):819-830

Pattanaik DR, Mohapatra M (2016) Seasonal forecasting of tropical cyclogenesis over the North Indian Ocean. Journal of Earth System Science 125(2):231-250

Philander SGH (1985) El Nino and La Nina. Journal of the Atmospheric Sciences 42(23):2652-2662

Philander SGH (1990) El Niño, La Niña and the Southern Oscillation. Academic Press, San Diego, Calif., p 293

Philander SGH (1992) Ocean-atmosphere interactions in the tropics: a review of recent theories and models. Journal of Applied Meteorology 31(8):938-945

Rajasekhar M, Kishtawal CM, Prasad MYS, Seshagiri Rao V, Rajeevan M (2014) Extended range tropical cyclone predictions for East Coast of India. In: Monitoring and Prediction of Tropical Cyclones in the Indian Ocean and Climate Change. pp 137-148

Ray A, Jaiswal N, Kishtawal CM (2012) Cyclone tracking over North Indian Ocean using Artificial Neural Network Models and implementation of regional and seasonal stratification,. In: Second WMO International Conference on Indian Ocean Tropical and Cyclone Change (IOTCCC-2012). New Delhi

Rigollet P, Vert R (2009) Optimal rates for plug-in estimators of density level sets. Bernoulli 15(4):1154-1178

Ropelewski CF, Halpert MS (1996) Quantifying southern oscillation-precipitation relationships. Journal of Climate 9(5):1043-1059

Ropelewski CF, Jones PD (1987) An Extension of the Tahiti–Darwin Southern Oscillation Index. Monthly Weather Review 115(9):2161-2165

Rumpf J, Weindl H, Höppe P, Rauch E, Schmidt V (2007) Stochastic modelling of tropical cyclone tracks. Mathematical Methods of Operations Research 66(3):475-490

Sahoo B, Bhaskaran PK (2016) Assessment on historical cyclone tracks in the Bay of Bengal, east coast of India. International Journal of Climatology 36(1):95-109

Sengupta D, Senan R, Goswami BN, Vialard J (2007) Intraseasonal Variability of Equatorial Indian Ocean Zonal Currents. Journal of Climate 20(13):3036-3055

Shaevitz DA, Camargo SJ, Sobel AH, Jonas JA, Kim D, Kumar A, Larow TE, Lim YK, Murakami H, Reed KA, Roberts MJ, Scoccimarro E, Vidale PL, Wang H, Wehner MF, Zhao M, Henderson N (2014) Characteristics of tropical cyclones in high-resolution models in the present climate. Journal of Advances in Modeling Earth Systems 6(4):1154-1172

Shaji C, Kar SK, Vishal T (2014) Storm surge studies in the North Indian Ocean: A review. Indian Journal of Marine Sciences 43(2):125-147

Singh OP, Ali Khan TM, Rahman MS (2000) Changes in the frequency of tropical cyclones over the North Indian Ocean. Meteorology and Atmospheric Physics 75(1-2):11-20

Singh OP, Ali Khan TM, Rahman MS (2001) Probable reasons for enhanced cyclogenesis in the Bay of Bengal during July-August of ENSO years. Global and Planetary Change 29(1-2):135-147

Srikanth L, Ramalingam M, George MS, Bertino L, Samuelsen A (2012) A study on the influence of oceanic and atmospheric parameters on tropical cyclones in the bay of Bengal. European Journal of Scientific Research 76(1):63-73

Tao L, Wu L, Wang Y, Yang J (2012) Influence of tropical Indian ocean warming and ENSO on tropical cyclone activity over the western North Pacific. Journal of the Meteorological Society of Japan 90(1):127-144

Turlach BA (1993) Bandwidth Selection in Kernel Density Estimation: A Review. CORE and Institut de Statistique 19:1-33

Tyagi A, Bandyopadhyay BK, Mohapatra M (2010) Monitoring and prediction of cyclonic disturbances over North Indian ocean by regional specialised meteorological centre, New Delhi (India): Problems and prospective. In: Indian Ocean Tropical Cyclones and Climate Change. pp 93-103

Vickery PJ, Skerjl P, Steckley AC, Twinsdale L (2000) Simulation of hurricane risk in the united states using an empirical storm track modeling technique. Journal of structural engineering 126:1222-1237

Vissa NK, Satyanarayana ANV, Prasad Kumar B (2013) Intensity of tropical cyclones during pre- and post-monsoon seasons in relation to accumulated tropical cyclone heat potential over Bay of Bengal. Natural Hazards 68(2):351-371

Wahiduzzaman M, Oliver E, Wotherspoon S, Holbrook N (2016) A climatological model of North Inidan Ocean tropical cyclone genesis, tracks and landfall. Climate Dynamics (revision submitted)

Wang B, Chan JCL (2002) How strong ENSO events affect tropical storm activity over the western North Pacific. Journal of Climate 15(13):1643-1658

Webster PJ (2008) Myanmar's deadly daffodil. Nature Geoscience 1(8):488-490

Werner A, Maharaj AM, Holbrook NJ (2012) A new method for extracting the ENSO-independent Indian Ocean Dipole: Application to Australian region tropical cyclone counts. Climate Dynamics 38(11-12):2503-2511

WMO (1997) Tropical Cyclone Operational Plan for the Bay of Bengal and the Arabian Sea,WMO Report 1997.

Yahyai SSA (2014) NWP forecast Guidance during Phet at Oman Meteorological Service. In: U.C. Mohanty MM, O.P. Singh, B.K. Bandyopadhyay, L.S. Rathore (ed) Monitoring and Prediction of Tropical Cyclones in the Indian Ocean and Climate Change,Springer, pp 240-262

Yonekura E, Hall TM (2011) A Statistical model of tropical cyclone tracks in the western North Pacific with ENSO-dependent cyclogenesis. Journal of Applied Meteorology and Climatology 50(8):1725-1739

Zhang W, Graf HF, Leung Y, Herzog M (2012) Different El Niño types and tropical cyclone landfall in East Asia. Journal of Climate 25(19):6510-6523

Zhao H, Wu L, Zhou W (2010) Assessing the influence of the ENSO on tropical cyclone prevailing tracks in the western North Pacific. Advances in Atmospheric Sciences 27(6):1361-1371

4.3 Chapter Summary

This chapter addresses the thesis aims of development of a forecast model to forecast the tropical cyclone genesis, tracks and landfall in the North Indian Ocean region. The model consists three components which are genesis distribution by kernel density estimation, tracks by generalised additive model, landfall by eular intergration with country mask approach. Also the model hindcast skills are quantified.

In detail we have presented a new statistical forecast model to forecast tropical cyclone activities in the North Indian Ocean region. Overall, the model has good cross-validated hindcast skill compared to climatology. Also, the model shows very good cross-validated hindcast performance of modeled landfalling cyclones against observations for most of the NIO rim countries. The components of model are found to be successful in forecasting TC activity of NIO region for the upcoming season. The model skill is assessed based on 1 to 6 months lead-lag analysis that confirms ENSO is a good predictor for 2 months advance to forecast. The distribution of TC genesis, tracks and landfall probabilities over the study period, as well as the hindcasted probabilities of TC landfall during ENSO events match remarkably well against observations over most of the study domain.

5 DEVELOPMENT OF STOCHASTIC MODEL FOR TROPICAL CYCLONE LANDFALL FREQUENCY IN THE NORTH INDIAN OCEAN REGION

5.1 Chapter Overview

This chapter introduces a Poisson regression and generalised additive model for the North Indian Ocean region tropical cyclone genesis, tracks and landfall. The development of Poisson model of tropical cyclone landfall probabilities are based on the observation and influence of predictors while the generalised additive model of tropical cyclone genesis, tracks and landfall for North Indian Ocean rim countries are based on kernel density estimation, velocity field including an Euler integration step, and landfall detection using a country mask approach and this model consider intensity during landfall. The model is fitted to the observed cyclone track velocities as a smooth function of location in each season and the distribution of cyclone genesis points is approximated by kernel density estimation. The model simulated TCs are randomly selected from the fitted kernel and the cyclonic tracks represented by the model together with the application of stochastic innovations at each step and simulated the first point of landfall. Separate cross validation hindcast methods are used to analyse the skill of model.

The main text of this chapter is a paper for submission to *Climate Dynamics (*Wahiduzzaman M, Wotherspoon S, Oliver E, Holbrook N (2017) Stochastic modelling of tropical cyclone landfall across the North Indian Ocean rim, Climate Dynamics, in prep)

5.2 Wahiduzzaman *et al.* 2017; *Climate Dynamics*

Stochastic modelling of tropical cyclone landfall across the North Indian Ocean rim

Md Wahiduzzaman[1], Simon J. Wotherspoon[1,2] , Eric C.J.Oliver[1, 3], and Neil J. Holbrook[1,3]

[1]Institute for Marine and Antarctic Studies, University of Tasmania, Australia

[2] Australian Antarctic Division, 203 Channel Highway, Kingston, Tasmania, Australia

[3]Australian Research Council Centre of Excellence for Climate System Science, Hobart, Tasmania, Australia

For submission to *Climate Dynamics*

Corresponding author address: Md Wahiduzzaman, Institute for Marine and Antarctic Studies, University of Tasmania, Australia | E-mail: **md.wahiduzzaman@utas.edu.au**

Abstract

This paper investigates the observation and prediction of Tropical Cyclone (TC) landfall by applying a Poisson regression and Generalised Additive Model (GAM) approach. TC data from the Joint Typhoon Warning Centre and climate mode data for a 50-year period (1964-2013) have been used in this study where the Poisson regression is fitted to analyse the landfall probabilities with consideration of climate modes, and the GAM model is fitted on observed cyclone track velocities as a smooth function of intensity to simulate the landfall point. Using Poisson regression, the annual average rate of TC occurrences is almost 3 over the North Indian Ocean (NIO) and it is predicted that there is only a 6% chance of not making landfall in a random year, whereas there is a 54% probability of landfall by more than two cyclones. Probabilities of TC landfall are higher during La Niña period compared to El Niño over the NIO rim countries except Indian coast in which no significant difference is seen.. In addition, TC occurrences have been simulated for each NIO rim by Markov Chain Monte Carlo approach, and climate modes have been used to predict the tropical cyclone landfall rate. Poisson regression is found skilful in hindcasting of tropical cyclone landfall frequency for the NIO region with a correlation coefficient in the forecasted hindcast time series of 0.57 and a mean absolute error and mean-square error of 19% and 32%, respectively better than climatology. In a separate study, the distribution of genesis points, movement and landfall is shown by GAM. This model previously demonstrated very skillfull to simulate TC landfall across the NIO rim by Wahiduzzaman *et al.* (2016) which deem skilful for this study and powerful compared to Poisson regression.

Keywords El Niño-Southern Oscillation, Indian Ocean Dipole, Stochastic modelling, Tropical cyclones, North Indian Ocean

1 Introduction

A tropical cyclone (TC) is one of the most noteworthy weather-related threats to shore and sea-based locations in tropical and sub-tropical latitudes (Regnier and Harr 2006). They are the most devastating weather systems because they can involve multiple hazards such as wind, rainfall and storm surge over the course of 1 or 2 days (Chand and Walsh 2012). As one of the deadliest natural catastrophes, tropical cyclones can cause loss of lives and enormous property damage in the North Indian Ocean (NIO) rim (Tyagi *et al.* 2010; Girishkumar and Ravichandran 2012; Nath *et al.* 2015) for instance the *TC Chittagong* in 1991 and *TC Nargis* in 2008. These TCs hit in Bangladesh and Myanmar respectively and caused economic damage around US$ 2.4 and 10 billion and 140,000 lives lost (Mydans and Cowell 2008; Alam and Collins 2010; Nath *et al.* 2015). The human and economic costs annually due to TCs that make landfall across the NIO rim can be massive.

The North Indian Ocean is cyclogenetically a very active zone of the world's oceans. The tropical disturbances over this region cause most of the hazardous impacts through wind action and floods caused by associated storm surges and heavy rainfall. The coastal zone of the countries Bangladesh, India, Myanmar, Pakistan and Sri Lanka are highly vulnerable to the tropical disturbances of different intensities. The different levels of damage to lives, properties, ecology and the environment are caused by various factors associated with tropical cyclones, including their intensity. The severe cyclone of 12 November 1970 that hit the coast of Bangladesh claimed the lives of over 300,000 people (Chowdhury *et al.* 1993). The tropical cyclone *Sidr* that hit the coast of Bangladesh was the most severe cyclone with a sustainable horizontal wind speed of about 250 km/hour and generating a surge of 6-8 m (Jakobsen *et al.* 2006). However, by virtue of the recent improvement of the early warning and preparedness system, the death toll was as low as 2,388 (Paul 2009).

Tropical cyclones are the most talked about weather events in Bangladesh, India, Myanmar, Sri Lanka and Oman. These cyclones originate in the North Indian Ocean (i.e. the Bay of Bengal and the Arabian Sea). The Bay of Bengal is a favourable breeding ground of tropical cyclones and the North Indian Ocean rim countries are the worst sufferers of cyclonic casualties in the world. The NIO claims 7% (about 5 per year) frequency (Mohapatra *et al.* 2014; Sahoo and Bhaskaran 2016) of the world's tropical

cyclones-four in the Bay of Bengal (Alam *et al.* 2003; Vissa *et al.* 2013; Balaguru *et al.* 2014; Mohapatra *et al.* 2014; Rajasekhar *et al.* 2014) and one in the Arabian Sea (Rajeevan *et al.* 2013; Mohapatra *et al.* 2014; Rajasekhar *et al.* 2014) and about 1% hit Bangladesh (Ali 1996, 1999).

Climate modes influence the tropical cyclone activities over the Indian Ocean, which is a portion of a large warm water pool and is adjacent to the pronounced monsoons of Asia that anchor the major convection centre of the atmosphere, and it states the climatic effects of large-scale events (Giannini *et al.* 2003; Hoerling *et al.* 2004). Sea surface temperature (SST) of the Indian Ocean controls atmospheric convection and circulation, employing an important effect on the El Niño-Southern Oscillation (ENSO) (Wu and Kirtman 2004; Annamalai *et al.* 2005). Tropical cyclone events are controlled by ENSO and Indian Ocean Dipole (IOD) activities. El Niño (La Niña) is the warm (cold) phase of the ENSO cycle. These events (El Niño and La Niña) are the main sources of weather and climate's year-to-year variability around the world (Zebiak and Cane 1987). The IOD is an array of connected ocean–atmosphere interface that is additional foundation of SST variability and it controls zonal SST gradients along the equator. On the other hand, the ENSO is known to affect the NIO through various teleconnection processes (Klein and Bloom 1989; Yulaeva and Wallace 1994; Alexander *et al.* 2002) and the equatorial Rossby waves motivated by ENSO-induced wind stress (Clarke and Liu 1994; Wijffels and Meyers 2004).

The forecasting of tropical cyclone landfall has pronounced importance because of the annual loss of life and destruction of property caused by these systems (Fraedrich and Leslie 1989). We studied the North Indian Ocean (NIO) whose impact is much larger compared to other basins (Singh 2010). The NIO TCs are characterised by a shorter life cycle and quicker development compared to other basins that allow less time for preparedness so the improvement of analysis and forecast over these regions is predominantly significant (Singh *et al.* 2012). Statistical models offer quantitative tools for the assessment and management of the risks posed by the frequency of tropical cyclone landfalls. Due to devastating nature of threat to life and property, the probability distribution of landfalls along the coastline creates an important role of resolving at the risk-relevant spatial resolutions from local to social infrastructures (Tolwinski-Ward 2015).

This study seeks to model the frequency and point of TC landfall in the context of the important climate modes of variability operating in the NIO. We have used a Poisson regression model with consideration of Sea Surface Temperature, Ocean Heat Content and Southern Oscillation Index to model the landfall frequency and also a Generalised Additive Model (GAM) to locate the simulated landfall point in each season by intensity. Finally, we examined the skill of both models.

The arrangement of this manuscript is as follows. The data and the workflow of model are described in section 2. In addition, the methods of Poisson regression, kernel density estimation for TC genesis distribution, General Additive Model for TC tracks simulation in each season jointly with intensity are described in section 2. Section 3 presents the results of Poisson regression, kernel density estimation and GAM simulations carried out with an implementation of the model and evaluates them in comparison to the observed data. In section 4, we present a summary and conclusions with an outlook on the possibilities for further model development.

2 Data and Methods

2.1 Data Sources

2.1.1 Tropical cyclone data

NOAA National Climatic Data Centre established the International Best Track Archive for Climate Stewardship (IBTrACS) dataset which focus was to integrate and merge best track data from all official Tropical Cyclone Warning Centres (TCWCs) and the WMO Regional Specialised Meteorological Centres (RSMCs) who are accountable to develop and archive best track data globally. Joint Typhoon Warning Centre (JTWC) data is a subset of IBTrACS that is commonly used by researchers worldwide (Knapp *et al.* 2010). We have used TC data from the JTWC over a 50-year period (1964-2013) for the North Indian Ocean (NIO) region, here defined as the region bounded meridionally from 0°--30°N and zonally from 50°E--100°E (Fig.1).

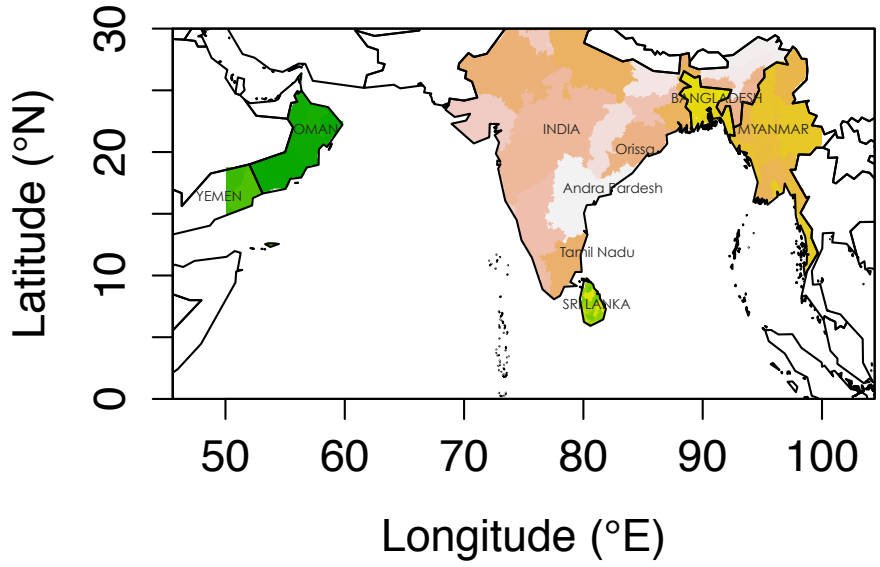

Fig.1 A map of six NIO rim countries (India, Bangladesh, Myanmar, Sri Lanka, Oman and Yemen) and three states (Orissa, Andhra Pradesh, Tamil Nadu) of India which is highly affected by tropical cyclone landfall and relevant to this study (Wahiduzzaman *et al.* 2016).

2.1.2 Climate indices data

There are three predictors (Sea Surface Temperature (SST), Ocean Heat Content (OHC) and Southern Oscillation Index (SOI)) that have been used in this study. The reanalysis of SST and OHC data (monthly-averaged data at 0.5 degree resolution) are collected from the US National Oceanographic Data Centre and SOI data from the National Climatic Data Centre (NCDC). We have also shown the predictability of TCs during ENSO and IOD years (See Table 1 in Appendix) and the years are considered from http://www.marine.csiro.au/~mcintosh/ENSO_IOD_years.htm.

We have predicted the rate of TC landfall probabilities for the specified values of the covariates (SST=-0.1, SOI=-0.5 and OHC=0) and selected the values of SOI, SST and OHC by considering bivariate relationships between covariates and TC landfall frequency (Fig.2). Scatter plots are not very useful for a given TC count (Elsner and Jagger 2013) as there is many covariates value so we plotted a summary of the covariate distribution of each count. Five-number summary provides information about the median, range and quartile values of a distribution. We compared the five-number summary of the covariates during years with no TC and during years with three TCs. Fig.2 shows the covariates are

likely important in statistically TC counts as there appears to be a systematic variation in counts across the range of values.

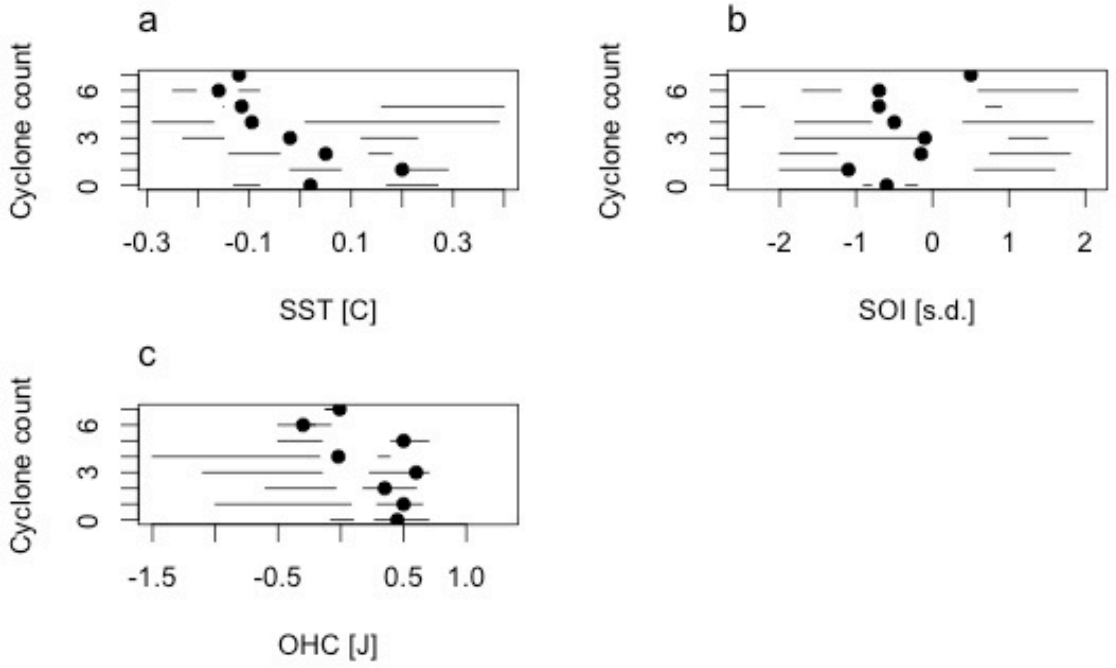

Fig.2 Bivariate relationships between covariates a) SST b) SOI c) OHC and TC landfall frequency. The dot represents the median; the ends of the lines toward the dot are the lower and upper quartiles, respectively; the ends of the horizontal lines are the minimum and maximum values, respectively.

2.2 Modelling Methods

The basic modelling approach comprises of two separate studies in which the landfall frequency is modelled through Poisson regression in one study and other one considers the modelling of TC landfall point through kernel density estimation for TC genesis, presentation of a generalised additive model for the velocity field and simulation of TC tracks anda country mask to determine the point of landfall.

The Poisson regression model closely follows the previous work of Elsner and Jagger (2013) for the counts of hurricanes hitting in the United States. In their research, they counted hurricane frequency and predicted with favourable and unfavourable conditions. Our approach follows the same however we fit the Poisson model by considering smooth function (part of GAM) whereas they have used general linear model.

The genesis, trajectories and landfall model developed here closely follows the previous work of Hall and Jewson (2007) for the North Atlantic and Yonekura and Hall (2011) for the Western North Pacific and Wahiduzzaman *et al.* (2016) for the NIO. The choice of a 6-hr increment for tracking and the landfall detection is consistent with the study by Hall and Jewson (2007), Yonekura and Hall (2011), Mestre and Hallegatte (2009), Weinkle *et al.* (2012) and Wahiduzzaman *et al.* (2016).

The analysis techniques are as follows:

2.2.1 Poisson Regression

We have applied the Poisson regression method to model the probabilities of TC landfall frequency. This regression analysis is an operational method (Gray *et al.* 1992, 1993, 1994; Nicholls 1999) and frequently used to model the rate of tornado counts, the droughts or cold spells (Wilks 1995). It is also perfect for modelling tropical cyclone occurrences (Elsner and Schmertmann 1993).

A Poisson process calls the probability distributional model for independent and rare event counts, for example, TCs. Given the Poisson intensity parameter λ (the mean seasonal TC rates), the probability mass function (PMF) of h TCs occurring in a unit of observation time (e.g., one season) is

$$\boldsymbol{P}\,(\boldsymbol{h}|\lambda) = \boldsymbol{exp}(-\boldsymbol{\lambda})\ \frac{(\lambda)^{\boldsymbol{h}}}{\boldsymbol{h}!}\text{, where } \boldsymbol{h}\text{=0, 1, 2, 3,. . . and } \lambda > 0$$

The Poisson mean is simply λ. For this research, we used *50-year* observations, and 4 relative predictors.

The advantage of Poisson regression over linear regression is that it is more relevant for the occurrence of infrequent, discrete event modelling such as the rates of tropical cyclones (Wilks 1995). This methods has been successful and effective to show the relationship between TC and the SOI (Solow and Nicholls, 1990) and TC genesis with Gray parameters (sea surface temperature (SST), conditional instability in the lower to mid-troposphere, absolute vorticity in the lower troposphere, mid-troposphere relative humidity, divergence in the upper troposphere, and low vertical shear of the horizontal winds between the lower and upper troposphere) by McDonnell and Holbrook (2004a)

In this paper, Poisson regression has been used to calculate the probabilities of TC

landfall frequency over the NIO as well as for four individual NIO rim countries. Besides, we calculated the probabilities of TC occurrence in ENSO and IOD-year. We have also focused the TC landfall probabilities by considering covariates (SST, SOI and OHC). Apart from this, the model cross-validation and forecast skill has been assessed. The main difference with GAM is to get the probability of number of cyclones without generating the vector field as well as model simulation. It's a simple process than complicated GAM process.

2.2.2 Genesis modelling by Kernel Density Estimation (KDE)

KDE approach is used to model the genesis points. The description of this approach has been discussed by Wahiduzzaman *et al.* (2016). Previously this approach successfully used by Vickery *et al.* (2000); James and Mason (2005); Emanuel *et al.* (2006), Hall and Jewson (2007) and Rumpf *et al.* (2007). If we denote the kernel function as K and its bandwidth by h, the estimated density at any point x is

$$\hat{f}(x) = \frac{1}{n}\sum_{i=1}^{n} K\left(\frac{x - x(i)}{h}\right)$$

The kernel K must fulfil the limit $\int K(x)dx = 1$ but is otherwise arbitrary.

$$K(x) = (2\,\pi)^{-1} \exp\left(-\frac{x^2}{2}\right)$$

A standard plug-in estimator (Rigollet and Vert 2009) has been used in the present study. We defined TC genesis by >=34kts wind speed (WMO 1997) and generated sample genesis points by probability density function. Also, we restricted genesis those are falling in <200m water depth by using masked kernel density.

2.2.3 Trajectories modelling by Generalised Additive Model (GAM)

GAM is fitted to the observed trajectory velocities for modelling of cyclone trajectories. By turn standard linear model is extended as generalised linear model and then further extended as GAM. GAM is an overview of linear regression where the linear terms are switched by smooth transformations of the predictors (Guisan *et al.* 2002; Hastie *et al.* 2009).

In regression, the mean, μ, can be modelled as a linear pattern of predictor variables, X_1, X_2, … , X_m

$$\mu = \beta_0 + \beta_1 X_1 + \beta_2 X_2 + \cdots + \beta_p X_p$$

where β_0 ,β_p are the regression coefficients.

GAM lessens the functional relation between the response and the predictors through a number of smooth transformations $f_1, f_2, \ldots, f_p$

$$\ell(\mu) = \eta = \beta_0 + f_1(x_1) + f_2(x_2) + \cdots + f_p(x_p)$$

The description of this approach has been discussed by Wahiduzzaman *et al.* (2016). In this paper, generalised additive model has been applied to the observed TC velocities which have been calculated from the difference between latitude and longitudinal positions in each step along the track. From random genesis points, trajectories have been simulated upto 7 days with a 6-hourly time step as 80% NIO region TC lifetimes are within 7 days of genesis and this will be a sensible and appropriate choice for the model (Wahiduzzaman *et al.* 2016).

2.2.3 Landfall modelling

To detect the position of landfall, a fine scale raster mask of the NIO rim countries was first constructed and then for each tropical cyclone, we traced along the trajectory to detect the first point that strikes land. The countries were represented as a set of polygon with locations, such that we recorded the country and state that the cyclones made landfall. To estimate the spatial location and time of a landfall, each trajectory was interpolated to a finer time scale with successive points along this fine-scale trajectory compared to the land mask. The first time and location crossing of the land mask is taken to be the point of landfall. The accuracy with which the precise point of a landfall is estimated depends on the interpolated resolution of the trajectory. Here we use an interpolated time increment of 6-hourly time steps up to a maximum lifetime of 7 days. We only considered first point of landfall as multiple landfalls are rarely seen in the NIO region (Wahiduzzaman *et al.* 2016).

3990 2.2.4 Validation techniques

3991 Leave one out cross validation (LOOCV) and distance measurement methods have been
3992 applied to validate the models. By deleting the trajectories in turn, we predict the
3993 trajectories from reduced data sets. Using GAM we predicted landfall by majority vote
3994 approach (Wahiduzzaman *et al.* 2016). Another approach examined the distance between
3995 observed and simulated landfall and histograms of the distance were formed.

3996

3997 **3 Results**

3998 **3.1 Probability of TC landfall over the NIO**

3999 The annual average rate of tropical cyclone landfall is found as a number of 2.86~3 over
4000 the NIO. Table 1 describes the observed and simulated (using the average rate λ =2.86)
4001 TC landfall percentage in any year. It is seen that there is only a 6% chance of not making
4002 landfall in any year, whereas the highest chance (54%) of making landfall is by more than
4003 two TCs over the NIO. By comparing with observation, it is found that TC landfall
4004 probability in a random year is well matched with model prediction by a number of 2 and
4005 2+ cyclones.

4006 Table 1: Tropical cyclone landfall probability (%) over the NIO by a set of numbers in a
4007 random year

	No	One	Two	Three	Four	Five	Six	Two+	Three+
Observation	8%	14%	24%	18%	20%	6%	6%	54%	36%
Model	**6%**	16%	24%	22%	16%	9%	4%	**54%**	32%

4008

4009 **3.2 TC occurrence over the NIO and its rim countries**

4010

4011 Annual TC occurrences in a time series and their distribution for a number of years are
4012 described in Fig. 3, and it is observed that the number of TC landfall is decreasing over
4013 time. A number of highest 7 TC is found in the year 1976, and it is also notable that a
4014 higher frequency of TC landfall is seen before 1980, whereas after the 80s the trend
4015 started decreasing (Fig. 3a). NIO rim countries are almost always stroked by TC landfall.

In a 50-year analysis period, it is found that 46 years saw TC landfall while 12 years saw a number of 2 TC landfalls. In addition, 38 years (76% in total time) are handled by at least 1 to 4 TC landfall (Fig 3b).

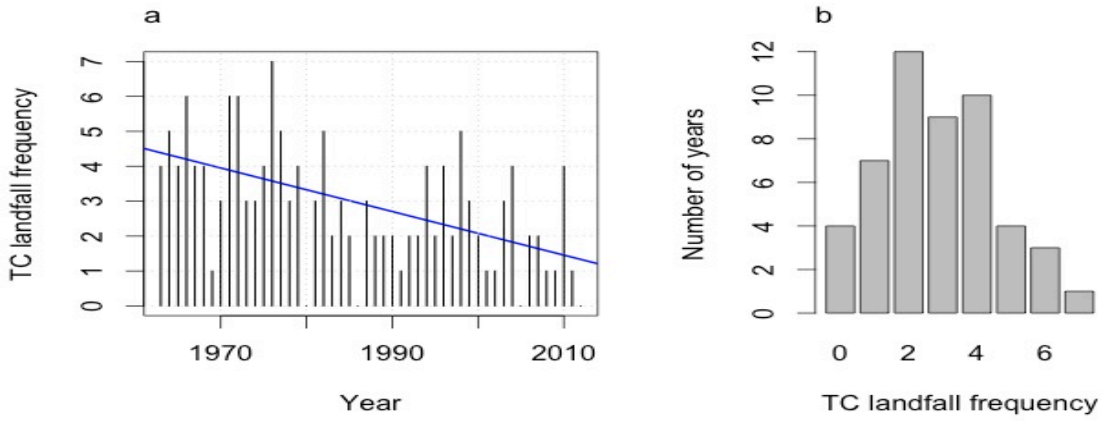

Fig.3 Annual TC landfall frequency over the NIO for a period of 50-year, (a) Time series and (b) distribution. The blue color line shows the linear trend of TC landfall frequency.

We have used the Monte Carlo (MC) simulation approach to simulate the TC landfall frequency. The real observation of landfall frequency and MC simulations are shown in Figs 4a-4d. A similar trend of observed landfall frequency in simulation is seen, though a few high predictions are seen for few years.

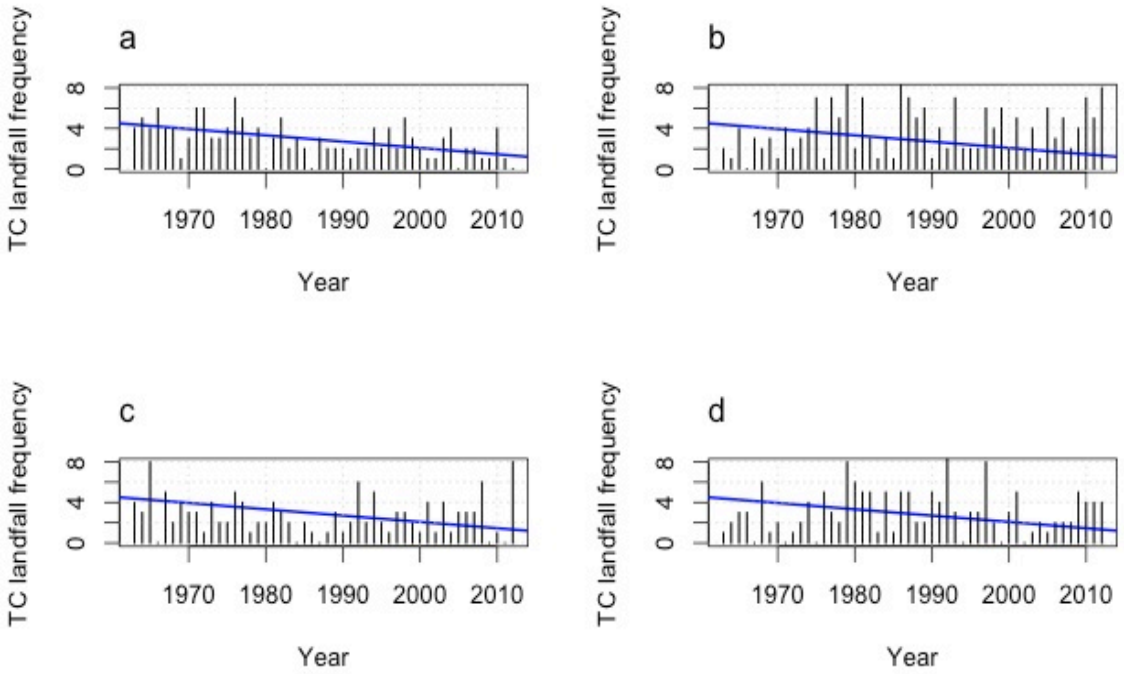

4027

4028 Fig.4 TC landfall frequency for a period of 50-year using MC approach (a) observed and (b-d)
4029 simulated counts. The blue color line shows the linear trend of TC landfall frequency.

4030 TC landfall frequency is also counted for individual NIO rim countries (Fig 5a-5d) and it
4031 is seen that India is stroked by the highest number of 4 TCs (Fig 5b). Bangladesh
4032 experienced one tropical cyclone landfall till 18th year (Fig 5a) whereas India faced them
4033 for 25 years, and before 1990 it is seen that India is getting 1 to 4 number of TC landfalls
4034 (Fig 5b) though the number of cyclone landfalls started decreasing after 1990. One TC
4035 landfall for Sri Lanka and Myanmar is seen for 10 and 12 years, respectively, and after
4036 1990 the number of TC landfalls started decreasing compared to before 1990 (Fig 5c, 5d).

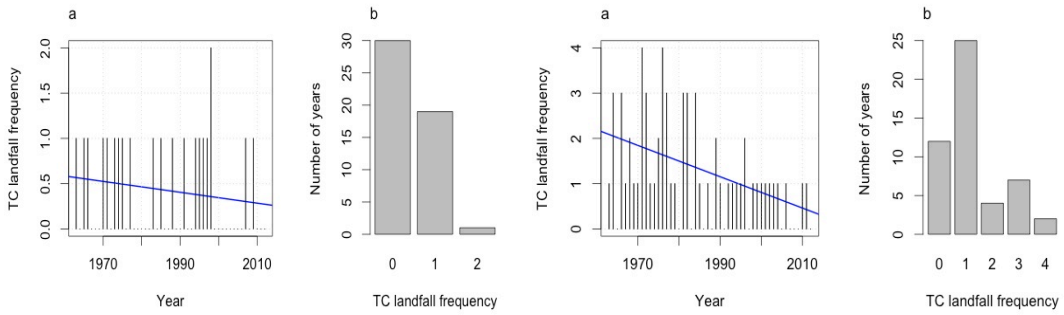

4037

4038 a. Bangladesh coast b. India coast

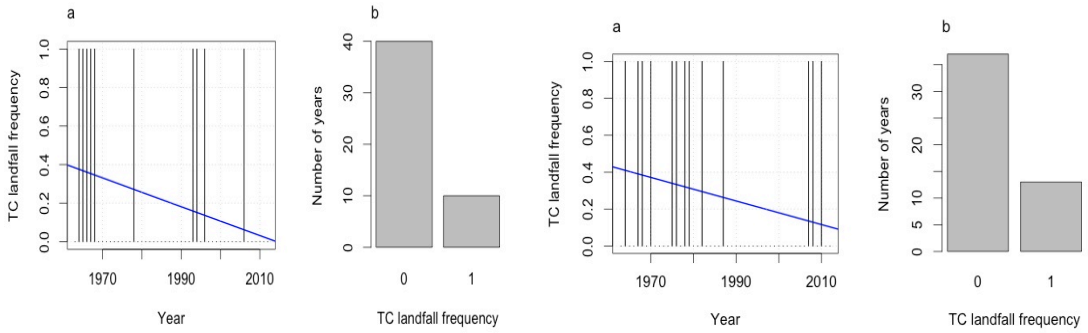

c. Sri Lanka coast d. Myanmar coast

Fig.5 Annual TC landfall frequency [(a) Time series and (b) distribution] over the NIO rim countries. The blue color line shows the linear trend of TC landfall frequency.

The observed and simulated TC landfall frequency by MC approach is shown in Fig 6 for each NIO rim countries. Compared with four countries it is seen that India is getting hit by more TCs and the number of TC landfalls is decreasing over time; however, the simulation shows a high predicted number for a few years in each country (Fig 6a-d).

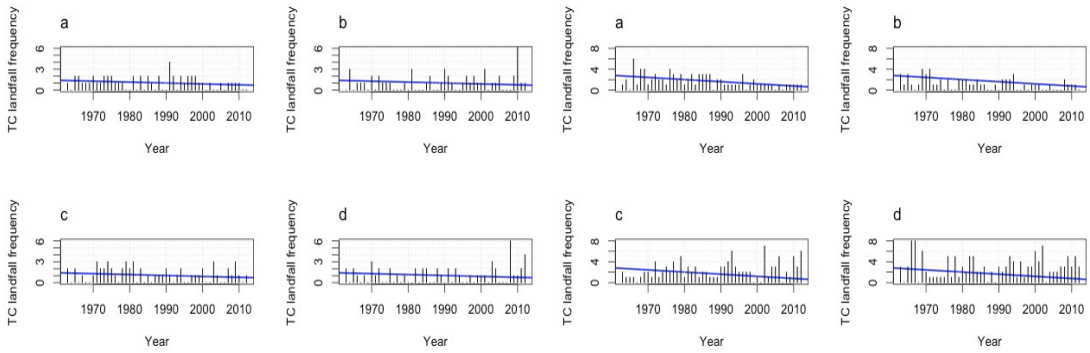

a. Bangladesh coast b. India coast

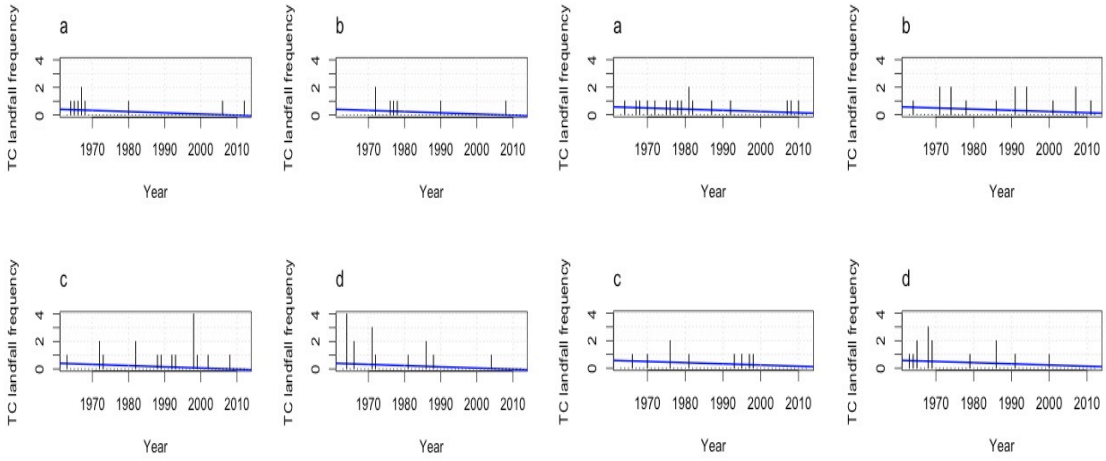

c. Sri Lanka coast d. Myanmar coast

Fig. 6 TC landfall frequency using (a) observed and (b-d) simulated counts over NIO rim countries. The blue color line shows the linear trend of TC landfall frequency.

3.3 Landfall probability with ENSO and IOD year

The probability percentage of cyclonic landfall across the NIO rim countries is calculated by Poisson regression (Fig 7). Bangladesh, India, Sri Lanka and Myanmar are considered to show the landfall percentage by different numbers of cyclone (like no cyclone, one cyclone, two cyclones, more than two cyclones) in a random year during El Niño, La Niña, positive IOD and negative IOD year. It is found that La Niña is a driver to make landfall in Bangladesh and Myanmar coasts compared to El Niño, though there are no significant differences for India coast, and negative IOD plays a significant role for more than two cyclonic landfalls in India. The Poisson model used the average rate of 1.02 for Bangladesh, 1.72 for India, 0.18 for Sri Lanka and 0.34 for Myanmar to generate the probability of TC landfalls in ENSO and IOD years (see appendix from Table 2 to 5).

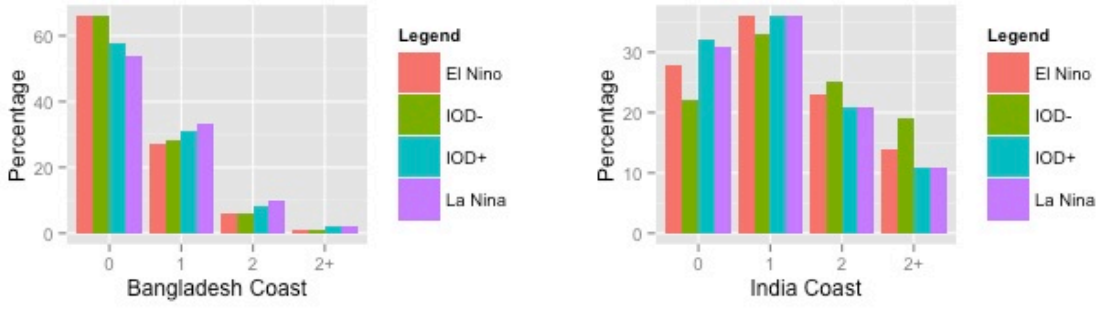

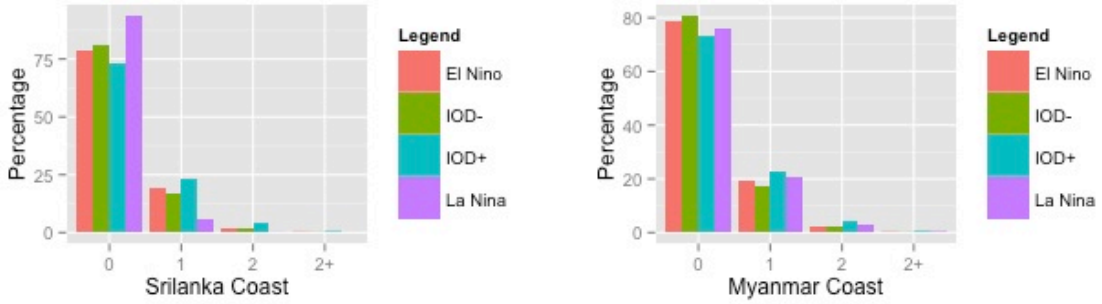

Fig.7 TCs landfall probability with ENSO (El Niño and La Niña) and IOD (Positive and negative) years. Number of landfall (No cyclone, 1, 2, 2+) against probability percentage has been presented for each NIO rim countries.

3.4 Model predictions with covariates

The probability by a number of TC landfalls is shown in Fig 8 when the model considered Sea Surface Temperature, Southern Oscillation Index and Ocean Heat Content as covariates (see the section 2.1.2) and it is found that there is an 84% chance of having two or more tropical cyclone landfalls in a single year, which decreases to 60% with climatological conditions (no predictors are considered). In addition, the probability of no landfall is 3% when the predictor is considered, whereas it is 13% probability with climatological conditions.

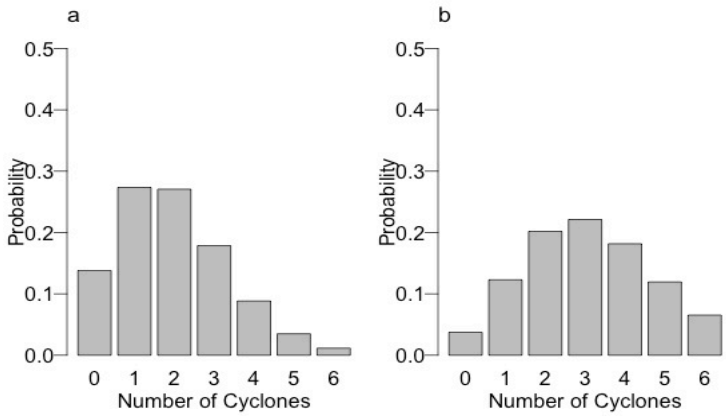

Fig.8 Forecast probabilities for (a) consideration of predictors and (b) climatological conditions

3.5 TC observation with intensity

Tropical cyclone can be categorized in different ways around the globe. They are known as different names and the classification for the North Indian Ocean is given in Table 2.

4083 Table 2: Tropical cyclone intensity scale (WMO 1997)

Category	Sustained winds (3-min average)	
Super Cyclonic Storm	≥120kt	≥221km/h
Extremely Severe Cyclonic Storm	90-119kt	166-220km/h
Very Severe Cyclonic Storm	64-89kt	118-165km/h
Severe Cyclonic Storm	48-63kt	89-117km/h
Cyclonic Storm	34-47kt	63-88km/h
Deep Depression	28-33kt	51-62km/h
Depression	17-27kt	31-50km/h

4084

4085 NIO tropical cyclone is categorised as cyclonic storm (34-47kt), severe cyclonic storm
4086 (48-63kt), very severe cyclonic storm (64-89 kt), extremely severe cyclonic storm (90-
4087 119 kt) and super cyclonic storm (≥ 120 kt). According to the Saffir-Simpon scale, very
4088 and extremely severe cyclonic storm will be category 1-3 whereas super cyclonic storm
4089 will be category 4-5. TC trajectories movement and landfall locations according to
4090 intensity scale are shown in Fig.9. Majority of cyclonic storms move northward and
4091 north-westward and make landfall in Andhra Pradesh, Orissa of India, Bangladesh and
4092 Myanmar. Severe cyclonic storms move north-westward and make landfall in Andhra
4093 Pradesh in India (genesis location in between 80-90^{0}E) however 90-95^{0}E storms are
4094 mainly move north-eastward and make landfall in south-eastern part of Bangladesh and
4095 Myanmar. Very and extremely severe cyclonic storms tend to move north-eastward
4096 direction and majority of them make landfall in Andhra Pradesh in India, Chittagong in
4097 Bangladesh and Ayerwardy in Myanmar. Super cyclonic storms move westward direction
4098 and make landfall in Orissa coast of India (Fig.9).

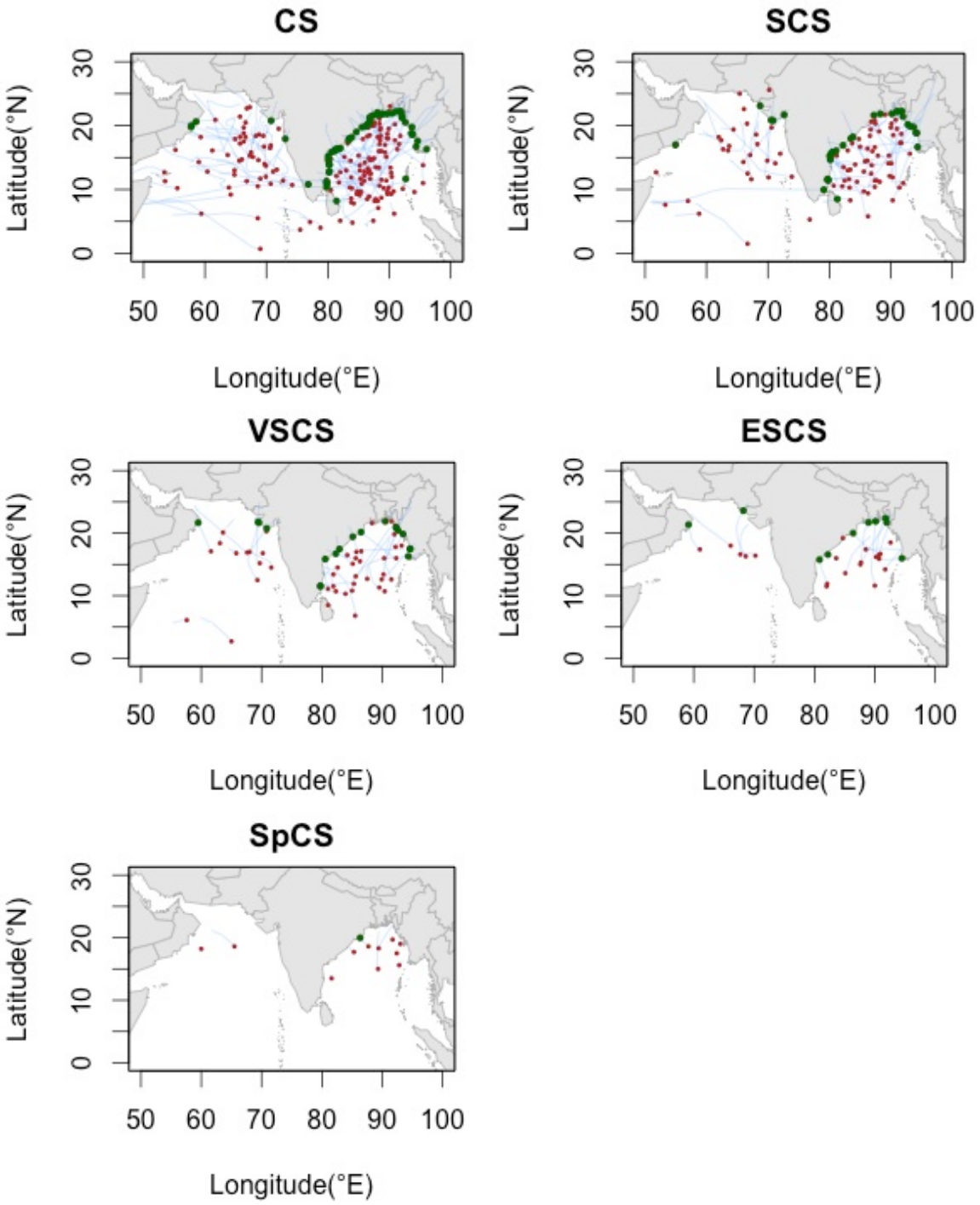

Fig.9 Observed TC genesis (red dots), tracks (blue lines) and landfall point (green dots) according to intensity scale in the NIO. Here CS, SCS, VSCS, ESCS and SpCS elaborates as cyclonic storm, severe cyclonic storm, very severe cyclonic storm, extremely severe cyclonic storm and Super cyclonic storm.

The distribution of TC velocities through fitting generalised additive model to the observed tracks for each tropical cyclone category is discussed in Fig.10. In cyclonic storm, the velocity field indicates a north-westward initial movement over the Bay of

Bengal and westward in Arabian Seas whereas the severe cyclonic storm follows the same pattern but above 15^0N velocity fields shows north-eastward movement. During severe cyclonic storm velocity field tends to move north-eastward in Bay of Bengal and south-westward in Arabian Sea.

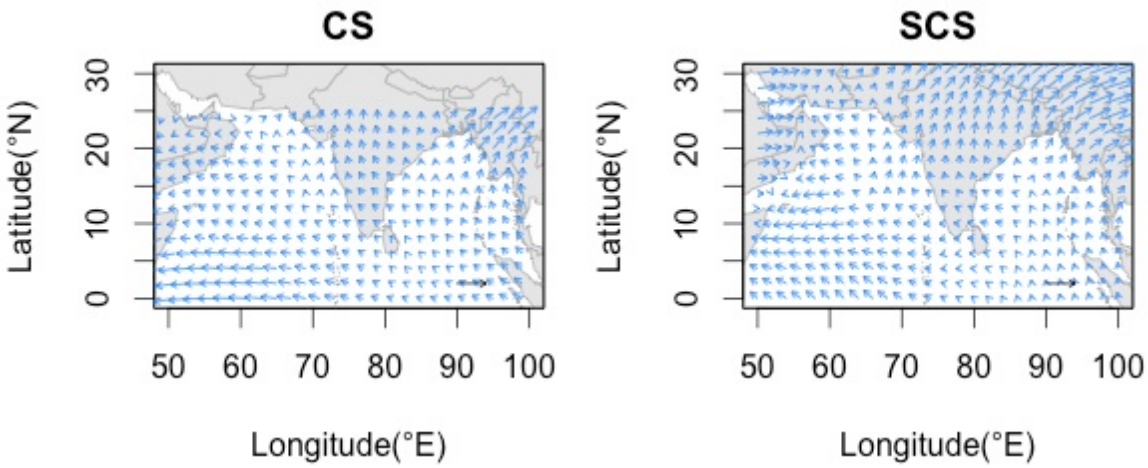

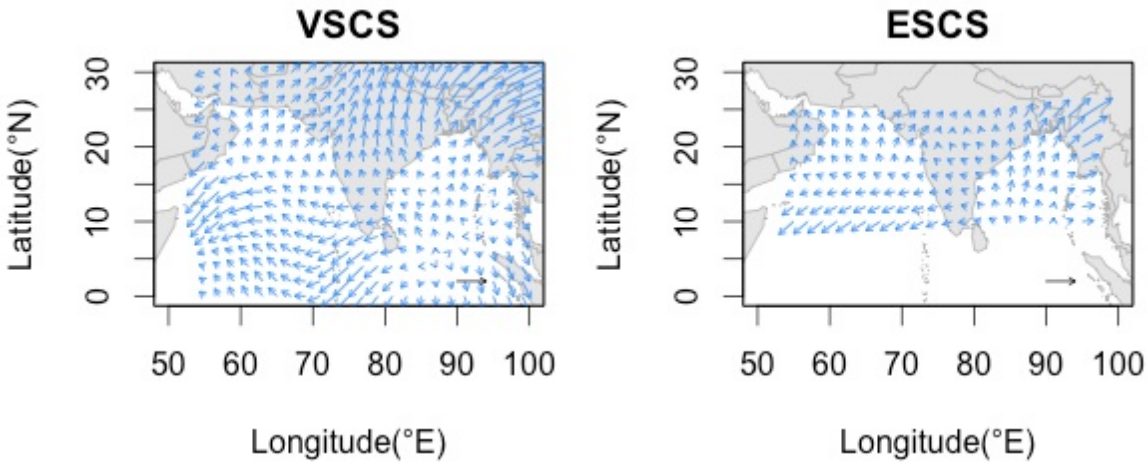

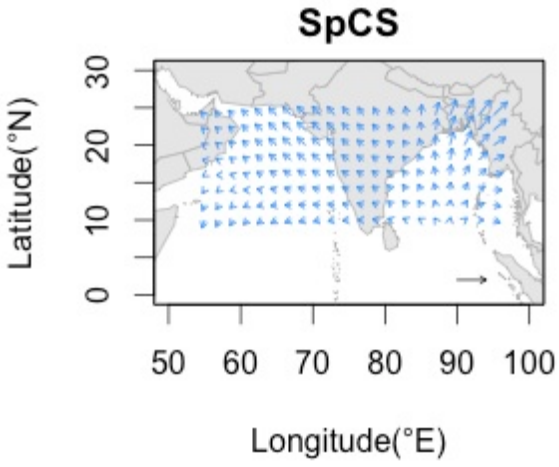

Fig.10 TC track velocities according to intensity scale in the NIO. Format is same as Fig.9. The reference arrow's magnitude is $10ms^{-1}$.

During the winter season, cyclone genesis occurs below 15°N and cyclonic storms are moving north-westward direction and make more landfall in Tamil Nadu of India. In the pre-monsoon season, most of cyclones genesis is seen above 10°N over the North Indian Ocean and they move eastward across the Bay of Bengal and it is clear that south-east part of Bangladesh and Myanmar has experienced more cyclonic storms. During the monsoon season, cyclone genesis occurs above 15°N and cyclonic storms are moving north-westward. The southwest part of Bangladesh is facing more landfalls during monsoon season. In the post-monsoon season, cyclone genesis occurs above 10°N over the Bay of Bengal and Arabian seas, but a few are under 10°N. They move westward/northward across the North Indian Ocean. Especially Andhra Pradesh and Orissa coast has experienced more landfalls during this period (Fig.11).

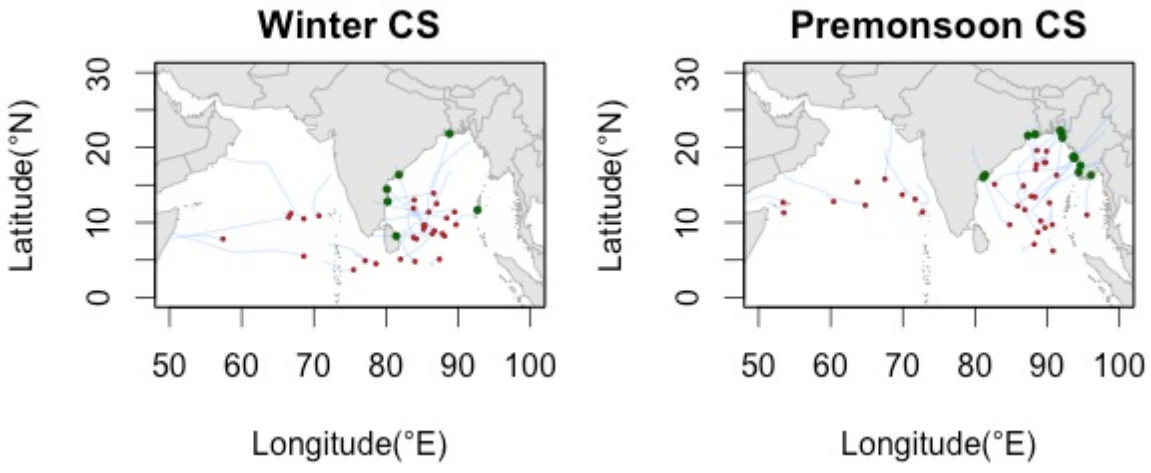

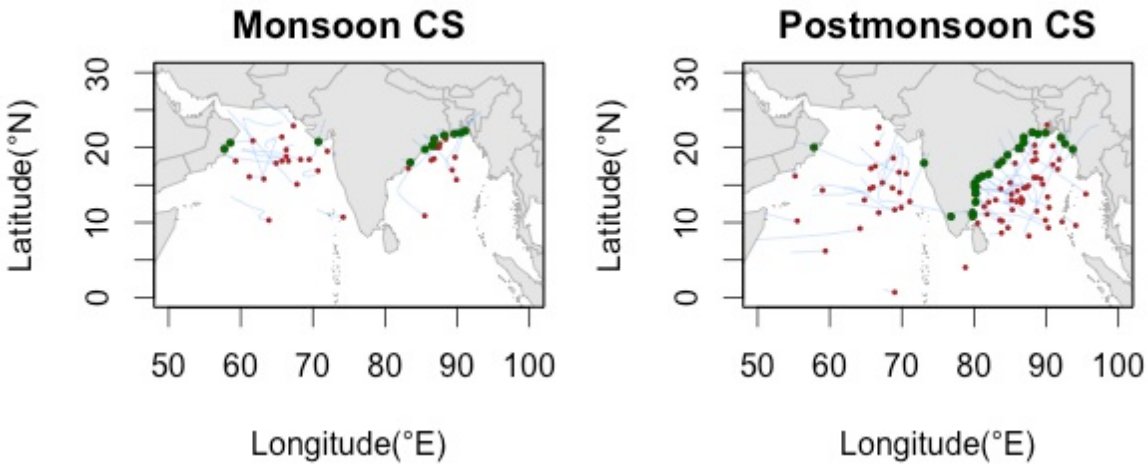

Fig.11 Seasonwise observed tropical cyclone genesis (red dots), tracks (blue lines) and landfall point (green dots) according to cyclonic storm intensity scale in the NIO.

Model simulations of TC trajectories (Fig.12) indicate their movement and point of landfall. During winter season, cyclonic storms move westward and make landfall Tamil Nadu coast in India and Sri Lanka. This is consistent with observation except landfall in Sri Lanka. In pre-monsoon season, cyclonic storms move northwestward across the NIO rim and make landfall in Sri Lanka and few states in India. The model didn't simulated well against observation in this season. A large number of genesis points are seen in Arabian seas during monsoon and they are moving northwestward and make landfall in Oman. In the post-monsoon season, cyclonic storms move westward and northwestward across the North Indian Ocean in which the Andhra Pradesh and Tamil Nadu coast in India (Fig 12).

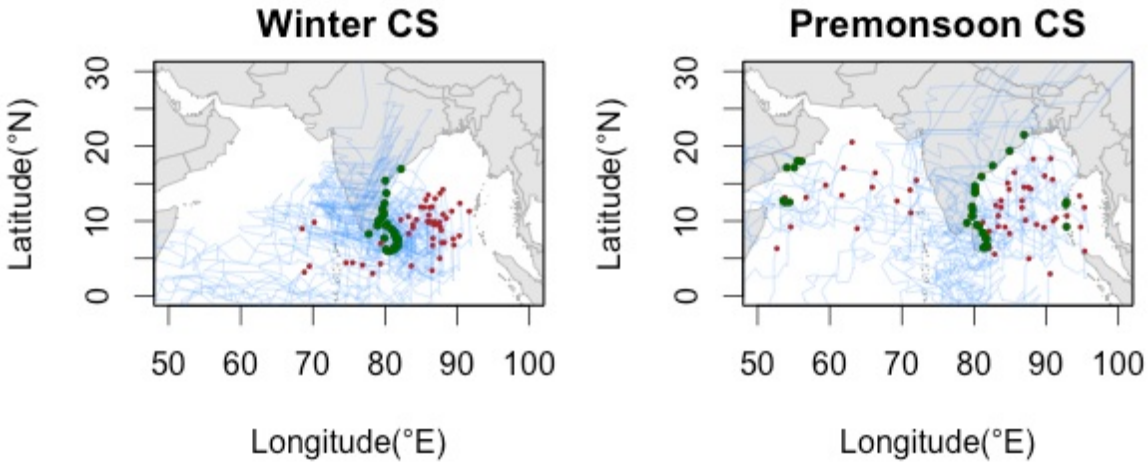

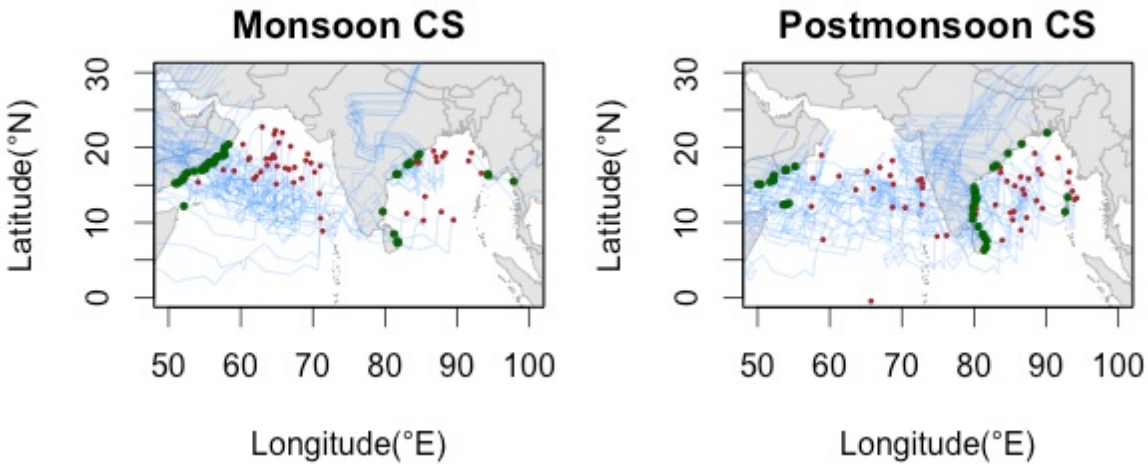

Fig.12 Simulated TC genesis (red dots), tracks (blue lines) and landfall point (green dots) according to cyclonic storm intensity scale in the NIO.

3.6 Prediction skills by model against observation

In this paper, the prediction skills for both models have been assessed. In the Poisson regression, the cross-validated hindcast phase variability is correlated where the Mean Squared Error (MSE) for these hindcasts are up to 10% improvement over climatology with a correlation coefficient in the crossvalidated hindcast time series of 0.33 (Table 7).

Table 7: Cross-validation skill of the Poisson Regression model. In the table 'MAE' stands for Mean Absolute Error; 'MSE' is Mean Squared Error; 'MAEp' is Mean Absolute Prediction Error; 'MSEp' is Mean Squared Prediction Error and 'Useful' in the percentage skill above climatology

	Poisson	Climatology	Useful
MAE	1.3076221	1.419592	7.887463
MSE	2.6844569	2.999167	**10.493251**
MAEp	1.8248665	1.907068	4.310357
MSEp	5.4969169	5.859154	6.182422

Forecast skill refers to how well your predictions match the observations. There are several ways to quantify this match. Here we consider three of the most common, the mean absolute error (MAE)

$$MAE = \frac{1}{n}\sum_{i=1}^{n}|\lambda_i - O_i|$$

4162 the mean squared error (MSE)

4163 $$MSE = \frac{1}{n}\sum_{i=1}^{n}\left(\lambda_i - O_i\right)^2$$

4164 and the correlation coefficient.
4165

$$r = \frac{\Sigma\left(\lambda_i - \bar{\lambda}\right)\left(O_i - \bar{O}\right)}{\sqrt{\Sigma\left(\lambda_i - \bar{\lambda}\right)^2 \Sigma\left(O_i - \bar{O}\right)^2}}$$

4166 Let λi be the predicted rate for year I, and o_i be the corresponding observed count for that
4167 year.

4168 Predicted rate for each year in the record is obtained by all tropical cyclone landfall
4169 frequencies with consideration of oceanic parameters and similar climatology. It is
4170 considered that oceanic parameters have no influence. A prediction model is deemed
4171 useful [useful is calculated by (climatology - poisson)/climatology * 100] if the skill level
4172 exceeds the level of a naive reference model. The percentage above the skill obtained
4173 from a naive model is referred to as a useful skill. The naive model is typically
4174 climatology.

4175 Table 8's results are an in-sample assessment of forecast skill. All years of data are used
4176 to estimate a single set of model coefficients with the model subsequently used to
4177 hindcast each year's tropical cyclone activity. To make predictions of the future then we
4178 have to check the model performance and it is done with an out-of-sample assessment of
4179 skill. An out-of-sample assessment (1) excludes a single year of observations, (2)
4180 determines the maximum likelihood estimation coefficients of the Poisson regression
4181 model using observations from the remaining years, and (3) uses the model to predict the
4182 hurricane count for the year left out. The forecast hindcast phase variability is correlated
4183 where the Mean Squared Error (MSE) for these hindcasts are up to 32% improvement
4184 over climatology with a correlation coefficient in the forecast hindcast time series of 0.57
4185 (Table 8).

4186 Table 8: Forecast skill of the Poisson regression model. Format as same as table 7.

	Poisson	Climatology	Useful
MAE	1.1177617	1.391200	19.654850

MSE	1.9500839	2.880400	32.298155
MAEp	1.6994765	1.886362	9.907184
MSEp	4.8096104	5.740388	16.214543

For the GAM model validation approach, the model skill is assessed through cross-validation by majority vote approach and distance calculation. The model simulation is matched well with observation for NIO rim countries except Bangladesh (Wahiduzzaman *et al.* 2016). The distance between the observed and predicted landfall point is presented for the number of TC, and it is found that the highest frequency (60.7%) of simulated track landfalls are within 0-500 km of those of the observed tracks (Fig 13). By considering the relative scale of tropical cyclones (~1000 km in size), predicted landfall within ~500 km of the observations suggests that the model is performing well.

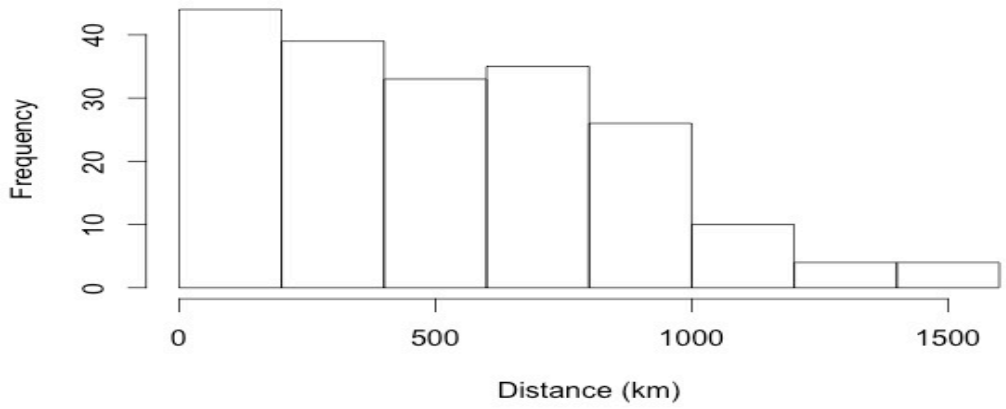

Fig 13. Distribution of distances between observed and simulated landfall point across the North Indian Ocean rim

4. Discussions and Summary

The paper represents a statistical model of tropical cyclone landfall frequency and point for the NIO region whether little skill has been found by dynamical model (Camargo *et al.* 2007a; Camp *et al.* 2015). Our approach comprises a statistical analysis to develop a model of tropical cyclone activities across the NIO rim. We have used both the Poisson regression model and general additive model approaches.

The bimodal seasonal distribution is seen in NIO. More number of cyclone is found in Bay of Bengal than Arabian sea except for Monsoon. Previous studies should be used to support the fact that there was almost no TC over BoB during the summer monsoon (Li *et al.* 2013) and it was due to the strengthened vertical wind shear starting from boreal spring, combined with decreasing sea surface temperature and relative vorticity that shut down TC activity during the monsoon. Over the NIO, on average a number of three TCs make landfall, and there is only a 6% chance of not making landfall in any year, whereas maximum 54% chance to make landfall by more than two TCs. The simulated landfall frequency using MCMC is matched with observation with few exceptions.

The influence of covariates for landfall probabilities is examined and it is found that La Niña is a driver to make landfall in Bangladesh and Myanmar coasts compared to El Niño, though there is no significant differences for India coast, but negative IOD plays a significant role for more than two cyclonic landfalls. The mechanism for more landfalls over India during negative IOD is discussed by Yuan and Cao (2013) who examined NIO TC activity under different phases of IOD and their study revealed that under negative IOD there are anomalous easterlies over BoB, which would steer TCs toward the east coast of India. Historically there were also many more landfalls over east coast of India under negative IOD. Using covariates, the model forecasts 84% chance to make landfall by two or more tropical cyclones in a random single year.

The findings suggest that most of the cyclones that make landfall during La Niña period across the NIO rim and covariates are likely to be a good predictor of tropical cyclone landfall for the NIO rim countries. The Poisson regression model and GAM showed skilful forecasts in this region. The MAE and MSE for these hindcasts are up to 32% improvement over climatology. The cross-validated hindcast phase variability is significantly correlated and the MAE and MSE for these hindcasts are up to 10% improvement over climatology. The GAM has been validated through majority votes and distance calculation and it is claimed that the distance for most of the simulated landfall was closest (within 500km) to observed landfall.

Acknowledgements: PhD research scholarship from University of Tasmania, Australia has supported Mohammad Wahiduzzaman to pursue this research.

References

Alam E , Collins AE. 2010. Cyclone disaster vulnerability and response experiences in coastal Bangladesh. *Disasters.* **34:** 931-954.

Alam MM , Hossain MA , Shafee S. 2003. Frequency of Bay of Bengal cyclonic storms and depressions crossing different coastal zones. *International Journal of Climatology.* **23:** 1119-1125.

Alexander MA , Bladé I , Newman M , Lazante JR , Lau NC , Scott JD. 2002. The atmospheric bridge: The influence of ENSO teleconnections on air–sea interaction over the global oceans. . *J. Climate.* **15:** 2205-2231.

Ali A. 1996. Vulnerability of Bangladesh to climate change and sea level rise through tropical cyclones and storm surges. *Water, Air and Soil Pollution,.* **vol. 94d,:** 171-179.

Ali A. 1999. Climate change impacts and adaptation assessment in Bangladesh. *Climate Research,.* **12:** 109-116.

Annamalai H , Liu P , Xie S-P. 2005. Southwest Indian Ocean SST Variability: Its Local Effect and Remote Influence on Asian Monsoons*. *Journal of Climate.* **18:** 4150-4167.

Balaguru K , Taraphdar S , Leung LR , Foltz GR. 2014. Increase in the intensity of postmonsoon Bay of Bengal tropical cyclones. *Geophysical Research Letters.* **41:** 3594-3601.

Bashtannyk DM , Hyndman RJ. 2001. Bandwidth selection for kernel conditional density estimation. *Computational Statistics & Data Analysis.* **36:** 279-98.

Camargo SJ , Barnston AG , Klotzbatch PJ , Landsea CW. 2007a. Seasonal Tropical cyclone forecasts. *Bulletin of the World Meterological Organization.* **56:** 297-307.

Camp J , Roberts M , Maclachlan C , Wallace E , Hermanson L , Brookshaw A , Arribas A , Scaife AA. 2015. Seasonal forecasting of tropical storms using the Met Office GloSea5 seasonal forecast system. *Quarterly Journal of the Royal Meteorological Society.* **141:** 2206-2219.

Chand SS , Walsh KJE. 2012. Modeling seasonal tropical cyclone activity in the Fiji region as a binary classification problem. *Journal of Climate.* **25:** 5057-5071.

Chowdhury AMR , Bhuyia AU , Choudhury AY , Sen R. 1993. The Bangladesh cyclone of 1991: why so many people died. *Disasters.* **17:** 291-304.

4267 Clarke AJ , Liu X. 1994. Interannual sea level in the northern and eastern Indian Ocean. *J. Phys.*
4268 *Oceanogr.* **24:** 1224–1235.

4269 Elsner JB , Jagger TH 2013. *Hurricane Climatology,* New York, Oxford University press.

4270 Elsner JB , Schmertmann CP. 1993. Improving extendedrange seasonal predictions of intense
4271 Atlantic hurricane activity. *Wea. Forecasting.* **8:** 345-51.

4272 Elsner JB , Schmertmann CP. 1994. Assessing forecast skill through cross validation. *Weather &*
4273 *Forecasting.* **9:** 619-624.

4274 Emanuel K , Ravela S , Vivant E , Risi C. 2006. A Statistical Deterministic Approach to
4275 Hurricane Risk Assessment. *Bulletin of the American Meteorological Society.* **87:** 299-
4276 314.

4277 Fraedrich K , Leslie LM. 1989. Estimates of cyclone track predictability. I: Tropical cyclones in
4278 the Australian region. *Quarterly Journal of the Royal Meteorological Society.* **115:** 79-92.

4279 Giannini A , Saravanan R , Chang P. 2003. Oceanic forcing of Sahel rainfall on interannual to
4280 interdecadal time scales. *Science.* **302:** 1027–1030.

4281 Girishkumar MS , Ravichandran M. 2012. The influences of ENSO on tropical cyclone activity in
4282 the Bay of Bengal during October-December. *Journal of Geophysical Research: Oceans.*
4283 **117**.

4284 Gray WM , Landsea CW , Mielke Jr PW , Berry KJ. 1992. Predicting Atlantic seasonal hurricane
4285 activity 6-11 months in advance. *Weather & Forecasting.* **7:** 440-455.

4286 Gray WM , Landsea CW , Mielke Jr PW , Berry KJ. 1993. Predicting Atlantic basin seasonal
4287 tropical cyclone activity by 1 August. *Weather & Forecasting.* **8:** 73-86.

4288 Gray WM , Landsea CW , Mielke Jr PW , Berry KJ. 1994. Predicting Atlantic Basin seasonal
4289 tropical cyclone activity by 1 June. *Weather & Forecasting.* **9:** 103-115.

4290 Guisan A , Edwards Jr TC , Hastie T. 2002. Generalized linear and generalized additive models in
4291 studies of species distributions: Setting the scene. *Ecological Modelling.* **157:** 89-100.

4292 Hall TM , Jewson S. 2007. Statistical modelling of North Atlantic tropical cyclone tracks. *Tellus,*
4293 *Series A: Dynamic Meteorology and Oceanography.* **59 A:** 486-498.

4294 Hastie T , Tibshirani R , Friedman J. 2009. The Elements of Statistical learning: Data Mining,
4295 Inference, and Prediction. *Springer Series in Statistics.* **Second Edition:** 295-333.

4296 Hess JC , Elsner JB. 1994. Extended-range hindcasts of tropical-origin Atlantic hurricane activity.
4297 *Geophysical Research Letters.* **21:** 365-368.

4298 Hoerling M , Hurrell J , Xu T , Bates GT , Phillips A. 2004. Twentieth century North Atlantic
4299 climate change. Part II: Understanding the effect of Indian Ocean warming. . *Climate*
4300 *Dyn.,.* **23:** 391-405.

4301 Jagger TH , Niu X , Elsner JB. 2002. A space-time model for seasonal hurricane prediction.
4302 *International Journal of Climatology.* **22:** 451-465.

4303 Jakobsen F , Azam MH , Ahmed MMZ , Mahboob-Ul-Kabir M. 2006. Cyclone storm surge levels
4304 along the Bangladeshi coastline in 1876 and 1960-2000. *Coastal Engineering Journal.*
4305 **48:** 295-307.

4306 James MK , Mason LB. 2005. Synthetic tropical cyclone database. *Journal of Waterway, Port,*
4307 *Coastal and Ocean Engineering.* **131:** 181-192.

4308 Klein WH , Bloom HJ. 1989. An Operational System for Specifying Monthly Precipitation
4309 Amounts over the United States from the Field of Concurrent Mean 700-mb Heights.
4310 *Weather and Forecasting.* **4:** 51-60.

4311 Knapp KR , Kruk MC , Levinson DH , Diamond HJ , Neumann CJ. 2010. The international best
4312 track archive for climate stewardship (IBTrACS). *Bulletin of the American*
4313 *Meteorological Society.* **91:** 363-376.

4314 Li Z , Yu W , Li T , Murty VSN , Tangang F. 2013. Bimodal character of cyclone climatology in
4315 the bay of bengal modulated by monsoon seasonal cycle. *Journal of Climate.* **26:** 1033-
4316 1046.

4317 Mcdonnell KA , Holbrook NJ. 2004a. A Poisson regression model of tropical cyclogenesis for the
4318 Australian-southwest Pacific Ocean region. *Weather and Forecasting.* **19:** 440-455.

4319 Mestre O , Hallegatte S. 2009. Predictors of tropical cyclone numbers and extreme hurricane
4320 intensities over the North Atlantic using generalized additive and linear models. *Journal*
4321 *of Climate.* **22:** 633-648.

4322 Mohapatra M , Bandyopadhyay BK , Tyagi A 2014. Status and Plans for Operational Tropical
4323 Cyclone Forecasting and Warning Systems in the North Inidan Ocean Region. *In:* U.C.
4324 Mohanty, MM, O.P. Singh, B.K. Bandyopadhyay, L.S. Rathore (ed.) *Monitoring and*
4325 *Prediction of Tropical Cyclones in the Indian Ocean and Climate Change.* Springer.

4326 Mydans S , Cowell A. 2008. "Myanmar Mourns Victims of Cyclone". . *New York Times.*

Nath S , Kotal SD , Kundu PK. 2015. Seasonal prediction of tropical cyclone activity over the North Indian Ocean using the neural network model. *Atmosfera.* **28:** 271-281.

Nicholls N. 1999. SOI-based forecast of Australian region tropical cyclone activity. . *Experimental Long-Lead Forecast Bulletin,Climate Prediction Center, National Weather Service, Washington,DC.* **Vol. 8, No.4, :** 71-72.

Paul BK. 2009. Why relatively fewer people died? The case of Bangladesh's cyclone sidr. *Natural Hazards.* **50:** 289-304.

Rajasekhar M , Kishtawal CM , Prasad MYS , Seshagiri Rao V , Rajeevan M 2014. Extended range tropical cyclone predictions for East Coast of India. *Monitoring and Prediction of Tropical Cyclones in the Indian Ocean and Climate Change.*

Rajeevan M , Srinivasan J , Niranjan Kumar K , Gnanaseelan C , Ali MM. 2013. On the epochal variation of intensity of tropical cyclones in the Arabian Sea. *Atmospheric Science Letters.* **14:** 249-255.

Regnier E , Harr PA. 2006. A Dynamic Decision Model Applied to Hurricane Landfall. *Weather and Forecasting.* **21:** 764-780.

Rigollet P , Vert R. 2009. Optimal rates for plug-in estimators of density level sets. *Bernoulli.* **15:** 1154-1178.

Rumpf J , Weindl H , Höppe P , Rauch E , Schmidt V. 2007. Stochastic modelling of tropical cyclone tracks. *Mathematical Methods of Operations Research.* **66:** 475-490.

Sahoo B , Bhaskaran PK. 2016. Assessment on historical cyclone tracks in the Bay of Bengal, east coast of India. *International Journal of Climatology.* **36:** 95-109.

Singh C , Das S , Verma RB , Verma BL , Bandyopadhyay BK. 2012. Rainfall estimation of landfalling tropical cyclones over indian coasts through satellite imagery. *Mausam.* **63:** 193-202.

Singh OP. 2010. Tropical cyclones: Trends, Forecasting and Mitigation. *Natural and Anthropogenic Disasters.* 256-274.

Solow A , Nicholls N. 1990. The Relationship between the Southern Oscillation and Tropical Cyclone Frequency in the Australian Region. *Journal of Climate.* **3:** 1097-1101.

Turlach BA. 1993. Bandwidth Selection in Kernel Density Estimation: A Review. *CORE and Institut de Statistique.* **19:** 1-33.

Tyagi A , Bandyopadhyay BK , Mohapatra M 2010. Monitoring and prediction of cyclonic disturbances over North Indian ocean by regional specialised meteorological centre, New Delhi (India): Problems and prospective. *Indian Ocean Tropical Cyclones and Climate Change.*

Vickery PJ , Skerjl P , Steckley AC , Twinsdale L. 2000. Simulation of hurricane risk in the united states using an empirical storm track modeling technique. *Journal of structural engineering.* **126:** 1222-1237.

Vissa NK , Satyanarayana ANV , Prasad Kumar B. 2013. Intensity of tropical cyclones during pre- and post-monsoon seasons in relation to accumulated tropical cyclone heat potential over Bay of Bengal. *Natural Hazards.* **68:** 351-371.

Wahiduzzaman M , Oliver ECJ , Wotherspoon SJ , Holbrook NJ. 2016. A climatological model of North Indian Ocean tropical cyclone genesis, tracks and landfall. *Climate Dynamics.* 1-19.

Weinkle J , Maue R , Pielke R. 2012. Historical global tropical cyclone landfalls. *Journal of Climate.* **25:** 4729-4735.

Wijffels S , Meyers G. 2004. An intersection of oceanic waveguides: Variability in the Indonesian throughflow region. *J. Phys. Oceanogr.* **34:** 1232-1253.

Wilks DS. 1995. Statistical Methods in the Atmospheric Sciences. *Academic Press.* 467.

Wmo 1997. Tropical Cyclone Operational Plan for the Bay of Bengal and the Arabian Sea,.

Wu R , Kirtman BP. 2004. Understanding the Impacts of the Indian Ocean on ENSO Variability in a Coupled GCM. *Journal of Climate.* **17:** 4019-4031.

Xie S-P , Annamalai H , Schott FA , Mccreary JP. 2002. Structure and Mechanisms of South Indian Ocean Climate Variability*. *Journal of Climate.* **15:** 864-878.

Yonekura E , Hall TM. 2011. A Statistical model of tropical cyclone tracks in the western North Pacific with ENSO-dependent cyclogenesis. *Journal of Applied Meteorology and Climatology.* **50:** 1725-1739.

Yuan JP , Cao J. 2013. North Indian Ocean tropical cyclone activities influenced by the Indian Ocean Dipole mode. *Science China Earth Sciences.* **56:** 855-865.

Yulaeva E , Wallace JM. 1994. The signature of ENSO inglobal temperature and precipitation fields derived from the Microwave Sounding Unit. *J. Climate.* **7:** 1719–1736.

Zebiak SE , Cane MA. 1987. A Model El Ni&ntilde–Southern Oscillation. *Monthly Weather Review*. **115:** 2262-2278.

Appendix

Table-1: IOD Year Categorization with ENSO

	Negative IOD	No IOD	Positive IOD
El Niño	**1930**	**1877 1888 1899 1911 1914** 1918 1925 **1940** 1941 **1965 1986 1987**	**1896 1902 1905 1923** 1957 **1963 1972 1982 1991 1997**
No ENSO	**1880 1958 1968 1974 1980 1985 1989 1992**	1881 **1882 1883 1884 1895 1898 1901 1904 1907 1908 1912** 1915 1920 **1921 1927 1929** 1931 **1932 1934 1936 1937 1939 1943 1947 1948** 1951 1952 **1953** 1956 1959 1960 **1962 1966 1969 1976 1979 1990** 1993 **1995**	**1885 1887 1891 1894** 1900 1913 **1919 1926 1935 1944 1945 1946 1961 1967** 1977 **1983** 1994
La Niña	**1906 1909 1910** 1916 **1917 1928 1933 1942 1950 1975** 1981	**1878** 1879 1886 1889 **1890 1892 1893 1897 1903** 1922 1924 **1938 1949** 1954 1955 **1964** 1970 1971 **1973** 1978 1984 **1988** 1996 1998	

Source: http://www.marine.csiro.au/~mcintosh/ENSO_IOD_years.htm

Boldface indicates a higher level of certainty in the classification (Meyers *et al,* 2007)

Table-2: Landfall rate and probability of TC during El Niño year

Oceanic Variable	TC Occurrence	Bangladesh Coast	India Coast	Srilanka Coast	Myanmar Coast	North Indian Ocean
El Niño	Rate	0.41	1.29	0.24	0.24	3.17
	Percentage	33%	35%	40%	31%	38%
	No	66%	28%	79%	79%	4%
	One	27%	36%	19%	19%	13%
	Two	6%	23%	2%	2%	21%
	Two or less	99%	86%	99%	99%	39%
	More than Two	1%	14%	<1%	<1%	61%

4399 Table-3: Landfall rate and probability of TC during La Niña year

4400

Oceanic Variable	TC Occurrence	Bangladesh Coast	India Coast	Srilanka Coast	Myanmar Coast	North Indian Ocean
La Niña	Rate	0.61	1.17	0.06	0.28	2.78
	Percentage	52%	34%	10%	38%	35%
	No	54%	31%	94%	76%	6%
	One	33%	36%	6%	21%	17%
	Two	1%	21%	<1%	3%	24%
	Two or less	98%	89%	99%	99%	47%
	More than Two	2%	11%	Nil	<1%	53%

4401

4402 Table-4: Landfall rate and probability of TC during IOD+ year

4403

Oceanic Variable	TC Occurrence	Bangladesh Coast	India Coast	Srilanka Coast	Myanmar Coast	North Indian Ocean
IOD+	Rate	0.54	1.15	0.31	0.31	3.38
	Percentage	33%	24%	40%	31%	31%
	No	58%	32%	73%	73%	3%
	One	31%	36%	23%	23%	12%
	Two	8%	21%	4%	4%	19%
	Two or less	98%	89%	99%	99%	34%
	More than Two	2%	11%	<1%	<1%	66%

4404

4405 Table-5: Landfall rate and probability of TC during IOD- year

4406

Oceanic Variable	TC Occurrence	Bangladesh Coast	India Coast	Srilanka Coast	Myanmar Coast	North Indian Ocean
IOD-	Rate	0.42	1.50	0.21	0.21	2.86
	Percentage	29%	34%	30%	23%	28%
	No	66%	22%	81%	81%	6%
	One	28%	33%	17%	17%	16%
	Two	6%	25%	2%	2%	23%
	Two or less	99%	81%	99%	99%	46%
	More than Two	1%	19%	<1%	<1%	54%

4407

4408

4409

4410

4411

5.3 Chapter Summary

This chapter addresses the thesis aims of development of a statistical model to predict the tropical cyclone landfall probabilities in the North Indian Ocean region. This paper consists two statistical model-Poisson regression and generalised additive model. Poisson regression considers predictors to forecast and three components based general additive model takes intensity into model. Also the model hindcast and forecast skills are quantified.

In detail we have presented a new statistical model for probabilities of tropical cyclone landfall frequency in the North Indian Ocean region. Overall, the model has good cross-validated and forecast skill over climatology.

III DISCUSSION AND SUMMARY

6 DISCUSSION AND SUMMARY

The NIO is a breeding ground for tropical cyclones and accounts for only 7% of the world's tropical cyclones but the number of deaths from TCs that make landfall in the region can be staggering. Therefore, it is important to assess the risks thoroughly and carefully. Models can be valuable tools for evaluation and management of the tropical cyclone risks by providing seasonal forecast and early warnings. Both dynamical and statistical model have been developed to forecast tropical cyclone in the NIO basin but there is very little skill is found using dynamical models (Pattanaik and Mohapatra 2016). In view of this, there is need to develop a suitable probabilistic seasonal forecast model. Seasonal forecasting and early warnings of tropical cyclone can help decision-makers, and residents in vulnerable coastal areas, to consider and plan potential action months in advance. The significance of skillful seasonal forecasts is important for many societal sectors and the framework of developing climate services. In addition, it is valuable among the larger community by increasing the acceptance of climate forecasts (Doblas-Reyes *et al.* 2013).

Now-a-days seasonal forecasting of tropical cyclone landfall by dynamical models is challenging (Camargo 2013; Shaevitz *et al.* 2014; Camp *et al.* 2015) and its skill varies (Camargo *et al.* 2005; Bengtsson *et al.* 2007; Camargo and Barnston 2009). Little accuracy was found in the simulation of seasonal cycle over the NIO region by Camp *et al.* (2015). Other dynamical models, including the Dynamical High Resolution Model (HRM), Consortium for small Scale Modeling (COSMO) and Artificial Neural Network System models, have been shown not to be able to forecast cyclone landfall well because of limited spatial resolution (Yahyai 2014) and number of simulations (Ray *et al.* 2012).

Interestingly, statistical models have shown some promise for TC count prediction in the NIO region (Nath *et al.* 2015). Skilful TC track studies have been previously also demonstrated using statistical forecast models in western North Pacific (Rumpf *et al.* 2010), North Atlantic (Emanuel *et al.* 2006) and South Pacific (James and Mason 2005) regions. There is no guarantee that statistical TC models, developed for the Atlantic and Pacific, will be similarly beneficial in the NIO in a seasonal context, since the seasonal cycle is characterised by the double peak that exists in the pre-monsoon and post-

monsoon periods. Compared to other ocean basins across the globe, the Indian Ocean has also received much less attention for statistical seasonal prediction of cyclones (Nath *et al.* 2015). Therefore, In this thesis, climatological and statistical seasonal forecast models are developed for TC genesis, tracks and landfall in the North Indian Ocean (NIO) rim countries based on kernel density estimation, Poisson regression, a generalised additive model (GAM) including an Euler integration step, and landfall detection using a country mask approach.

We have applied a Kernel density approach to model the spatial distribution of observed tropical cyclone genesis locations. This approach has been previously used successfully by Vickery *et al.* (2000); James and Mason (2005); Emanuel *et al.* (2006) and Rumpf *et al.* (2007). Cyclone tracks were estimated by fitting a Generalized Additive Model (GAM) to the observed trajectories velocity. The GAM is an extension of linear regression model in which the linear relationships are changed by smooth changes of the predictors Cyclone trajectories are simulated using the fitted GAM to predict mean increment velocities at each step along the simulated track, together with random (stochastic) innovations also at each step – starting from randomly selected genesis locations drawn from the kernel for each NIO region TC season. Based on the mean vector field estimated by the GAM fit, a Euler step is used to project trajectories forward in time from this genesis point. A stochastic innovation is added at each time step to account for the variable nature of the vector field that is not captured by the GAM, with a variance determined by the residual error of the GAM fit. For each simulated genesis point, 50 trajectories (and each trajectory has an independent set of innovations applied) were simulated 7 days forward in time with a 6 hourly time step. To determine the points of landfall, each trajectory is interpolated in time to finer increments, with successive points along the trajectory compared to the land mask and the first land mask crossing is taken to be the point of landfall. From the literature and our own analysis, we note that multiple landfalls are rare in the NIO region; it is almost never seen that a cyclone strikes a country in the NIO rim and then comes back again to strike land a second time (Evan and Camargo 2010; Weinkle *et al.* 2012; Alam and Dominey-Howes 2015). In the study period, 95.2% of NIO region TCs made landfall (95.7% is reported by Alam and Dominey-Howes (2015) based on their long-term catalogue (from 1000AD to 2009) of landfall occurrences in surrounding countries of the Bay of Bengal) and none make

secondary landfalls. Based on this observation, we have only considered the first point of landfall for this region, while being consistent with other previous research across other basins by Weinkle *et al.* (2012) where they assume that even in TC multiple landfall cases, only the first point of landfall is counted. We have endeavoured to be both pragmatic with our lifetime choice and consistent with typical TC lifetime scales for the region in our modelling. This choice of a 7-day lifetime for TCs in the model is based both reported research and our own analysis of historical NIO region TC observations from genesis to landfall.

There are four TC seasons in the NIO region, i.e. the winter (December-February), pre-monsoon (March-May), monsoon (June-September) and post-monsoon (October-November). A bimodal characteristics of tropical cyclones are observed in the NIO region (Yanase *et al.* 2012; Li *et al.* 2013; Xing and Huang 2013; Akter and Tsuboki 2014). More number of cyclone is found in Bay of Bengal than Arabian sea except for Monsoon. Previous studies should be used to support the fact that there was almost no TC over BoB during the summer monsoon (Li *et al.* 2013) and it was due to the strengthened vertical wind shear starting from boreal spring, combined with decreasing sea surface temperature and relative vorticity that shut down TC activity during the monsoon. A distictly bimodal cyclone season in the NIO is pre-monson and post-monsoon (Camargo *et al.* 2007c; Kikuchi and Wang 2010; Akter and Tsuboki 2014; Wahiduzzaman *et al.* 2016) with the primary (secondary) peak in cyclone frequency is in November (May). Previous studies (Gray 1968; Camargo *et al.* 2007c; Evan and Camargo 2011; Yanase *et al.* 2012; Li *et al.* 2013) suggested that the bimodal feature of TC frequency in the BoB and AS is attributable to the annual cycle of the background vertical shear. Another study by Xing and Huang (2013) is shown that the bimodal distribution of TC genesis events is due to potential intensity.

The climate of the Indian Ocean region is strongly influenced by ocean variability on various spatial and temporal scales (Schott and McCreary Jr 2001). Tropical cyclone activity over the North Indian Ocean is strongly influenced by El Niño - Southern Oscillation (Girishkumar and Ravichandran 2012; Girishkumar *et al.* 2015), Quasi-Biennial Oscillation (Fadnavis *et al.* 2011; Fadnavis *et al.* 2014), Pacific Decadal Oscillation (Girishkumar *et al.* 2014), Boreal Summer Intraseasonal Oscillation (Kikuchi and Wang 2010), Indian Ocean Dipole (Saji *et al.* 1999), Madden Julian Oscillation

(Kikuchi and Wang 2010; Mohapatra and Adhikary 2011; Girishkumar *et al.* 2015) but their role varies from the weakest to strongest. This thesis investigates the forecast potential of TC genesis, trajectories and landfall in the NIO region using an index of the stratospheric Quasi-Biennial Oscillation (QBO) and El Niño - Southern Oscillation (ENSO) as the predictor variable in a new statistical seasonal forecast model. ENSO is a predictor variable that influences the global tropical cyclone frequency, genesis, tracks and landfall on seasonal time-scales (Camargo *et al.* 2008; Camp *et al.* 2015) Many earlier studies have investigated the relationship between ENSO and seasonal TC activity in NIO basins (Ho *et al.* 2006; Kuleshov *et al.* 2008; Girishkumar *et al.* 2012; Srikanth *et al.* 2012; Girishkumar *et al.* 2014; Camp *et al.* 2015; Girishkumar *et al.* 2015). Recently, a potentially useful climatic relationship has been demonstrated between the stratospheric Quasi-Biennial Oscillation (QBO) and TC tracks in the Bay of Bengal region of the NIO (Fadnavis *et al.* 2014).

The Quasi-Biennial Oscillation (QBO) index is based on a time series of National Centers for Environmental Prediction (NCEP) Reanalysis zonal mean wind shear at the equator. We have calculated the QBO index as the east-west wind velocity difference between the 30hPa and 50hPa levels (30hpa-50hpa). A number of studies (Balachandran and Guhathakurta 1999; Camargo and Sobel 2010; Fadnavis *et al.* 2011; Yadav 2012; Fadnavis *et al.* 2014) suggest that the QBO has a notable and potentially important influence on TC frequency and track. However, Chan (1995) finds that the relationship between TCs and the QBO does not hold well during strong ENSO events. Our analysis in the present study therefore takes this into account and excludes data for previously classified strong ENSO events. A few studies have investigated the frequency and tracks of TCs in the Bay of Bengal and their relationship with the QBO (Balachandran and Guhathakurta 1999; Fadnavis *et al.* 2011; Fadnavis *et al.* 2014), but no previous study that we are aware of has developed a statistical forecast model to simulate and forecast TC tracks as well as provide probabilistic forecasts of landfall months in advance. Here, we have developed a statistical seasonal forecast model of TC genesis, tracks and landfall in the North Indian Ocean region for four seasons, utilising the QBO as a predictor. The QBO index used in this study is smoothed using a 3-month running average, and then a 1 to 6 month lead-lag analysis is performed to assess the best predictor timescale based on TC forecast skill.

We assessed the best predictor timescale based on a lead-lag analysis between the QBO, SOI index and the TCs by considering two approaches to assess the overall model skill. The first approach was based on LOOCV. The second approach was based on the distance between the observed and simulated landfall points. The highest percentage is seen for a 3-month lead of the QBO predictor and 2-month lead of the ENSO predictor. We therefore used this QBO 3-month lead and ENSO 2-month lead for the remainder of our analysis.

The observed distribution of TC genesis points appeared to have a clear dependence on the QBO phase, with a higher frequency of total genesis occurrences observed during the easterly QBO phase (60% of the total) than in the westerly QBO phase (40%), in keeping with the findings of Fadnavis *et al.* (2014). For the three phases of ENSO, the highest average frequency of genesis was observed in the La Niña years (3.67/yr), whereas El Niño and the Neutral years corresponded to the 2.9 and 2.76 respectively over the NIO. This results matched with previous studies done by Girishkumar and Ravichandran (2012); Felton *et al.* (2013) and Mahala *et al.* (2015) over the BoB.

The movement of TC is determined by the driving force of steering flow (Fadnavis *et al.* 2014). Earlier studies by Girishkumar and Ravichandran (2012) found that 200 hPa wind patterns during ENSO regimes do not confirm any substantial difference however George (1976) explained 500 hpa wind patterns as best for TC motion. We have shown 500hpa wind patters for pre-monsoon and post-monsoon during QBO and ENSO phases.

By using Poisson regression it was found that La Nina was a driver of landfall in Bangladesh and Myanmar. It was also found that the negative IOD plays a significant role for more than two cyclonic landfalls in India. The mechanism for more landfalls over India during negative IOD is discussed by Yuan et al. (2013) who examined NIO TC activity under different phases of IOD and their study revealed that under negative IOD there are anomalous easterlies over BoB, which would steer TCs toward the east coast of India. Historically there were also many more landfalls over east coast of India under negative IOD.

A comparison of the percentages of country-based statistics of cyclone landfalls from observations against the model simulations was also performed to assess the model skill

when the predictor is used in model forecasts. It was found that the model performs better overall compared to the climatological model of Wahiduzzaman *et al.* (2016). We found that the seasonal forecast model performed with approximately 25% improvement over results from the corresponding climatological model by using QBO and 15% improvement over results from the corresponding climatological model by using ENSO. Poisson regression model performed 10% improvement over climatology.

Separately, we have also explored the skill of independent model forecasts (hindcasts) for each season of the year for data from 2010-2013, taking into account the QBO and ENSO phase. To assess the forecast skill more broadly, we have performed a hold-one-out validation by running the model 30 times, each time holding out one year and validating based on that held-out year. Then we aggregate the validation statistics by averaging across all these results to get single maps, by season and QBO, ENSO phase, showing the landfall probabilities across all years for the QBO and ENSO forecast model and the change relative to the climatological model.

One limitation of the statistical modelling approach is the lower sharpness (the tendency of the forecast to predict extreme values) that comes with such models (Vitart *et al.* 2010). Statistical models rarely predict very low or very high probabilities largely because of the constraints provided by climatology (Slade and Maloney 2013). There is also room for the TC genesis kernel density estimation to be better tuned to the observations. Future improvements to the genesis model may translate to a bias reduction in the track simulations and thus landfall estimates. The KDE/GAM formalism as applied in this study is a unique method to model TC genesis and tracks. By generating random genesis points from the KDE distribution and then following the GAM velocity field, “future” TC tracks have been resulted. This formalism is different from regression-based forecast models. In regression-based forecast models, it is intended that the physical mechanisms behind how the predictors affect TC activity be represented, as least indirectly, in the models. Comparatively, the KDE/GAM is purely phenomenological model that replicates the climatological distribution.

KDE and GAM distributions derived from climatology likely do not apply to the future climate however the KDE/GAM formalism can be extended to model by changing TC genesis locations for example increasing sample size or clustering sample size. Therefore, Future research would benefit from considering the clustering genesis points and tracks.

In the current study, the predictors have been modelled separately and if the KDE/GAM formalism is applied as an operational seasonal forecast model, it will consider the combined climate effects from predictors so the framework to incorporate all these factors in a single model would be clustering the specified values of the covariates/predictors and values will be selected by considering bivariate relationships between covariates and TC activities. For example, using Poisson regression we have predicted the rate of TC landfall probabilities for the specified values of the covariates (SST=-0.1, SOI=-0.5 and OHC=0) and selected the values of SOI, SST and OHC by considering bivariate relationships between covariates and TC landfall frequency.

This model will be highly beneficial for the seasonal prediction at the expense of climate change. Single predictor is still favorable for the model as predictors like ENSO, QBO, IOD are seasonally locked however the combined predictors could be useful in a single model though there will be less sample size. In future, the predictors selection can follow the bivariate relationships between TC and covariates. Again, possible future efforts could then regard the impact of rainfall due to TCs across the NIO rim using the existing model approach. Last but not least, the Kernel density estimation, generalised additive model, eular integration with country mask approach could be implemented in Atlantic and Pacific basin.

REFERENCES

Akter N (2015) Mesoscale convection and bimodal cyclogenesis over the Bay of Bengal. Monthly Weather Review 143(9):3495-3517

Akter N, Tsuboki K (2014) Role of synoptic-scale forcing in cyclogenesis over the Bay of Bengal. Climate Dynamics 43:2651-2662

Alam E, Collins AE (2010) Cyclone disaster vulnerability and response experiences in coastal Bangladesh. Disasters 34(4):931-954

Alam E, Dominey-Howes D (2015) A new catalogue of tropical cyclones of the northern Bay of Bengal and the distribution and effects of selected landfalling events in Bangladesh. International Journal of Climatology 35(6):801-835

Alam MM, Hossain MA, Shafee S (2003) Frequency of Bay of Bengal cyclonic storms and depressions crossing different coastal zones. International Journal of Climatology 23(9):1119-1125

Alexander MA, Bladé I, Newman M, Lazante JR, Lau NC, Scott JD (2002) The atmospheric bridge: The influence of ENSO teleconnections on air–sea interaction over the global oceans. J. Climate 15:2205-2231

Ali A (1996) Vulnerability of Bangladesh to climate change and sea level rise through tropical cyclones and storm surges. Water, Air and Soil Pollution, vol. 94d,:171-179

Ali A (1999) Climate change impacts and adaptation assessment in Bangladesh. Climate Research, 12:109-116

Ali MM, Jagadeesh PSV, Jain S (2007) Effects of Eddies on bay of Bengal cyclone intensity. Eos 88(8)

Ali MM, Kishtawal CM, Jain S (2007) Predicting cyclone tracks in the north Indian Ocean: An artificial neural network approach. Geophysical Research Letters 34(4)

Allan RJ (1988) El Nino Southern Oscillation influences in the Australasian region. Progress in Physical Geography 12(3):313-348

An S-I, Kug J-S, Timmermann A, Kang I-S, Timm O (2007) The Influence of ENSO on the Generation of Decadal Variability in the North Pacific*. Journal of Climate 20(4):667-680

Annamalai H, Liu P, Xie S-P (2005) Southwest Indian Ocean SST Variability: Its Local Effect and Remote Influence on Asian Monsoons. Journal of Climate 18(20):4150-4167

Annamalai H, Potemra J, Murtugudde R, McCreary JP (2005) Effect of Preconditioning on the Extreme Climate Events in the Tropical Indian Ocean. Journal of Climate 18(17):3450-3469

Arpe K, Leroy SAG (2009) Atlantic hurricanes-Testing impacts of local SSTs, ENSO, stratospheric QBO-Implications for global warming. Quaternary International 195(1-2):4-14

Ashok K, Guan Z, Yamagata T (2003) Influence of the Indian Ocean Dipole on the Australian winter rainfall. Geophysical Research Letters 30(15):CLM 6-1 - 6-4

Ashok K, Saji N (2007) On the impacts of ENSO and Indian Ocean dipole events on sub-regional Indian summer monsoon rainfall. Natural Hazards 42(2):273-285

Baik JJ, Paek JS (1998) A climatology of sea surface temperature and the maximum intensity of western North Pacific tropical cyclones. Journal of the Meteorological Society of Japan 76(1):129-137

Balachandran S, Geetha B (2012) Statistical prediction of seasonal cyclonic activity over North Indian Ocean. Mausam 63(1):17-28

Balachandran S, Guhathakurta P (1999) On the influence of QBO over North Indian Ocean storm and depression tracks. Meteorology and Atmospheric Physics 70(1-2):111-118

Balaguru K, Taraphdar S, Leung LR, Foltz GR (2014) Increase in the intensity of postmonsoon Bay of Bengal tropical cyclones. Geophysical Research Letters 41(10):3594-3601

Baldwin MP, Gray LJ, Dunkerton TJ, Hamilton K, Haynes PH, Randel WJ, Holton JR, Alexander MJ, Hirota I, Horinouchi T, Jones DBA, Kinnersley JS, Marquardt C, Sato K, Takahashi M (2001) The quasi-biennial oscillation. Reviews of Geophysics 39(2):179-229

Bashtannyk DM, Hyndman RJ (2001) Bandwidth selection for kernel conditional density estimation. Computational Statistics & Data Analysis 36:279-298

Basu BK, Bhagyalakshmi K (2010) Forecast of the track and intensity of the tropical cyclone AILA over the bay of bengal by the global spectral atmospheric model VARSHA. Current Science 99(6):765-774

Behera SK, Luo JJ, Masson S, Rao SA, Sakuma H, Yamagata T (2006) A CGCM Study on the Interaction between IOD and ENSO. Journal of Climate 19(9):1688-1705

Belanger JI, Webster PJ, Curry JA, Jelinek MT (2012) Extended prediction of North Indian Ocean tropical cyclones. Weather and Forecasting 27(3):757-769

Belmadani A, Dewitte B, An S-I (2010) ENSO Feedbacks and Associated Time Scales of Variability in a Multimodel Ensemble. Journal of Climate 23(12):3181-3204

Bengtsson L, Hodges KI, Esch M (2007) Tropical cyclones in a T159 resolution global climate model: Comparison with observations and re-analyses. Tellus, Series A: Dynamic Meteorology and Oceanography 59 A(4):396-416

Bjerknes J (1969) Atmospheric teleconnections from the equatorial Pacific. Mon.Wea. Rev. 97:163-172

Black E, Slingo J, Sperber KR (2003) An observational study of the relationship between excessively strong short rains in coastal East Africa and Indian ocean SST. Monthly Weather Review 131(1):74-94

Brian B (2015) Tropical Cyclone ACE Climatology. Climate Blog Published on 8th Nov, 2015

Cai W, Whetton PH, Pittock AB (2001) Fluctuations of the relationship between ENSO and northeast Australian rainfall. Climate Dynamics 17(5-6):421-432

Camargo SJ (2013) Global and regional aspects of tropical cyclone activity in the CMIP5 models. Journal of Climate 26(24):9880-9902

Camargo SJ, Barnston AG (2009) Experimental dynamical seasonal forecasts of tropical cyclone activity at IRI. Weather and Forecasting 24(2):472-491

Camargo SJ, Barnston AG, Klotzbatch PJ, Landsea CW (2007a) Seasonal Tropical cyclone forecasts. Bulletin of the World Meterological Organization 56:297-307

Camargo SJ, Barnston AG, Zebiak SE (2005) A statistical assessment of tropical cyclone activity in atmospheric general circulation models. Tellus, Series A: Dynamic Meteorology and Oceanography 57(4):589-604

Camargo SJ, Emanuel KA, Sobel AH (2007) Use of a genesis potential index to diagnose ENSO effects on tropical cyclone genesis. Journal of Climate 20(19):4819-4834

Camargo SJ, Robertson AW, Barnston AG, Ghil M (2008) Clustering of eastern North Pacific tropical cyclone tracks: ENSO and MJO effects. Geochemistry, Geophysics, Geosystems 9(6)

Camargo SJ, Sobel AH (2010) Revisiting the influence of the quasi-biennial oscillation on tropical cyclone activity. Journal of Climate 23(21):5810-5825

Camp J, Roberts M, Maclachlan C, Wallace E, Hermanson L, Brookshaw A, Arribas A, Scaife AA (2015) Seasonal forecasting of tropical storms using the Met Office GloSea5 seasonal forecast system. Quarterly Journal of the Royal Meteorological Society 141(691):2206-2219

Cane MA, Zebiak SE, Dolan SC (1986) Experimental forecasts of El Nino. Nature 321(6073):827-832

Carson DJ (1998) Seasonal forecasting. Quarterly Journal of the Royal Meteorological Society 124:1-26

Carter MM, Elsner JB (1997) A Statistical Method for Forecasting Rainfall over Puerto Rico. Weather and Forecasting 12(3):515-525

Casson E, Coles S (2000) Simulation and extremal analysis of hurricane events. Journal of the Royal Statistical Society. Series C: Applied Statistics 49(2):227-245

Chan JCL (1985) Tropical cyclone activity in the northwest Pacific in relation to the El Nino/Southern Oscillation phenomenon. Monthly Weather Review 113(4):599-606

Chan JCL (1995) Tropical cyclone activity in the western North Pacific in relation to the stratospheric quasi-biennial oscillation. Mon. Wea. Rev. 123:2567-2571

Chan JCL, Shi JE (1999) Prediction of the summer monsoon rainfall over South China. International Journal of Climatology 19(11):1255-1265

Chan JCL, Shi JE, Lam CM (1998) Seasonal forecasting of tropical cyclone activity over the western North Pacific and the South China Sea. Weather and Forecasting 13(4):997-1004

Chan JCL, Shi JE, Liu KS (2001) Improvements in the seasonal forecasting of tropical cyclone activity over the Western North Pacific. Weather and Forecasting 16(4):491-498

Chand SS, Walsh KJE (2010) Forecasting Tropical Cyclone Formation in the Fiji Region: A Probit Regression Approach Using Bayesian Fitting. Weather and Forecasting 26(2):150-165

Chand SS, Walsh KJE (2011) Forecasting tropical cyclone formation in the Fiji region: A probit regression approach using bayesian fitting. Weather and Forecasting 26(2):150-165

Chand SS, Walsh KJE (2011) Influence of ENSO on Tropical Cyclone Intensity in the Fiji Region. Journal of Climate 24(15):4096-4108

Chand SS, Walsh KJE (2012) Modeling seasonal tropical cyclone activity in the Fiji region as a binary classification problem. Journal of Climate 25(14):5057-5071

Chowdhury AMR, Bhuyia AU, Choudhury AY, Sen R (1993) The Bangladesh cyclone of 1991: why so many people died. Disasters 17(4):291-304

Chu P-S (2004) ENSO and tropical cyclone activity. Hurricanes and Typhoons: Past, Present, and Potential. Columbia University Press,

Chu P-S, Zhao X (2007) A Bayesian Regression Approach for Predicting Seasonal Tropical Cyclone Activity over the Central North Pacific. Journal of Climate 20(15):4002-4013

Chu PS, Zhao X, Ho CH, Kim HS, Lu MM, Kim JH (2010) Bayesian forecasting of seasonal typhoon activity: A track-pattern-oriented categorization approach. Journal of Climate 23(24):6654-6668

Clark CO, Webster PJ, Cole JE (2003) Interdecadal variability of the relationship between the Indian Ocean zonal mode and East African coastal rainfall anomalies. . Journal of Climate 16:548-554

Clarke AJ, Liu X (1994) Interannual sea level in the northern and eastern Indian Ocean. J. Phys. Oceanogr. 24:1224–1235.

Collimore CC, Martin DW, Hitchman MH, Huesmann A, Waliser DE (2003) On the relationship between the QBO and tropical deep convection. Journal of Climate 16(15):2552-2568

Doblas-Reyes FJ, García-Serrano J, Lienert F, Biescas AP, Rodrigues LRL (2013) Seasonal climate predictability and forecasting: Status and prospects. Wiley Interdisciplinary Reviews: Climate Change 4(4):245-268

Drosdowsky W, Williams M (1991) The Southern Oscillation in the Australian Region. Part I: Anomalies at the Extremes of Oscillation. J. Climate 4:619-638

Du YG, Song JJ, Tang JP (2013) Impacts of different kinds of ENSO on landfalling tropical cyclones in China. Journal of Tropical Meteorology 19(1):39-48

4786 Ebert EE, Turk M, Kusselson SJ, Yang J, Seybold M, Keehn PR, Kuligowski RJ (2010) Ensemble
4787 Tropical Rainfall Potential (eTRaP) Forecasts. Weather and Forecasting 26(2):213-224
4788 Eichler T, Higgins W (2006) Climatology and ENSO-Related Variability of North American
4789 Extratropical Cyclone Activity. Journal of Climate 19(10):2076-2093
4790 Elsner JB, Jagger TH (2004) A hierarchical Bayesian approach to seasonal hurricane modeling.
4791 Journal of Climate 17(14):2813-2827
4792 Elsner JB, Jagger TH (2006) Prediction models for annual U.S. hurricane counts. Journal of
4793 Climate 19(12):2935-2952
4794 Elsner JB, Jagger TH (2013) Hurricane Climatology. Oxford University press, New York, pp 161-
4795 193
4796 Elsner JB, Jagger TH, Dickinson M, Rowe D (2008) Improving multiseason forecasts of North
4797 Atlantic hurricane activity. Journal of Climate 21(6):1209-1219
4798 Elsner JB, Kara AB (1999) Hurricanes of the North Atlantic: Climate and Society
4799 Elsner JB, Murnane RJ, Jagger TH (2006) Forecasting U.S. hurricanes 6 months in advance.
4800 Geophysical Research Letters 33(10)
4801 Elsner JB, Schmertmann CP (1993) Improving extendedrange seasonal predictions of intense
4802 Atlantic hurricane activity. Wea. Forecasting 8:345-351
4803 Elsner JB, Schmertmann CP (1994) Assessing forecast skill through cross validation. Weather &
4804 Forecasting 9(4):619-624
4805 Emanuel K (1986) An air-sea interaction theory for tropical cyclones. Part I. J.Atmos. Sci 43:585-
4806 604
4807 Emanuel K (1991) The Theory of Hurricanes. Annu. Rev. Fluid Mech 23:179-196
4808 Emanuel K (2005a) Divine wind: the history and science of hurricanes. Oxford University press,
4809 pp 1-182
4810 Emanuel K (2005b) Increasing destructiveness of tropical cyclones over the past 30 years. Nature
4811 436(7051):686-688
4812 Emanuel K (2006) Hurricanes: Tempests in a greenhouse. Physics Today 59(8):74-75
4813 Emanuel K, Ravela S, Vivant E, Risi C (2006) A Statistical Deterministic Approach to Hurricane
4814 Risk Assessment. Bulletin of the American Meteorological Society 87(3):299-314
4815 Emanuel K, Sundararajan R, Williams J (2008) Hurricanes and global warming: Results from
4816 downscaling IPCC AR4 simulations. Bulletin of the American Meteorological Society
4817 89(3):347-367
4818 Emanuel KA (1988) The maximum intensity of hurricanes. Journal of the Atmospheric Sciences
4819 45(7):1143-1155
4820 Evan AT, Camargo SJ (2010) A Climatology of Arabian Sea Cyclonic Storms. Journal of Climate
4821 24(1):140-158

Evan AT, Camargo SJ (2011) A climatology of Arabian Sea cyclonic storms. Journal of Climate 24(1):140-158

Fadnavis S, Chakraborty T, Ghude SD, Beig G, Ernest Raj P (2011) Modulation of Cyclone tracks in the Bay of Bengal by QBO. Journal of Atmospheric and Solar-Terrestrial Physics 73(13):1868-1875

Fadnavis S, Ernest Raj P, Buchunde P, Goswami BN (2014) In search of influence of stratospheric Quasi-Biennial Oscillation on tropical cyclones tracks over the Bay of Bengal region. International Journal of Climatology 34(3):567-580

Felton CS, Subrahmanyam B, Murty VSN (2013) ENSO-modulated cyclogenesis over the Bay of Bengal. Journal of Climate 26(24):9806-9818

Fraedrich K, Leslie LM (1989) Estimates of cyclone track predictability. I: Tropical cyclones in the Australian region. Quarterly Journal of the Royal Meteorological Society 115(485):79-92

Frank WM (1987) Tropical cyclone formation. A Global View of Tropical Cyclones:53-90

Garreaud RD, Battisti DS (1999) Interannual (ENSO) and interdecadal (ENSO-like) variability in the Southern Hemisphere tropospheric circulation. J.Climate Dynamics 12:2113–2123

George JE, Gray WM (1976) TROPICAL CYCLONE MOTION AND SURROUNDING PARAMETER RELATIONSHIPS. Journal of Applied Meteorology 15(12):1252-1264

Giannini A, Saravanan R, Chang P (2003) Oceanic forcing of Sahel rainfall on interannual to interdecadal time scales. Science 302:1027–1030.

Girishkumar MS, Ravichandran M (2012) The influences of ENSO on tropical cyclone activity in the Bay of Bengal during October-December. Journal of Geophysical Research: Oceans 117(2)

Girishkumar MS, Ravichandran M, Pant V (2012) Observed chlorophyll-a bloom in the southern Bay of Bengal during winter 2006-2007. International Journal of Remote Sensing 33(4):1264-1275

Girishkumar MS, Suprit K, Vishnu S, Prakash VPT, Ravichandran M (2015) The role of ENSO and MJO on rapid intensification of tropical cyclones in the Bay of Bengal during October–December. Theoretical and Applied Climatology 120(3-4):797-810

Girishkumar MS, Thanga Prakash VP, Ravichandran M (2014) Influence of Pacific Decadal Oscillation on the relationship between ENSO and tropical cyclone activity in the Bay of Bengal during October–December. Climate Dynamics 44(11-12):3469-3479

Goh AZC, Chan JCL (2010) An improved statistical scheme for the prediction of tropical cyclones making landfall in South China. Weather and Forecasting 25(2):587-593

Goswami BN, Ajayamohan RS, Xavier PK, Sengupta D (2003) Clustering of synoptic activity by Indian summer monsoon intraseasonal oscillations. Geophysical Research Letters 30(8):14-11

4859 Goyal S, Mohapatra M, Dube SK, Kumari P, de I (2016) Mesoscale convective systems in
4860 association with tropical cyclones over Bay of Bengal. Natural Hazards:1-17
4861 Gray MW (1990) Tropical cyclone formation. Proceedings of the Second WMO International
4862 Workshop on Tropical Cyclones (IWTC-II)
4863 Gray WM (1968) Global view of the origin of tropical disturbances and storms. Mon. Wea. Rev.
4864 96:669-700
4865 Gray WM (1968) Gloval view of the origin of tropical disturbances and storms. Mon.Wea.Rev
4866 96:669-700
4867 Gray WM (1975) Tropical cyclone genesis. dept. of Atm.Sci.Paper No.234,Colorado State
4868 University, Fort Collins, CO:121
4869 Gray WM (1979) Hurricanes: Their formation, structure and likely role in the tropical circulation.
4870 Meteorology over the Tropical Oceans:155-218
4871 Gray WM (1984) Atlantic seasonal hurricane frequency, Part I: El Nino and 30 mb Quasi-
4872 Biennial Oscillation influences. Monthly Weather Review 112(9)
4873 Gray WM (1984) Atlantic seasonal hurricane frequency. Part II: forecasting its variability.
4874 Monthly Weather Review 112(9):1669-1683
4875 Gray WM (1998) The formation of tropical cyclones. Meteorology and Atmospheric Physics
4876 67(1-4):37-69
4877 Gray WM, Landsea CW, Mielke Jr PW, Berry KJ (1992) Predicting Atlantic seasonal hurricane
4878 activity 6-11 months in advance. Weather & Forecasting 7(3):440-455
4879 Gray WM, Landsea CW, Mielke Jr PW, Berry KJ (1993) Predicting Atlantic basin seasonal
4880 tropical cyclone activity by 1 August. Weather & Forecasting 8(1):73-86
4881 Gray WM, Landsea CW, Mielke Jr PW, Berry KJ (1994) Predicting Atlantic Basin seasonal
4882 tropical cyclone activity by 1 June. Weather & Forecasting 9(1):103-115
4883 Guisan A, Edwards Jr TC, Hastie T (2002) Generalized linear and generalized additive models in
4884 studies of species distributions: Setting the scene. Ecological Modelling 157(2-3):89-100
4885 Haggag M, Badry H (2012) Hydrometeorological Modeling Study of Tropical Cyclone Phet in
4886 the Arabian Sea in 2010 Atmospheric and Climate Sciences 2:174-190
4887 Hall T, Yonekura E (2013) North American tropical cyclone landfall and SST: A statistical model
4888 study. Journal of Climate 26(21):8422-8439
4889 Hall TM, Jewson S (2007) Statistical modelling of North Atlantic tropical cyclone tracks. Tellus,
4890 Series A: Dynamic Meteorology and Oceanography 59 A(4):486-498
4891 Harold JM, Bigg GR, Turner J (1999) Mesocyclone activity over the North-East Atlantic. Part 1:
4892 Vortex distribution and variability. International Journal of Climatology 19(11):1187-1204
4893 Hastie T, Tibshirani R, Friedman J (2009) The Elements of Statistical learning: Data Mining,
4894 Inference, and Prediction. Springer Series in Statistics Second Edition:295-333

Hess JC, Elsner JB (1994) Extended-range hindcasts of tropical-origin Atlantic hurricane activity. Geophysical Research Letters 21(5):365-368

Hess JC, Elsner JB (1994) Historical developments leading to current forecast models of annual Atlantic hurricane activity. Bulletin - American Meteorological Society 75(9):1611-1620

Ho CH, Kim JH, Jeong JH, Kim HS, Chen D (2006) Variation of tropical cyclone activity in the South Indian Ocean: El Niño-Southern Oscillation and Madden-Julian Oscillation effects. Journal of Geophysical Research D: Atmospheres 111(22)

Ho CI, Kim HS, Jeong JH, Son SW (2009) Influence of stratospheric quasi-biennial oscillation on tropical cyclone tracks in the western North Pacific. Geophysical Research Letters 36(6)

Hoerling M, Hurrell J, Xu T, Bates GT, Phillips A (2004) Twentieth century North Atlantic climate change. Part II: Understanding the effect of Indian Ocean warming. . Climate Dyn., 23:391-405

Holland G (1987) Chapter 3 of A Global View of Tropical Cyclones. WMO Bangkok TC Workshop Textbook:13-52

Holland GJ (1997) The maximum potential intensity of tropical cyclones. Journal of the Atmospheric Sciences 54(21):2519-2541

Holland GJ, Webster PJ (2007) Heightened tropical cyclone activity in the North Atlantic: Natural variability or climate trend? Philosophical Transactions of the Royal Society A: Mathematical, Physical and Engineering Sciences 365(1860):2695-2716

Hopsch SB, Thorncroft CD, Tyle KR (2010) Analysis of African easterly wave structures and their role in influencing tropical cyclogenesis. Monthly Weather Review 138(4):1399-1419

Hossain MN, Paul SK (2015) Simulation of physical and socioeconomic factors of vulnerability to cyclones and storm surges using GIS: a case study. GeoJournal

Hsu PC, Ho CR, Liang SJ, Kuo NJ (2013) Impacts of two types of El Niño and la Niña events on typhoon activity. Advances in Meteorology 2013

Huang B, Kinter Iii JL (2002) Interannual variability in the tropical Indian Ocean. Journal of Geophysical Research C: Oceans 107(11):20-21

Huesmann AS, Hitchman MH (2001) The stratospheric quasi-biennial oscillation in the NCEP reanalyses: Climatological structures. Journal of Geophysical Research: Atmospheres 106(D11):11859-11874

IMD (1979) "Tracks of Storms and Depressions in the Bay of Bengal and the Arabian Sea, 1877-1970".

Islam T, Peterson RE (2009) Climatology of landfalling tropical cyclones in Bangladesh 1877-2003. Natural Hazards 48(1):115-135

Jagger TH, Elsner JB (2010) A consensus model for seasonal hurricane prediction. Journal of Climate 23(22):6090-6099

Jagger TH, Niu X, Elsner JB (2002) A space-time model for seasonal hurricane prediction. International Journal of Climatology 22(4):451-465

Jakobsen F, Azam MH, Ahmed MMZ, Mahboob-ul-Kabir M (2006) Cyclone storm surge levels along the Bangladeshi coastline in 1876 and 1960-2000. Coastal Engineering Journal 48(3):295-307

James MK, Mason LB (2005) Synthetic tropical cyclone database. Journal of Waterway, Port, Coastal and Ocean Engineering 131(4):181-192

Jury MR (1993) A preliminary study of climatological associations and characteristics of tropical cyclones in the SW Indian Ocean. Meteorology and Atmospheric Physics 51(1-2):101-115

Jury MR, Pathack B, Parker B (1999) Climatic determinants and statistical prediction of tropical cyclone days in the southwest Indian Ocean. Journal of Climate 12(6):1738-1746

Kang NY, Lim MS, Elsner JB, Shin DH (2016) Bayesian updating of track-forecast uncertainty for tropical cyclones. Weather and Forecasting 31(2):621-626

Karoly DJ (1989) Southern Hemisphere circulation features associated with El Niño–Southern Oscillation. J. Climate 2:1239– 1252.

Kikuchi K, Wang B (2010) Formation of tropical cyclones in the Northern Indian ocean associated with two types of tropical intraseasonal oscillation modes. Journal of the Meteorological Society of Japan 88(3):475-496

Kikuchi K, Wang B, Fudeyasu H (2009) Genesis of tropical cyclone Nargis revealed by multiple satellite observations. Geophysical Research Letters 36(6)

Killworth PD, Blundell JR (2003) Long extratropical planetary wave propagation in the presence of slowly varying mean flow and bottom topography. Part I: The local problem. Journal of Physical Oceanography 33(4):784-801

Killworth PD, Blundell JR (2003) Long extratropical planetary wave propagation in the pressence of slowly varying mean flow and bottom topography. Part II: Ray propagation and comparison with observations. Journal of Physical Oceanography 33(4):802-821

Klein WH, Bloom HJ (1989) An Operational System for Specifying Monthly Precipitation Amounts over the United States from the Field of Concurrent Mean 700-mb Heights. Weather and Forecasting 4(1):51-60

Kleinschmidt E (1951) Principles of the theory of tropical cyclones. Arch. Meteor.Geophys., Bioklimatol 4:53-72

Klotzbach PJ (2007) Recent developments in statistical prediction of seasonal Atlantic basin tropical cyclone activity. Tellus, Series A: Dynamic Meteorology and Oceanography 59 A(4):511-518

Klotzbach PJ (2011) El Niño-Southern Oscillation's impact on Atlantic basin hurricanes and U.S. Landfalls. Journal of Climate 24(4):1252-1263

Klotzbach PJ, A. Barnston, G. Bell, S.J. Camargo, J.C.L. Chan, A. Lea, M.Saunders, and, Vitart F (2010) Seasonal Forecasting of Tropical Cyclones. Global Guide to Tropical Cyclone Forecasting C. Guard (ed), WMO Report, 2nd edition.

Knapp KR, Kruk MC, Levinson DH, Diamond HJ, Neumann CJ (2010) The international best track archive for climate stewardship (IBTrACS). Bulletin of the American Meteorological Society 91(3):363-376

Knutson TR, Zeng F, Wittenberg A, Kim SH, Sirutis J, Bender M, Zhao M, Tuleya R (2014) Recent Research at GFDL on Surface Temperature Trends and Simulations of Tropical Cyclone Activity in the Indian Ocean Region. In: U.C. Mohanty MM, O.P. Singh, B.K. Bandyopadhyay, L.S. Rathore (ed) Monitoring and Prediction of Tropical Cyclones in the Indian Ocean and Climate Change. Springer, pp 50-62

Kossin JP, Olander TL, Knapp KR (2013) Trend analysis with a new global record of tropical cyclone intensity. Journal of Climate 26(24):9960-9976

Kuleshov Y, Qi L, Fawcett R, Jones D (2008) On tropical cyclone activity in the Southern Hemisphere: Trends and the ENSO connection. Geophysical Research Letters 35(14)

Lander MA, Guard CP (1998) A look at global tropical cyclone activity during 1995: Contrasting high Atlantic activity with low activity in other basins. Monthly Weather Review 126(5):1163-1173

Landsea CW (1993) A climatology of intense (or major) Atlantic hurricanes. Monthly Weather Review 121(6):1703-1713

Landsea CW (2007) Counting Atlantic tropical cyclones back to 1900. Eos 88(18)

Landsea CW, Bell GD, Gray WM, Goldenberg SB (1998) The extremely active 1995 Atlantic hurricane season: Environmental conditions and verification of seasonal forecasts. Monthly Weather Review 126(5):1174-1193

Landsea CW, Gray WM (1992) The strong association between western Sahel monsoon rainfall and intense Atlantic hurricanes. J. Climate 5:435-453

Larson S, Lee SK, Wang C, Chung ES, Enfield D (2012) Impacts of non-canonical El Niño patterns on Atlantic hurricane activity. Geophysical Research Letters 39(14)

Lau (1985) Elements of a stochastic-dynamical theory of the long-term variability of the El Niño/Southern Oscillation. J. Atmos. Sci. 42:1552-1558

Lehmiller GS, Kimberlain TB, Elsner JB (1997) Seasonal prediction models for North Atlantic basin hurricane location. Monthly Weather Review 125(8):1780-1791

Leroy A, Wheeler MC (2008) Statistical prediction of weekly tropical cyclone activity in the southern hemisphere. Monthly Weather Review 136(10):3637-3654

Li RCY, Zhou W (2013) Modulation of western north pacific tropical cyclone activity by the ISO. Part II: Tracks and landfalls. Journal of Climate 26(9):2919-2930

5003 Li Z, Yu W, Li T, Murty VSN, Tangang F (2013) Bimodal character of cyclone climatology in
5004 the bay of bengal modulated by monsoon seasonal cycle. Journal of Climate 26(3):1033-
5005 1046
5006 Liang CK, Eldering A, Gettelman A, Tian B, Wong S, Fetzer EJ, Liou KN (2011) Record of
5007 tropical interannual variability of temperature and water vapor from a combined AIRS-
5008 MLS data set. Journal of Geophysical Research: Atmospheres 116(6)
5009 Liebmann B, Hendon HH, Glick JD (1994) The relationship between tropical cyclones of the
5010 western Pacific and Indian Oceans and the Madden-Julian oscillation. J. Meteor. Soc. Japan
5011 72:401-411
5012 Liess S, Geller MA (2012) On the relationship between QBO and distribution of tropical deep
5013 convection. Journal of Geophysical Research: Atmospheres 117(3)
5014 Lim EP, Hendon HH, Hudson D, Wang G, Alves O (2009) Dynamical forecast of inter-el Niño
5015 variations of tropical SST and Australian spring rainfall. Monthly Weather Review
5016 137(11):3796-3810
5017 Lin II, Chen CH, Pun IF, Liu WT, Wu CC (2009) Warm ocean anomaly, air sea fluxes, and the
5018 rapid intensification of tropical cyclone Nargis (2008). Geophysical Research Letters 36(3)
5019 Liu KS, Chan JCL (2003) Climatological characteristics and seasonal forecasting of tropical
5020 cyclones making landfall along the South China Coast. Monthly Weather Review 131(8
5021 PART 1):1650-1662
5022 Liu KS, Chan JCL (2012) Interannual variation of Southern Hemisphere tropical cyclone activity
5023 and seasonal forecast of tropical cyclone number in the Australian region. International
5024 Journal of Climatology 32(2):190-202
5025 Loader CR (1999) Bandwidth Selection: Classical or Plug-In? The Annals of Statistics 27(2):415-
5026 438
5027 Lu J, Chen G, Frierson DMW (2008) Response of the zonal mean atmospheric circulation to El
5028 Niño versus global warming. Journal of Climate 21(22):5835-5851
5029 Mahala BK, Nayak BK, Mohanty PK (2015) Impacts of ENSO and IOD on tropical cyclone
5030 activity in the Bay of Bengal. Natural Hazards 75(2):1105-1125
5031 Mallik MAK, Ahsan MN, Chowdhury MAM (2015) Simulation of Track and Landfall of Tropical
5032 Cyclone Viyaru and Its Associated Strom Surges Using NWP Models. American Journal of
5033 Marine Science 3(1):11-21
5034 Mandal GS (1991) "Tropical Cyclones and Their Forecasting and Warning Systems in the North
5035 Indian Ocean". In, pp 139-188
5036 McBride JL (1995) Tropical cyclone formation. Global Perspectives on Tropical Cyclones:63-105
5037 McBride JL, Zehr R (1981) Observational analysis of tropical cyclone formation. Part II:
5038 comparison of non-developing versus developing systems. Journal of the Atmospheric
5039 Sciences 38(6):1132-1151

5040 McDonnell KA, Holbrook NJ (2004a) A Poisson regression model of tropical cyclogenesis for the
5041 Australian-southwest Pacific Ocean region. Weather and Forecasting 19(2):440-455
5042 McDonnell KA, Holbrook NJ (2004b) A Poisson regression model approach to predicting tropical
5043 cyclogenesis in the Australian/southwest Pacific Ocean region using the SOI and saturated
5044 equivalent potential temperature gradient as predictors. Geophysical Research Letters
5045 31(20):L20110 20111-20115
5046 McDonnell KA, Holbrook NJ, Shaik H (2006) Seasonal forecasts of tropical cyclone numbers in
5047 the Australian/southwest Pacific Ocean region using a new Poisson regression model:
5048 verification of 2005/06 season forecast and forecast for 2006/07 season. Bull. Austr. Met.
5049 Oceanogr. Soc., 19(6):126-128
5050 McGauley MG, Nolan DS (2011) Measuring environmental favorability for tropical cyclogenesis
5051 by statistical analysis of threshold parameters. Journal of Climate 24(23):5968-5997
5052 McPhaden MJ, Foltz GR, Lee T, Murty VSN, Ravichandran M, Vecchi GA, Vialard J, Wiggert
5053 JD, Yu L (2009) Ocean-atmosphere interactions during cyclone nargis. Eos 90(7):53-54
5054 Mestre O, Hallegatte S (2009) Predictors of tropical cyclone numbers and extreme hurricane
5055 intensities over the North Atlantic using generalized additive and linear models. Journal of
5056 Climate 22(3):633-648
5057 Meyers G, McIntosh P, Pigot L, Pook M (2007) The years of El Niño, La Niña and interactions
5058 with the tropical Indian Ocean. Journal of Climate 20(13):2872-2880
5059 Mohapatra M, Adhikary S (2011) Modulation of cyclonic disturbances over the North Indian
5060 ocean by madden - Julian oscillation. Mausam 62(3):375-390
5061 Mohapatra M, Bandyopadhyay BK, Tyagi A (2012) Best track parameters of tropical cyclones
5062 over the North Indian Ocean: A review. Natural Hazards 63(3):1285-1317
5063 Mohapatra M, Bandyopadhyay BK, Tyagi A (2014) Status and Plans for Operational Tropical
5064 Cyclone Forecasting and Warning Systems in the North Inidan Ocean Region. In: U.C.
5065 Mohanty MM, O.P. Singh, B.K. Bandyopadhyay, L.S. Rathore (ed) Monitoring and
5066 Prediction of Tropical Cyclones in the Indian Ocean and Climate Change. Springer, pp
5067 149-162
5068 Montgomery MT, Farrell BF (1993) Tropical cyclone formation. Journal of the Atmospheric
5069 Sciences 50(2):285-310
5070 Mydans S, Cowell A (2008) "Myanmar Mourns Victims of Cyclone". . New York Times
5071 Nath S, Kotal SD, Kundu PK (2015) Seasonal prediction of tropical cyclone activity over the
5072 North Indian Ocean using the neural network model. Atmosfera 28(4):271-281
5073 Naujokat B (1986) An update of the observed quasi-biennial oscillation of the stratospheric winds
5074 over the Tropics. Journal of the Atmospheric Sciences 43(17):1873-1877
5075 NCDC (June 2009) "El Niño-Southern Oscillation (ENSO) June 2009". National Oceanic and
5076 Atmospheric Administration. Retrieved 2009-07-26.

5077 Neumann CJ (1972) An alternate to the hurran (hurrican analog) tropical cyclone forecast system.
5078 NOAA Tech. Memo., NWS SR-62,:22
5079 Ng EKW, Chan JCL (2012) Interannual variations of tropical cyclone activity over the north
5080 Indian Ocean. International Journal of Climatology 32(6):819-830
5081 Nicholls N (1979) A possible method for predicting seasonal tropical cyclone activity in the
5082 Australian region. Monthly Weather Review 107(9):1221-1224
5083 Nicholls N (1985) Predictability of interannual variations of Australian seasonal tropical cyclone
5084 activity. Monthly Weather Review 113(7):1144-1149
5085 Nicholls N (1999) SOI-based forecast of Australian region tropical cyclone activity.Experimental
5086 Long-Lead Forecast Bulletin,Climate Prediction Center, National Weather Service,
5087 Washington,DC Vol. 8, No.4, :71-72
5088 Nicholls N, Landsea C, Gill J (1998) Recent trends in Australian region tropical cyclone activity.
5089 Meteorology and Atmospheric Physics 65(3-4):197-205
5090 O'Hare G (2001) Hurricane 07B in the Godivari Delta, Andhra Pradesh, India: Vulnerability,
5091 mitigation and the spatial impact. Geographical Journal 167(1):23-38
5092 Owens BF, Landsea CW (2003) Assessing the Skill of Operational Atlantic Seasonal Tropical
5093 Cyclone Forecasts. Weather and Forecasting 18(1):45-54
5094 Paliwal M, Patwardhan A (2013) Identification of clusters in tropical cyclone tracks of North
5095 Indian Ocean. Natural Hazards:1-12
5096 Paliwal M, Patwardhan A, Sarda NL (2011) Analyzing tropical cyclone tracks of North Indian
5097 Ocean. In: ACM International Conference Proceeding Series.
5098 Palmen E (1956) A review of knowledge on the formation and development of tropical cyclones.
5099 Proc. of the Tropical Cyclone Symposium:213-232
5100 Paterson LA, Hanstrum BN, Davidson NE, Weber HC (2005) Influence of environmental vertical
5101 wind shear on the intensity of hurricane-strength tropical cyclones in the Australian region.
5102 Monthly Weather Review 133(12):3644-3660
5103 Pattanaik DR, Mohapatra M (2016) Seasonal forecasting of tropical cyclogenesis over the North
5104 Indian Ocean. Journal of Earth System Science 125(2):231-250
5105 Paul BK (2009) Why relatively fewer people died? The case of Bangladesh's cyclone sidr. Natural
5106 Hazards 50(2):289-304
5107 Philander SGH (1985) El Nino and La Nina. Journal of the Atmospheric Sciences 42(23):2652-
5108 2662
5109 Philander SGH (1990) El Niño, La Niña and the Southern Oscillation. Academic Press, San
5110 Diego, Calif., p 293
5111 Philander SGH (1992) Ocean-atmosphere interactions in the tropics: a review of recent theories
5112 and models. Journal of Applied Meteorology 31(8):938-945

5113 Rajasekhar M, Kishtawal CM, Prasad MYS, Seshagiri Rao V, Rajeevan M (2014) Extended range
5114 tropical cyclone predictions for East Coast of India. In: Monitoring and Prediction of
5115 Tropical Cyclones in the Indian Ocean and Climate Change. pp 137-148
5116 Rajeevan M, Srinivasan J, Niranjan Kumar K, Gnanaseelan C, Ali MM (2013) On the epochal
5117 variation of intensity of tropical cyclones in the Arabian Sea. Atmospheric Science Letters
5118 14(4):249-255
5119 Ramage CS (1950) Hurricane Development. J. Met. 21(9):917-925
5120 Ramsay HA, Leslie LM, Lamb PJ, Richman MB, Leplastrier M (2008) Interannual Variability of
5121 Tropical Cyclones in the Australian Region: Role of Large-Scale Environment. Journal of
5122 Climate 21(5):1083-1103
5123 Rasmusson EM (1984) 'El Niño: the ocean/atmosphere connection'. Oceanus 27:36-39
5124 Ray A, Jaiswal N, Kishtawal CM (2012) Cyclone tracking over North Indian Ocean using
5125 Artificial Neural Network Models and implementation of regional and seasonal
5126 stratification,. In: Second WMO International Conference on Indian Ocean Tropical and
5127 Cyclone Change (IOTCCC-2012). NEW DELHI
5128 Rayhun KMZ, Quadir DA, Chowdhury MAM, Ahsan MN, Haque MS (2015) Simulation of
5129 structure, track and landfall of tropical cyclone Bijli using WRF-ARW model. J.
5130 Bangladesh Acad. Sci 39(2):157-167
5131 Regnier E, Harr PA (2006) A Dynamic Decision Model Applied to Hurricane Landfall. Weather
5132 and Forecasting 21(5):764-780
5133 Riehl H (1954) Tropical Meteorology:392
5134 Rigollet P, Vert R (2009) Optimal rates for plug-in estimators of density level sets. Bernoulli
5135 15(4):1154-1178
5136 Ritchie EA, Holland GJ (1999) Large-scale patterns associated with tropical cyclogenesis in the
5137 western Pacific. Monthly Weather Review 127(9):2027-2043
5138 Rodriguez J, F. Vos., R. Below., Guha-Sapir D (2009) Annual disaster statistical review 2008. In:
5139 Centre for Research on the Epidemiology of Disasters (CRED), Brussels, Belgium, p 33
5140 Ropelewski CF, Halpert MS (1996) Quantifying southern oscillation-precipitation relationships.
5141 Journal of Climate 9(5):1043-1059
5142 Ropelewski CF, Jones PD (1987) An Extension of the Tahiti–Darwin Southern Oscillation Index.
5143 Monthly Weather Review 115(9):2161-2165
5144 Rumpf J, Weindl H, Faust E, Schmidt V (2010) Structural variation in genesis and landfall
5145 locations of North Atlantic tropical cyclones related to SST. Tellus, Series A: Dynamic
5146 Meteorology and Oceanography 62(3):243-255
5147 Rumpf J, Weindl H, Höppe P, Rauch E, Schmidt V (2007) Stochastic modelling of tropical
5148 cyclone tracks. Mathematical Methods of Operations Research 66(3):475-490

Sağır S, Atıcı R, Özcan O, Yüksel N (2015) The effect of the stratospheric QBO on the neutral density of the D region. Annals of Geophysics 58(3)

Sahoo B, Bhaskaran PK (2016) Assessment on historical cyclone tracks in the Bay of Bengal, east coast of India. International Journal of Climatology 36(1):95-109

Saji NH, Goswami BN, Vinayachandran PN, Yamagata T (1999) A dipole mode in the tropical Indian ocean. Nature 401(6751):360-363

Saunders MA, Lea AS (2005) Seasonal prediction of hurricane activity reaching the coast of the United States. Nature 434(7036):1005-1008

Schott FA, McCreary Jr JP (2001) The monsoon circulation of the Indian Ocean. Progress in Oceanography 51(1):1-123

Sengupta D, Senan R, Goswami BN, Vialard J (2007) Intraseasonal Variability of Equatorial Indian Ocean Zonal Currents. Journal of Climate 20(13):3036-3055

Shaevitz DA, Camargo SJ, Sobel AH, Jonas JA, Kim D, Kumar A, Larow TE, Lim YK, Murakami H, Reed KA, Roberts MJ, Scoccimarro E, Vidale PL, Wang H, Wehner MF, Zhao M, Henderson N (2014) Characteristics of tropical cyclones in high-resolution models in the present climate. Journal of Advances in Modeling Earth Systems 6(4):1154-1172

Shaji C, Kar SK, Vishal T (2014) Storm surge studies in the North Indian Ocean: A review. Indian Journal of Marine Sciences 43(2):125-147

Shankar D, Vinayachandran PN, Unnikrishnan AS (2002) The monsoon currents in the north Indian Ocean. Progress in Oceanography 52(1):63-120

Shapiro LJ (1989) The relationship of the quasi-biennial oscillation to Atlantic tropical storm activity. Monthly Weather Review 117(7):1545-1552

Singh C, Das S, Verma RB, Verma BL, Bandyopadhyay BK (2012) Rainfall estimation of landfalling tropical cyclones over indian coasts through satellite imagery. Mausam 63(2):193-202

Singh OP (2010) Tropical cyclones: Trends, Forecasting and Mitigation. Natural and Anthropogenic Disasters: 256-274

Singh OP, Ali Khan TM, Rahman MS (2000) Changes in the frequency of tropical cyclones over the North Indian Ocean. Meteorology and Atmospheric Physics 75(1-2):11-20

Singh OP, Ali Khan TM, Rahman MS (2001) Probable reasons for enhanced cyclogenesis in the Bay of Bengal during July-August of ENSO years. Global and Planetary Change 29(1-2):135-147

Singh R, Kishtawal CM, Pal PK, Joshi PC (2012) Improved tropical cyclone forecasts over north Indian Ocean with direct assimilation of AMSU-A radiances. Meteorology and Atmospheric Physics 115(1-2):15-34

Slade SA, Maloney ED (2013) An intraseasonal prediction model of atlantic and east Pacific tropical cyclone genesis. Monthly Weather Review 141(6):1925-1942

Smith RK, Montgomery MT, Vogl S (2008) A critique of Emanuel's hurricane model and potential intensity theory. Quarterly Journal of the Royal Meteorological Society 134(632):551-561

SMRC (1998) The impact of tropical cyclones on the coastal region of SAARC countries and their influence in the region. In: SMRC No-1, SMRC Publication. Bangladesh, 1998

Solow A, Nicholls N (1990) The Relationship between the Southern Oscillation and Tropical Cyclone Frequency in the Australian Region. Journal of Climate 3(10):1097-1101

Song Q, Vecchi GA, Rosati AJ (2007) Indian Ocean Variability in the GFDL Coupled Climate Model. Journal of Climate 20(13):2895-2916

Srikanth L, Ramalingam M, George MS, Bertino L, Samuelsen A (2012) A study on the influence of oceanic and atmospheric parameters on tropical cyclones in the bay of Bengal. European Journal of Scientific Research 76(1):63-73

Tailleux R (2003) Comments on "The effect of bottom topography on the speed of long extratropical planetary waves". Journal of Physical Oceanography 33(7):1536-1541

Tanabe S (1963) Low Latitude Analysis at the Formative Stage of Typhoons in 1962. Kishocho Kenkyu Jiho 15(6):405-418

Tang B, Emanuel K (2010) Midlevel ventilation's constraint on tropical cyclone intensity. Journal of the Atmospheric Sciences 67(6):1817-1830

Tao L, Wu L, Wang Y, Yang J (2012) Influence of tropical Indian ocean warming and ENSO on tropical cyclone activity over the western North Pacific. Journal of the Meteorological Society of Japan 90(1):127-144

Taskin S, Lodree Jr EJ (2011) A Bayesian decision model with hurricane forecast updates for emergency supplies inventory management. Journal of the Operational Research Society 62(6):1098-1108

Tolwinski-Ward SE (2015) Uncertainty quantification for a climatology of the frequency and spatial distribution of North Atlantic tropical cyclone landfalls. Journal of Advances in Modeling Earth Systems

Tomczak M, Godfrey JS (1994) Regional oceanography: an introduction. Elsevier Sci.

Turlach BA (1993) Bandwidth Selection in Kernel Density Estimation: A Review. CORE and Institut de Statistique 19:1-33

Tyagi A, Bandyopadhyay BK, Mohapatra M (2010) Monitoring and prediction of cyclonic disturbances over North Indian ocean by regional specialised meteorological centre, New Delhi (India): Problems and prospective. In: Indian Ocean Tropical Cyclones and Climate Change. pp 93-103

Ummenhofer CC, England MH, McLntosh PC, Meyers GA, Pook MJ, Risbey JS, Gupta AS, Taschetto AS (2009) What causes southeast Australia's worst droughts? Geophysical Research Letters 36(4)

5223 UNDP (2009) Tropical Cyclones. UNDP Report,pp 179-184
5224 Van Loon H, Shea DJ (1987) The Southern Oscillation. Part VI: anomalies of sea level pressure
5225 on the Southern Hemisphere and of Pacific sea surface temperature during the development
5226 of a warm event. Monthly Weather Review 115(2):370-379
5227 Vickery PJ, Skerjl P, Steckley AC, Twinsdale L (2000) Simulation of hurricane risk in the united
5228 states using an empirical storm track modeling technique. Journal of structural engineering
5229 126:1222-1237
5230 Vissa NK, Satyanarayana ANV, Prasad Kumar B (2013) Intensity of tropical cyclones during pre-
5231 and post-monsoon seasons in relation to accumulated tropical cyclone heat potential over
5232 Bay of Bengal. Natural Hazards 68(2):351-371
5233 Vitart F, Leroy A, Wheeler MC (2010) A comparison of dynamical and statistical predictions of
5234 weekly tropical cyclone activity in the Southern Hemisphere. Monthly Weather Review
5235 138(9):3671-3682
5236 Wahiduzzaman M, Oliver ECJ, Wotherspoon SJ, Holbrook NJ (2016) A climatological model of
5237 North Indian Ocean tropical cyclone genesis, tracks and landfall. Climate Dynamics:1-19
5238 Wang B, Chan JCL (2002) How strong ENSO events affect tropical storm activity over the
5239 western North Pacific. Journal of Climate 15(13):1643-1658
5240 Wang L, Koblinsky CJ, Howden S (2001) Annual rossby wave in the Southern Indian ocean:
5241 Why does It "Appear" to break down in the middle ocean? Journal of Physical
5242 Oceanography 31(1):54-74
5243 Warrick RA, MAccines KL, Pittock AB, Kench PS (2000) Climate change, severe storms and sea
5244 level. Floods edited by Dennis J. Parker Taylor and Francis group, London:139
5245 Webster PJ (2008) Myanmar's deadly daffodil. Nature Geoscience 1(8):488-490
5246 Webster PJ, Moore AM, Loschnigg JP, Leben RR (1999) Coupled ocean-atmosphere dynamics in
5247 the Indian Ocean during 1997-98. Nature 401(6751):356-360
5248 Weinkle J, Maue R, Pielke R (2012) Historical global tropical cyclone landfalls. Journal of
5249 Climate 25(13):4729-4735
5250 Werner A (2011) Seasonal forecasting of tropical cyclone formation in the Australian region.
5251 PhD Thesis, Deparment of Environmental Sciences. Macquaire University, Australia
5252 Werner A, Holbrook NJ (2011) A Bayesian Forecast Model of Australian Region Tropical
5253 Cyclone Formation. Journal of Climate 24(23):6114-6131
5254 Werner A, Maharaj AM, Holbrook NJ (2012) A new method for extracting the ENSO-
5255 independent Indian Ocean Dipole: Application to Australian region tropical cyclone counts.
5256 Climate Dynamics 38(11-12):2503-2511
5257 Whitney LD, Hobgood JS (1997) The relationship between sea surface temperatures and
5258 maximum intensities of tropical cyclones in the eastern North Pacific Ocean. Journal of
5259 Climate 10(11):2921-2930

Wijffels S, Meyers G (2004) An intersection of oceanic waveguides: Variability in the Indonesian throughflow region. J. Phys. Oceanogr 34:1232-1253

Wilks DS (1995) Statistical Methods in the Atmospheric Sciences. Academic Press:467

Williams RT, Chan JCL (1994) Numerical studies of the beta effect in tropical cyclone motion. Part II: zonal mean flow effects. Journal of the Atmospheric Sciences 51(8):1065-1076

WMO (1997) Tropical Cyclone Operational Plan for the Bay of Bengal and the Arabian Sea,WMO Report, 1997.

Wright PB, Mitchell TP, Wallace JM (1984) Relationships between Surface Observations over the Global Oceans and the Southern Oscillation. NOAA, Seattle, WA, Data Report ERL PMEL-I2, :61

Wu R, Kirtman BP (2004) Understanding the Impacts of the Indian Ocean on ENSO Variability in a Coupled GCM. Journal of Climate 17(20):4019-4031

Xie S-P, Annamalai H, Schott FA, McCreary JP (2002) Structure and Mechanisms of South Indian Ocean Climate Variability*. Journal of Climate 15(8):864-878

Xing W, Huang F (2013) Influence of summer monsoon on asymmetric bimodal pattern of tropical cyclogenesis frequency over the Bay of Bengal. Journal of Ocean University of China 12(2):279-286

Yadav RK (2012) Emerging role of Indian ocean on Indian northeast monsoon. Climate Dynamics:1-12

Yahyai SSA (2014) NWP forecast Guidance during Phet at Oman Meteorological Service. In: U.C. Mohanty MM, O.P. Singh, B.K. Bandyopadhyay, L.S. Rathore (ed) Monitoring and Prediction of Tropical Cyclones in the Indian Ocean and Climate Change. Springer, pp 240-262

Yanai M (1964) Formation of tropical cyclones. Reviews of Geophysics 2(2):367-414

Yanase W, Satoh M, Taniguchi H, Fujinami H (2012) Seasonal and intraseasonal modulation of tropical cyclogenesis environment over the bay of bengal during the extended summer monsoon. Journal of Climate 25(8):2914-2930

Yonekura E, Hall TM (2011) A Statistical model of tropical cyclone tracks in the western North Pacific with ENSO-dependent cyclogenesis. Journal of Applied Meteorology and Climatology 50(8):1725-1739

Yuan JP, Cao J (2013) North Indian Ocean tropical cyclone activities influenced by the Indian Ocean Dipole mode. Science China Earth Sciences 56(5):855-865

Yulaeva E, Wallace JM (1994) The signature of ENSO inglobal temperature and precipitation fields derived from the Microwave Sounding Unit. J. Climate 7:1719–1736

Zebiak SE, Cane MA (1987) A Model El Ni&ntilde–Southern Oscillation. Monthly Weather Review 115(10):2262-2278

5296 Zhang W, Graf HF, Leung Y, Herzog M (2012) Different El Niño types and tropical cyclone
5297 landfall in East Asia. Journal of Climate 25(19):6510-6523
5298 Zhang Y, Wallace JM, Battisti DS (1997) ENSO-like Interdecadal Variability: 1900–93. Journal
5299 of Climate 10(5):1004-1020
5300 Zhao H, Wu L, Zhou W (2010) Assessing the influence of the ENSO on tropical cyclone
5301 prevailing tracks in the western North Pacific. Advances in Atmospheric Sciences
5302 27(6):1361-1371
5303 Zhao M, Held IM, Lin SJ, Vecchi GA (2009) Simulations of global hurricane climatology,
5304 interannual variability, and response to global warming using a 50-km resolution GCM.
5305 Journal of Climate 22(24):6653-6678
5306 Zhou XL, Geller MA, Zhang M (2004) Temperature fields in the tropical tropopause transition
5307 layer. Journal of Climate 17(15):2901-2906

5308